frontiers | Research Topics

Chronic airway diseases, lung cancer, and their interaction

Edited by
Yi Liu, Dong Yang, Zheng-Guo Cui, Qiang Wan and Youming Zhang

Published in
Frontiers in Medicine

ISSN 1664-8714
ISBN 978-2-8325-2695-8
DOI 10.3389/978-2-8325-2695-8

About Frontiers

Frontiers is more than just an open access publisher of scholarly articles: it is a pioneering approach to the world of academia, radically improving the way scholarly research is managed. The grand vision of Frontiers is a world where all people have an equal opportunity to seek, share and generate knowledge. Frontiers provides immediate and permanent online open access to all its publications, but this alone is not enough to realize our grand goals.

Frontiers journal series

The Frontiers journal series is a multi-tier and interdisciplinary set of open-access, online journals, promising a paradigm shift from the current review, selection and dissemination processes in academic publishing. All Frontiers journals are driven by researchers for researchers; therefore, they constitute a service to the scholarly community. At the same time, the *Frontiers journal series* operates on a revolutionary invention, the tiered publishing system, initially addressing specific communities of scholars, and gradually climbing up to broader public understanding, thus serving the interests of the lay society, too.

Dedication to quality

Each Frontiers article is a landmark of the highest quality, thanks to genuinely collaborative interactions between authors and review editors, who include some of the world's best academicians. Research must be certified by peers before entering a stream of knowledge that may eventually reach the public - and shape society; therefore, Frontiers only applies the most rigorous and unbiased reviews. Frontiers revolutionizes research publishing by freely delivering the most outstanding research, evaluated with no bias from both the academic and social point of view. By applying the most advanced information technologies, Frontiers is catapulting scholarly publishing into a new generation.

What are Frontiers Research Topics?

Frontiers Research Topics are very popular trademarks of the *Frontiers journals series*: they are collections of at least ten articles, all centered on a particular subject. With their unique mix of varied contributions from Original Research to Review Articles, Frontiers Research Topics unify the most influential researchers, the latest key findings and historical advances in a hot research area.

Find out more on how to host your own Frontiers Research Topic or contribute to one as an author by contacting the Frontiers editorial office: frontiersin.org/about/contact

Chronic airway diseases, lung cancer, and their interaction

Topic editors

Yi Liu — Shandong Provincial Hospital, China
Dong Yang — Fudan University, China
Zheng-Guo Cui — University of Fukui, Japan
Qiang Wan — Shandong Provincial Hospital, China
Youming Zhang — Imperial College London, United Kingdom

Citation

Liu, Y., Yang, D., Cui, Z.-G., Wan, Q., Zhang, Y., eds. (2023). *Chronic airway diseases, lung cancer, and their interaction*. Lausanne: Frontiers Media SA. doi: 10.3389/978-2-8325-2695-8

Table of contents

frontiers | Frontiers in Medicine

TYPE Editorial
PUBLISHED 31 May 2023
DOI 10.3389/fmed.2023.1201894

OPEN ACCESS

EDITED AND REVIEWED BY
Dawei Yang,
Fudan University, China

*CORRESPONDENCE
Youming Zhang
✉ y.zhang@imperial.ac.uk

RECEIVED 07 April 2023
ACCEPTED 16 May 2023
PUBLISHED 31 May 2023

CITATION
Liu Y and Zhang Y (2023) Editorial: Chronic airway diseases, lung cancer, and their interaction. *Front. Med.* 10:1201894. doi: 10.3389/fmed.2023.1201894

Editorial: Chronic airway diseases, lung cancer, and their interaction

Yi Liu[1] and Youming Zhang[2]*

[1]Department of Pulmonary and Critical Care Medicine, Shandong Provincial Hospital Affiliated to Shandong First Medical University, Jinan, Shandong, China, [2]Section of Genomic and Environmental Medicine, National Heart and Lung Institute, Imperial College London, London, United Kingdom

KEYWORDS

asthma, COPD, infection, lung cancer, microbiome

Editorial on the Research Topic
Chronic airway diseases, lung cancer, and their interaction

Chronic respiratory diseases include chronic airway diseases, chronic cough, pulmonary fibrosis, pulmonary infection, and lung cancer. Asthma and chronic obstructive pulmonary disease (COPD) are the most common chronic respiratory diseases, both are inflammatory diseases in small airways. Asthma affects 300 million people in the world (1). Important components of the asthma syndrome include severity, age of onset and the presence of eosinophilia and IgE-mediated allergy to inhaled proteins. Type 2 immune responses are dominant in asthma in Westernized societies, but most cases of asthma in the developing world are non-atopic (2). COPD is also a heterogeneous disease and a leading cause of death and disability worldwide. It characterizes as persistent airflow obstruction and respiratory symptoms. The disease is caused by exposure to inhale cigarette smoke and air pollutants, in combination with genetic, developmental, and social factors (3). Lung cancer can be classified into two broad histologic classes: small cell lung carcinomas (SCLC) and non-small cell lung carcinomas (NSCLC). It is the leading cause of cancer mortality worldwide. Smoking is also the major cause of lung cancer (about 90% of cases). Radon gas, asbestos, air pollution exposures, and chronic infections can also contribute to lung carcinogenesis (4).

With the advanced omics technologies, clinical managements for chronic airway diseases and lung cancer have been revolutionized. For asthma, IgE-specific antibodies, leukotriene receptor antagonists, Th2 type cytokines, therapies against tumor necrosis factor (TNF), vitamin D, probiotics, pathogen-associated molecular patterns (PAMPs) and toll-like receptors (TLRs) agonists, and interferons (IFNs) are all possible treatment means (5). Inhaled corticosteroids (ICS) are still the mainstay for asthma treatment and short-acting beta-agonists (SABAs) can also rapidly reduce airway bronchoconstriction. Although these advanced biologic therapies have reduced the exacerbations rates of moderate to severe asthma by 50% (6), two-thirds of patients with severe asthma treated with biologics continue to have uncontrolled diseases (7). For COPD, there's currently no cure for the disease, but treatments can help to slow the progression of the condition. The effective managements of COPD include stopping tobacco, inhalers, pulmonary rehabilitation, surgery, or lung transplant. For lung cancer, treatments include surgery, radiation therapy, chemotherapy, targeted therapy, and immunotherapy (4). Treatments with tyrosine kinase inhibitors (TKIs) and immune checkpoint inhibitors (ICPIs) have been emerged as valuable therapies for some lung cancer patients. Combining with other traditional therapeutic options, targeted therapies and immunotherapies show great potential in lung cancer treatments.

Personized medicine or precision medicine requires to understand host genetic factors and environmental factors. Chronic airway diseases and lung cancer are caused by combinations of the two factors. Asthma and COPD exacerbations are often linked to the bacterial and viral infections. Human rhinovirus (HRV) and non-typeable Haemophilus Influenzae (NTHi) infections contribute to airway diseases (8, 9). Lower respiratory tract infections (LRTI) are leading causes of morbidity and mortality in the world, accounting for 4.4% of deaths among all ages (10). *Klebsiella pneumoniae* (Kp) is a nosocomial gram-negative bacterial pathogen and can cause community-acquired bacteraemia, liver abscess, urinary tract infection and pneumonia. In this special collection Yang et al. identified 49 patients had sequence type 11 (ST11) from 139 patients infected *Klebsiella pneumoniae*. Patients with ST11 Kp infection can increase mortality in hospital and the infection could be regarded as an independent risk factor for mortality in respiratory ward. The human microbiota plays an important role in immune system development and tissue homeostasis. Microbiome in human lungs exhibits a low biomass and is dominated by dynamic fluxes of microbial clearance and immigration. Respiratory diseases can disrupt the microbial-host interface and affect disease development (11). Zhu et al. presented a cross-sectional study of sputum samples from 36 healthy volunteers and 34 patients with an acute exacerbation of chronic obstructive pulmonary disease (AECOPD) in Inner Mongolia area in China with high-throughput sequencing of 16S rDNA. The airway microbiota of the AECOPD population was different from that of the healthy population. The diversity of airway microbiota was lower than that of the healthy population. Long-term use of ICS plus long-acting beta agnoist (LABA) leads to lower alpha diversity in AECOPD patients. In a meta-analysis, Liu et al. analyzed testosterone deficiency in COPD patients. They found uncertainty for improving the quality of life of COPD patients with anabolic-androgenic steroids (AASs) treatment, suggesting longer and larger future studies for better clarifying the efficacy of AASs. Dendritic cells (DCs) are important bridges to connect innate and adaptive immunity. Xuan et al. presented a systematic review on the roles in respiratory diseases such as lung carcinoma, asthma, pulmonary fibrosis, and pulmonary Langerhans cell histiocytosis, COPD and microbial infection. Hui et al. presented another meta-analysis to summarize the association between polymorphism of angiotensin-converting enzyme (*ACE*) gene and asthma risk. The genotypes DD and ID of *ACE* gene associated with circulating ACE levels. High circulating ACE levels contributed to the development of asthma. Acupuncture at the sphenopalatine ganglion (SPG) for seasonal allergic rhinitis (SAR) is widely applied to treat seasonal allergic rhinitis in China, but the effectiveness is not clear. Wang et al. provided a protocol for a parallel-design, three-armed, patient-assessor blinded randomized controlled trial. The results of the clinical trials would bring the outcomes of the effectiveness of acupuncture treatment on SAR.

Lung cancer is still the most common cancer in China. Li et al. investigated the epidemiology of lung cancer in China from 1990 to 2019. They identified top five risk factors including smoking, ambient particulate matter pollution, second hand smoke, high fasting plasma glucose, and household air pollution from solid fuels. The results provided valuable clues for the prevention and treatment of lung cancer in China. Liang et al. found rapid on-site evaluation (ROSE) examination can increase the diagnostic accuracy of malignant diseases during endobronchial ultrasound-guided transbronchial needle aspiration (EBUS-TBNA). The method can reduce the number of intraoperative punctures. Shen et al. analyzed patients with multiple lung nodules, they applied four factors including chronic inflammation history, human Th cell, imaging vascular convergence sign and mixed ground-glass nodules (GGNs) to assess GGNs. They established a prediction model that can greatly improve the accuracy of malignancy or benignancy prediction of sub-centimeter pulmonary GGNs. Immune checkpoint inhibitors (ICIs) have brought revolutionary breakthroughs to lung cancer, but the therapy has adverse events such as hepatitis, nephritis, dermatitis, and myocarditis. Zhou et al. reported one case of myocarditis with the treatment of PD-L1 inhibitor. The myocardial injury in this case happened in a short time and returned to normal after applying glucocorticoids therapy.

This Research Topic contains 10 valuable articles for the chronic airway diseases and lung cancers and the interaction. Further research in the field can provide more exciting evidence for understanding the pathophysiology of the diseases. Novel therapeutic means will give respiratory patients better, and personalized care in future.

Author contributions

YL and YZ drafted the manuscript, revised the version, and gave approval for the submission. All authors contributed to the article and approved the submitted version.

Acknowledgments

We wish to thank all authors who submitted articles to this Research Topic and all experts who provided critical comments as reviewers.

Conflict of interest

The authors declare that the research was conducted in the absence of any commercial or financial relationships that could be construed as a potential conflict of interest.

Publisher's note

References

1. Dharmage SC, Perret JL, Custovic A. Epidemiology of asthma in children and adults. *Front Pediatr.* (2019) 7:246. doi: 10.3389/fped.2019.00246

2. Worldwide variation in prevalence of symptoms of asthma, allergic rhinoconjunctivitis, and atopic eczema: ISAAC. The international study of asthma and allergies in childhood (ISAAC) steering committee. *Lancet.* (1998) 351:1225–32. doi: 10.1016/S0140-6736(97)07302-9

3. Fermont JM, Masconi KL, Jensen MT, Ferrari R, Di Lorenzo VAP, Marott JM, et al. Biomarkers and clinical outcomes in COPD: a systematic review and meta-analysis. *Thorax.* (2019) 74:439–46. doi: 10.1136/thoraxjnl-2018-211855

4. Lemjabbar-Alaoui H, Hassan OU, Yang YW, Buchanan P. Lung cancer: biology and treatment options. *Biochim Biophys Acta.* (2015) 1856:189–210. doi: 10.1016/j.bbcan.2015.08.002

5. Edwards MR, Bartlett NW, Hussell T, Openshaw P, Johnston SL. The microbiology of asthma. *Nat Rev Microbiol.* (2012) 10:459–71. doi: 10.1038/nrmicro2801

6. McGregor MC, Krings JG, Nair P, Castro M. Role of biologics in asthma. *Am J Respir Crit Care Med.* (2019) 199:433–45. doi: 10.1164/rccm.201810-1944CI

7. Reibman J, Tan L, Ambrose C, Chung Y, Desai P, Llanos JP, et al. Clinical and economic burden of severe asthma among US patients treated with biologic therapies. *Ann Allergy Asthma Immunol.* (2021) 127:318–25. doi: 10.1016/j.anai.2021.03.015

8. Ito K, Zhang Y. Fighting the common cold: ORMDL3 in the crosshairs? *Am J Respir Cell Mol Biol.* (2020) 62:676–7. doi: 10.1165/rcmb.2020-0052ED

9. Brown MA, Jabeen M, Bharj G, Hinks TSC. Non-typeable Haemophilus influenzae airways infection: the next treatable trait in asthma? *Eur Respir Rev.* (2022) 31:22. doi: 10.1183/16000617.0008-2022

10. Collaborators GBDLRI. Estimates of the global, regional, and national morbidity, mortality, and aetiologies of lower respiratory infections in 195 countries, 1990–2016: a systematic analysis for the Global Burden of Disease Study 2016. *Lancet Infect Dis.* (2018) 18:1191–210. doi: 10.1016/S1473-3099(18)30310-4

11. Natalini JG, Singh S, Segal LN. The dynamic lung microbiome in health and disease. *Nat Rev Microbiol.* (2023) 21:222–35. doi: 10.1038/s41579-022-00821-x

frontiers | Frontiers in Medicine

ORIGINAL RESEARCH
published: 16 May 2022
doi: 10.3389/fmed.2022.889020

Clinical Outcomes and Microbiological Characteristics of Sequence Type 11 *Klebsiella pneumoniae* Infection

Ping Yang[1,2], *Zhenchao Wu*[2], *Chao Liu*[3], *Jiajia Zheng*[4], *Nan Wu*[2], *Zhangli Wu*[1,2], *Juan Yi*[1], *Ming Lu*[2,3*†] and *Ning Shen*[1,2,3*†]

[1] Institute of Medical Technology, Peking University Health Science Center, Beijing, China, [2] Department of Pulmonary and Critical Care Medicine, Peking University Third Hospital, Beijing, China, [3] Department of Infectious Diseases, Peking University Third Hospital, Beijing, China, [4] Laboratory of Clinical Microbiology, Peking University Third Hospital, Beijing, China

Background: Sequence type 11 (ST11) *Klebsiella pneumoniae* (Kp) is highly prevalent in China and is a typical sequence type among KPC-producing isolates. This study aimed to evaluate the clinical outcomes and microbiological features of ST11 Kp infections.

Methods: A retrospective cohort study was conducted at Peking University Third Hospital from January 2017 to March 2021. Clinical data were collected from medical records. Antimicrobial susceptibility testing and string tests were performed. Whole-genome sequencing was used to analyze the capsular serotypes, detect virulence-associated genes, and perform multilocus sequence typing. The risk of all-cause mortality in ST11 Kp-infected patients was compared to that in non-ST11 Kp-infected patients.

Results: From 139 patients infected with Kp, 49 ST11 Kp (35.3%) strains were isolated. The Charlson comorbidity index in the ST11 group was higher than that in the non-ST11 group (3.94 ± 1.59 vs. 2.41 ± 1.54, $P = 0.001$). A greater number of ST11 Kp-infected patients required ICU admission (46.9 vs. 16.7%, $P < 0.001$) and mechanical ventilation (28.6 vs. 10.0%, $P = 0.005$). All ST11 isolates presented a multidrug-resistant (MDR) phenotype, and twenty-nine (59.2%) hypervirulent Kp (hvKp) were identified. Twenty-four ST11 strains presented with hypermucoviscosity. The presence of capsular types K47 and K64 was frequent in the ST11 Kp strains ($P < 0.001$). The key virulence-associated genes *rmpA*, *rmpA2*, *iucA*, *iroB*, and *peg344* were present in 26.5, 42.9, 59.2, 0, and 26.5% of the isolates, respectively, in the ST11 group. Twenty-one ST11 isolates harbored the combination of *iucA+rmpA2*. The 30-day mortality rate and sequential organ failure assessment (SOFA) score were significantly higher in ST11 Kp-infected patients than in non-ST11 Kp-infected patients ($P < 0.01$). ST11 Kp infection appeared to be an independent risk factor for mortality in ST11 Kp-infected patients.

Conclusions: A high prevalence of the ST11 clone was found in the hospital, which accounted for elevated antimicrobial resistance and exhibited great molecularly inferred virulence. Patients with ST11 Kp infection had a tendency toward increased 30-day mortality and SOFA scores. ST11 Kp infection was an independent risk factor for mortality, suggesting that enhanced surveillance and management are essential.

Keywords: ***Klebsiella pneumoniae*, ST11, risk factor, virulence, multidrug resistance**

OPEN ACCESS

Edited by:
Yi Liu,
Shandong Provincial Hospital, China

Reviewed by:
Farzad Badmasti,
Pasteur Institute of Iran, Iran
Suchanda Dey,
Siksha O Anusandhan University, India

***Correspondence:**
Ming Lu
lumingpuh3@163.com
Ning Shen
shenningputh@163.com

† These authors have contributed equally to this work

Specialty section:
This article was submitted to Pulmonary Medicine, a section of the journal Frontiers in Medicine

Received: *03 March 2022*
Accepted: *19 April 2022*
Published: *16 May 2022*

Citation:
Yang P, Wu Z, Liu C, Zheng J, Wu N, Wu Z, Yi J, Lu M and Shen N (2022) Clinical Outcomes and Microbiological Characteristics of Sequence Type 11 Klebsiella pneumoniae Infection. Front. Med. 9:889020. doi: 10.3389/fmed.2022.889020

INTRODUCTION

Klebsiella pneumoniae (Kp), an important community-acquired and nosocomial gram-negative bacterial pathogen, causes fatal infections, including pneumonia, urinary tract infection, pyogenic liver abscess, bacteremia and so on (1). Two distinct pathotypes are currently circulating: hypervirulent *Klebsiella pneumoniae* (hvKp) and classical *Klebsiella pneumoniae* (cKp), each of which poses great challenges in clinical practice (2–5). cKp infection mainly occurs in immunocompromised hosts and patients with physiological barrier breakdown in the medical environment. cKp has the ability to acquire various antibiotic resistance genes and rapidly become resistant to all available antibiotics, which is a serious threat to public health. The worldwide spread of multidrug-resistant (MDR) cKp is mainly driven by a special clone termed sequence type 11 (ST11) (6, 7). In China, ST11 Kp is endemic, and most KPC-producing isolates are typically of this sequence type (8). In stark contrast, hvKp infection is mainly acquired by healthy individuals of any age in the community and is highly associated with aggressive invasive infections in hospitals, such as bacteremia and pyogenic liver abscess (4, 9, 10). The previous definition of hvKp was determined by the hypermucoviscosity phenotype (string test showing a positive result) (11).

In fact, not all hvKp isolates possess the hypermucoviscosity phenotype, as confirmed by *in vitro* and *in vivo* studies (3, 5, 12–14). Studies have demonstrated that genetic traits perform better than hypermucoviscosity as a marker for differentiating hvKp and cKp (14, 15). Five key virulence-associated genes, *iucA*, *iroB*, *peg-344*, *rmpA* and *rmpA2*, showed higher diagnostic accuracy for defining hvKp than the hypermucoviscosity phenotype and other virulence-associated genes (15).

ST11, previously identified as cKp, commonly presents with lower virulence (16, 17). However, Gu et al. (18) first demonstrated a fatal outbreak caused by ST11 carbapenem-resistant (CR) hvKp in the ICU. The acquisition of pVir-CR-hvKp4 contributed to the convergence of carbapenem resistance and hypervirulence (18). In addition, the emergence of hybrid conjugative virulence plasmids triggered MDR hvKp formation (19, 20).

Contrary to common belief, the phenomenon of convergence of carbapenem resistance and hypervirulence in Kp is increasing in frequency, which may lead to worse clinical outcomes (18, 19). Few studies have focused on the outcomes and microbiological characteristics of ST11 Kp strains. Liu et al. (21) revealed that the 3-year survival rate of ST11 Kp-infected patients was 73.68%. Another study reported that the in-hospital mortality in the ST11 group was 36.7% (22). However, these previous studies on the mortality of ST11 Kp infection compared to that of non-ST11 infection were controversial. Therefore, we conducted a retrospective study to analyze the clinical outcomes, antibiotic resistance, virulence, and all-cause mortality risk of ST11 Kp infection. We found that ST11 Kp isolates accounted for elevated antimicrobial resistance and exhibited great molecularly inferred virulence. ST11 Kp infection was an independent risk factor for mortality and an increased sequential organ failure assessment (SOFA) score.

MATERIALS AND METHODS

Enrolled Patients

A retrospective cohort study was conducted on Kp culture-positive patients enrolled from January 2017 to March 2021 at Peking University Third Hospital. Clinical data and patient information were obtained from medical records, which included basic demographics, medical history, usage of invasive devices, infection site, infection type, blood examination results, ICU admission, and mechanical ventilation after Kp infection. The Charlson comorbidity index (CCI) was calculated based on the medical history.

The main inclusion criteria were as follows: (1) age $\geq$ 18 years old and (2) Kp was cultured positively and was associated with clinical infectious manifestations at the same time. The exclusion criteria included the following: (1) the bacterial strain not viable after storage and (2) duplicate isolates from the same patient within 3 months. The primary outcome was survival and all-cause mortality at 30 days after Kp infection, and the secondary outcome was the SOFA score.

Hospital-acquired infection and community-acquired infection were defined as previously described (4). The definition of metastatic infection was based on the clinical diagnosis (the presence of $>$ 1 infection site) in the same patient (23).

This study protocol was approved by the Peking University Third Hospital Medical Science Research Ethics Committee (M2021545).

Strain Identification and Antimicrobial Susceptibility Profiling

These specimens were from the respiratory system, urine, blood, drainage fluid, and other body sites. The standardized isolation, culture, and identification were conducted in the Department of Clinical Microbiology. All strains were stored at −80°C.

Strain identification and antimicrobial susceptibility testing (AST) were performed by a Vitek 2 system (bioMérieux, Marcy-l'Étoile, France). If necessary, we also applied the disk diffusion method. The AST results were interpreted according to the 2020 Clinical and Laboratory Standards Institute (CLSI) guidelines (24). The following antimicrobial agents were tested: piperacillin/tazobactam, cefoperazone/sulbactam, ceftazidime, cefepime, imipenem, meropenem, levofloxacin, amikacin, minocycline, and trimethoprim/sulfamethoxazole. The definition of an MDR strain was resistance to three or more different antimicrobial categories (25). Carbapenem-resistant *Klebsiella pneumoniae* (CRKP) was defined based on resistance to imipenem or meropenem.

DNA Extraction and Whole-Genome Sequencing

The DNA of all the isolated Kp strains was extracted by using a GenePure Pro Automatic Nucleic Acid Purification System (NPA-32P, Bioer Technology, Hangzhou, Zhejiang, China) and MagaBio Bacterium DNA Fast Purification Kit (BSC45S1E, Bioer Technology, Hangzhou, Zhejiang, China). Each Kp sample was fully mixed with 180 μL of TET buffer (with added lysozyme) and incubated at 37°C for 30∼60 min. Two microliters of RNase

A (RT405-02, TIANGEN, Beijing, China) was added, and the samples were shaken for 15 s and incubated at 15–25°C for 5 min. Next, each prepared sample and 20 μl of Proteinase K were transferred into kit columns 1 and 7, and then plugged in 8-strip tip and ran the machine program. DNA concentration and purity were evaluated by a NanoDrop (ThermoFisher, Waltham, America).

All strains were sequenced using the Illumina HiSeq 2500 platform by constructing paired-end libraries to obtain 150 bp reads. The clean data were obtained using FastQC and assembled using SPAdes (v.3.13) with the default parameters.

Bioinformation Analysis and Phenotypic Features

Whole-genome sequencing was used to analyze the capsular serotypes, identify virulence-associated genes, and perform multilocus sequence typing (MLST). Raw data were filtered to remove low-quality reads and then assembled using SPAdes (v.3.13). The definition of ST11 Kp was based on MLST using MLST (v.2.0) (Center for Genomic Epidemiology). Capsular types were analyzed using Kleborate software (v.0.3.0). Resistance and virulence genes were annotated by comparison with relevant databases (ResFinder, Virulence Factor Database) using BLAST software (v.2.2.18). HvKp is defined based on the combination of *peg-344*, *iroB*, *iucA*, *rmpA*, or *rmpA2* positivity (15).

Sequencing reads were mapped to the *K. pneumoniae* HS11286 using bowtie 2 v2.2.8 and single nucleotide polymorphisms (SNPs) were identified by using Samtools v1.9 and combined according to the reference genome (SGH-10) using the iSNV-calling pipeline (https://github.com/generality/iSNV-calling). High-quality SNPs (more than 5 reads of mapping quality $>$ 20) were retained. Regions of recombination were detected by Gubbins (26), and the polymorphic sites located in recombination regions were removed. The concatenated sequences of filtered polymorphic sites conserved in all genomes (core genome SNPs, cgSNPs) were used to perform phylogenetic analysis using the maximum likelihood method by iqTree2.1.2 (27).

The hypermucoviscous phenotype was determined by the string test as described previously (2). All isolates were inoculated onto Columbia agar with sheep blood (PB0123A, OXOID, Beijing, China) and incubated at 37°C overnight. The string test was considered positive when a bacteriology inoculation loop was able to generate a viscous string $>$ 5 mm in length by touching and pulling a single colony upward.

Statistical Analysis

Data analysis was performed using SPSS software (v.25.0). Measurement data were assessed as the mean ± standard deviation, and count data are reported as percentages. We used the *T* test and Wilcoxon test for the analysis of continuous variables. We performed the χ^2 or Fisher's exact test for categorical variables. All tests were 2-tailed. A *P*-value $<$ 0.05 was considered statistically significant. The all-cause mortality within 30 days between the two groups was estimated using a Kaplan–Meier curve and log-rank tests. Univariate logistic regression analyses were performed to identify the risk factors associated with death. A multivariable logistic regression analysis was conducted for independent risk factors for death (the variables with $P < 0.05$ were included). Univariate linear regression analyses were performed to identify the factors associated with death. A multivariable linear regression analysis was conducted for independent risk factors for elevated SOFA scores (the variables with $P < 0.05$ were included).

RESULTS

Clinical Characteristics of ST11 Kp Infection

Isolates from 139 Kp infection cases were collected from January 2017 to March 2021. Among these isolates, 49 strains (35.3%, 49/139) were identified as ST11, which was the most prevalent sequence type in this study. Non-ST11 strains (64.7%, 90/139) mainly included ST23 (18.9%, 17/90), ST15 (8.9%, 8/90), ST86 (6.7%, 6/90) and so on. The median age of patients with ST11 Kp infections was 80.04 ± 12.41 years, and 29 patients (59.2%) were male. Most ST11 Kp strains were isolated from patients in the emergency department and ICU (55.1 and 26.5%, respectively), followed by the geriatric department (10.2%) (**Supplementary Figure 1**). Compared with those in the non-ST11 group, more patients in the ST11 group had cardiovascular disease (93.9 vs. 64.4%, $P < 0.001$), cerebrovascular disease (63.3 vs. 36.7%, $P = 0.003$), and urinary disease (51.0 vs. 28.9%, $P = 0.010$). Furthermore, the CCI was higher in the ST11 group (3.94 ± 1.59 vs. 2.41 ± 1.54, $P = 0.001$). In addition, the ST11 group showed significantly more antibiotic exposure within the previous 90 days (100.0 vs. 60.0%, $P < 0.001$). A significant number of patients with invasive catheters were infected by ST11 Kp isolates (100.0 vs. 55.6%, $P < 0.001$), which included central intravenous catheters (67.3 vs. 26.0%, $P < 0.001$), urinary catheters (91.8 vs. 70.0%, $P = 0.006$), endotracheal tubes (32.7 vs. 14.0%, $P = 0.028$) and gastrostomy tubes (89.8 vs. 60.0%, $P = 0.001$). In this study, the most common ST11 Kp infection sites were the respiratory system (65.3%), followed by urine (16.3%). Fewer patients suffered from bloodstream infection in the ST11 group than in the non-ST11 group (6.1 vs. 18.9%, $P = 0.040$), whereas there was no significant difference among other sites between the two groups. Compared to non-ST11 Kp strains, ST11 Kp strains were more closely related to hospital-acquired infections (100.0 vs. 74.4%, $P < 0.001$). In contrast, more community-acquired infections occurred in non-ST11 isolates (0 vs. 25.6%, $P < 0.001$). Furthermore, blood testing indicators (red blood cell count, hemoglobin, and albumin) of patients with ST11 Kp infection were significantly lower than those of the non-ST11 group ($P < 0.01$). However, patients with ST11 Kp infection had a higher hematocrit ($P = 0.013$). In addition, a significant number of patients with ST11 Kp infection required ICU admission (46.9 vs. 16.7%, $P < 0.001$) and mechanical ventilation after Kp detection (28.6 vs. 10.0%, $P = 0.005$) (**Table 1**).

Subgroup analysis was performed according to cKp and hvKp infection. The clinical characteristics of ST11 Kp infection in the hvKp and cKp subgroups were mostly similar to the

TABLE 1 | Clinical Characteristics of ST11 vs. Non-ST11 Kp.

Clinical characteristics	ST11 ($n = 49$)	Non-ST11 ($n = 90$)	*P*-value
Basic demographics			
Age	80.04 ± 12.41	68.66 ± 19.27	0.005
Male	29 (59.2%)	61 (67.8%)	0.311
Medical history			
Diabetes	20 (40.8%)	30 (33.3%)	0.380
Pulmonary disease	18 (36.7%)	22 (24.4%)	0.126
Cardiovascular disease	46 (93.9%)	58 (64.4%)	0.000
Cerebrovascular disease	31 (63.3%)	33 (36.7%)	0.003
Digestive disease	15 (30.6%)	34 (37.8%)	0.398
Urinary disease	25 (51.0%)	26 (28.9%)	0.010
Cancer	10 (20.4%)	11 (12.2%)	0.198
CCI[a]	3.94 ± 1.59	2.41 ± 1.54	0.001
Surgery within 3 months	3 (6.1%)	8 (8.9%)	0.804
Antibiotic exposure within 90 days	49 (100.0%)	54 (60.0%)	0.000
Usage of invasive catheters	49 (100.0%)	50 (55.6%)	0.000
Central intravenous catheter	33 (67.3%)	13 (26.0%)	0.000
Urinary catheter	45 (91.8%)	35 (70.0%)	0.006
Endotracheal tube	16 (32.7%)	7 (14.0%)	0.028
Gastrostomy tube	44 (89.8%)	30 (60.0%)	0.001
Drainage tube	13 (26.5%)	11 (22.0%)	0.599
Metastatic infection	13 (26.5%)	13 (14.4%)	0.081
Infection site			
Respiratory tract	32 (65.3%)	47 (52.2%)	0.137
Urinary tract	8 (16.3%)	12 (13.3%)	0.631
Blood	3 (6.1%)	17 (18.9%)	0.040
Drainage	1 (2.0%)	3 (3.3%)	1.000
Other	5 (10.2%)	11 (12.2%)	0.722
Infection type			
Hospital-acquired infection	49 (100.0%)	67 (74.4%)	0.000
Community-acquired infection	0 (0.0%)	23 (25.6%)	0.000
Laboratory examination result			
Red blood cell count	3.03 ± 0.80	3.64 ± 0.93	0.000
Hemoglobin	94.47 ± 23.82	110.18 ± 25.65	0.001
White blood cell count	10.03 ± 4.90	10.48 ± 5.17	0.611
Platelet count	180.92 ± 128.76	218.12 ± 98.02	0.082
NEU%[b]	77.87 ± 15.68	78.60 ± 15.77	0.986
Total protein	61.81 ± 7.73	63.87 ± 10.23	0.202
Albumin	30.78 ± 3.96	32.84 ± 6.00	0.018
Hematocrit	0.73 ± 3.03	0.33 ± 0.08	0.013
Vasoactive drug use after Kp detection	10 (20.4%)	10 (11.1%)	0.136
Admitted in the ICU[c]	23 (46.9%)	15 (16.7%)	0.000
Mechanical ventilation after Kp detection	14 (28.6%)	9 (10.0%)	0.005
SOFA[d]	6.31 ± 6.04	2.47 ± 2.97	0.000
30-day mortality	18 (38.3%)	11 (12.5%)	0.001

[a]*CCI, Charlson comorbidity index.*
[b]*NEU%, Neutrophil percentage.*
[c]*Patients infected with Kp were then transferred to the ICU.*
[d]*SOFA, Sequential organ failure assessment.*

above results. Notably, more metastatic infection occurred with ST11 Kp strains of the hvKp subgroup (34.5 vs. 10.9%, $P = 0.013$) (**Supplementary Table 2**). In the cKp subgroup, more patients suffered from respiratory system infection in the ST11 group than in the non-ST11 group (75.0 vs. 47.7%, $P = 0.041$) (**Supplementary Table 2**). Additionally, in the ST11 group, the ICU admission rate was higher in patients with cKp infection than in those with hvKp infection (34.5 vs. 65.0%, $P = 0.035$),

while the other clinical characteristics showed no significant differences (**Supplementary Table 3**).

Microbiological Characteristics of ST11 Kp Infection

All the ST11 Kp isolates (100.0%) were MDR, while only 28 of 90 non-ST11 (31.1%) Kp strains were MDR. Moreover, CRKP in the ST11 group and non-ST11 group accounted for 100 and 14.4%, respectively. Notably, all 49 ST11 Kp strains (100.0%) were resistant to piperacillin/tazobactam, cefoperazone/sulbactam, ceftazidime, cefepime, imipenem, and meropenem. Significantly, the rates of resistance to all antibiotics in the non-ST11 group were <50%. However, except for minocycline and trimethoprim/sulfamethoxazole, the rates of resistance to most antibiotics were approximately 100% in ST11 Kp isolates. Additionally, for the antibiotics commonly used in clinical practice, such as β-lactamase inhibitors and carbapenems, the resistance rate of the ST11 group was significantly higher than that of the non-ST11 group ($P < 0.001$) (**Table 2**, **Supplementary Table 1**).

In terms of resistance genes, all the ST11 Kp strains harbored the beta-lactamase gene bla_{KPC-2}. Additionally, a large number of ST11 isolates presented the beta-lactamase gene bla_{TEM-1D} (93.9%) and the fosfomycin resistance gene *fosA3* (91.8%). Over half of the ST11 isolates possessed the aminoglycoside resistance gene *aadA2* and the beta-lactamase genes $bla_{CTX-M-65}$ and bla_{SHV-11}, which were significantly more frequently detected than in the non-ST11 group ($P < 0.001$, $P < 0.001$ and $P = 0.022$, respectively). There was a strong tendency for the presence of *K47* (53.1 vs. 1.1%, $P < 0.001$) and *K64* (42.9 vs. 1.1%, $P < 0.001$) in ST11 Kp strains. In contrast, there was a tendency for the presence of *K1* (0 vs. 20.0%, $P < 0.001$) and *K2* (0 vs. 15.6%, $P = 0.002$) in non-ST11 Kp isolates. Twenty-four ST11 strains showed a hypermucoviscous phenotype, which was a significantly lower number than that in the non-ST11 group (49.0 vs. 68.9%, $P = 0.021$). The virulence-associated genes *rmpA, rmpA2, iucA, iroB,* and *peg344* were present in 26.5, 42.9, 59.2, 0, and 26.5% of the isolates in the ST11 group, respectively. Notably, all the ST11 Kp isolates harbored the siderophore yersiniabactin genes. Additionally, the *ybt-ICEKp3* cluster was highly clustered in the ST11 group (100.0 vs. 6.7%, $P < 0.001$). *peg589*, which is related to a poor prognosis in an animal model, was highly associated with the ST11 group (61.2 vs. 41.1%, $P = 0.023$). Importantly, twenty-nine (59.2%) ST11 Kp strains were MDR hvKp. Additionally, twenty-one ST11 isolates harbored the combination of *iucA+rmpA2*, which showed no significant difference in both groups ($P = 0.649$) (**Figure 1**, **Supplementary Table 4**).

Among all the ST11 Kp strains, two distinguished clades were identified by the phylogenetic analysis. Clade a contained 23 strains, and clade b comprised 26 strains. Notably, a great number of hvKp belonged to the clade a (21/29). Besides, two clades had the same 30-day mortality (**Figure 2**).

TABLE 2 | Antibiotic resistance patterns of ST11 Kp.

Antibiotic agent	ST11	Non-ST11	*P*-value
MDR[a]	49 (100.0%)	28 (31.1%)	0.000
CR[b]	49 (100.0%)	13 (14.4%)	0.000
Piperacillin/tazobactam (TZP)	49 (100.0%)	15 (16.7%)	0.000
Cefoperazone/sulbactam (CSL)	49 (100.0%)	14 (15.6%)	0.000
Ceftazidime (CAZ)	49 (100.0%)	22 (24.4%)	0.000
Cefepime (FEP)	49 (100.0%)	24 (26.7%)	0.000
Imipenem (IPM)	49 (100.0%)	12 (13.3%)	0.000
Meropenem (MEM)	49 (100.0%)	13 (14.4%)	0.000
Levofloxacin (LVX)	48 (98.0%)	25 (27.8%)	0.000
Amikacin (AMK)	42 (85.7%)	5 (5.6%)	0.000
Minocycline (MNO)	23 (46.9%)	19 (21.1%)	0.002
Trimethoprim/sulfamethoxazole (SXT)	22 (44.9%)	18 (20.0%)	0.002

[a]*MDR, multidrug resistant.*
[b]*CR, carbapenem resistant.*

Risk Factors for 30-Day Mortality in Patients With Kp Infection

The survival curve revealed that the 30-day mortality rate in patients with ST11 Kp infection was significantly higher than that in patients without ST11 Kp infection (38.3 vs. 12.5%, $P = 0.001$) (**Figure 3**). Similar results were observed in the hvKp (35.7 vs. 8.9%, $P = 0.005$) and cKp subgroups (42.1 vs. 16.3%, $P = 0.029$) (**Supplementary Figure 2**). In the ST11 group, the mortality among patients with cKp and hvKp infections was similar (35.7 vs. 42.1%, $P = 0.644$) (**Supplementary Figure 3**).

Univariate regression analysis showed that ST11 Kp infection [odds ratio (OR) = 4.345] and the CCI (OR = 1.598) were statistically significant risk factors associated with 30-day mortality. In addition, multivariate analysis revealed that ST11 Kp infection appeared to be an independent risk factor for ST11 Kp infection (OR = 2.786) (**Table 3**).

Risk Factors for Elevated SOFA Scores in Patients With Kp Infection

The SOFA score was significantly higher in patients with ST11 infection than in the non-ST11 infection patients (6.31 ± 6.04 vs. 2.47 ± 2.97, $P < 0.001$) (**Table 1**, **Supplementary Figure 4**). The results of univariate linear analysis revealed that the risk factors for an elevated SOFA score included ST11 Kp infection [risk ratio (RR) = 3.839]) and increased CCI (RR = 0.597). Multivariate analysis showed that compared to non-ST11 infection, ST11 Kp infection caused an increase in SOFA score (RR = 3.579) (**Table 4**).

DISCUSSION

The prevalent sequence types of Kp are diverse worldwide. In China, previous studies revealed that ST11 Kp is the main endemic clone, typically presenting as CRKP (7, 28, 29). Similarly, we found that ST11 Kp was highly prevalent in our study. We found that the CCI was significantly higher in patients with ST11 Kp infection than in the non-ST11 infection patients. In addition, our data revealed that the ST11 group was highly

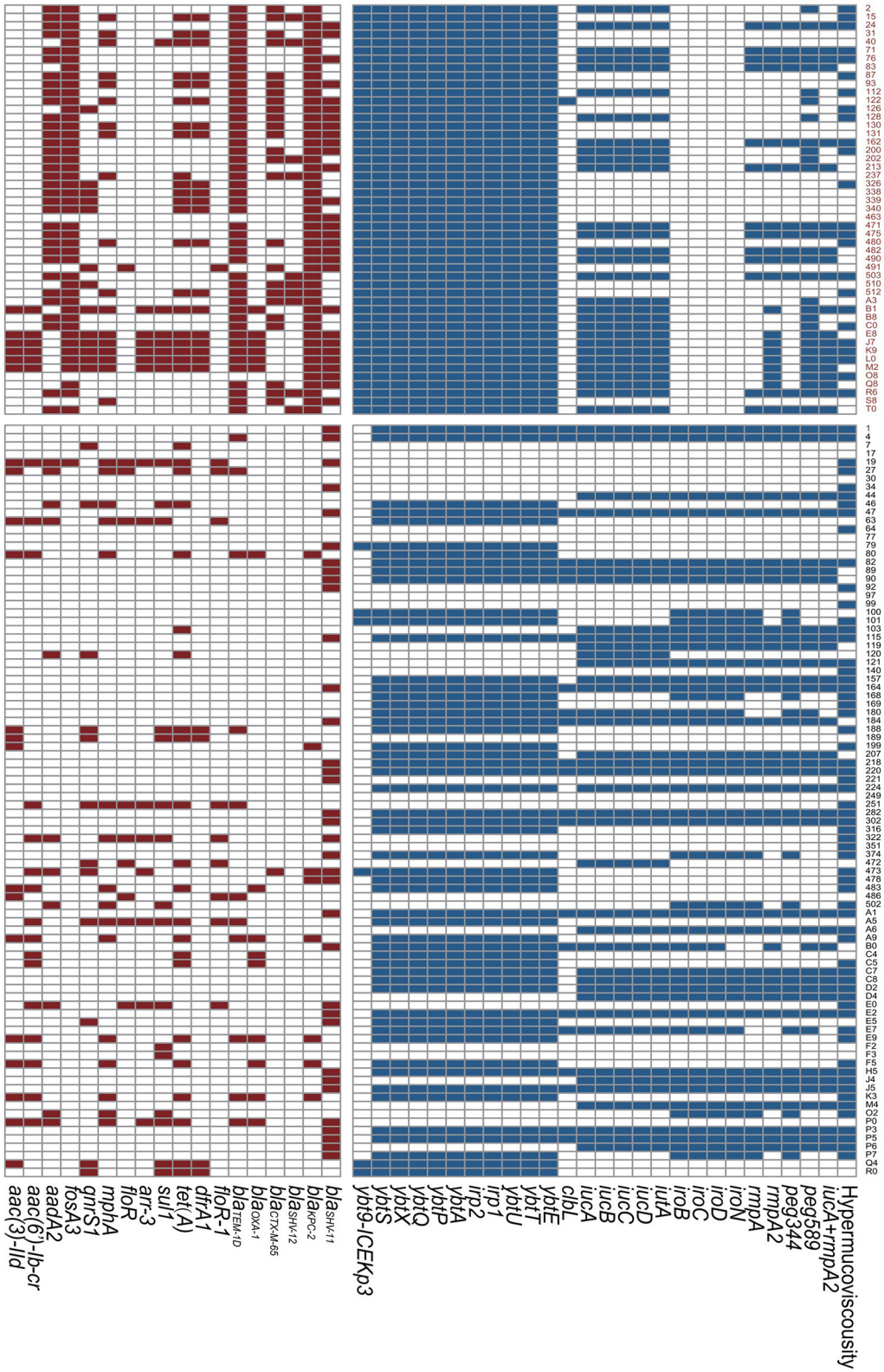

FIGURE 1 | Resistance genes and virulence genes of *Klebsiella pneumoniae* strains. The colored blocks represent existence of genes. Red, ST11 group; Black, Non-ST11 group.

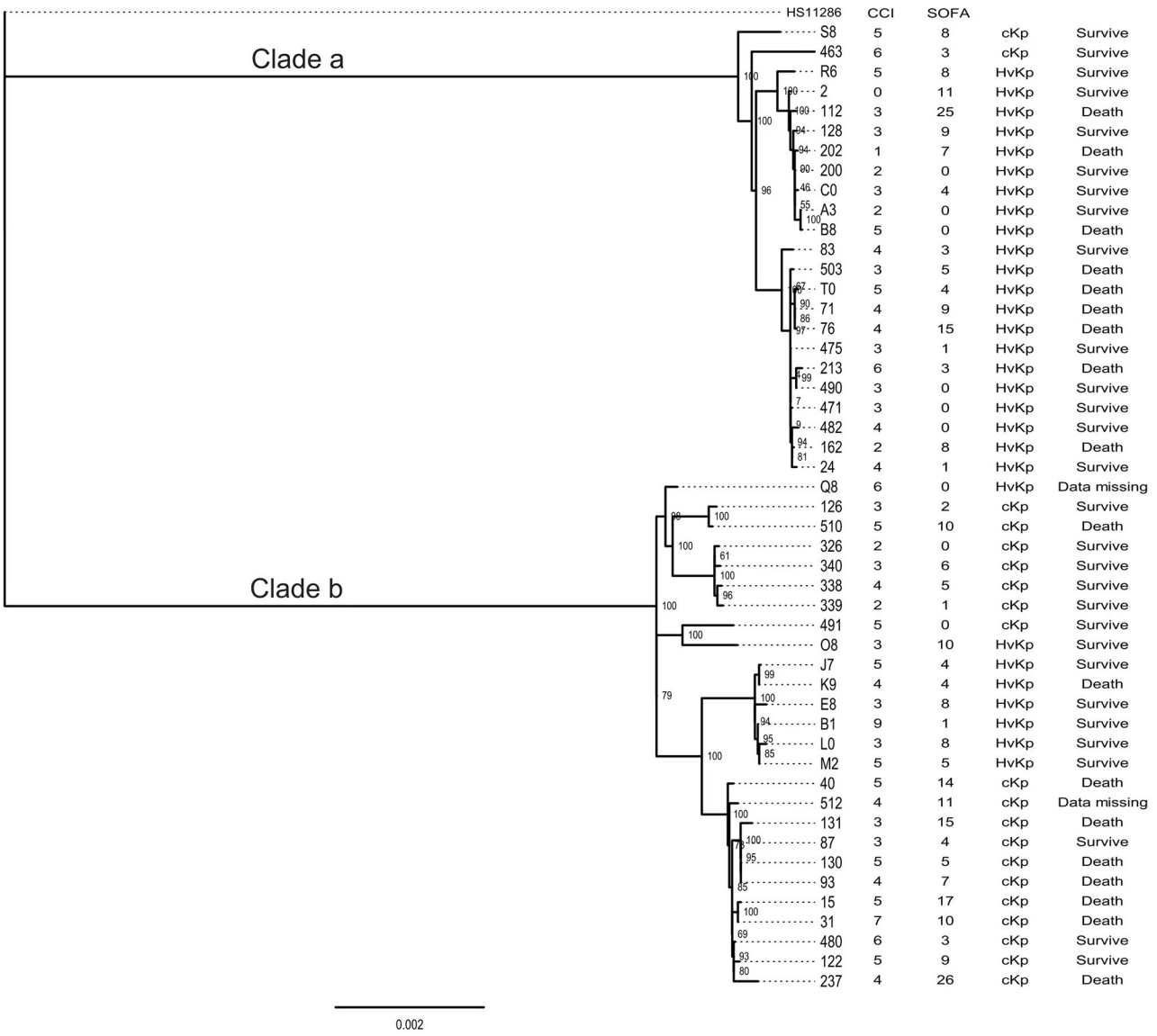

FIGURE 2 | The phylogenetic tree of ST11 strains isolated in this study.

associated with catheter usage, ICU admission and mechanical ventilation after Kp detection. It seemed that ST11 Kp-infected patients might have a complicated status. Importantly, the results suggested that all ST11 Kp strains were MDR. Surprisingly, the majority of MDR ST11 isolates were hvKp. The emergence of MDR ST11 hvKp strains threatens the viability of the current therapeutic approach, increasing the severity of infection. The nosocomial dissemination of MDR ST11 hvKp isolates is alarming, and medical staff need to enhance the infection control and management of ST11 strains with "superbug" characteristics and high virulence.

A previous study demonstrated that ST11 Kp was a common class of cKp and was notorious for acquiring various antibiotic resistance genes (30). Notably, the ratio of MDR strains has increased rapidly among ST11 isolates (7, 31). Previous studies reported that ST11 isolates had higher levels of resistance to aztreonam, fosfomycin, amikacin and meropenem than non-ST11 strains (7, 32). Our results also revealed that all ST11 isolates presented with an MDR phenotype, while the drug resistance rate in the non-ST11 group was generally low. Importantly, most MDR-ST11 Kp acquired virulence-associated genes and then evolved into MDR ST11 hvKp strains (18). In terms of the virulence gene spectrum, our data showed that the prevalence of *rmpA2* (42.9%) and *iucA* (59.2%) was very high, and most of the MDR ST11 hvKp possessed *iucA*+*rmpA2*, similar to previous reports, suggesting that they might carry pVir-CR-hvKP4-like virulence plasmids (18, 33, 34). Studies have reported that these strains tested positive on the string test and presented

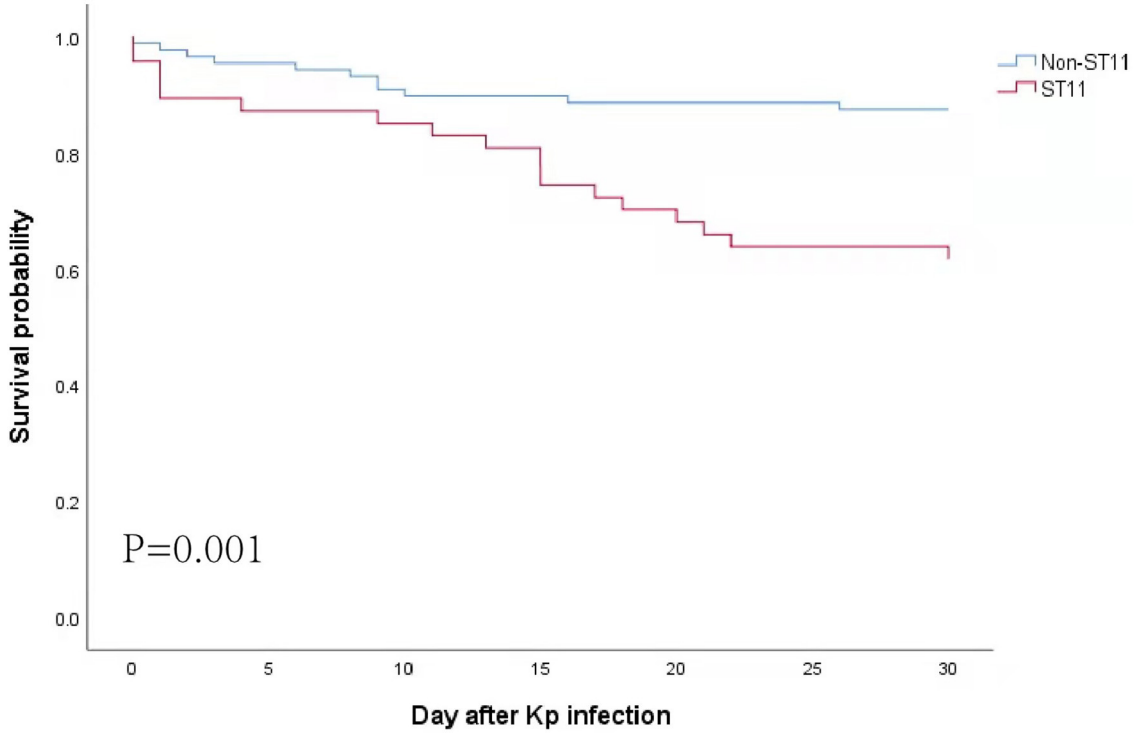

FIGURE 3 | Kaplan–Meier curves for all-cause 30-day mortality. Statistical significance was determined by the log-rank test.

TABLE 3 | Risk factors for death.

Variable	Univariate OR[a] (95% CI[b])	P-value	Multivariate OR (95% CI)	P-value
ST11 Kp infection	4.345(1.833–10.300)	0.001	2.786(1.089–7.126)	0.032
CCI	1.598(1.206–2.117)	0.001	1.418(1.048–1.918)	0.024

[a]*OR, Odds ratio.*
[b]*CI, Confidence interval.*

hypervirulence in *Galleria mellonella* infection and human neutrophil models (18, 35). Compared with pLVPK, a 41,231 bp depletion occurred in pVir-CR-hvKP4 that resulted in the loss of the virulence genes *rmpA* and *iro*, but the *iuc* and *rmpA2* genes were retained (18, 34). Further investigations are required to determine whether genetic deletion has a potential effect on the hypervirulence phenotype. Previous studies demonstrated that the K1 and/or K2 capsule serotypes were commonly associated with enhanced virulence (36, 37). However, none of the MDR hvKp strains possessed the K1/K2 serotype in this study. The K47 and K64 serotypes were common within the ST11 group, which is similar to previous studies (38, 39). This result suggested that other genetic elements may play key roles in virulence. A previous study showed that ST11-KL47 was replaced by ST11-KL64 as the endemic subclone (40), which should be further confirmed in a large study. ICE*Kp* represents a key virulence element that exerts a strong influence on the pathogenicity of Kp isolates. ICE*Kp* is responsible for scavenging iron from host transport proteins, thereby enhancing survival and replication within the host (41, 42). Lam et al. (41) reported that *ybt 9* and *ybt 10* were predominant within the ST11 group, and the ICE*Kp3* element was highly associated with *ybt 8* and *ybt 9*. In this study, *ybt9*-ICE*Kp3* was dominant in ST11 isolates, which was similar to a previous study with longitudinal genomic surveillance (43).

As described above, ST11 Kp strains presented all kinds of virulence determinants and showed both MDR and hypervirulent phenotypes, indicating that the prognosis of the patients infected with MDR ST11 hvKp was poor. Gu et al. (18) first reported an outbreak caused by ST11 CR-hvKp in the ICU, and all the patients presented with a poor prognosis. Compared with that of non-ST11 Kp-infected patients (18/20, 90.00%), the 3-year survival rate (28/38, 73.68%) was lower in a report from Liu et al. (21). However, another study reported no significant difference in in-hospital mortality between the ST11 and non-ST11 groups ($P = 0.795$) (22). Remarkably, previous studies have set different endpoints that lead to contradictory

TABLE 4 | Risk factors for an elevated SOFA score.

Variable	Univariate RR[a] (95% CI[b])	*P*-value	Multivariate RR (95% CI[a])	*P*-value
ST11 Kp infection	3.839(2.329–5.350)	0.000	3.579(1.906–5.253)	0.000
CCI	0.597(0.149–1.045)	0.009	0.170(-0.297–0.638)	0.472

[a]*RR, Risk ratio.*
[b]*CI, Confidence interval.*

conclusions. Too long or too short of a study period results in confounding factors that affect the conclusion. Some studies have indicated that 30-day mortality is a better indicator to analyze the clinical outcomes of infected patients. Of note, the previous study enrolled patients with hospital-acquired pneumonia caused by CRKP, while we enrolled patients with all kinds of Kp infections. Our study highlighted that ST11 Kp infection was significantly associated with higher 30-day mortality than non-ST11 infection. Interestingly, our subgroup analysis revealed that the mortality among patients with cKp and hvKp infections was similar in patients with ST11 strain infection. Notably, the ST11 isolates themselves, not the cKp or hvKp, might be responsible for the poor prognosis. Increased attention should be given to the prevention and control of ST11 Kp infections.

A previous study reported that CRKP appeared to be an independent risk factor for 1-year postoperative mortality in patients after kidney transplantation (44). Additionally, some studies demonstrated that CRKP infection was one of the independent risk factors for death from Kp bloodstream infection (45, 46). However, these studies did not distinguish the specific sequence types that might exert different influences on the mortality of Kp-infected patients. Li et al. observed a high percentage (20/35, 57.1%) of KPC-producing isolates among hvKp strains, in which ST11 strains were dominant (17/35, 48.6%). They found that the KPC-producing isolates were an independent predictor for 30-day mortality of Kp bacteremia patients (47). Similarly, another previous study revealed that ST11 was the most prevalent (66.7%), nearly all of the ST11 isolates were bla_{KPC} positive, and bla_{KPC} was an independent risk factor for 14-day mortality. It is believed that ST11 strains are the dominant Kp clone in CRKP strains in China, typically carrying bla_{KPC} and producing carbapenemase (8, 31). Similarly, all the CRKP isolates were ST11 in our study. In this study, ST11 Kp infection was independently associated with 30-day mortality in Kp-infected patients, indicating that close attention should be given to ST11 strains, not only CRKP.

The SOFA score, a universally recognized indicator to evaluate sepsis, was significantly associated with 30-day mortality in patients with KPC-producing Kp and CRKP infection (48–51). Our study showed that patients with ST11 Kp infection had an elevated SOFA score (RR = 3.579). Moreover, multivariable linear regression revealed that ST11 Kp infection could lead to an increase in the SOFA score, indicating that ST11 Kp strains could cause more serious infections, a higher risk of sepsis and a worse prognosis than non-ST11 Kp strains.

The main limitation of our study is the selection bias and small sample size because it was a retrospective study conducted at a single center. Therefore, further prospective multicenter studies are desirable. Additionally, apart from virulence-associated genes detected by whole-genome sequencing, identification of Kp virulence in *in vitro* and *in vivo* models by using objective evidence, such as *Galleria mellonella*, mouse, or human neutrophil assays, is needed.

In summary, ST11 Kp infection was an independent risk factor for mortality and an elevated SOFA score. Our research demonstrated the notable conclusion that a high prevalence of ST11 Kp strains might be the main cause of high 30-day mortality and SOFA scores in Kp-infected patients. All the ST11 strains presented an MDR phenotype and exhibited great molecularly inferred virulence. For this superbug, it is of great importance to enhance clinical awareness, control and management of ST11 Kp infections.

DATA AVAILABILITY STATEMENT

The genome sequences in this study were deposited into the China National Center for Bioinformation under BioProject accession no. PRJCA007641. The datasets used and/or analyzed during the current study are available from the corresponding author on reasonable request.

ETHICS STATEMENT

The studies involving human participants were reviewed and approved by Peking University Third Hospital Medical Science Research Ethics Committee. Written informed consent for participation was not required for this study in accordance with the national legislation and the institutional requirements.

AUTHOR CONTRIBUTIONS

NS and ML contributed to the study design. NW, ZheW, and JY collected the clinical data. JZ and PY collected the laboratory data and performed the tests. CL and ZhaW analyzed and interpreted the data. ZheW and PY drafted the manuscript. CL revised the manuscript. All authors have reviewed and approved the final version of the manuscript.

FUNDING

This study was supported by Beijing Key Clinical Specialty Funding (010071) and by the Clinical Cohort Construction Program of Peking University Third Hospital (BYSYDL2019007).

ACKNOWLEDGMENTS

We would like to thank Peking University Third Hospital for providing a laboratory for the experiments.

SUPPLEMENTARY MATERIAL

The Supplementary Material for this article can be found online at: https://www.frontiersin.org/articles/10.3389/fmed.2022.889020/full#supplementary-material

REFERENCES

1. Paczosa MK, Mecsas J. Klebsiella pneumoniae: Going on the offense with a strong defense. *Microbiol Mol Biol Rev.* (2016) 80:629–61. doi: 10.1128/MMBR.00078-15
2. Shon AS, Bajwa RP, Russo TA. Hypervirulent (hypermucoviscous) Klebsiella pneumoniae: a new and dangerous breed. *Virulence.* (2013) 4:107–18. doi: 10.4161/viru.22718
3. Catalan-Najera JC, Garza-Ramos U, Barrios-Camacho H. Hypervirulence and hypermucoviscosity: two different but complementary Klebsiella spp. phenotypes? *Virulence.* (2017) 8:1111–23. doi: 10.1080/21505594.2017.1317412
4. Li W, Sun G, Yu Y, Li N, Chen M, Jin R, et al. Increasing occurrence of antimicrobial-resistant hypervirulent (hypermucoviscous) Klebsiella pneumoniae isolates in China. *Clin Infect Dis.* (2014) 58:225–32. doi: 10.1093/cid/cit675
5. Liu C, Shi J, Guo J. High prevalence of hypervirulent Klebsiella pneumoniae infection in the genetic background of elderly patients in two teaching hospitals in China. *Infect Drug Resist.* (2018) 11:1031–41. doi: 10.2147/IDR.S161075
6. Tóth A, Damjanova I, Puskás E, Jánvári L, Farkas M, Dobák A, et al. Emergence of a colistin-resistant KPC-2-producing Klebsiella pneumoniae ST258 clone in Hungary. *Eur J Clin Microbiol Infect Dis.* (2010) 29:765–9. doi: 10.1007/s10096-010-0921-3
7. Wang Q, Wang X, Wang J, Ouyang P, Jin C, Wang R, et al. Phenotypic and genotypic characterization of carbapenem-resistant enterobacteriaceae: data from a longitudinal large-scale CRE study in China (2012-2016). *Clin Infect Dis.* (2018) 67:S196–205. doi: 10.1093/cid/ciy660
8. Liu Y, Zhang X, Cai L, Zong Z. Enhanced survival of ST-11 carbapenem-resistant Klebsiella pneumoniae in the intensive care unit. *Infect Control Hosp Epidemiol.* (2020) 41:740–2. doi: 10.1017/ice.2020.68
9. Pomakova DK, Hsiao CB, Beanan JM, Olson R, MacDonald U, Keynan Y, et al. Clinical and phenotypic differences between classic and hypervirulent Klebsiella pneumonia: an emerging and under-recognized pathogenic variant. *Eur J Clin Microbiol Infect Dis.* (2012) 31:981–9. doi: 10.1007/s10096-011-1396-6
10. Siu LK, Yeh KM, Lin JC, Fung CP, Chang FY. Klebsiella pneumoniae liver abscess: a new invasive syndrome. *Lancet Infect Dis.* (2012) 12:881–7. doi: 10.1016/S1473-3099(12)70205-0
11. Fang CT, Chuang YP, Shun CT, Chang SC, Wang JT. A novel virulence gene in Klebsiella pneumoniae strains causing primary liver abscess and septic metastatic complications. *J Exp Med.* (2004) 199:697–705. doi: 10.1084/jem.20030857
12. Zhang Y, Zhao C, Wang Q, Wang X, Chen H, Li H, et al. High prevalence of hypervirulent klebsiella pneumoniae infection in China: geographic distribution, clinical characteristics, and antimicrobial resistance. *Antimicrob Agents Chemother.* (2016) 60:6115–20. doi: 10.1128/AAC.01127-16
13. Lin YC, Lu MC, Tang HL, Liu HC, Chen CH, Liu KS, et al. Assessment of hypermucoviscosity as a virulence factor for experimental Klebsiella pneumoniae infections: comparative virulence analysis with hypermucoviscosity-negative strain. *BMC Microbiol.* (2011) 11:50. doi: 10.1186/1471-2180-11-50
14. Russo TA, Olson R, MacDonald U, Beanan J, Davidson BA. Aerobactin, but not yersiniabactin, salmochelin, or enterobactin, enables the growth/survival of hypervirulent (hypermucoviscous) Klebsiella pneumoniae ex vivo and in vivo. *Infect Immun.* (2015) 83:3325–33. doi: 10.1128/IAI.00430-15
15. Russo TA, Olson R, Fang CT, Stoesser N, Miller M, MacDonald U, et al. Identification of Biomarkers for Differentiation of Hypervirulent Klebsiella pneumoniae from Classical K. pneumoniae. *J Clin Microbiol.* (2018) 56:e00776–18. doi: 10.1128/JCM.00776-18
16. Chiang TT, Yang YS, Yeh KM, Chiu SK, Wang NC, Lin TY, et al. Quantification and comparison of virulence and characteristics of different variants of carbapenemase-producing klebsiella pneumoniae clinical isolates from Taiwan and the United States. *J Microbiol Immunol Infect.* (2016) 49:83–90. doi: 10.1016/j.jmii.2015.08.011
17. Liu Y, Liu PP, Wang LH, Wei DD, Wan LG, Zhang W. Capsular polysaccharide types and virulence-related traits of epidemic KPC-producing klebsiella pneumoniae isolates in a Chinese university hospital. *Microb Drug Resist.* (2017) 23:901–7. doi: 10.1089/mdr.2016.0222
18. Gu D, Dong N, Zheng Z, Lin D, Huang M, Wang L, et al. A fatal outbreak of ST11 carbapenem-resistant hypervirulent Klebsiella pneumoniae in a Chinese hospital: a molecular epidemiological study. *Lancet Infect Dis.* (2018) 18:37–46. doi: 10.1016/S1473-3099(17)30489-9
19. Dong N, Yang X, Zhang R, Chan EW, Chen S. Tracking microevolution events among ST11 carbapenemase-producing hypervirulent Klebsiella pneumoniae outbreak strains. *Emerg Microbes Infect.* (2018) 7:146. doi: 10.1038/s41426-018-0146-6
20. Yang X, Wai-Chi Chan E, Zhang R, Chen S. A conjugative plasmid that augments virulence in Klebsiella pneumoniae. *Nat Microbiol.* (2019) 4:2039–43. doi: 10.1038/s41564-019-0566-7
21. Liu S, Wang X, Ge J, Wu X, Zhao Q, Li YM, et al. Analysis of carbapenemase-resistant genotypes of highly virulent klebsiella pneumoniae and clinical infection characteristics of different MLST types. *Evid Based Complement Alternat Med.* (2021) 2021:3455121. doi: 10.1155/2021/3455121
22. Zuo Y, Zhao D, Song G, Li J, Xu Y, Wang Z. Risk factors, molecular epidemiology, and outcomes of carbapenem-resistant klebsiella pneumoniae infection for hospital-acquired pneumonia: a matched case-control study in eastern China during 2015-2017. *Microb Drug Resist.* (2021) 27:204–11. doi: 10.1089/mdr.2020.0162
23. Wang JH, Liu YC, Lee SS, Yen MY, Chen YS, Wang JH, et al. Primary liver abscess due to Klebsiella pneumoniae in Taiwan. *Clin Infect Dis.* (1998) 26:1434–8. doi: 10.1086/516369
24. Institute CaLS. *Performance Standards for Antimicrobial Susceptibility Testing, 30th ed.* Wayne, PA: CLSI supplement M100 CLSI (2020).
25. Magiorakos AP, Srinivasan A, Carey RB, Carmeli Y, Falagas ME, Giske CG, et al. Multidrug-resistant, extensively drug-resistant and pandrug-resistant bacteria: an international expert proposal for interim standard definitions for acquired resistance. *Clin Microbiol Infect.* (2012) 18:268–81. doi: 10.1111/j.1469-0691.2011.03570.x
26. Croucher NJ, Page AJ, Connor TR, Delaney AJ, Keane JA, Bentley SD, et al. Rapid phylogenetic analysis of large samples of recombinant bacterial whole genome sequences using Gubbins. *Nucleic Acids Res.* (2015) 43:e15. doi: 10.1093/nar/gku1196
27. Nguyen LT, Schmidt HA, von Haeseler A, Minh BQ, IQ-TREE a fast and effective stochastic algorithm for estimating maximum-likelihood phylogenies. *Mol Biol Evol.* (2015) 32:268–74. doi: 10.1093/molbev/msu300
28. Lee CR, Lee JH, Park KS, Kim YB, Jeong BC, Lee SH. Global dissemination of carbapenemase-producing klebsiella pneumoniae: epidemiology, genetic context, treatment options, and detection methods. *Front Microbiol.* (2016) 7:895. doi: 10.3389/fmicb.2016.00895
29. Li H, Zhang J, Liu Y, Zheng R, Chen H, Wang X, et al. Molecular characteristics of carbapenemase-producing Enterobacteriaceae in China from 2008 to 2011: predominance of KPC-2 enzyme. *Diagn Microbiol Infect Dis.* (2014) 78:63–5. doi: 10.1016/j.diagmicrobio.2013.10.002
30. Kuehn BM. "Nightmare" bacteria on the rise in US hospitals, long-term care facilities. *Jama.* (2013) 309:1573–4. doi: 10.1001/jama.2013.2922

31. Qi Y, Wei Z, Ji S, Du X, Shen P, Yu Y. ST11 the dominant clone of KPC-producing Klebsiella pneumoniae in China. *J Antimicrob Chemother.* (2011) 66:307–12. doi: 10.1093/jac/dkq431
32. Zhou M, Yang Q, Lomovskaya O, Sun D, Kudinha T, Xu Z, et al. In vitro activity of meropenem combined with vaborbactam against KPC-producing Enterobacteriaceae in China. *J Antimicrob Chemother.* (2018) 73:2789–96. doi: 10.1093/jac/dky251
33. Russo TA, Marr CM. Hypervirulent Klebsiella pneumoniae. *Clin Microbiol Rev.* (2019) 32:e00001–19. doi: 10.1128/CMR.00001-19
34. Yang X, Dong N, Chan EW, Zhang R, Chen S. Carbapenem resistance-encoding and virulence-encoding conjugative plasmids in klebsiella pneumoniae. *Trends Microbiol.* (2021) 29:65–83. doi: 10.1016/j.tim.2020.04.012
35. Zhang Y, Jin L, Ouyang P, Wang Q, Wang R, Wang J, et al. Evolution of hypervirulence in carbapenem-resistant Klebsiella pneumoniae in China: a multicentre, molecular epidemiological analysis. *J Antimicrob Chemother.* (2020) 75:327–36. doi: 10.1093/jac/dkz446
36. Yeh KM, Kurup A, Siu LK, Koh YL, Fung CP, Lin JC, et al. Capsular serotype K1 or K2, rather than magA and rmpA, is a major virulence determinant for Klebsiella pneumoniae liver abscess in Singapore and Taiwan. *J Clin Microbiol.* (2007) 45:466–71. doi: 10.1128/JCM.01150-06
37. Wang TC, Lin JC, Chang JC, Hiaso YW, Wang CH, Chiu SK, et al. Virulence among different types of hypervirulent Klebsiella pneumoniae with multi-locus sequence type (MLST)-11, Serotype K1 or K2 strains. *Gut Pathog.* (2021) 13:40. doi: 10.1186/s13099-021-00439-z
38. Dong N, Zhang R, Liu L, Li R, Lin D, Chan EW, et al. Genome analysis of clinical multilocus sequence Type 11 Klebsiella pneumoniae from China. *Microb Genom.* (2018) 4:e000149. doi: 10.1099/mgen.0.000149
39. Liu C, Du P, Xiao N, Ji F, Russo TA, Guo J. Hypervirulent Klebsiella pneumoniae is emerging as an increasingly prevalent K. pneumoniae pathotype responsible for nosocomial and healthcare-associated infections in Beijing, China. *Virulence.* (2020) 11:1215–24. doi: 10.1080/21505594.2020.1809322
40. Zhou K, Xiao T, David S, Wang Q, Zhou Y, Guo L, et al. Novel subclone of carbapenem-resistant klebsiella pneumoniae sequence type 11 with enhanced virulence and transmissibility, China. *Emerg Infect Dis.* (2020) 26:289–97. doi: 10.3201/eid2602.190594
41. Lam MMC, Wick RR, Wyres KL, Gorrie CL, Judd LM, Jenney AWJ, et al. Genetic diversity, mobilisation and spread of the yersiniabactin-encoding mobile element ICEKp in Klebsiella pneumoniae populations. *Microb Genom.* (2018) 4:e000196. doi: 10.1099/mgen.0.000196
42. Holden VI, Bachman MA. Diverging roles of bacterial siderophores during infection. *Metallomics.* (2015) 7:986–95. doi: 10.1039/C4MT00333K
43. Zhu C, Li C, Lai CKC, Ng R, Chau KY, Wong KT, et al. Longitudinal genomic characterization of carbapenemase-producing enterobacteriaceae (CPE) reveals changing pattern of CPE isolated in Hong Kong hospitals. *Int J Antimicrob Agents.* (2021) 58:106430. doi: 10.1016/j.ijantimicag.2021.106430
44. Zhang F, Zhong J, Ding H, Pan J, Yang J, Lan T, et al. Analysis of risk factors for carbapenem-resistant klebsiella pneumoniae infection and its effect on the outcome of early infection after kidney transplantation. *Front Cell Infect Microbiol.* (2021) 11:726282. doi: 10.3389/fcimb.2021.726282
45. Xiao T, Zhu Y, Zhang S, Wang Y, Shen P, Zhou Y, et al. A retrospective analysis of risk factors and outcomes of carbapenem-resistant klebsiella pneumoniae bacteremia in nontransplant patients. *J Infect Dis.* (2020) 221:S174–s83. doi: 10.1093/infdis/jiz559
46. Chang H, Wei J, Zhou W, Yan X, Cao X, Zuo L, et al. Risk factors and mortality for patients with Bloodstream infections of klebsiella pneumoniae during 2014-2018: clinical impact of carbapenem resistance in a large tertiary hospital of China. *J Infect Public Health.* (2020) 13:784–90. doi: 10.1016/j.jiph.2019.11.014
47. Li J, Ren J, Wang W, Wang G, Gu G, Wu X, et al. Risk factors and clinical outcomes of hypervirulent Klebsiella pneumoniae induced bloodstream infections. *Eur J Clin Microbiol Infect Dis.* (2018) 37:679–89. doi: 10.1007/s10096-017-3160-z
48. Falcone M, Bassetti M, Tiseo G, Giordano C, Nencini E, Russo A, et al. Time to appropriate antibiotic therapy is a predictor of outcome in patients with bloodstream infection caused by KPC-producing Klebsiella pneumoniae. *Crit Care.* (2020) 24:29. doi: 10.1186/s13054-020-2742-9
49. Freire MP, Abdala E, Moura ML, de Paula FJ, Spadão F, Caiaffa-Filho HH, et al. Risk factors and outcome of infections with Klebsiella pneumoniae carbapenemase-producing K. pneumoniae in kidney transplant recipients. *Infection.* (2015) 43:315–23. doi: 10.1007/s15010-015-0743-4
50. Wu D, Xiao J, Ding J, Jia Y, Guo Z, Liu H, et al. Predictors of mortality and drug resistance among carbapenem-resistant enterobacteriaceae-infected pancreatic necrosis patients. *Infect Dis Ther.* (2021) 10:1665–76. doi: 10.1007/s40121-021-00489-5
51. Freire MP, Pierrotti LC, Filho HH, Ibrahim KY, Magri AS, Bonazzi PR, et al. Infection with klebsiella pneumoniae carbapenemase (KPC)-producing klebsiella pneumoniae in cancer patients. *Eur J Clin Microbiol Infect Dis.* (2015) 34:277–86. doi: 10.1007/s10096-014-2233-5

Conflict of Interest: The authors declare that the research was conducted in the absence of any commercial or financial relationships that could be construed as a potential conflict of interest.

Publisher's Note: All claims expressed in this article are solely those of the authors and do not necessarily represent those of their affiliated organizations, or those of the publisher, the editors and the reviewers. Any product that may be evaluated in this article, or claim that may be made by its manufacturer, is not guaranteed or endorsed by the publisher.

frontiers | Frontiers in Medicine

CASE REPORT
published: 21 June 2022
doi: 10.3389/fmed.2022.866068

Case Report: Acute Myocarditis Due to PD-L1 Inhibitor Durvalumab Monotherapy in a Patient With Lung Squamous Cell Carcinoma

Bo Zhou[1]*, *Manxiang Li*[1], *Tianjun Chen*[1] and *Jianqing She*[2]*

[1] Respiratory and Critical Care Medicine, The First Affiliated Hospital of Xi'an Jiaotong University, Xi'an, China, [2] Cardiology Department, The First Affiliated Hospital of Xi'an Jiaotong University, Xi'an, China

Background: Durvalumab, as a PD-L1 inhibitor, is commonly used for the treatment of various cancers. Adverse events associated with the therapy include hepatitis, nephritis, dermatitis, and myocarditis. Especially, myocarditis as an adverse event after PD-L1 inhibitor therapy is characterized for its low incidence and high mortality.

Case Summary: Here we present a rare case of a 67-year-old male with lung squamous cell carcinoma complicated with empyema who experienced myocarditis after only PD-L1 inhibitor durvalumab monotherapy. He presented with markedly decrease left ventricular ejection fraction, elevated Natriuretic peptide BNP, Troponin T, Troponin I, ESR, CRP and interleukin-6. The electrocardiogram showed sinus tachycardia, low voltage of limb leads, T wave inversion in anterior waves and V1-V3 QS type. Myocardial injury occurred in a short period and quickly returned to normal after glucocorticoids therapy.

Conclusion: This case report is of clinical value for the treatment of PD-L1 related myocarditis.

Keywords: durvalumab, PD-L1 inhibitor, myocarditis, empyema, lung squamous cell carcinoma

OPEN ACCESS

Edited by:
Yi Liu,
Shandong Provincial Hospital, China

Reviewed by:
Akshay Avula,
UPMC Pinnacle, United States
Francesco Poti,
University of Parma, Italy

***Correspondence:**
Bo Zhou
zb_bob@stu.xjtu.edu.cn
Jianqing She
jianqingshe@xjtu.edu.cn

Specialty section:
This article was submitted to Pulmonary Medicine, a section of the journal Frontiers in Medicine

Received: *30 January 2022*
Accepted: *01 June 2022*
Published: *21 June 2022*

Citation:
Zhou B, Li M, Chen T and She J (2022) Case Report: Acute Myocarditis Due to PD-L1 Inhibitor Durvalumab Monotherapy in a Patient With Lung Squamous Cell Carcinoma. Front. Med. 9:866068. doi: 10.3389/fmed.2022.866068

INTRODUCTION

Immune checkpoint inhibitors (ICIs) has brought revolutionary breakthroughs to tumor therapy (1–3). However, with the increased utilization of ICIs, the associated adverse events are becoming more and more recognized. ICIs treatment was originally intended to enhance the body's immunity. But in some cases, the immune system was overcorrected, causing its own immune cells to attack the host tissues and organs, which led to the corresponding ICIs related adverse reactions (irAEs). Specifically, myocarditis as one of the irAEs is characterized by its low incidence and high mortality, which deserves immediate recognition (4, 5). Previously, cases of myocarditis and fatal heart failure have been reported among patients with lung cancer treated with ICIs, especially among those receiving programmed cell death 1 (PD-1) inhibitor with or with chemical therapy as combination treatment (6, 7). Nevertheless, clinical evidence regarding myocarditis after programmed cell death ligand-1 (PD-L1) inhibitor treatment are still lacking due to its low incidence. Here, we presented the case of acute immune-mediated myocarditis associated with a PD-L1 inhibitor durvalumab monotherapy in a patient with lung squamous cell carcinoma complicated with empyema.

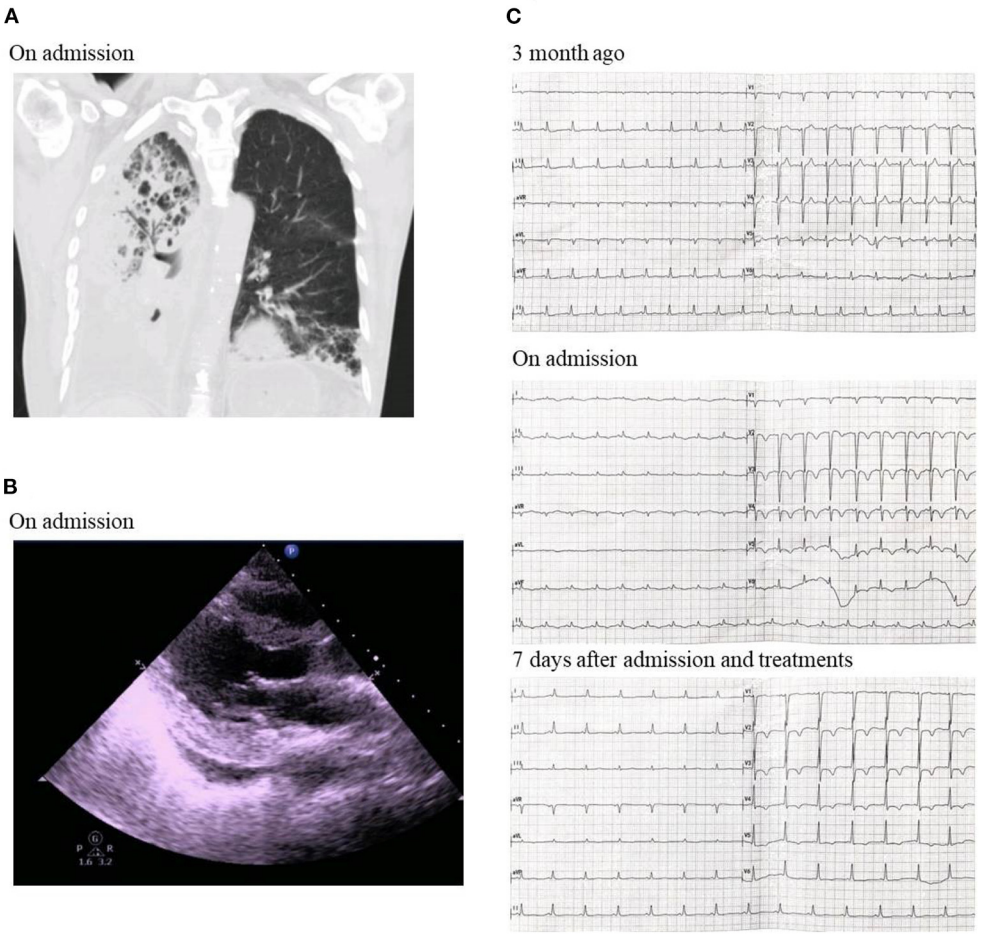

FIGURE 1 | (A) Chest CT on admission. **(B)** Echocardiography showing ventricle size within normal range, increased atrium size and markedly decrease cardiac ejection fraction on admission. **(C)** Electrocardiogram showing sinus tachycardia, low voltage of limb leads, T wave inversion in anterior waves and V1–V3 QS type on admission.

CASE REPORT

A 67-year-old male patient was admitted to the hospital with new onset fever, chest pain and dyspnea for 7 days and previous diagnose of right lung squamous cell carcinoma. His previous medical history was notable for right lung squamous cell carcinoma stage IV ($T_3N_3M_1$) complicated with mediastinal lymph nodes and liver metastasis 1 year before. Cardiac and pulmonary function was normal at that time. Four cycles of chemotherapy with paclitaxel-cisplatin regimen was initiated but afterwards stopped due to 2019 coronavirus outbreak. Ten months thereafter, he was admitted to the hospital because of right massive pleural effusion. Twice bacterial culture of pleural effusion displayed *Prevotella nigrescens,* indicating right lung squamous cell carcinoma complicated with empyema. With subsequent treatment of meropenem as the anti-bacterial agent, his symptoms were relieved and his temperature was normal. As a result, chemotherapy was discontinued and replaced with PD-L1 immune checkpoint inhibitor, durvalumab monotherapy for four cycles (500 mg intravenous drip). And he presented with the symptom of fever, chest pain and dyspnea 7 days after last cycle of durvalumab. Moreover, the previous medical, family, and psychosocial history as well as genetic information showed nothing special.

Physical and laboratory examination was done for the patients upon this admission. The highest temperature was 39.4°C. His blood pressure was 121/69 mmHg. Chest computed tomography (CT) examination indicated right bronchial obstruction, obstructive pneumonia and right pleural effusion (**Figure 1A**). Echocardiography revealed ventricle size within normal range (left ventricle end diastolic dimension 46 mm), increased atrium size (left atrium dimension LA 36 mm) and markedly decrease cardiac ejection fraction (left ventricular ejection fraction 41%), tracing 2 mm pericardial effusion (**Figure 1B**). The electrocardiogram showed sinus tachycardia, low voltage of limb leads, T wave inversion in anterior waves and V1–V3 QS type (**Figure 1C**). Markers of myocardial injury were elevated: Natriuretic peptide BNP 18 942 ng/L; Troponin T 0.066 ng/L;

Troponin I 200.83 ng/L; Creatine kinase (CK) and Creatine kinase isoenzyme (CKMB) normal. Moreover, inflammatory indicators were significantly elevated. Erythrocyte sedimentation rate (ESR) was markedly increased with the level of 101 mm/h, and C-reactive protein (CRP) 268.2 mg/L. Interleukin-6 was 44.93 pg/mL.

Judging by the decreased cardiac function and elevated myocardial injury markers at this admission, the patient was diagnosed of acute immune-associated myocarditis and right lung squamous cell carcinoma complicated with empyema. Treatments included methylprednisolone to suppress inflammation (40 mg, once per day, iv), meropenem to control infection (1.0 g, q8h, iv.drip) and symptomatic and supportive treatments. Seven days after admission, the patient's symptoms were relieved. Myocardial injury and inflammation markers were significantly decreased: Natriuretic peptide BNP was down to 2,298 ng/L; Troponin T, Troponin I, CK and CKMB normal; ESR 41 mm/h; CRP 29.8 mg/L; and Interleukin-6 normal. The electrocardiogram showed normal sinus rate and V2–V5 T wave inversion (**Figure 1C**). Echocardiography revealed ventricle size within normal range (left ventricle end diastolic dimension 48 mm), increased atrium size (left atrium dimension LA 30 mm) and markedly recovered cardiac ejection fraction (left ventricular ejection fraction 66%). The patient was discharged with prescription of continuing oral methylprednisolone (20 mg, once per day, po) and anti-bacterial therapy of faroenem to control infection (150 mg, q8h, po). No further heart failure exacerbations have occurred to date.

DISCUSSION

ICIs have substantially improved clinical outcomes in multiple cancer types (8, 9). Mechanistically, tumor cells realize immune escape by activating immune checkpoint molecular related signal pathway, and immune checkpoint inhibitors can awaken T lymphocytes to enhance the body's clearance of tumor cells. However, blocking immune checkpoints to restore antitumor immune response may also break immune tolerance to self-antigens and induce specific immune-related adverse events (10). With the widespread use of these drugs, immune related toxicity is increasingly recognized, including fatal myocarditis. Physicians should be aware of these infrequent, but potentially fatal toxicities associated with ICIs as their therapeutic use becomes widespread (11).

The ICI related myocarditis is generally considered highly arrhythmogenic and fatal; however, the exact pathogenesis is still poorly recognized and understood (12, 13). Myocarditis caused by ICIs represents <1% of immune-related adverse events. It is a potentially fatal condition associating with a mortality rate of 42% (14, 15). Judging by its high mortality rate, the incidence of ICI related myocarditis might be higher than expected. There are many manifestations of cardiotoxicity, such as myocarditis, heart failure, pericardial effusion, arrhythmia, acute coronary syndrome and valve disease. Treatment with ICIs can lead to severe and disabling inflammatory cardiovascular adverse-events soon after commencement of therapy (16). It is noteworthy that PD-L1 as monotherapy for lung cancer has been rarely reported to cause acute myocarditis. Previously it has also been reported of a patient diagnosed of non-small-cell lung cancer and developed durvalumab-associated myocarditis (17). As a result, it is worthy of further research and exploration whether there are differences in myocardial injury caused by different PD-L1 monotherapy and in patients with various baseline health state.

The keys to the diagnosis of ICIs related myocarditis in the present case are the previous history of PD-L1 utilization, elevated biomarkers suggesting cardiac damage, EKG presentation, negative coronary stenosis and decreased left ventricular ejection fraction.It is worthy of attention that in this case, PD-L1 monotherapy of durvalumab was chosen because of the right lung squamous cell carcinoma stage IV complicated with Prevotella nigrescens infection leading to empyema. In addition, due to the empyema, small dose of corticosteroids treatment was utilized in the present patient. Myocardial injury occurred in a short period and quickly returned to normal after treatment.

CONCLUSION

In this study, we report a rare case of a 67-year-old male with lung squamous cell carcinoma complicated with empyema who experienced myocarditis after only PD-L1 inhibitor durvalumab monotherapy. As clinical evidence for myocarditis related to PD-L1 treatment has been limited, the present case report is of clinical value for the treatment and prognosis of PD-L1 related myocarditis.

DATA AVAILABILITY STATEMENT

The original contributions presented in the study are included in the article/supplementary material, further inquiries can be directed to the corresponding author/s.

ETHICS STATEMENT

The studies involving human participants were reviewed and approved by The First Affiliated Hospital of Xi'an Jiaotong University. The patients/participants provided their written informed consent to participate in this study.

AUTHOR CONTRIBUTIONS

BZ and TC collected the clinical and laboratory data. JS and BZ summarized the data and drafted the manuscript. BZ, ML, and TC revised the final manuscript. All authors contributed to the article and approved the submitted version.

FUNDING

This study was funded by Key Research and Development Program of Shaanxi (Program No. 2020KW-049).

ACKNOWLEDGMENTS

We thank the patient involved in the study.

REFERENCES

1. Curti BD, Faries MB. Recent advances in the treatment of melanoma. *N Engl J Med*. (2021) 384:2229–40. doi: 10.1056/NEJMra2034861
2. Xie X, Wang X, Liang Y, Yang J, Wu Y, Li L, et al. Evaluating cancer-related biomarkers based on pathological images: a systematic review. *Front Oncol*. (2021) 11:763527. doi: 10.3389/fonc.2021.763527
3. Xiong A, Wang J, Zhou C. Immunotherapy in the first-line treatment of NSCLC: current status and future directions in China. *Front Oncol*. (2021) 11:757993. doi: 10.3389/fonc.2021.757993
4. Wong SK, Nebhan CA, Johnson DB. Impact of patient age on clinical efficacy and toxicity of checkpoint inhibitor therapy. *Front Immunol*. (2021) 12:786046. doi: 10.3389/fimmu.2021.786046
5. Di Wang KS, Wang T, Zhang D, Sun F, Cui Y, Zhao H, et al. Adverse effects and toxicity of immune checkpoint inhibitors for patients with urothelial carcinoma. *Front Pharmacol*. (2021) 12:710943. doi: 10.3389/fphar.2021.710943
6. Lechner O, Hu Y, Jafarian-Tehrani M, Dietrich H, Schwarz S, Herold M, et al. Disturbed immunoendocrine communication via the hypothalamo-pituitary-adrenal axis in murine lupus. *Brain Behav Immun*. (1996) 10:337–50. doi: 10.1006/brbi.1996.0030
7. Zamami Y, Niimura T, Okada N, Koyama T, Fukushima K, Izawa-Ishizawa Y, et al. Factors associated with immune checkpoint inhibitor-related myocarditis. *JAMA Oncol*. (2019) 5:1635–7. doi: 10.1001/jamaoncol.2019.3113
8. Wang DY, Salem JE, Cohen JV, Chandra S, Menzer C, Ye F, et al. Fatal toxic effects associated with immune checkpoint inhibitors: a systematic review and meta-analysis. *JAMA Oncol*. (2018) 4:1721–8. doi: 10.1001/jamaoncol.2018.3923
9. Palaskas N, Lopez-Mattei J, Durand JB, Iliescu C, Deswal A. Immune checkpoint inhibitor myocarditis: pathophysiological characteristics, diagnosis, and treatment. *J Am Heart Assoc*. (2020) 9:e013757. doi: 10.1161/JAHA.119.013757
10. Anquetil C, Salem JE, Lebrun-Vignes B, Johnson DB, Mammen AL, Stenzel W, et al. Immune checkpoint inhibitor-associated myositis: expanding the spectrum of cardiac complications of the immunotherapy revolution. *Circulation*. (2018) 138:743–5. doi: 10.1161/CIRCULATIONAHA.118.035898
11. Ball S, Ghosh RK, Wongsaengsak S, Bandyopadhyay D, Ghosh GC, Aronow WS, et al. Cardiovascular toxicities of immune checkpoint inhibitors: JACC review topic of the week. *J Am Coll Cardiol*. (2019) 74:1714–27. doi: 10.1016/j.jacc.2019.07.079
12. Li C, Bhatti SA, Ying J. Immune checkpoint inhibitors-associated cardiotoxicity. *Cancers*. (2022) 14:1145. doi: 10.3390/cancers14051145
13. Power JR, Alexandre J, Choudhary A, Ozbay B, Hayek S, Asnani A, et al. Electrocardiographic manifestations of immune checkpoint inhibitor myocarditis. *Circulation*. (2021) 144:1521–3. doi: 10.1161/CIRCULATIONAHA.121.055816
14. Hu JR, Florido R, Lipson EJ, Naidoo J, Ardehali R, Tocchetti CG, et al. Cardiovascular toxicities associated with immune checkpoint inhibitors. *Cardiovasc Res*. (2019) 115:854–68. doi: 10.1093/cvr/cvz026
15. Chan KK, Bass AR. Autoimmune complications of immunotherapy: pathophysiology and management. *BMJ*. (2020) 369:m736. doi: 10.1136/bmj.m736
16. Salem JE, Manouchehri A, Moey M, Lebrun-Vignes B, Bastarache L, Pariente A, et al. Cardiovascular toxicities associated with immune checkpoint inhibitors: an observational, retrospective, pharmacovigilance study. *Lancet Oncol*. (2018) 19:1579–89. doi: 10.1016/S1470-2045(18)30608-9
17. Maetani T, Hamaguchi T, Nishimura T, Marumo S, Fukui M. Durvalumab-associated late-onset myocarditis successfully treated with corticosteroid therapy. *Intern Med*. (2022) 61:527–31. doi: 10.2169/internalmedicine.7644-21

Conflict of Interest: The authors declare that the research was conducted in the absence of any commercial or financial relationships that could be construed as a potential conflict of interest.

frontiers | Frontiers in Medicine

TYPE Systematic Review
PUBLISHED 06 September 2022
DOI 10.3389/fmed.2022.915159

OPEN ACCESS

EDITED BY
Yi Liu,
Shandong Provincial Hospital, China

REVIEWED BY
Rodolfo P. Vieira,
Centro Universitário UniEvangélica, Brazil
Akihiro Shiroshita,
Vanderbilt University Medical Center, United States

*CORRESPONDENCE
Guochao Shi
shiguochao@hotmail.com

SPECIALTY SECTION
This article was submitted to Pulmonary Medicine, a section of the journal Frontiers in Medicine

RECEIVED 07 April 2022
ACCEPTED 18 August 2022
PUBLISHED 06 September 2022

CITATION
Liu Y, Huang C, Du J, Lan G, Du X, Sun Y and Shi G (2022) Anabolic-androgenic steroids for patients with chronic obstructive pulmonary disease: A systematic review and meta-analysis. *Front. Med.* 9:915159. doi: 10.3389/fmed.2022.915159

Anabolic-androgenic steroids for patients with chronic obstructive pulmonary disease: A systematic review and meta-analysis

Yahui Liu[1,2,3], Chunrong Huang[1,2,3], Juan Du[1,2,3], Gelei Lan[1,2,3], Xueqing Du[1,2,3], Yidan Sun[1,2,3] and Guochao Shi[1,2,3]*

[1]Department of Respiratory and Critical Care Medicine, Ruijin Hospital, Shanghai Jiao Tong University School of Medicine, Shanghai, China, [2]Institute of Respiratory Diseases, Ruijin Hospital, Shanghai Jiao Tong University School of Medicine, Shanghai, China, [3]Shanghai Key Laboratory of Emergency Prevention, Diagnosis and Treatment of Respiratory Infectious Diseases, Ruijin Hospital, Shanghai Jiao Tong University School of Medicine, Shanghai, China

Background: Testosterone deficiency is common in chronic obstructive pulmonary disease (COPD) patients. There has been a growing interest in the potential use of anabolic-androgenic steroids (AASs) in patients with COPD recently. However, whether AASs could improve their clinical outcomes remains unknown.

Methods: In order to explore the efficacy of AASs in patients with COPD, systematic search of MEDLINE, Embase, the Cochrane Library and ClinicalTrials.gov for randomized controlled trials (RCTs) of AASs for COPD published before March 17, 2022 was performed.

Results: Data were extracted from 8 articles involving 520 participants. The median number of participants per study was 39.5 and the mean follow up was 14.2 weeks. As compared to the control group, AASs therapy could significantly improve body weight (weighted mean difference (WMD), 1.38 kg; 95% CI, 0.79 to 1.97 kg), fat-free mass (WMD, 1.56 kg; 95% CI, 0.94 to 2.18 kg) and peak workload (WMD, 6.89W; 95% CI, 3.97 to 9.81W) of COPD patients, but no improvements in spirometry indicators and six-minute walking distances (WMD, 16.88 m; 95%, −3.27 to 37.04 m). Based on the available research data, it is uncertain whether AASs treatment could improve the quality of life of COPD patients.

Conclusions: Limited published evidence indicates that AASs therapy provides clinical benefits in patients with COPD. However, longer and larger studies are needed to better clarify the efficacy of AASs and draw final conclusions.

KEYWORDS

chronic obstructive pulmonary disease, anabolic-androgenic steroids, meta-analysis, systematic review, randomized controlled trials

Introduction

Chronic obstructive pulmonary disease (COPD) is a globally prevalent illness, which affects millions of people and becomes the fourth leading cause of death in the world (1). The Global Burden of Disease study estimated that 174.5 million adults worldwide had prevalent COPD and 3.2 million deaths were estimated to be due to COPD in 2015 (2, 3). The burden of COPD is expected to increase in coming decades by reason of aging of the population and continued exposure to COPD risk factors (4). Additionally, COPD often coexists with other diseases (comorbidities) that may influence the disease course. Many people suffer from this disease for years and die prematurely from it or its comorbidities. Involuntary weight loss, decreased muscle function and impaired exercise capacity are common comorbidities of COPD, which are associated with poor health status and prognosis (1). Comorbidities like these remain largely under-recognized and underdiagnosed, especially in low-income and middle-income countries (5). In the meantime, medical treatment is predominantly focused on the primary organ dysfunction. However, treatment of these comorbidities is of great importance, as they are potentially remediable.

Androgens belong to a class of steroid hormones. Testosterone (TT) and dehydroepiandrosterone (DHEA) are the principal circulating androgens. Anabolic-androgenic steroids (AASs) are synthetic derivatives of TT that were originally developed as adjunct therapy for a variety of medical conditions. In the past few decades, various studies have demonstrated that androgens could exert anti-inflammatory and protective effects through direct or indirect effects in pulmonary diseases (6–8). Several randomized controlled trials (RCTs) investigated the influence of exogenous androgen therapy on body composition, muscle strength, exercise capacity and health-related quality of life (HRQoL) in patients with COPD (9–19).

Atlantis et al. included six RCTs about TT supplementation in COPD for meta-analysis (8). However, they only focused on exercise capacity and HRQoL, and did not pay attention to spirometry and body composition (8). Pan et al. reperformed meta-analysis on this issue including eight RCTs. TT or androgen derivative treatment was the trial arm of six RCTs, and the other two involved recombinant human growth hormone and ghrelin, which greatly affected our confidence in the certainty of evidence (20). More importantly, two recently published large-scale clinical studies have demonstrated that higher levels of TT are associated with better lung function in men, and low dehydroisoandrosterone sulfate (DHEA-S) levels in women were associated with impaired lung function and a greater risk of developing airflow limitation later in adult life (21, 22). Additionally, Baillargeon et al. conducted two retrospective cohort studies, and found that TT replacement therapy may slow disease progression and decrease hospitalization rate in patients with COPD (23). Thus, we believe that studies on the efficacy of AASs therapy for COPD are far from over. In the light of the above considerations, we conduct a meta-analysis of RCTs to evaluate the potential benefits of exogenous AASs therapy on COPD patients, mainly concentrating on body composition, lung function, exercise capacity and HRQoL, hoping to call on more researchers to pay attention to this kind of therapy.

Methods

Search strategy and study selection

Two reviewers performed a comprehensive literature search for RCTs evaluating the effects of AASs in patients with COPD. We employed a highly sensitive search strategy to retrieve articles and supplementary materials contain the search strategies developed for MEDLINE database interfaces, which we adapted to search other databases. Databases to search in retrieving relevant papers included the following: MEDLINE, Embase, the Cochrane Library and ClinicalTrials.gov. The databases were searched for studies published before March 17, 2022. Furthermore, we reviewed citations in the retrieved articles to search for additional relevant studies.

Criteria for considering studies for this review

For evidence on the effectiveness of AASs for the treatment of COPD, we considered only RCTs written in English. Reviews and animal studies were excluded. Studies that were not published as full reports were not included, either. The most comprehensive publication was used when there were several involving the same study population. Two reviewers independently checked the relevant studies obtained from databases. Any difference in opinion about eligibility was resolved by consensus.

Inclusion criteria were: (1) population: adults ($\geq$18 years), diagnosed with COPD, (2) intervention: using AASs defined as receiving oral or intramuscular injection of TT, DHEA, nandrolone, oxymetholone, dihydrotestosterone (DHT), oxandrolone or anabolic steroids, (3) outcomes: refer to "type of outcome measures." Based on the searched results, we selected the primary outcomes to be: improvements in lung function, body composition, and exercise capacity from baseline to follow up in subjects treated with AASs. The secondary outcomes were the changes of HRQoL.

Data extraction

Data from included RCTs were independently extracted by two investigators and checked by other authors in agreement with Data Extraction for Complex Meta-Analysis

recommendations (24, 25). The concordance rate was 91% between the two authors. Discrepancies in data extraction were resolved by discussion or arbitration by a third reviewer if agreement could not be reached. The following information was abstracted: authors, publication year, participant inclusion and exclusion criteria, sample size, duration of treatment, geographic locale in which the study took place, mean or median participant age, route of medication, dosage of administration, outcomes and adverse events.

Assessment of study quality

The Cochrane risk-of-bias tool was used to assess the quality of the RCTs concerning on selection bias, performance bias, detection bias, attrition bias, reporting bias and other bias. Two reviewers independently assessed the quality of individual studies, and any difference in opinion about the quality score was resolved by consensus. The degree of bias found in the individual studies were categorized into high, moderate, or low risk of bias according to the Cochrane risk of bias tool.

Date synthesis and analysis

The meta-analysis was conducted using Review Manager 5.4 (Cochrane Collaboration, London, England). The weighted mean differences (WMD) and 95% confidence interval (CI) measured prior to initiating and then after treatment with either exogenous androgens or placebo were calculated for each individual study. The standardized mean differences (SMD) and 95% CI were applied between the two groups when the studies all assessed the same outcome but measured it in a variety of ways (for example, some studies measured HRQoL, but they use different scales). If the associated information was present merely in figures in eligible studies, three investigators would use Engauge Digitizer 12.1 to collect data from the statistical graphs independently. Then, the mean values would be adopted. Q statistic and I^2 index were used to examine statistical heterogeneity. Moderate to high levels of heterogeneity were considered for $P_{heterogeneity} < 0.10$ or $I^2 > 50\%$. Random effects meta-analysis was used for high between-study heterogeneity. Publication bias was evaluated by funnel plots. Sensitivity and subgroup analysis were conducted to determine the robustness of the pooled results and to explore the possible source of heterogeneity. Statistical tests were two-sided and used a significance threshold of $P < 0.05$.

Results

Study characteristics and risk of bias

The selection process for the studies included in the meta-analysis was outlined in Figure 1. Eight RCTs involving 520 patients with COPD were included in this meta-analysis (Table 1). The median number of participants was 39.5 (range, 16–203), and the mean duration of follow-up was 14.2 weeks. Two studies took place in the Netherland, one in Brazil, one in Norway, one in the United Stated of America, one in Canada, one in France and one in India. Five studies recruited only male patients as subjects. The detailed inclusion and exclusion criteria presented in Supplementary Table S1. Most of the studies investigated body composition, exercise capacity and HRQoL as outcomes. All studies reported the treatment-related adverse events. If any, the numbers and reasons of withdrawals were also mentioned. Venous blood concentration changes of sex hormone were measured in five trials. Two studies did not specify how serum testosterone levels were measured.

The majority of studies were found to be at low risk of bias (Figure 2). However, insufficient details were reported about allocation concealment and outcome assessors in the study by Sharma et al. which was discontinued following the interim analysis (15). In addition, according to the experimental design by Pison et al., blinding during the trial can be difficult or even impossible, and the rate of lost to follow-up was more than 10% (16).

Meta-analysis results

Effects of AASs on body composition

There were seven studies with a total number of 335 participants investigating the effects of AASs on changes in body composition of COPD patients. The meta-analysis indicated that exogenous AASs therapy significantly improved body weight (WMD, 1.38 kg; 95% CI, 0.79 to 1.97 kg; I^2, 25%; $P < 0.001$; Figure 3A) and fat-free mass (FFM) (WMD, 1.56 kg; 95% CI, 0.94 to 2.18 kg; I^2, 0%; $P < 0.001$; Figure 3B). In addition, funnel plots were produced which showed only slight evidence of publication bias for body weight and FFM (Figure 3). There was no statistically significant difference in pooled changes in midarm circumference (WMD, 0.36 cm; 95% CI, −0.33 to 1.04cm; I^2, 20%; $P = 0.31$) and percentage of body fat mass (WMD, −1.14%; 95% CI, −2.56 to 0.28%; I^2, 0%; $P = 0.12$) from baseline to follow up in COPD patients treated with AASs compared with those receiving placebo.

Effects of AASs on spirometry and exercise capacity

To measure effects of AASs on spirometry of individuals with COPD, several studies were involved in this meta-analysis. No significant differences were found on the improvements of maximal inspiratory muscle strength, peak oxygen uptake, predicted forced expiratory volume in the first second (FEV1 % pred), PaO2, and PaCO2 (Table 2).

Exercise capacity of COPD patients in these studies included were assessed using maximal inspiratory muscle

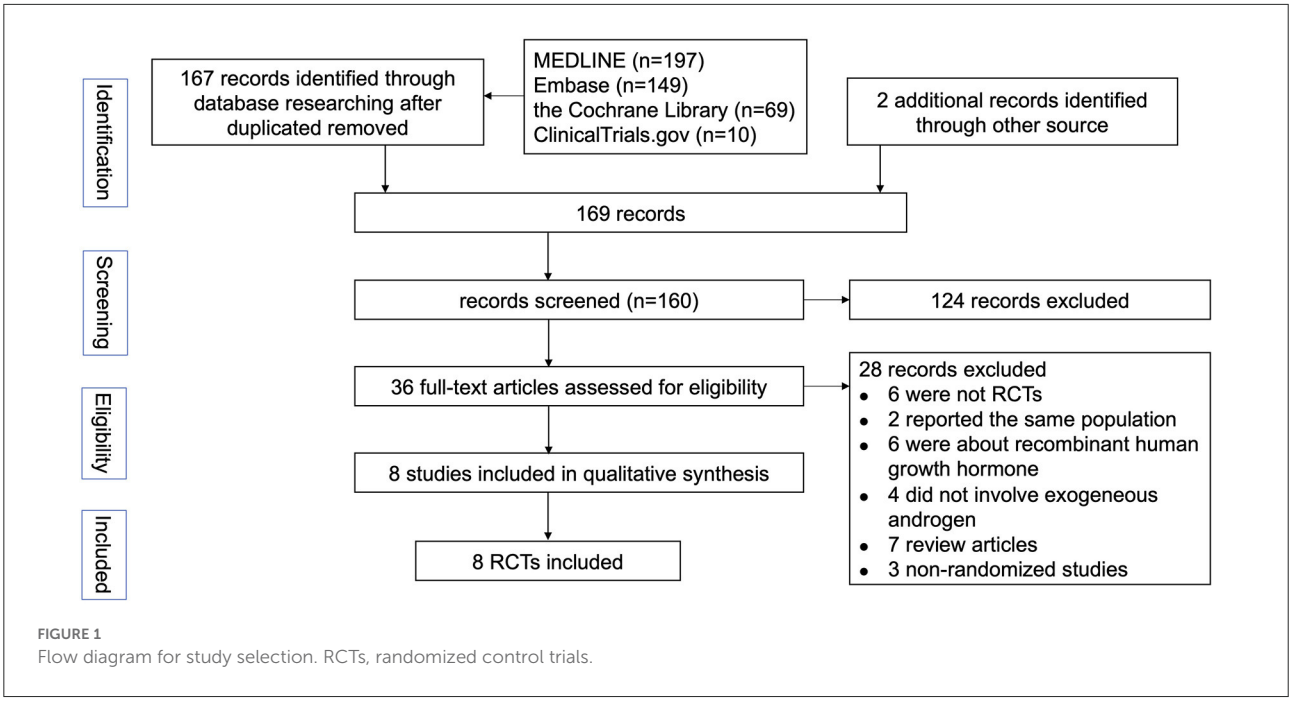

FIGURE 1
Flow diagram for study selection. RCTs, randomized control trials.

strength, peak oxygen consumption, peak workload and 6-min walking distances (6MWD). The treatment of AASs to COPD patients could not improve their maximal inspiratory muscle strength and peak oxygen consumption, but increase the peak workload (WMD, 6.89W; 95% CI, 3.97 to 9.81W; I^2, 0%; $P = 0.49$) (Table 2). There were five studies with a number of 213 participants investigating the effects of AASs on 6MWD. Our results showed no statistically significant difference in 6MWD between the two groups (WMD, 16.88 m; 95%, −3.27 to 37.04 m; I^2, 31%; $P = 0.21$; Figure 4).

Effects of AASs on HRQoL

Four RCTs investigated the effects of AASs therapy on COPD patients' HRQoL. There were two types of criteria used for judging HRQoL: one was that the higher the score, the higher the quality of life, including chronic respiratory disease questionnaire (CRQ) and HRQoL index (assessed by Seattle Obstructive Lung Disease Questionnaire); the other was just the opposite, including St George's respiratory questionnaire (SGRQ) and Maugeri Foundation Respiratory Failure questionnaire (MRF-28). Meta-analysis of the former type of scales showed that the treatment of AASs did not improve HRQoL of COPD participants (Figure 5A). However, the results of the latter types did not result in the same conclusion (Figure 5B). This means that we need more high-quality clinical trials to clarify this issue.

Effects of AASs on biochemical indicators

While improving some clinical outcomes, AASs for COPD patients will also cause changes in a series of biochemical indicators. Treatment of AASs could significantly decrease serum levels of luteinizing hormone (LH) (WMD, −3.79IU/L; 95% CI, −5.92 to −1.65 IU/L; I^2, 0%; $P < 0.001$), and increased serum free testosterone concentration (SMD, 1.13; 95% CI, 0.64 to 1.62; I^2, 0%; $P < 0.001$) and hemoglobin levels (WMD 8.86 g/L; 95% CI, 5.58 to 12.14 g/L; I^2, 19%; $P < 0.001$) in COPD patients (Figure 6).

Sensitivity analysis

The influence of individual studies on the overall summary estimates was examined by serially excluding each study in a sensitivity analysis. The pooled WMDs or SMDs for most of the outcomes were robust, except for peak workload and 6MWD. As shown in Table 3, the pooled WMD for peak workload changed after exclusion of one study which recruited malnourished patients with chronic respiratory failure, including not only COPD but also bronchiectasis, restrictive disorders and mixed respiratory disorders (16). As for 6MWD, three studies enrolled only male participants, but different route of medication and dosage of administration were used (10, 13, 18). Experimental group of one study received multimodal nutritional rehabilitation combining health education, oral nutritional supplements, exercise and oral testosterone treatment (16). Therefore, it is difficult to perform subgroup analysis for 6MWD.

TABLE 1 Selected characteristics of the eight RCTs included in this systematic review.

Authors	Year of publication	Area	Number of randomized populations	Per-protocol population	Sex (M/W)	Mean age (years) Experimental/ Control	Types of androgens and dosage	Grouping	Duration of treatment	Safety measures
Schols et al.	1995	The Netherlands	217	203	M/W	NR	ND on day 1, 15, 29 and 43	P: placebo N: placebo + nutrition N+A: ND + nutrition	8 weeks	no
Ferreira et al.	1998	Brazil	23	17	M	70.3/66.1	testosterone	placebo group and testosterone group	27 weeks	no
Creutzberg et al.	2003	The Netherlands	63	56	M	66/67	50 mg ND on day 1, 15, 29 and 43	placebo group and ND group	8 weeks	ESR declined. LDH elevated.
Svartberg et al.	2004	Norway	29	27	M	64.5/67.5	250 mg testosterone every fourth week	placebo group and testosterone group	26 weeks	no
Casaburi et al.	2004	USA	53	47	M	No training: 66.6/67.6 Training: 66.4/68.9	100 mg/week of testosterone	placebo; testosterone; placebo + training; testosterone + training.	10 weeks	Hemoglobin elevated
Sharma et al.	2008	Canada	16	16	M/W	71.0/64.2	50 mg testosterone biweekly for men and 25 mg for women	Placebo group and ND group	16 weeks	no
Pison et al.	2011	France	126	122	M/W	66.6/65.1	oral testosterone undecanoate, M 80 mg/W 40 mg twice daily with PR	Control group and multimodal+ nutritional+ rehabilitation group	90 days	no
Daga et al.	2014	India	32	32	M	60.05/56.75	25 mg ND on days 1, 8, 15, 22, 29, and 35	placebo group and ND group	6 weeks	no

RCTs, randomized controlled trials; W, women; M, man; NR, not reported; ND, nandrolone decanoate; P, placebo; N, nutrition supplementation; PR, pulmonary rehabilitation; ESR, erythrocyte sedimentation rate; LDH, lactate dehydrogenase.

10.3389/fmed.2022.915159

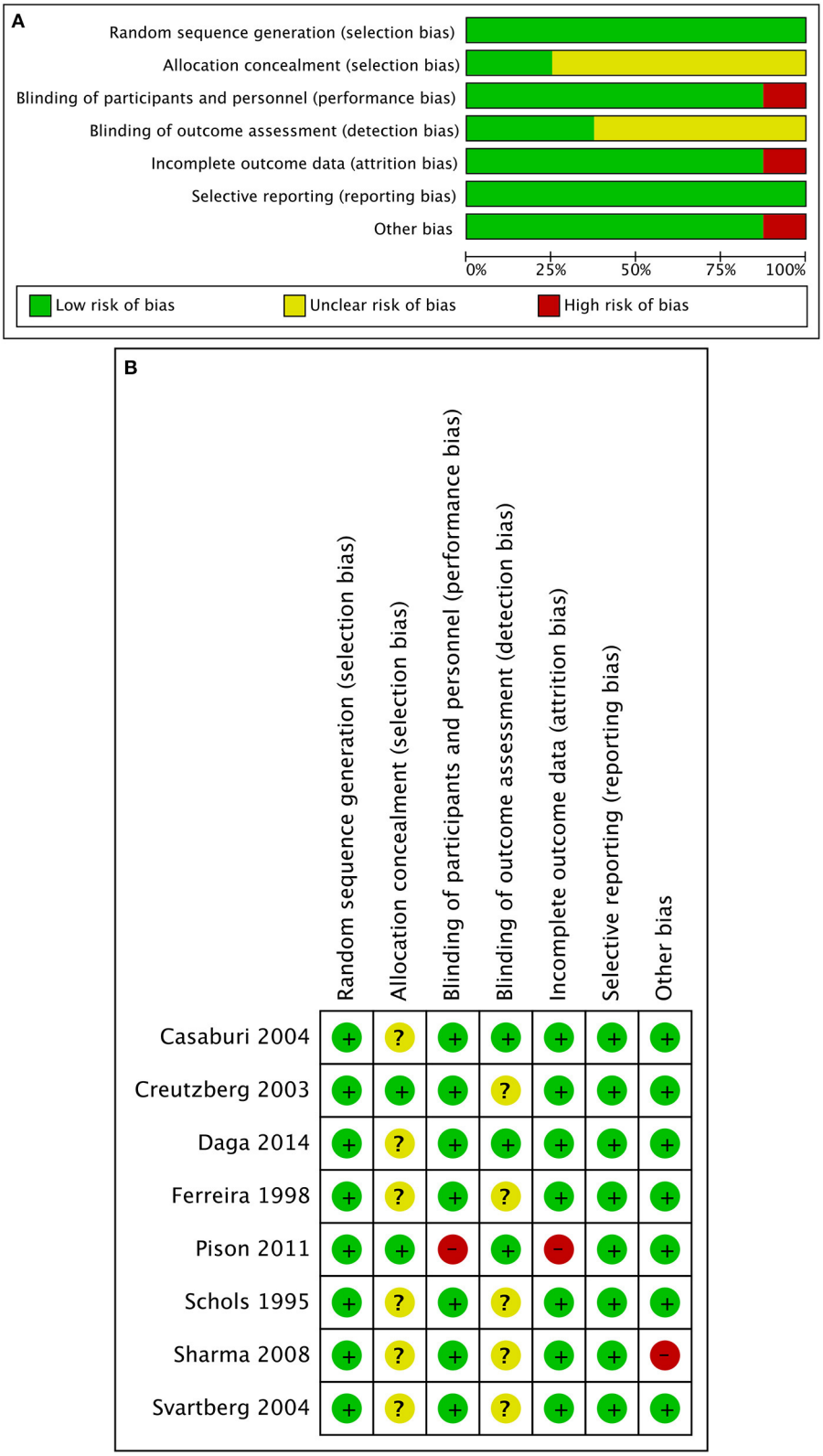

FIGURE 2
Quality assessment of included randomized control trials. **(A)** Risk of bias graph judging by Cochrane risk-of-bias tool. **(B)** Risk of bias summary. Insufficient details were reported about allocation concealment of the studies by Casaburi 2004 and Daga 2014. Insufficient details were reported about allocation concealment and outcome assessors of the studies by Ferreira 1998, Schols 1995, and Svartberg 2004. Insufficient details were reported about outcome assessors of the study by Creutzberg 2003. Blinding can be difficult, and the rate of lost to follow-up was more than 10% in the study by Pison 2011. Insufficient details were reported about allocation concealment and outcome assessors of the study by Sharma 2008, and the study was discontinued following the interim analysis.

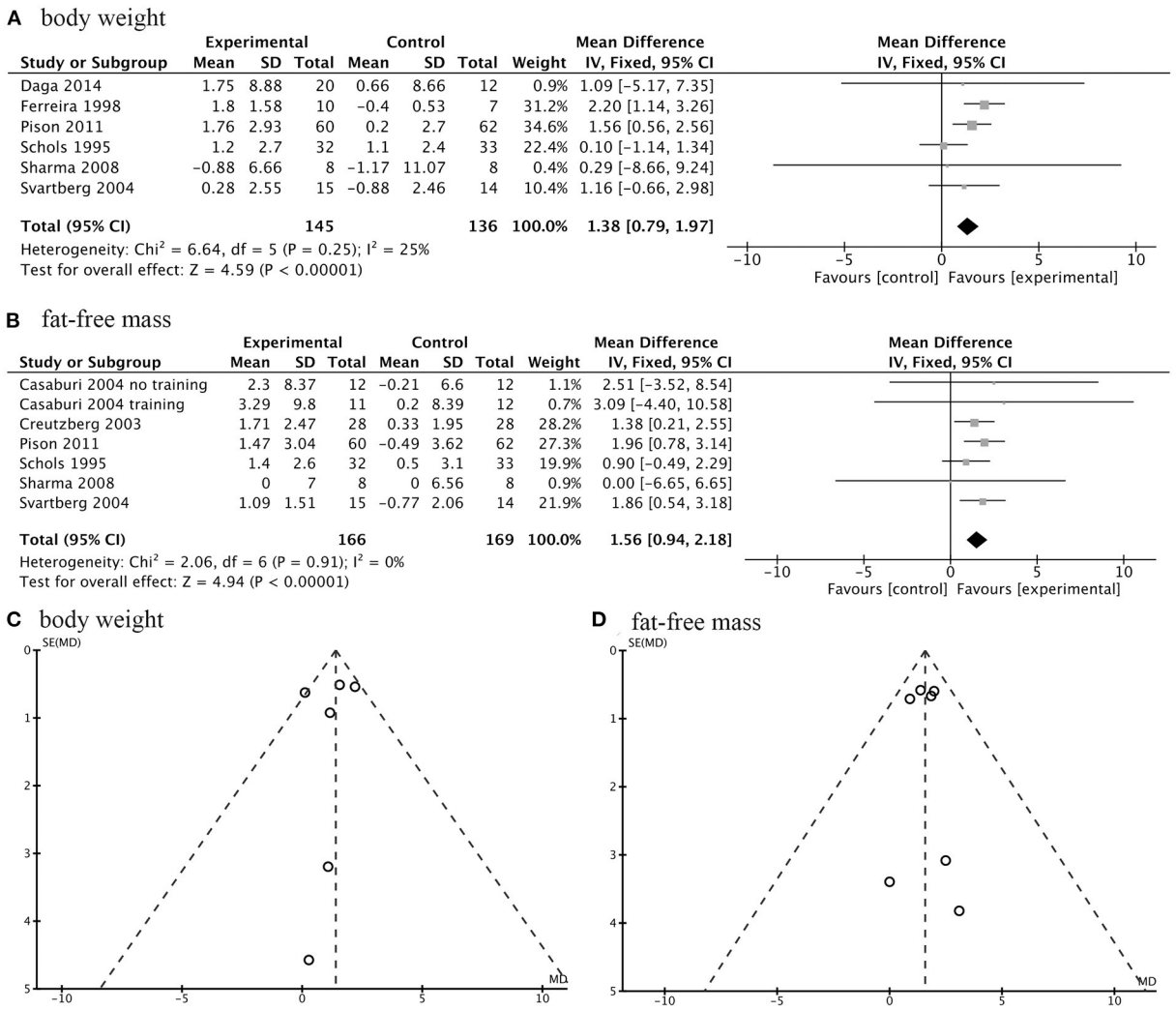

FIGURE 3
Forest plots of meta-analysis of body composition and publication bias assessed by funnel plot. Fixed-effects meta-analysis of effectiveness of AASs on body weight **(A)** and fat-free mass (FFM) **(B)** of COPD. Funnel plot of meta-analysis on body weight **(C)** and FFM **(D)**.

Discussion

Summary of the main results

Eight RCTs were included in this meta-analysis. Our results indicated that exogenous AASs therapy could improve body mass, FFM, peak workload of COPD patients, with no significant changes in spirometry. Simultaneously, the treatment of AASs on 6MWD and HRQoL of COPD patients still needs further research (Supplementary Table S2).

Interpretation of the results

Weight loss and decreased muscle function are common systemic manifestations in COPD, portending negative outcomes independent of the degree of airflow limitation, which occurred in more than 20% of COPD patients (2, 26). Besides, studies have shown that parameters of body composition are associated with exercise capacity, disease severity, mortality, disease prognosis, and quality of life (2–4, 26, 27). Decreased muscle function is in part the result of involuntary weight loss and muscle wasting in patients with COPD. The prevalence of muscle dysfunction increased from 20% in clinically stable outpatients up to 35% in patients eligible for pulmonary rehabilitation (PR) (28, 29). As the disease progresses, weight loss and muscle dysfunction may cause damage to skeletal muscle, affecting not only respiratory musculature, but also making an impact on peripheral skeletal muscle function, leading to fatigue, progressively deteriorating dyspnea and impaired exercise capacity. Dyspnea, muscle dysfunction, and airflow limitation deserve the blame for impaired exercise

TABLE 2 The results of pooled meta-analysis on spirometry and exercise capacity.

	No. studies	Heterogeneity		Effect measure	WMD (95% CI)/ SMD (95% CI)
		$P_{heterogeneity}$	I^2, %	Random effects/Fixed effects	
Spirometry					
FEV_1, % pred	3	0.87	0	fixed	−1.61 (−7.07, 3.84)*
PaO_2, mmHg	4	0.72	0	fixed	0.52 (−3.07, 4.10)*
$PaCO_2$, mmHg	3	0.74	0	fixed	−1.4 (−4.15, 1.35)*
Exercise capacity					
maximal inspiratory muscle strength	4	0.61	0	fixed	0.23 (−0.11, 0.57)†
peak oxygen consumption	4	0.43	0	fixed	0.07 (−0.27, 0.41)†
peak workload	5	0.49	0	fixed	6.89 (3.97, 9.81)*
6MWD	5	0.21	31	fixed	16.88 (−3.27, 37.04)*

FEV_1, % pred, predicted forced expiratory volume in the first second; 6MWD, 6–min walking distances; CI, confidence interval; WMD, weighted mean difference; SMD, standardized mean difference.
†SMD (95% CI).
*WMD (95% CI).

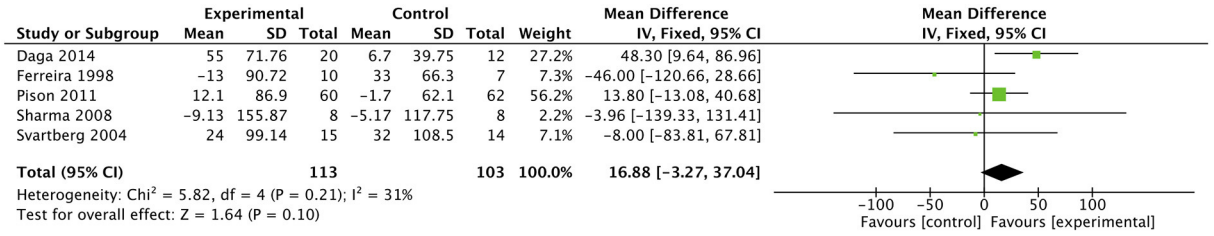

FIGURE 4
Forest plots of meta-analysis of 6-min walking distances.

capacity, which stops patients from attending PR to alleviates symptoms, improves (HRQoL), and reduces hospital admissions and mortality (30). Thus, patients with COPD are trapped in a vicious circle of unfavorable prognosis. In addition to this, increases in body weight and physical activity were shown to relief symptoms, improve HRQoL, and reduce mortality (27).

Previous studies demonstrated that testosterone therapy could increase bone mineral density, FFM and muscle strength, reduce whole body fat, and improve maximal voluntary strength and muscle in healthy young hypogonadal men (31). Androgens can act on a variety of cells to exert protective effects, which may help partially explain androgen therapy for COPD. Androgens can easily diffuse across cell membranes without the need for receptor, or bind to classical and non-classical androgen receptors (ARs) to mediate genomic and non-genomic androgen effects, respectively (32–34). The DNA binding-dependent actions of the AR promote cardiac growth, kidney hypertrophy, cortical bone growth and regulate trabecular bone architecture (35). In addition, androgens generate anabolic effects on carbohydrate metabolism and protein, maintain insulin sensitivity, and impact brain function and mood (34). Exogenous supplementation of androgens could alleviate pulmonary artery hypertension, increase serum insulin-like growth factor (IFG) 1 and IGF-binding protein-1, reverse the loss in diaphragm force-generating capacity, improve mitochondrial and muscle function, increase myosin expression and attenuate pulmonary epithelial inflammation in COPD mouse model or patients (36–42). RCTs in older men with hypogonadism showed that exogenous testosterone therapy consistently increased bone mineral density and decreased fat mass, but the effects on muscle strength, physical function, energy, and mood were variable (31).

We found that AASs treatment could improve body composition, including body weight and FFM. Our conclusions obtained were not exactly the same as the previous studies, because the researches included and statistical methods adopted were different from the previous analysis (20). Additionally, sensitivity analysis showed that these results were robust, and no obvious heterogeneity and publication bias were found. Schols et al. showed that nutritional intervention alone helped COPD

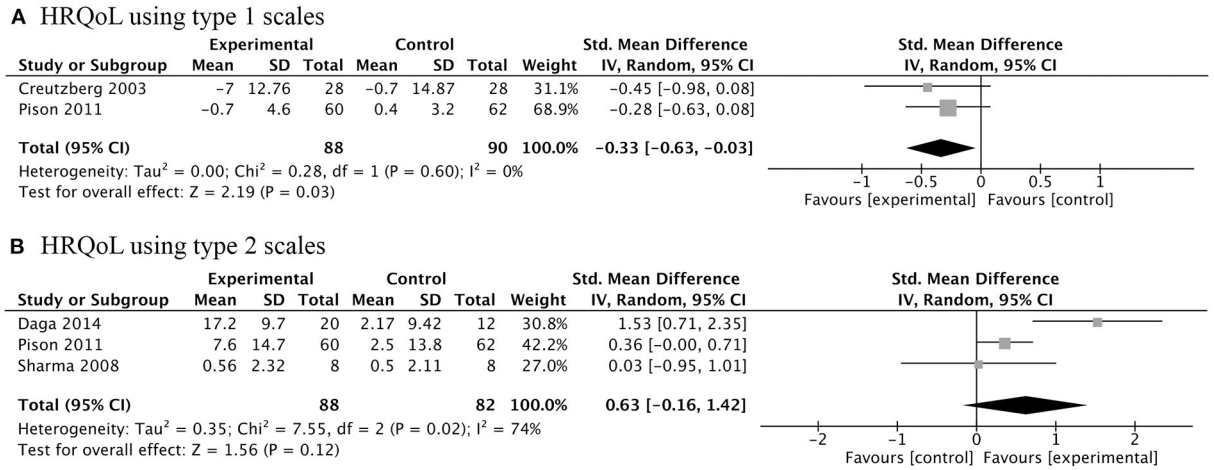

FIGURE 5
Forest plots of meta-analysis of health-related quality of life (HRQoL). Random-effects meta-analysis using type 1 scales **(A)** and type 2 scales **(B)** of effectiveness of AASs on HRQoL of COPD. Type 1 scales: Creutzberg 2003, St George's respiratory questionnaire; Pison 2011, Maugeri Foundation Respiratory Failure questionnaire. Type 2 scales: Daga 2014, Seattle Obstructive Lung Disease Questionnaire; Pison 2011, chronic respiratory disease questionnaire; Sharma 2008, chronic respiratory disease questionnaire.

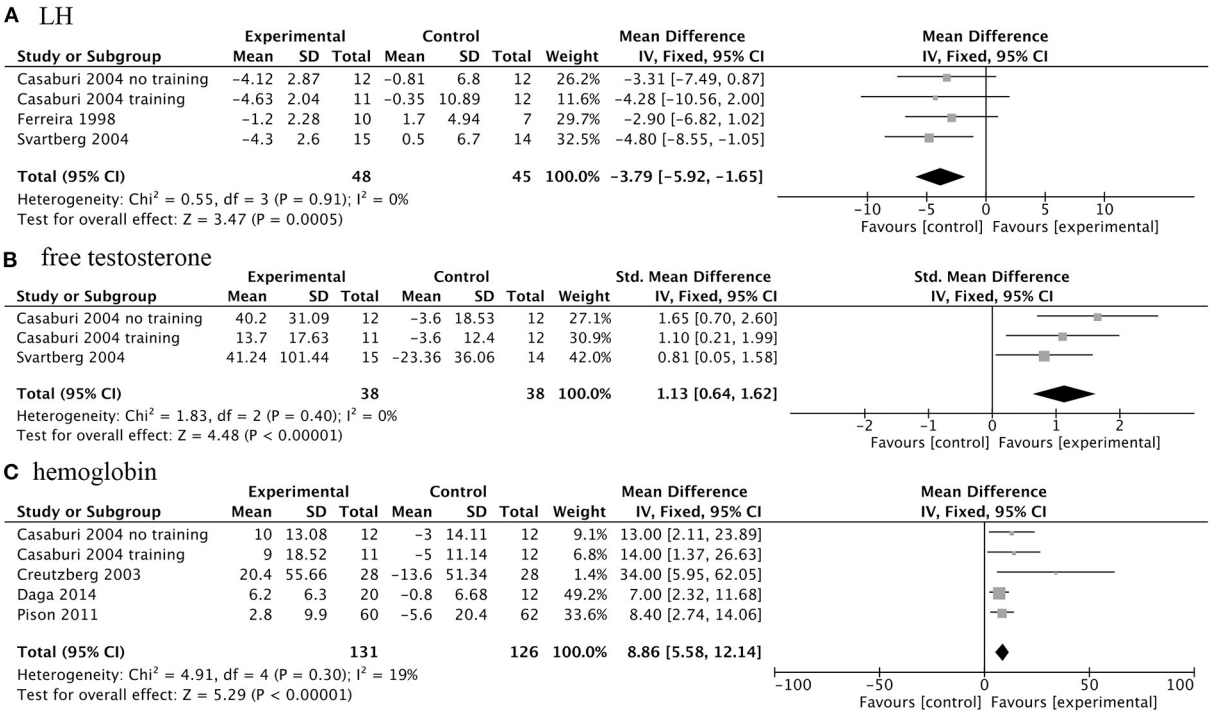

FIGURE 6
Forest plots of meta-analysis of biochemical indicators. Fixed-effects meta-analysis of effectiveness of AASs on luteinizing hormone (LH) **(A)**, free testosterone concentration **(B)** and hemoglobin **(C)** of COPD.

patients gain total weight (9). Under a combination treatment of exogenous androgens and nutrition supplementation, the weight gain of COPD patients is mainly FFM, which will benefit patients even more.

FFM is significantly associated with muscle strength, spirometry, physical function, quality of life, and survival in patients with COPD (20). However, no improvements in maximal inspiratory muscle strength, peak oxygen uptake,

TABLE 3 Sensitivity analysis of included randomized controlled trials for the outcome of peak workload and 6MWD.

Outcomes		Number of studies	WMD (95% CI)	Heterogeneity	
				$P_{heterogeneity}$	I^2, %
Peak workload	Fixed effects model	5	6.89 (3.97, 9.81)	0.49	0
	Exclusion of Casaburi 2004 no training	4	7.12 (4.18, 10.06)	0.64	0
	Exclusion of Casaburi 2004 training	4	6.91 (3.98, 9.85)	0.34	11
	Exclusion of Creutaberg 2003	4	7.01 (4.03, 9.98)	0.36	8
	Exclusion of Piosn 2011	4	0.22 (−8.65, 9.09)	0.81	0
	Exclusion of Sharma 2008	4	7.26 (4.28, 10.25)	0.56	0
6MWD	Fixed effects model	5	16.88 (−3.27, 37.04)	0.21	31
	Exclusion of Dage 2014	4	5.16 (−18.47, 28.78)	0.51	0
	Exclusion of Ferreira 1998	4	21.83 (0.89, 42.76)	0.41	0
	Exclusion of Pison 2011	4	20.85 (−9.63, 51.32)	0.13	47
	Exclusion of Sharma 2008	4	17.36 (−3.03, 37.74)	0.13	48
	Exclusion of Svartberg 2004	4	18.78 (−2.13, 39.69)	0.15	44

WMD, weighted mean difference; CI, confidence interval; 6MWD, 6–min walking distance.

FEV1 %predicted, PaO2 and PaCO2 were observed in our meta-analysis. It was reported that men with severe COPD had lower free testosterone levels, and free testosterone was positively and independently associated with forced vitality capacity and FEV1 (43). Our analysis indicated that AASs improved free testosterone levels, but there was no improvement in spirometry. Diversities in quality of trials and inclusion criteria and small sample size may partially explain this difference.

As for exercise capacity, others found that testosterone supplementation therapy significantly improved several exercise capacity outcomes, such as peak muscle strength and peak oxygen outcomes (8). Another analysis indicated that anabolic steroids administration increased maximal inspiratory pressure and maximal expiratory pressure (20). We found that exogenous AASs therapy could increase patients' peak workload, with uncertain roles in 6MWD. The results of all analyses are not that robust, and additional large-scale studies are needed to determine whether exercise capacity could be improved with exogenous AASs treatment in COPD patients.

Alantis et al. pooled four clinical trials and drew a conclusion that TT treatment failed to improve HRQoL, but they did not classify different scales of HRQoL (8). On the contrary, others found that anabolic steroid administration improved HRQoL as measured by SGRQ total score and symptoms score (20). It is worth noting that there were only two trials included in latter analysis, so the conclusion was not that convincing, not to mention that the two studies in this meta-analysis were not limited to the use of AASs. Given that different scales were used to assess patients' HRQoL in different RCTs, we classified them into two categories. Combined with our meta-analysis results and sensitivity analysis, we think additional trials must be conducted to assess the significance of this intervention.

Our meta-analysis shows that AASs therapy could significantly decrease serum LH, increase free testosterone and hemoglobin levels. We particularly emphasize that when applying exogenous AASs to treat patients with COPD, the changes of these treatment-related parameters need to be closely monitored.

The implication for future studies

The therapeutic use of AASs in patients with chronic disease is appealing and the theoretic basis for it appears sound. However, the results from studies exploring the effects in patients with COPD are mixed, showing limited positive effects on muscle function or exercise capacity. There are lots of reasons why we believe it is premature to deny its potential efficacy. The definition of testosterone deficiency, dosages used for replacement (sub-physiological vs. supra-physiological), small trials with variable inclusion criteria and study populations varied widely across the studies.

In other clinical trials, doses up to 600 mg of testosterone per week for a healthy man were administered, which caused relatively few adverse events and improved muscle mass and strength in healthy men (44). It can be expected that the administered dose of exogenous AASs in the above-mentioned studies is probably too low to exert a clinically meaningful effect, since the highest dose of androgens applied in the eight trials was 250 mg (Table 1). For a clinically meaningful effect, higher doses of androgens maybe used, preferably in combination with PR and nutritional supplementation. Additionally, nandrolone is an anabolic steroid that cannot be converted to DHT, and is considered to be less androgenic than testosterone. Compared with testosterone, nandrolone may be expected to be better

tolerated, especially in women. Therefore, we believe that it is suggesting that exogenous AASs therapy was likely to be an acceptable type of administration used in COPD patients, especially those with advanced COPD, involuntary weight loss, muscle wasting and on chronic corticosteroid therapy.

Limitations

Some limitations of this review are summarized as follows. Only a small number of studies were included and the small sample size was also a major limitation. Gender composition was different in this meta-analysis. Three trials recruited both male and female subjects, and five trials included only men. The duration of treatment for these studies ranged from 6 weeks to 27 weeks. Four trials looked at the effect of exogenous testosterone, whereas others used nandrolone. In addition, there were also differences in the route of administration, the dosage of exogenous androgens, whether the intervention included nutritional supplements and exercise training or not. All of these may contribute to the risk of bias.

Conclusion

In general, the main findings from our meta-analysis indicate that AASs therapy can increase body weight, FFM and peak workload in COPD patients. However, because of the limited number of included trials, we are not certain whether it has improvements on spirometry, 6MWD and HRQoL. More multi-center RCTs in the future are of great essence, especially these with higher quality and longer follow-up duration.

Data availability statement

The original contributions presented in the study are included in the article/Supplementary material, further inquiries can be directed to the corresponding author.

Author contributions

Conceived and designed the experiments: GS. Performed the experiments: YL, JD, CH, GL, and XD. Analyzed the data: YL, JD, and YS. Contributed reagents, materials and analysis tools: YL, CH, and GL. All authors contributed to drafting and revising the article, and gave final approval of the version to be published.

Funding

This study was supported by Grant 22YF1424800 from Shanghai Sailing Program, Grant 82170023, 81970020 from National Natural Science Foundation of China, Grant 2019SY006 from Shanghai Municipal Health Commission, Grant 20dz2261100 from Shanghai Key Laboratory of Emergency Prevention, Diagnosis and Treatment of Respiratory Infectious Diseases, Grant shslczdzk02202 from Shanghai Municipal Key Clinical Specialty, Grant 20dz2210500 from Cultivation Project of Shanghai Major Infectious Disease Research Base, Grant 2017ZZ02014 from Shanghai key discipline for respiratory diseases.

Conflict of interest

The authors declare that the research was conducted in the absence of any commercial or financial relationships that could be construed as a potential conflict of interest.

Publisher's note

Supplementary material

The Supplementary Material for this article can be found online at: https://www.frontiersin.org/articles/10.3389/fmed.2022.915159/full#supplementary-material

References

1. *Global Strategy for the Diagnosis. Management, and Prevention of Chronic Obstructive Pulmonary Disease 2021 Report*. Available online at: https://goldcopd.org. (accessed November 6, 2021).

2. Ingadottir AR, Beck AM, Baldwin C, Weekes CE, Geirsdottir OG, Ramel A, et al. Two components of the new ESPEN diagnostic criteria for malnutrition are independent predictors of lung function in hospitalized patients with chronic obstructive pulmonary disease (COPD). *Clin Nutr.* (2018) 37:1323–31. doi: 10.1016/j.clnu.2017.05.031

3. Vestbo J, Prescott E, Almdal T, Dahl M, Nordestgaard BG, Andersen T, et al. Body mass, fat-free body mass, and prognosis in patients with chronic obstructive

pulmonary disease from a random population sample. *Am J Respir Crit Care Med.* (2006) 173:79–83. doi: 10.1164/rccm.200506-969OC

4. Luo Y, Zhou L, Li Y, Guo S, Li X, Zheng J, et al. Fat-Free mass index for evaluating the nutritional status and disease severity in COPD. *Respir Care.* (2016) 61:680–8. doi: 10.4187/respcare.04358

5. World Health Organization. *Chronic Obstructive Pulmonary Disease. Burden of COPD*. Available online at: www.who.int/respiratory/copd/burden/en/ (accessed 25 March 2020).

6. Mohan SS, Knuiman MW, Divitini ML, James AL, Musk AW, Handelsman DJ, et al. Higher serum testosterone and dihydrotestosterone, but not oestradiol, are independently associated with favourable indices of lung function in community-dwelling men. *Clin Endocrinol (Oxf).* (2015) 83:268–76. doi: 10.1111/cen.12738

7. Fuentes N, Silveyra P. Endocrine regulation of lung disease and inflammation. *Exp Biol Med.* (2018) 243:1313–22. doi: 10.1177/1535370218816653

8. Atlantis E, Fahey P, Cochrane B, Wittert G, Smith S. Endogenous testosterone level and testosterone supplementation therapy in chronic obstructive pulmonary disease (COPD): a systematic review and meta-analysis. *BMJ Open*. (2013) 3:3127. doi: 10.1136/bmjopen-2013-003127

9. Schols A, Soeters P, Mostert R, Pluymers R, Wouters E. Physiologic effects of nutritional support and anabolic steroids in patients with chronic obstructive pulmonary disease: A placebo-controlled randomized trial. *Am J Respir Crit Care Med.* (1995) 152:1268–74. doi: 10.1164/ajrccm.152.4.7551381

10. Ferreira IM, Verreschi IT, Nery LE, Goldstein RS, Zamel N, Brooks D, et al. The influence of 6 months of oral anabolic steroids on body mass and respiratory muscles in undernourished COPD patients. *Chest.* (1998) 114:19–28. doi: 10.1378/chest.114.1.19

11. Yeh SS, DeGuzman B, Kramer T, Albin RJ, Anderson L, Bowen R, et al. Reversal of COPD-associated weight loss using the anabolic agent oxandrolone. *Chest.* (2002) 122:421–8. doi: 10.1378/chest.122.2.421

12. Creutzberg EC, Wouters EFM, Mostert R, Pluymers RJ, Schols AMWJ, A. Role for anabolic steroids in the rehabilitation of patients with copd? A double-blind, placebo-controlled, randomized trial. *Chest.* (2003) 124:1733–42. doi: 10.1378/chest.124.5.1733

13. Svartberg J, Aaseboø U, Hjalmarsen A, Sundsfjord J, Jorde R. Testosterone treatment improves body composition and sexual function in men with COPD, in a 6-month randomized controlled trial. *Respir Med.* (2004) 98:906–13. doi: 10.1016/j.rmed.2004.02.015

14. Casaburi R, Bhasin S, Cosentino L, Porszasz J, Somfay A, Lewis MI, et al. Effects of testosterone and resistance training in men with chronic obstructive pulmonary disease. *Am J Respir Crit Care Med.* (2004) 170:870–8. doi: 10.1164/rccm.200305-617OC

15. Sharma S, Arneja A, McLean L, Duerksen D, Leslie W, Sciberras D, et al. Anabolic steroids in COPD: a review and preliminary results of a randomized trial. *Chron Respir Dis.* (2008) 5:169–76. doi: 10.1177/1479972308092350

16. Pison CM, Cano NJ, Chérion C, Caron F, Court-Fortune I, Antonini MT, et al. Multimodal nutritional rehabilitation improves clinical outcomes of malnourished patients with chronic respiratory failure: a randomised controlled trial. *Thorax.* (2011) 66:953–60. doi: 10.1136/thx.2010.154922

17. Dumas de. La Roque E, Savineau JP, Metivier AC, Billes MA, Kraemer JP, Doutreleau S, et al. Dehydroepiandrosterone (DHEA) improves pulmonary hypertension in chronic obstructive pulmonary disease (COPD): a pilot study. *Ann Endocrinol (Paris).* (2012) 73:20–5. doi: 10.1016/j.ando.2011.12.005

18. Daga MK, Khan NA, Malhotra V, Kumar S, Mawari G, Hira HS. Study of body composition, lung function, and quality of life following use of anabolic steroids in patients with chronic obstructive pulmonary disease. *Nutr Clin Pract.* (2014) 29:238–45. doi: 10.1177/0884533614522832

19. Casaburi R, Nakata J, Bistrong L, Torres E, Rambod M, Porszasz J. Effect of megestrol acetate and testosterone on body composition and hormonal responses in COPD cachexia. *Chronic Obstr Pulm Dis COPD Found.* (2016) 3:389–97. doi: 10.15326/jcopdf.3.1.2015.0128

20. Pan L, Wang M, Xie X, Du C, Guo Y. Effects of anabolic steroids on chronic obstructive pulmonary disease: A meta-analysis of randomised controlled trials. *PLoS One.* (2014) 9:84855. doi: 10.1371/journal.pone.0084855

21. Lenoir A, Fuertes E, Gómez-Real F, Leynaert B, van der Plaat DA, Jarvis D. Lung function changes over 8 years and testosterone markers in both sexes: UK Biobank. *ERJ Open Res.* (2020) 6:00070–2020. doi: 10.1183/23120541.00070-2020

22. Pesce G, Triebner K, van der Plaat DA, Courbon D, Hustad S, Sigsgaard T, et al. Low serum DHEA-S is associated with impaired lung function in women. *EClinicalMedicine*. (2020) 23:100389. doi: 10.1016/j.eclinm.2020.100389

23. Baillargeon J, Urban RJ, Zhang W, Zaiden MF, Javed Z, Sheffield-Moore M, et al. Testosterone replacement therapy and hospitalization rates in men with COPD. *Chron Respir Dis.* (2018) 16:1–9. doi: 10.1177/1479972318793004

24. Moher D, Liberati A, Tetzlaff J, Altman DG. Preferred reporting items for systematic reviews and meta-analyses: the PRISMA statement. *PLoS Med.* (2009) 6:e1000097. doi: 10.1371/journal.pmed.1000097

25. Liberati A, Altman DG, Tetzlaff J, Mulrow C, Gøtzsche PC, Ioannidis JPA, et al. The PRISMA statement for reporting systematic reviews and meta-analyses of studies that evaluate health care interventions: explanation and elaboration. *PLoS Med.* (2009) 6:e1000100. doi: 10.1371/journal.pmed.1000100

26. Choudhury G, Rabinovich R, Macnee W. Comorbidities and systemic effects of chronic obstructive pulmonary disease. *Clin Chest Med.* (2014) 35:101–30. doi: 10.1016/j.ccm.2013.10.007

27. Yang L, Zhu Y, Huang JA, Jin J, Zhang X, A. Low lean-to-fat ratio reduces the risk of acute exacerbation of chronic obstructive pulmonary disease in patients with a normal or low body mass index. *Med Sci Monit.* (2019) 25:5229–36. doi: 10.12659/MSM.914783

28. Engelen MPKJ, Schols AMWJ, Baken WC, Wesseling GJ, Wouters EFM. Nutritional depletion in relation to respiratory and peripheral skeletal muscle function in out-patients with COPD. *Eur Respir J.* (1994) 7:1793–7. doi: 10.1183/09031936.94.07101793

29. Schols AMWJ, Soeters PB, Dingemans AMC, Mostert R, Frantzen PJ, Wouters EFM. Prevalence and characteristics of nutritional depletion in patients with stable COPD eligible for pulmonary rehabilitation. *Am Rev Respir Dis.* (1993) 147:1151–6. doi: 10.1164/ajrccm/147.5.1151

30. Kerti M, Balogh Z, Kelemen K, Varga J. The relationship between exercise capacity and different functional markers in pulmonary rehabilitation for COPD. *Int J Chron Obstruct Pulmon Dis*. (2018) 13:717–24. doi: 10.2147/COPD.S153525

31. Bhasin S, Brito JP, Cunningham GR, Hayes FJ, Hodis HN, Matsumoto AM, et al. Testosterone therapy in men with hypogonadism: an endocrine society. *J Clin Endocrinol Metab.* (2018) 103:1715–44. doi: 10.1210/jc.2018-00229

32. Sallon C, Provost PR, LeBlanc D, Soulet D, Tremblay Y. Essential Intracrine Androgenic Action in Lung Development for Both Sexes. *J Steroid Biochem Mol Biol.* (2018) 183:184–91. doi: 10.1016/j.jsbmb.2018.06.012

33. Sellau J, Groneberg M, Lotter H. Androgen-dependent immune modulation in parasitic infection. *Semin Immunopathol.* (2019) 41:213–24. doi: 10.1007/s00281-018-0722-9

34. Pihlajamaa P, Sahu B, Jänne OA. Determinants of receptor- and tissue-specific actions in androgen signaling. *Endocr Rev.* (2015) 36:357–84. doi: 10.1210/er.2015-1034

35. MacLean HE, Moore AJ, Sastra SA, Morris HA, Ghasem-Zadeh A, Rana K, et al. DNA-binding-dependent androgen receptor signaling contributes to gender differences and has physiological actions in males and females. *J Endocrinol.* (2010) 206:93–103. doi: 10.1677/JOE-10-0026

36. Bonnet S. Dumas-de-La-Roque E, Bégueret H, Marthan R, Fayon M, Dos Santos P, et al. Dehydroepiandrosterone (DHEA) prevents and reverses chronic hypoxic pulmonary hypertension. *Proc Natl Acad Sci U S A.* (2003) 100:9488–93. doi: 10.1073/pnas.1633724100

37. Klinge CM, Clark BJ, Prough RA. Dehydroepiandrosterone research: past, current, and future. Vol 108 1st ed Elsevier Inc. (2018).

38. Van Balkom RHH, Dekhuijzen PNR, Van Der Heijden HFM, Folgering HTM, Fransen JAM, Van Herwaarden CLA. Effects of anabolic steroids on diaphragm impairment induced by methylprednisolone in emphysematous hamsters. *Eur Respir J.* (1999) 13:1062–9. doi: 10.1034/j.1399-3003.1999.13e21.x

39. Wijnhoven HJH, Ennen L, Rodenburg RJT, Dekhuijzen PNR. Mitochondrial function in diaphragm of emphysematous hamsters after treatment with nandrolone. *Int J Chron Obstruct Pulmon Dis.* (2006) 1:83–9. doi: 10.2147/copd.2006.1.1.83

40. Lewis MI, Fournier M, Storer TW, Bhasin S, Porszasz J, Ren SG, et al. Skeletal muscle adaptations to testosterone and resistance training in men with COPD. *J Appl Physiol.* (2007) 103:1299–310. doi: 10.1152/japplphysiol.00150.2007

41. Chavoshan B, Fournier M, Lewis MI, Porszasz J, Storer TW Da X, et al. Testosterone and resistance training effects on muscle nitric oxide synthase isoforms in COPD men. *Respir Med.* (2012) 106:269–75. doi: 10.1016/j.rmed.2011.07.018

42. Wang X, Huang L, Jiang S, Cheng K, Wang D, Luo Q, et al. Testosterone attenuates pulmonary epithelial inflammation in male rats of COPD model through preventing NRF1-derived NF-κB signaling. *J Mol Cell Biol.* (2021) 13:128–40. doi: 10.1093/jmcb/mjaa079

43. Svartberg J, Schirmer H, Medbø A, Melbye H, Aasebø U. Reduced pulmonary function is associated with lower levels of endogenous total and free testosterone. The Tromsø study. *Eur J Epidemiol.* (2007) 22:107–12. doi: 10.1007/s10654-006-9095-9

44. Velema MS, Kwa BHB, De Ronde W. Should androgenic anabolic steroids be considered in the treatment regime of selected chronic obstructive pulmonary disease patients? *Curr Opin Pulm Med.* (2012) 18:118–24. doi: 10.1097/MCP.0b013e32834e9001

frontiers | Frontiers in Medicine

TYPE Study Protocol
PUBLISHED 06 September 2022
DOI 10.3389/fmed.2022.904864

OPEN ACCESS

EDITED BY
Yi Liu,
Shandong Provincial Hospital, China

REVIEWED BY
Kai Guan,
Peking Union Medical College Hospital (CAMS), China
Sergey Karpishchenko,
Saint-Petersburg Research Institute of Ear, Throat, Nose and Speech, Russia
Im Quah-Smith,
Royal Hospital for Women, Australia

*CORRESPONDENCE
Zhishun Liu
zhishunjournal@163.com

†These authors have contributed equally to this work

SPECIALTY SECTION
This article was submitted to Pulmonary Medicine, a section of the journal Frontiers in Medicine

RECEIVED 26 March 2022
ACCEPTED 29 July 2022
PUBLISHED 06 September 2022

CITATION
Wang W, Chen H, Gao N, Yu S, Liao J, Wang S, Gao Z and Liu Z (2022) Effect of acupuncture at the sphenopalatine ganglion for the treatment of moderate to severe seasonal allergic rhinitis: Study protocol for a three-armed randomized controlled trial.
Front. Med. 9:904864.
doi: 10.3389/fmed.2022.904864

Effect of acupuncture at the sphenopalatine ganglion for the treatment of moderate to severe seasonal allergic rhinitis: Study protocol for a three-armed randomized controlled trial

Weiming Wang[1†], Hui Chen[2†], Ning Gao[1], Shudan Yu[1], Jiahua Liao[2], Shijie Wang[3], Ziqi Gao[3] and Zhishun Liu[1*]

[1]Department of Acupuncture and Moxibustion, China Academy of Chinese Medical Sciences Guang'anmen Hospital, Beijing, China, [2]Department of Traditional Chinese Medicine, China Aerospace Science & Industry Corporation 731 Hospital, Beijing, China, [3]Department of Otolaryngology, China Aerospace Science & Industry Corporation 731 Hospital, Beijing, China

Introduction: Seasonal allergic rhinitis (SAR) is a major health problem with a relatively high worldwide prevalence that severely limits the quality of life for sufferers. Acupuncture is widely used for SAR treatment in China; however, the evidence on the efficacy of acupuncture at the sphenopalatine ganglion (SPG) for SAR is inconclusive. Therefore, this study aims to investigate the efficacy and safety of acupuncture at the SPG acupoint for the treatment of SAR.

Methods and analysis: A total of 120 participants with SAR will be recruited and randomly assigned to the acupuncture group, placebo acupuncture (PA) group, or rescue medication (RM) group with a 1:1:1 allocation ratio. Participants in the acupuncture group and PA group will receive 8 sessions of acupuncture stimulus at the SPG plus RM or 8 sessions of shallow needling at the SPG acupoint plus RM for 4 weeks with a 4-week follow-up in the first year and a 1-week follow-up in the second year. Participants in the RM group will only receive RM throughout the study. The primary outcome is the change from baseline in the average daily combined symptoms and medication score (CSMS) over weeks 1–4. All analysis will be based on an intention-to-treat principle. All statistical tests will be two-sided and a p-value < 0.05 will be considered to be statistically significant.

KEYWORDS

acupuncture, seasonal allergic rhinitis, sphenopalatine ganglion, randomized controlled trial, protocol

Strengths and limitations of this study

► Acupuncture at the SPG might have a specific effect on the treatment of SAR. This study is the first randomized controlled trial that compares acupuncture at the SPG plus RM with shallow needling at SPG plus RM and only RM for participants suffering from SAR.

► This study was rigorously designed with strict inclusion and exclusion criteria, and the measurement of the primary outcome was recommended by the European Academy of Allergy and Clinical Immunology (EAACI), blinding participants, and outcome assessors.

► Due to the difficulty of inserting an acupuncture needle into the SPG, the acupuncturist must receive specialist training before the initiation of the trial.

► This is a single-center study that will only recruit patients with SAR in Asian populations, which might limit the generalizability of the study among other types of allergic rhinitis and other ethnic patients.

► The acupuncturists will not be blinded, which could potentially introduce bias in the results.

Background

Allergic rhinitis (AR) is an immunoglobulin E-mediated inflammatory disease (1) that is caused by the hypersensitivity of the immune system to an allergen, which affects 100 million people in Europe (2) and 400 million people globally (3). Typical symptoms of AR include nasal congestion, rhinorrhea, itching, and sneezing (4), other common non-nasal symptoms include itchy eyes, tearing, and eye redness (5). Many patients with AR are susceptible to several comorbidities, such as asthma, rhinosinusitis, obstructive sleep apnea, and other related airway conditions (6). AR can result in impaired physical, emotional, and social functions, as well as poor quality of life (7), and therefore, has a substantial economic burden on society. The etiology of AR is multifactorial, which results primarily from a genetic predisposition, immunological response, and environmental pollutants (8). AR has traditionally been classified as seasonal allergic rhinitis (SAR) or perennial allergic rhinitis (PAR) depending on the causes and duration of symptoms (9).

In addition to avoiding allergens, current treatments for AR mainly include pharmacotherapy and immunotherapy (10). These treatments are effective to control and improve AR symptoms, but each treatment modality has unique challenges: it is impractical to eliminate all environmental allergens, pharmacotherapy (i.e., histamine antagonists) is often associated with adverse events, such as fatigue (11), and adherence with immunotherapy is often poor (12). Therefore, some patients with AR prefer complementary and alternative medicine to alleviate their symptoms, with approximately 20% receive acupuncture (13).

Acupuncture, which is one of the most studied Chinese medical techniques, involves stimulation of specific locations (acupoints) on the body, usually by the insertion of a fine needle (14). Many studies have reported the efficacy of acupuncture to treat AR (15–17), and a 2020 meta-analysis of 39 randomized clinical trials (RCTs) claimed that acupuncture methods were effective and safe for the treatment of AR (18). However, according to the updated practice parameters for rhinitis in 2020, the use of acupuncture for the treatment of AR was not recommended due to a lack of well-controlled studies (19).

The sphenopalatine ganglion (SPG), which is located under a thin (1–2 mm) layer of mucosa in the pterygopalatine fossa, consists of sensory fibers that innervate the nasopharynx, nasal cavity, and palate (20). Several studies reported the benefits of SPG stimulation for chronic cluster headaches (21), and acute ischemic stroke (22). Compared with traditional acupoints that are selected based on traditional meridian theory, acupuncture at the SPG (inserting a needle through the SPG acupoint near ST7, Xiaguan (23) to reach and directly stimulate the SPG) might help patients improve nasal symptoms immediately and improve their quality of life (24) by increasing sympathetic nerve excitability (25); however, the evidence is inconclusive.

This three-armed, randomized trial will investigate the efficacy and safety of acupuncture at the SPG for the treatment of SAR. Acupuncture at the SPG plus rescue medication (RM) might be superior to placebo acupuncture (PA) plus RM, and only RM for the treatment of SAR.

Methods and design

Study design

This is a parallel-design, three-armed, patient-assessor blinded randomized (1:1:1) controlled trial. This protocol has been developed according to the standard protocol items included in the *Recommendations for Interventional Trials* (26) and the *Standards for Reporting Interventions in Clinical Trials of Acupuncture* (27) guidelines. The trial flow diagram and treatment schedule are shown in **Figures 1** and **2**.

Study setting and recruitment

This trial will be carried out at No. 731 Hospital of China Aerospace Science and Industry Corporation from May 2021 to August 2023. A total of 120 participants will be recruited. The trial duration will be 10 weeks: 1 week baseline (run-in phase), 4 weeks treatment, 4 weeks follow-up in the first year, and the first week following symptom onset in the second year.

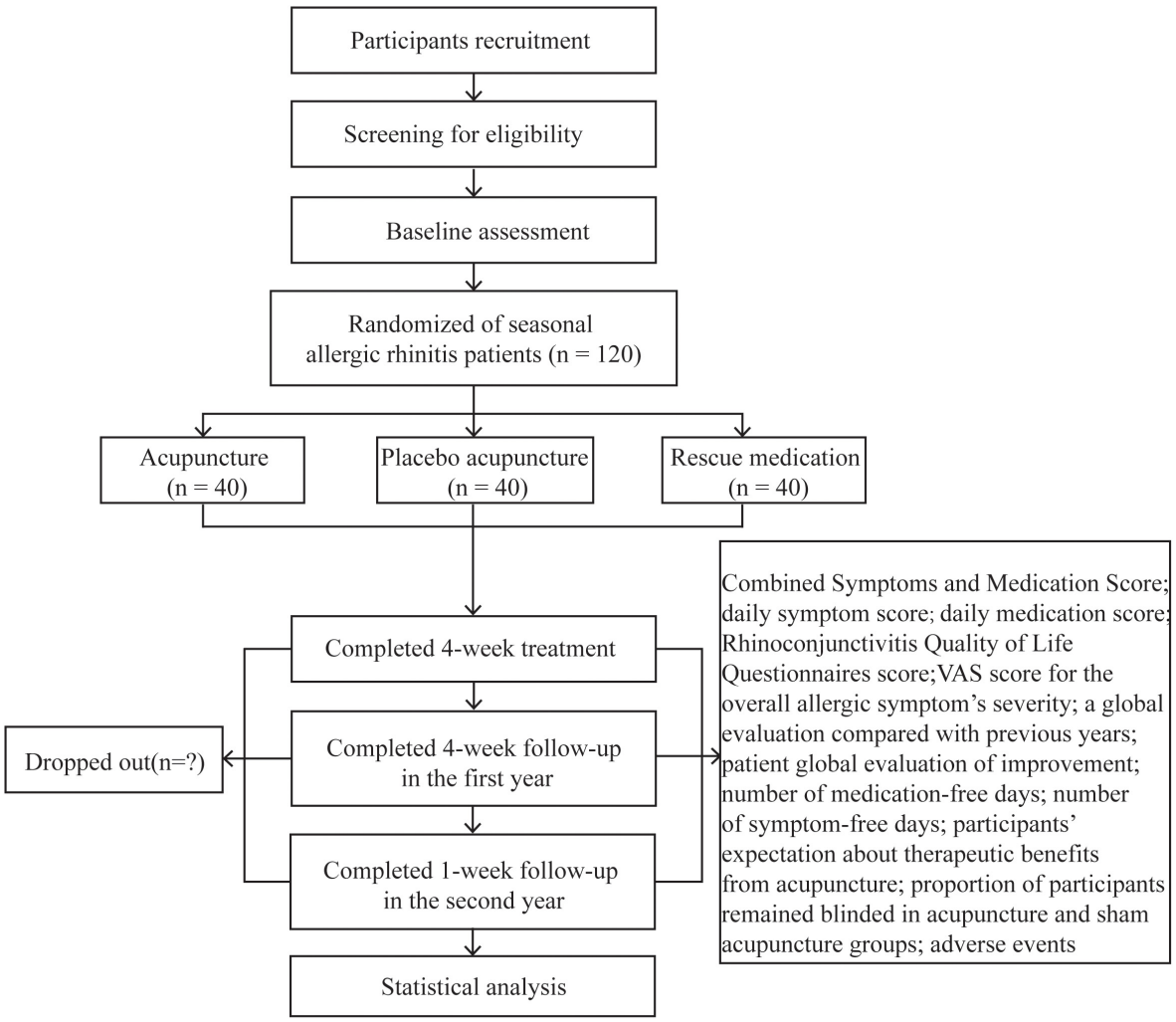

FIGURE 1
Study flow diagram.

At baseline, participants would not take any anti-histamines and will record their SARs symptoms in a daily participant diary.

Randomization and blinding

Participants who agreed to randomization will be allocated to the acupuncture, PA, or RM groups in a 1:1:1 ratio that uses a fixed block size of 6. The randomization number of the allocation sequence will be generated using PROC PLAN of SAS software, version 9.4 (SAS Institute Inc., Cary, NC, United States). An independent researcher will prepare consecutively numbered, sealed, opaque envelopes that contain the information about group allocation. These envelopes will be consecutively opened by a research coordinator that is not involved in recruitment, therapy, and outcome assessments immediately after the baseline assessments.

Because of the two different acupuncture techniques that will be used in this trial, the acupuncturist will know which group each participant is in. However, the participants in the acupuncture and PA groups, outcome evaluators, and statisticians will be blinded to the group allocation throughout the trial. To ensure blinding, all researchers will receive the same training before the trial, and each participant will be treated in a separate room. Participants in the RM group will not be blinded.

Participants

The participants will have previously been diagnosed with SAR by a lung physician or allergist, according to the Allergic Rhinitis and Its Impact on Asthma (ARIA) criteria (28). Participants will be recruited during the pollen season, which is defined as the period with pollen levels $\geq$ 20 grains/m (3, 29).

	Study Period				
	Baseline	**Allocation**	**Treatment**	**Follow-up in first year**	**Follow-up in second year**
TIME POINT [W (week)]			W 4 ± 2 days	W 8 ± 2 days	W 9 ± 2 days
Enrollment					
Eligibility criteria	×				
Demography characteristics	×				
Disease history of seasonal allergic rhinitis	×				
Eligibility screen	×				
Informed consent	×				
Allocation		×			
Interventions					
Acupuncture			×(weeks 1 –4)		
Placebo acupuncture			×(weeks 1 –4)		
Rescue medication			×(weeks 1 –4)	×(weeks 5 –8)	×
Assessments					
Combined Symptoms and Medication Score	×		×	×	×
Daily symptom score	×		×	×	×
Daily medication score	×		×	×	×
Rhinoconjunctivitis Quality of Life Questionnaires score	×		×	×	×
VAS score for the overall allergic symptom's severity	×		×	×	×
A global evaluation compared with previous years	×		×	×	×
Patient global evaluation of improvement	×		×	×	×
Number of medication-free days			×(weeks 1 –4)	×(weeks 5 –8)	
Number of symptom-free days			×(weeks 1 –4)	×(weeks 5 –8)	
Participants' expectation of therapeutic benefits from acupuncture	×				
Proportion of participants remained blinded in acupuncture and sham acupuncture groups			×		
Adverse events	×		×	×	×

FIGURE 2
Study schedule.

According to a previous study, the pollen season annually in Beijing was set from 17 March to the end of October (30). To ensure that participants are recruited within pollen season from baseline to the end of the 4 weeks follow-up period in the first year, patients would not be involved in the same year, if pollen season is over in less than 9 weeks. Participants will be eligible if they meet all the inclusion criteria and have none of the exclusion criteria. The last participant is expected to complete treatment in September 2021.

Inclusion criteria

1. Aged ≥ 18 years and ≤ 75 years.

2. A history of moderate to severe SAR symptoms [visual analog scale (VAS) > 50 mm, range from 0 cm (not at all troublesome) to 100 mm (extremely bothersome)] (31) for > 4 days per weeks, and > 4 consecutive weeks with ≥ 2 years duration.
3. Participants' SAR symptoms severity scores at baseline > 50 mm for at least 4 consecutive days at baseline.
4. Positive skin prick test response, defined as wheal diameter greater than or equal to 3 mm, to grass and birch pollen (rather than dust mite or mold), or a serum-specific IgE test, or both.
5. Ability to complete the medical information form and sign a written informed consent.

Exclusion criteria

1. A history or current evidence of PAR, acute sinusitis, allergic asthma, pneumonia, autoimmune disorders, or severe chronic inflammatory diseases.
2. A history of nasal rhinopolypus or abnormalities.
3. Taking antihistamines, anticholinergics, corticosteroids, decongestants, or antibiotics 1 month before starting the study.
4. A history of systemically administered corticosteroids within 6 months or specific immunotherapy, or allergy desensitization therapy 1 year before enrollment.
5. Serious uncontrolled blood coagulation disorder, cardiovascular disorder, severe hepatic or renal insufficiency, or a mental disorder.
6. Pregnancy or planning for pregnancy;
7. Known allergy, or contraindication to RM or related drugs.
8. Known phobia to acupuncture or have received acupuncture treatment, or SPG stimulation, or other complementary and alternative medicine within 1 month of enrollment.

Interventions

Acupuncture group

The acupuncture regimen was determined based on previous reports (23, 24, 32). The licensed acupuncturists have > 5 years of practical experience. Before the study, the acupuncturists will receive special training in the SPG stimulation technique and will perform the technique clinically. The SPG acupoint is located under the zygomatic arch between the coronoid process and mandibular condyle (24). Sterile single-use stainless steel needles (0.35 mm × 55 mm; YiDaiFu brand, Suzhou Tianyi Acupuncture Instrument Co., Ltd., Suzhou, China) will be used. Participants will be in the lateral position and the acupoints area will be sterilized with 75% alcohol. To stimulate the SPG, the needles will be inserted into the medial superior anterior direction to a depth of approximately 55 mm (33), until the participants report a special (deqi) sensation that radiates toward the nose or the upper teeth (**Figure 3**). Then, the needle will be withdrawn slightly. The needles will be retained for 30 min and stimulated 3 times during the needling period.

Placebo acupuncture group

The acupuncture procedure is similar to that of the acupuncture group. After sterilizing the skin, the 0.35 × 25 mm disposable needle will be vertically inserted at the SPG acupoint approximately 3–5 mm. The needles will also be retained for 30 min, yet no needle manipulation would be carried out to avoid the deqi (unique) response.

Acupuncture is administrated unilaterally. The SPG acupoint will be stimulated alternatively in each session. After randomization, participants receive treatment twice per week for eight sessions for four consecutive weeks. All participants will be treated separately to prevent communication and will be advised to avoid allergens during the trial.

Rescue medication group

Participants in the RM group will not receive acupuncture treatment during the study period. They could use the RM described in the following section. They have the option of 4 weeks (≤ 8 sessions) of acupuncture free of charge at the end of the follow-up period.

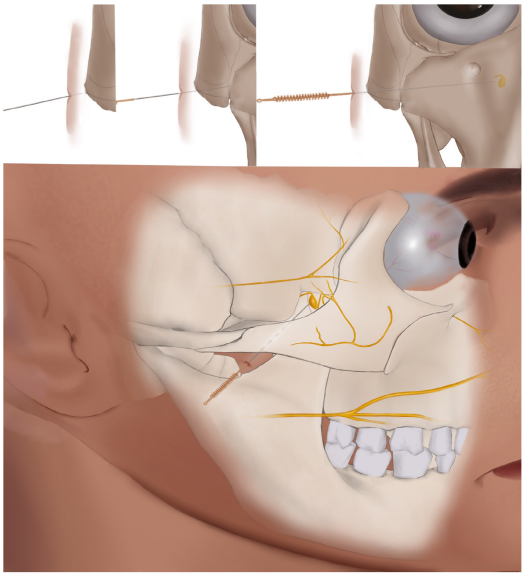

FIGURE 3
Schematic diagram of acupuncture.

Rescue medication

The following RM; non-sedative H1 antihistamines, intranasal, or oral corticosteroids are permitted in each group based on a standardized approach (34), only when participants feel that their symptoms are intolerable. Administration for prophylactic purposes is prohibited. Additional medications, such as leukotriene receptor antagonists, anticholinergic agents, α-adrenergic agonists, allergen immunotherapy, nasal ipratropium, decongestants, or any form of alternative therapy are not allowed at any time during the study period. The daily medication score (dMS) will be recorded every day in case report forms (CRFs) based on the following scores: 0 = no RM; 1 = use of oral, or topical non-sedative H1 antihistamines, or both (e.g., Clarityne or Patanol); 2 = use of intranasal corticosteroids (Rhinocort) with or without H1 antihistamines; and 3 = use of oral corticosteroids (Prednisone) with or without intranasal corticosteroids, with or without H1 antihistamines (34). When a participant takes $\geq$ 2 rescue medications, the higher score will be retained for the corresponding day.

Outcome measures

Primary outcome

The primary outcome is the change from baseline in the average daily combined symptoms and medication score (CSMS) over weeks 1–4, which measures the symptoms of AR and the use of RM. It has been widely used in previous studies and is recommended by the EAACI (34). The average daily CSMS is the sum of the daily symptom score (dSS) plus dMS. The dSS contains a 6-item scale that refers to nasal symptoms (4 items) and ocular symptoms (2 items), and each item is scored using a Likert scale of 0–3. The dSS is calculated as a mean of all entered dSS divided by the number of individual symptoms (range 0–3). The dMS is calculated as an average of the daily symptom relief medication score, with a range of 0–3. Therefore, the potential CSMS score could be from 0 to 6, with high scores indicating more severe nasal symptoms. In addition, the changes from baseline over weeks 5–8 during the first year and the first week following symptoms onset in the second year will be assessed.

Secondary outcomes

The secondary outcomes are:

1. Change in the average dSS and dMS from baseline over weeks 1–4, weeks 5–8 in the first year, and the first week following symptoms onset in the second year.
2. The proportion of participants with a minimum of 23% improvement in the average daily CSMS from baseline over weeks 1–4, weeks 5–8 in the first year, and at the first week following symptoms onset in the second year. Based on the previous data, a difference of 23% (35) in the average daily CSMS was chosen to demonstrate a minimum clinically significant difference.
3. A change in the Rhinoconjunctivitis Quality of Life Questionnaires (RQLQ) (36) total score and subscale scores from baseline to the end of weeks 4 and 8 in the first year and the first week following symptoms onset in the second year. The RQLQ is a well-established and validated questionnaire that consists of 28 questions that cover 7 domains: (1) sleep (3 items); (2) practical problems (3 items); (3) non-nasal and eye symptoms (7 items); (4) nasal symptoms (4 items); (5) eye symptoms (4 items); (6) activities that have been limited by nose or eye symptoms (3 items); and (7) and emotional function (4 items). Each item was evaluated on a 7-point rating scale from 0 (no impairment) to 6 (severe impairment) (36) during the previous week. The analysis of the RQLQ total score is the average of the answers to the 28 items and the subscale scores are the average of the answers in those subscales. The total score or the subscale score is between 0 and 6, with high values indicating the lower disease-specific quality of life. Changes in scores by $\geq$ 0.5 were considered clinically significant (37). In this study, the validated Chinese version of RQLQ is used (38).
4. A Change in the VAS score for the overall allergic symptom's severity from baseline to the end of weeks 4 and 8 in the first year and the first week following symptoms onset in the second year. Patients will be asked to grade the severity of allergic symptoms using the self-rated 0–100 mm VAS (0 = no symptoms and 100 = worst-ever symptoms, in 1-point increments). The VAS is a reliable and valid tool to quantitatively evaluate AR severity (31).
5. A global evaluation will compare previous years by each participant at the end of weeks 4 and 8 in the first year and the first week following symptoms onset in the second year. Each participant will be asked the following question: Compared with your symptoms in previous grass pollen seasons, how have you felt overall in this grass pollen season? (select only one). The possible answers are coded follows:1 = very much better; 2 = much better; 3 = a little better; 4 = no change; 5 = a little worse; 6 = much worse; and 7 = very much worse.
6. Patient global evaluation of improvement at the end of weeks 4 and 8 in the first year and the first week following symptoms onset in the second year. Patient global evaluation of improvement will be rated by the participants using a 7-point Likert scale with the following options: 1 = very much better; 2 = much better; 3 = a little better; 4 = no change; 5 = a little worse; 6 = much worse; and 7 = very much worse, at each study visit.
7. The average weekly number of medication-free days during weeks 1–4 and weeks 5–8 in the first year.
8. The average weekly number of symptom-free days during weeks 1–4 and weeks 5–8 in the first year.

9. Participants expectation about the therapeutic benefits of acupuncture at baseline. At baseline, participants in the acupuncture and PA groups will be asked the following question: How helpful you believe the acupuncture modality you received would be for your AR. Participants will be instructed to choose one of the given answers: (1) very helpful; (2) moderately helpful; (3) slightly helpful; (4) not helpful; and (5) unclear.
10. The participants remained blinded to the treatment arm in the acupuncture and PA groups. Five minutes after the end of the final treatment in week 4, each participant in the acupuncture and PA groups will be asked the following question: Which treatment do you think you received (acupuncture or PA). Participants will be allowed to choose only one answer, acupuncture, "PA," or unclear. Before the question, participants will be told that they might have received acupuncture with a deeper insertion or PA with shallow penetration.

Safety assessment

Any potential adverse events (AEs) will be monitored and documented in the CRFs within 24 h of their occurrence during treatment and the follow-up period. Based on their potential association with acupuncture, AEs will be categorized as acupuncture-associated AEs (e.g., subcutaneous hemorrhage, dizziness, fainting, serious pain, local infection, and localized hematoma), and non-treatment-related AEs. Any serious adverse events, for example, an event that is life-threatening, or requires hospitalization, or results in death, hospitalization, or significant disability will be reported immediately to the study principal investigator and ethics committee. The ethics committee will decide whether to suspend the trial if required, and the statistician will break the blinding. Any participant that suffers an SAE will be withdrawn from the study.

Sample size calculation

This trial hypothesizes that 4 weeks of acupuncture treatment plus RM could be superior for the improvement of the average daily CSMS over PA plus RM and only RM. Based on previous studies (15, 16), the differences in total nasal symptom score that changed at week 4 and the RM score that changed at week 8 between acupuncture and PA were 1.00 and 1.1, respectively. The between-group difference of 1.65 (1 point change in symptom score and 0.55 point change in RM score) with a standard deviation of 2.0 in the improvement of total CSMS could be detected at week 4 in the first pollen season period. Assuming an $\alpha = 0.05$ level of significance (two-sided test), 90% power, and a 20% drop-out rate, 120 patients (40 in each group) will be considered.

Statistical analysis

The null hypothesis is that the change from baseline in the average daily CSMS over weeks 1–4 in the first year could be the same in the acupuncture, the PA group and RM groups. Data will be presented as means with standard deviations, or medians with interquartile ranges for continuous variables, and frequencies (number of cases) or relative frequencies (%) for categorical variables. The repeated measure of the analysis of variance (ANOVA) will be performed for normally distributed variables, and a non-parametrical Kruskal–Wallis test will be used for non-normally distributed variables. The categorical variables will be compared using the Chi-squared (χ^2) test. A two-tailed p-value < 0.05 will be considered statistically significant. All analyses will be conducted based on an intention-to-treat approach with all randomized participants included using SPSS software V.20.0 (IBM SPSS Statistics; IBM Corp, Somers, NY). Missing primary outcome data will be handled by multiple imputation techniques according to the missing at random assumption. Missing data will not be imputed for secondary outcomes.

Quality control

To guarantee the quality of the trial, all participating staff will receive the same study training before the study starts. The training includes the aim of the trial, case screening and recruitment, intervention protocols, outcome measures, and data processing. The licensed acupuncturists have ≥ 5 years of clinical acupuncture practice and will receive special training in the SPG stimulation technique. The principal investigator has overall responsibility for the trial and is supported by a research coordinator for the CRFs review, data entry verification and storage, and quality control checks. Dropouts and withdrawals from the study will be documented during the trial. All paper data will be stored in a fire-proof safe, and all-electric data saved on a secure server within No. 731 Hospital of China Aerospace Science and Industry Corporation.

Patient and public involvement

The research question was first proposed by a patient that failed the conventional acupuncture treatment. Patients were not involved in the development or implementation of this study. The results of this study will be communicated to all participants after completion of the study upon their request.

Discussion

AR is a global health problem, which severely impairs the sufferers quality of life (7). Previously, acupuncture has

been widely used to alleviate associated symptoms that are induced by AR. However, there is an ongoing debate on the effect of acupuncture on SAR. To the best of our knowledge, this is the first trial that aims to evaluate the clinical efficacy of acupuncture at the SPG for SAR that uses the CSMS recommended by the EAACI. The results of this trial could help to determine the effect of acupuncture at the SPG to improve SAR symptoms and reduce RM.

Although the SPG is relatively small and varies in size between individuals, it is possible to reach the SPG by inserting a needle through the SPG acupoint (33). A previous study found that acupuncture at the SPG led to significant improvement in nasal ventilation and nasal patency, and increased sympathetic nerve excitability (25) in healthy volunteers. In addition, one pilot study revealed the effect of acupuncture at the SPG acupoint for the prevention of PAR development (24). In this study, the effect of acupuncture at the SPG for SAR will be determined. Due to ethical considerations, the participants will be allowed to use relief medication, and therefore, the total CSMS was selected as the primary outcome measure as recommended by the EAACI (34). The CSMS is easy to understand and is an analysis of the daily burden of the disease, which equally combines symptom scores and medication scores.

This prospective study is a registered, concealed-allocation, three-armed, randomized controlled trial. The strengths of the trial include strict inclusion and exclusion criteria, the measurement of the primary outcome as recommended by the EAACI, evaluation of the participant's expectation for acupuncture, blinding of the participants and outcome assessors, and is analyses based on the principle of intent-to-treat. In addition, this trial has several limitations. First, this is a single-center study in an Asian population, which might limit the generalizability of the study among other ethnic patients. Second, only patients with SAR were included, and therefore, the result might not apply to other types of AR (i.e., PAR). Third, the acupuncturists cannot be blinded due to the nature of acupuncture, which might bias the results of this study.

Ethics statement

This study will be conducted in compliance with the principles of the Declaration of Helsinki 2008. This study was approved by the Medical Ethics Committee of No. 731 Hospital of China Aerospace Science and Industry Corporation (approval No: 2021-0102-01) on March 12, 2021. The registration number provided by ClinicalTrials.gov is NCT04815668. All investigators will adhere to a strict confidentiality regulation before, during, and after the trial. All participants will be asked to voluntarily sign the informed consent form if they agree to participate and will be reminded that they can withdraw from the study at any time without giving a reason. They also can be discontinued from the trial by the investigator if based upon his clinical judgment, continuation in the trial is deemed inappropriate. Any modifications to the protocol that might impact the conduct of this study will be submitted to the ethics committee and will be updated in the clinical trial registry. After completing data analysis, the results of this study will be published in an international peer-reviewed medical journal and will be disseminated via national conferences and scientific meetings.

Author contributions

WW, ZL, and HC contributed to the conception and design of the study. HC, JL, SW, and NG will be responsible for clinical recruitment, intervention, data collection, and outcome assessment, respectively. ZG will be responsible for statistical analysis. This manuscript was drafted by WW and revised by SY and ZL. All authors read and approved the final manuscript.

Funding

This RCT was funded by the Science Foundation of Aerospace Medical & Healthcare Technology Group Co., Ltd., and the Fundamental Research Funds for the Central Public Welfare Research Institutes of China Academy of Chinese Medical Sciences. The funding source has no role in the design, conduct or reporting of the study.

Acknowledgments

The authors appreciate the patients who will participate in this study.

Conflict of interest

The authors declare that the research was conducted in the absence of any commercial or financial relationships that could be construed as a potential conflict of interest.

Publisher's note

References

1. Seidman MD, Gurgel RK, Lin SY, Schwartz SR, Baroody FM, Bonner JR, et al. Clinical practice guideline: allergic rhinitis executive summary. *Otolaryngol Head Neck Surg.* (2015) 152:197–206. doi: 10.1177/0194599814562166

2. European Academy of Allergy and Clinical Immunology. *Advocacy Manifesto: Tackling the Allergy Crisis in Europe-Concerted Policy Action Needed*. Brussels: EAACI – EU Liaison Office (2015).

3. Pawanker R, Canonica G, Holgate S editors. *White Book on Allergy: Update*. (Vol. 2013). Milwaukee, WI: World Allergy Organization (2013).

4. Dykewicz MS, Wallace DV, Baroody F, Bernstein J, Craig T, Finegold I, et al. Treatment of seasonal allergic rhinitis: an evidence-based focused 2017 guideline update. *Ann Allergy Asthma Immunol.* (2017) 119:489–511. doi: 10.1016/j.anai.2017.08.012

5. Wallace DV, Dykewicz MS, Bernstein DI, BlessingMoore J, Cox L, Khan DA, et al. The diagnosis and management of rhinitis: an updated practice parameter. *J Allergy ClinImmunol.* (2008) 122(Suppl. 2):S1–84. doi: 10.1016/j.jaci.2008.06.003

6. Hadley JA, Derebery MJ, Marple BF. Comorbidities and allergic rhinitis: not just a runny nose. *J FamPract.* (2012) 61(Suppl. 2):S11–5.

7. Horak F. Clinical advantages of dual activity in allergic rhinitis. *Allergy.* (2000) 55 (Suppl. 64):34–9. doi: 10.1034/j.1398-9995.2000.00805.x

8. Lim R, Fedulov AV, Kobzik L. Maternal stress during pregnancy increases neonatal allergy susceptibility: role of glucocorticoids. *Am J Physiol Lung Cell Mol Physiol.* (2014) 307:L141–8. doi: 10.1152/ajplung.00250.2013

9. Us Department of Health and Human Services. *Allergic Rhinitis: Developing Drug Products for Treatment Guidance for Industry: Draft Guidelines 2016*. Rockville, MD: Federal Register (2020).

10. May JR, Dolen WK. Management of allergic rhinitis: a review for the community pharmacist. *ClinTher.* (2017) 39:2410–9. doi: 10.1016/j.clinthera.2017.10.006

11. Yanai K, Rogala B, Chugh K, Paraskakis E, Pampura AN, Boev R. Safety considerations in the management of allergic diseases: focus on antihistamines. *Curr Med Res Opin.* (2012) 28:623–42. doi: 10.1185/03007995.2012.672405

12. Meltzer EO, Blaiss MS, Naclerio RM, Stoloff SW, Derebery MJ, Nelson HS, et al. Burden of allergic rhinitis: allergies in America, Latin America, and Asia-Pacific adult surveys. *Allergy Asthma Proc.* (2012) 33(Suppl. 1):S113–41. doi: 10.2500/aap.2012.33.3603

13. Krouse JH, Krouse HJ. Patient use of traditional and complementary therapies in treating rhinosinusitis before consulting an otolaryngologist. *Laryngoscope.* (1999) 109:1223–7. doi: 10.1097/00005537-199908000-00007

14. Vickers A, Wilson P, Kleijnen J. Acupuncture. *QualSaf Health Care.* (2002) 11:92–7. doi: 10.1136/qhc.11.1.92

15. Choi SM, Park JE, Li SS, Jung H, Zi M, Kim TH, et al. A multicenter, randomized, controlled trial testing the effects of acupuncture on allergic rhinitis. *Allergy.* (2013) 68:365–74. doi: 10.1111/all.12053

16. Brinkhaus B, Ortiz M, Witt CM, Roll S, Linde K, Pfab F, et al. Acupuncture in patients with seasonal allergic rhinitis: a randomized trial. *Ann Intern Med.* (2013) 158:225–34. doi: 10.7326/0003-4819-158-4-201302190-00002

17. McDonald JL, Smith PK, Smith CA, Xue CC, Golianu B, Cripps AW, et al. Effect of acupuncture on house dust mite specific IgE, substance P, and symptoms in persistent allergic rhinitis. *Ann Allergy Asthma Immunol.* (2016) 116:497–505. doi: 10.1016/j.anai.2016.04.002

18. Yin Z, Geng G, Xu G, Zhao L, Liang F. Acupuncture methods for allergic rhinitis: a systematic review and bayesian meta-analysis of randomized controlled trials. *Chin Med.* (2020) 15:109. doi: 10.1186/s13020-020-00389-9

19. Dykewicz MS, Wallace DV, Amrol DJ, Baroody FM, Bernstein JA, Craig TJ, et al. Rhinitis 2020: a practice parameter update. *J Allergy ClinImmunol.* (2020) 146:721–67. doi: 10.1016/j.jaci.2020.07.007

20. Robbins MS, Robertson CE, Kaplan E, Ailani J, Charleston IVL, Kuruvilla D, et al. The sphenopalatine ganglion: anatomy, pathophysiology, and therapeutic targeting in headache. *Headache.* (2016) 56:240–58. doi: 10.1111/head.12729

21. Goadsby PJ, Sahai-Srivastava S, Kezirian EJ, Calhoun AH, Matthews DC, McAllister PJ, et al. Safety and efficacy of sphenopalatine ganglion stimulation for chronic cluster headache: a double-blind, randomised controlled trial. *Lancet Neurol.* (2019) 18:1081–90. doi: 10.1016/S1474-4422(19)30322-9

22. Bornstein NM, Saver JL, Diener HC, Gorelick PB, Shuaib A, Solberg Y, et al. An injectable implant to stimulate the sphenopalatine ganglion for treatment of acute ischaemic stroke up to 24 h from onset (ImpACT-24B): an international, randomised, double-blind, sham-controlled, pivotal trial. *Lancet.* (2019) 394:219–29. doi: 10.1016/S0140-6736(19)31192-4

23. Li XW, Tian ZP. A preliminary summary of the treatment on rhinitis puncturing sphenopalatine ganglion. *Beijing Chin Med.* (1990) 9:36–8.

24. Mi J, Chen X, Lin X, Guo J, Chen H, Wei L, et al. Treatment of persistent allergic rhinitis via acupuncture at the sphenopalatine acupoint: a randomized controlled trial. *Trials.* (2018) 19:28. doi: 10.1186/s13063-017-2339-z

25. Wang K, Chen L, Wang Y, Wang C, Zhang L. Sphenopalatine ganglion acupuncture improves nasal ventilation and modulates autonomic nervous activity in healthy volunteers: a randomized controlled study. *Sci Rep.* (2016) 6:29947. doi: 10.1038/srep29947

26. Chan AW, Tetzlaff JM, Gøtzsche PC, Altman DG, Mann H, Berlin JA, et al. SPIRIT 2013 explanation and elaboration: guidance for protocols of clinical trials. *BMJ.* (2013) 346:e7586. doi: 10.1136/bmj.e7586

27. MacPherson H, Altman DG, Hammerschlag R, Youping L, Taixiang W, White A, et al. Revised STandards for reporting interventions in clinical trials of acupuncture (STRICTA): extending the CONSORT statement. *Acupunct Med.* (2010) 28:83–93. doi: 10.1136/aim.2009.001370

28. Bousquet J, Khaltaev N, Cruz AA, Denburg J, Fokkens WJ, Togias A, et al. Allergic rhinitis and its impact on asthma (ARIA) 2008 update (in collaboration with the World Health Organization, GA(2)LEN and Aller- Gen). *Allergy.* (2008) 63(Suppl. 86):8–160.

29. Rondón C, Blanca-López N, Campo P, Mayorga C, Jurado-Escobar R, Torres MJ, et al. Specific immunotherapy in local allergic rhinitis: a randomized, double-blind placebo-controlled trial with *Phleum pratense* subcutaneous allergen immunotherapy. *Allergy.* (2018) 73:905–15. doi: 10.1111/all.13350

30. Meng L, Wang XK, Ouyang ZY, Ren YF, Lu F. Seasonal dynamics of airborne pollen in Beijing Urban area. *Acta Ecol Sin.* (2013) 33:2381–7. doi: 10.5846/stxb201204100502

31. Bousquet PJ, Combescure C, Neukirch F, Klossek JM, Mechin H, Daures JP, et al. Visual analog scales can assess the severity of rhinitis graded according to ARIA guidelines. *Allergy.* (2007) 62:367–72. doi: 10.1111/j.1398-9995.2006.01276.x

32. Zhang WG, Wang ZF, Wu BH. Acupuncture with warmed needle in treating 30 cases of knee osteoarthritis. *J Fujian Coll TCM.* (2007) 17:39–41.

33. Zhang L, Fang DL, Jiang DW, Gao Y, Shi DZ. Can the sphenopalatine ganglion be reached by an acupuncture needle? *Acupunct Med.* (2017) 35:153–5. doi: 10.1136/acupmed-2016-011216

34. Pfaar O, Demoly P, Gerth van Wijk R, Bonini S, Bousquet J, Canonica GW, et al. Recommendations for the standardization of clinical outcomes used in allergen immunotherapy trials for allergic rhinoconjunctivitis: an EAACI position paper. *Allergy.* (2014) 69:854–67. doi: 10.1111/all.12383

35. Pfaar O, Bachert C, Kuna P, Panzner P, Džupinová M, Klimek L, et al. Sublingual allergen immunotherapy with a liquid birch pollen product in patients with seasonal allergic rhinoconjunctivitis with or without asthma. *J Allergy ClinImmunol.* (2019) 143:970–7. doi: 10.1016/j.jaci.2018.11.018

36. Juniper EF, Thompson AK, Ferrie PJ, Roberts JN. Validation of the standardized version of the rhinoconjunctivitis quality of life questionnaire. *J Allergy ClinImmunol.* (1999) 104 (2 Pt 1):364–9. doi: 10.1016/S0091-6749(99)70380-5

37. Juniper EF, Guyatt GH, Griffith LE, Ferrie PJ. Interpretation of rhinoconjunctivitis quality of life questionnaire data. *J Allergy ClinImmunol.* (1996) 98:843–5. doi: 10.1016/S0091-6749(96)70135-5

38. Chen Q, Zhang Q, Jiang L, Li X, Liu Y, Xie Y, et al. Effectiveness of strengthened stimulation during acupuncture for the treatment of allergic rhinitis: study protocol for a randomized controlled trial. *Trials.* (2014) 15:301. doi: 10.1186/1745-6215-15-301

frontiers | Frontiers in Medicine

TYPE Review
PUBLISHED 07 September 2022
DOI 10.3389/fmed.2022.909057

OPEN ACCESS

EDITED BY
Yi Liu,
Shandong Provincial Hospital, China

REVIEWED BY
Andrew Nicholas Harman,
The University of Sydney, Australia
Beatrice Ludovica Ritondo,
University of Rome Tor Vergata, Italy

*CORRESPONDENCE
Xin Yao
yaoxin@njmu.edu.cn

SPECIALTY SECTION
This article was submitted to Pulmonary Medicine, a section of the journal Frontiers in Medicine

RECEIVED 31 March 2022
ACCEPTED 12 August 2022
PUBLISHED 07 September 2022

CITATION
Xuan S, Li Y, Wu Y, Adcock IM, Zeng X and Yao X (2022) Langerin-expressing dendritic cells in pulmonary immune-related diseases. *Front. Med.* 9:909057. doi: 10.3389/fmed.2022.909057

Langerin-expressing dendritic cells in pulmonary immune-related diseases

Shurui Xuan[1], Yuebei Li[1], Yunhui Wu[1], Ian M. Adcock[2], Xiaoning Zeng[1] and Xin Yao[1]*

[1]Department of Respiratory and Critical Care Medicine, The First Affiliated Hospital of Nanjing Medical University, Nanjing, China, [2]Airway Disease Section, National Heart and Lung Institute, Faculty of Medicine, Imperial College London, London, United Kingdom

Dendritic cells (DCs) are "frontline" immune cells dedicated to antigen presentation. They serve as an important bridge connecting innate and adaptive immunity, and express various receptors for antigen capture. DCs are divided into various subclasses according to their differential expression of cell surface receptors and different subclasses of DCs exhibit specific immunological characteristics. Exploring the common features of each sub-category has became the focus of many studies. There are certain amounts of DCs expressing langerin in airways and peripheral lungs while the precise mechanism by which langerin$^+$ DCs drive pulmonary disease is unclear. Langerin-expressing DCs can be further subdivided into numerous subtypes based on the co-expressed receptors, but here, we identify commonalities across these subtypes that point to the major role of langerin. Better understanding is required to clarify key disease pathways and determine potential new therapeutic approaches.

KEYWORDS

pulmonary immune-related disease, langerin, dendritic cells, immunity, pathogenesis

Introduction

Langerin, a C-type lectin receptor (CLR) also known as CD207, was originally found to be highly expressed on Langerhans cells (LCs) that reside in the epidermis of the human skin (1). Later, the existence of langerin$^+$ dermal DCs was clarified as well (2, 3). The disease with a relatively high association with langerin is Langerhans cell histiocytosis (LCH). LCH is a rare disease characterized by heterogeneous lesions, e.g., granulomatous lesions and histiocytosis X lesions, and the pathological features of affected tissues usually manifests as positive staining of CD1a and langerin (4, 5).

Langerin$^+$ DCs were also found in tissues apart from skin including the lung, liver, kidney, and lymphoid tissue (6). To date, there is no comprehensive understanding of the specific function of these langerin$^+$ DCs although LCs have some similar characteristics to other langerin-expressing DCs (7). However, these are not completely equivalent (7), e.g., murine epidermal LCs and dermal langerin-expressing DCs exhibit distinct repopulation kinetics and migratory characteristics *in vitro* and *in vivo*, and play distinct roles in humoral and cellular responses generated by gene gun immunization (7, 8).

There are recent papers declaring that langerin-expressing DCs play a role in pulmonary immune-related disease settings. This article summarizes the immune and pathological relationship between langerin-expressing DCs and pulmonary immune-related diseases whose understanding will provide potential new therapeutic directions.

The expression and characteristics of langerin in MNPs

Langerin was first recognized as an epitope specific to LCs by monoclonal antibody (mAb) DCGM4 staining (1, 9). Langerin mRNA is abundant in freshly isolated LCs while resting DCs generated from $CD34^+$ progenitors treated with GM-CSF and TNFα are identified lower levels of langerin expression (1). LCs were traditionally regarded as a subset of immature DCs residing in epidermis and other mucosal epithelia due to their comparable function and dendritic processes (10, 11). Even though LCs are currently best classified as a type of mononuclear phagocytes (MNPs) distinct from DCs for that LCs are derived similarly to macrophages from the yolk sac during embryogenesis differently from DCs (12). According to the recent literature, we summarize the expression and distribution of langerin in the MNPs in tissue and blood of human and mouse. In human tissue, langerin is expressed by certain conventional DC2 (cDC2) cells from the dermis, lung, tonsil, and liver apart from epidermal LCs under healthy conditions, and it is rapidly induced in blood cDC2 upon tumor growth factor (TGF)-β stimulation (6, 13, 14). With the development of immunological knowledge of DC classification, human inflammatory blood DC3 were identified to express the langerin gene (15). It differs in murine normal tissue for that the expression of langerin was described in mouse cDC1 in view that the co-expressing CD103 (also named αE integrin) is a marker of cDC1 in mouse peripheral tissues (16, 17). Specifically, langerin was reported expressed by 15% of cDC1s in the murine lung (18).

The expression of langerin is regulated by various factors. Mononuclear cells can be induced to form LCs or LC-like DCs using factors such as GM-CSF and IL-4. Bone marrow-derived monocytes enter the peripheral blood and constitute 5% of circulating white blood cells. In response to appropriate stimuli, they migrate from the bloodstream into various peripheral tissues. A study has compared the responses to different maturation signals and antigen-presenting functions between LCs induced by GM-CSF and by M-CSF and demonstrated that GM-CSF can be replaced by M-CSF to some extent (19). Furthermore, TNF-α markedly increased the induction of $langerin^+$ $CD83^-$ LCs from both CD14-negative and CD14-positive precursors (20) whilst TGF-β1 can also affect the development of $langerin^+$ epidermal LCs (21). In addition to some inflammatory factors that promote the increase of langerin, estrogen promotes the formation of a DC population with the unique features of epidermal LCs. The data suggest that differentiation of LCs *in vivo* will be dependent upon the local estrogen levels and estrogen receptor-mediated signaling events in the skin (22). $Langerin^+$ cDCs and LCs are profoundly regulated by the retinoic acid (RA)-RA receptor (RARα) axis in a concentration-dependent manner (23). In addition to cytokines and growth factors such as GM-CSF and TGF-β1, the Notch receptor ligand Delta-1 is a regulator of the induction of human LC development from blood monocytes (24). Moreover, signaling by another Notch ligand JAG2 induces differentiation of $CD14^+$ monocytes into LCH-like cells (25). In addition, inhibition of TNFAIP3, the negative regulator of NF-κB signaling affects Th cell differentiation in the presence of pulmonary $langerin^+$ DCs (18).

Birbeck et al. elucidated the ultrastructure of LCs using electron microscopy (26). LCs have a lobular nucleus surrounded by a clear cytoplasm devoid of tonofilaments, desmosomes, or melanosomes. However, they possess an unique intracytoplasmic organelle which is their characteristic ultrastructural feature: the Birbeck granule (BG) (26, 27). Langerin is involved in the rapid internalization of BGs after mannose-binding *via* endocytosis. Intracellular tracing using an anti-langerin antibody demonstrated that following mannose-binding, langerin was internalized from the cell membrane into the BG (1). Indeed, the distribution and transport of langerin in immature LCs is mainly through the endosomal recycling of BGs. After internalization, langerin relocates back to the cell surface as part of a cell membrane-pericentriolar BG-cell membrane loop (28). Langerin appears to be a key structural element in BG formation due to langerin aggregation (1, 28), and presumably facilitates the uptake of mannans present on the cell surface of bacteria (9). BGs are characterized by the unusual cytoplasmic rod-like or tennis-racket-shaped structures, which can be visualized by electron microscopy as two apposed membranes separated by a striated zipper-like lamella (29). Langerin-deficient mice lack BG and the introduction of the langerin gene into embryonic fibroblasts induces the formation of BG (20). Oda et al. rebuilt the 3D structure of isolated BGs using cryo-electron tomography and identified a flexible loop region within langerin trimers that is crucial for BG formation and viral internalization (30).

Langerin polymorphisms affect both stability and sugar-binding activity. As such, langerin haplotypes may differ in their binding to pathogens and thus might be associated with susceptibility to infection. For example, the W264R form of langerin exhibits large changes in the structure of the CRD that alter its sugar-binding activity. In addition to structural factors, sugar-binding activity is also affected by other physical factors such as pH, temperature, and protein concentrations (31). Other mutations can result in thickened membrane structures compared with the typical cytomembrane sandwiching structures (CMS) of BG. In addition to BG

structures, the affinity for high mannose glycoconjugates is to some extend affected (32).

Immunological functions of langerin in MNPs

Advances in structural biology have provided evidence for the functional role of langerin. Langerin is a type II transmembrane cell surface receptor belonging to the $Ca2^{+}$-dependent CLR family (33, 34). The extracellular domain (ECD) of langerin consists of a neck region containing a series of heptad repeats and a C-terminal C-type carbohydrate-recognition domain (CRD) featuring a glutamate-proline-asparagine (EPN) motif (position 285–287) (22, 35, 36). The extracellular region of langerin exists as a stable trimer kept together by a coiled coil of α-helices formed by the neck region. The CRD exhibits selectivity for mannose, N-Acetylglucosamine (GlcNAc), and fucose (37), but only the trimeric ECD fragment binds to glycoprotein ligands. The ECD binds human high-mannose oligosaccharides as well as yeast invertase mannose-containing structures but not complex glycan structures (36). After antigen capture, langerin internalizes the antigen, e.g., Candida albicans (38), Mycobacterium leprae (39), or HIV-1 (40) *via* the BG. Considering that the expression levels of langerin was markedly reduced along with LCs maturation, Valladeau et al. further confirmed that Langerin is restricted to immature DC (41). While Stoitzner et al. demonstrated that certain expression of langerin on the surface of matured and emigrated DCs were retained in a time-course-dependent manner which suggested that LCs or other langerin^{+} DCs can be traced to the draining lymph nodes by their langerin expression (42). In recent research, langerin were used as one of the markers for immature monocyte-derived DCs (moDCs) (43).

As a sugar-binding protein expressed on the surface of DCs, langerin has a key role in antigen-uptaking when DCs serve as professional antigen-presenting cells to exert immune function. In leprosy, for example, LC-like DCs and freshly isolated epidermal LCs present non-peptide antigens of Mycobacterium leprae to T cell clones derived from a leprosy patient in a CD1a-restricted and langerin-dependent manner (39). In addition, GM-CSF-dependent langerin^{+} CD103^{+} dermal DCs promote CD4^{+} effector Th cell differentiation and play a role in autoimmune pathogenesis (44). Human primary LCs capture the measles virus (MV) through langerin, which then presents MV-derived antigens in the context of HLA class II to MV-specific CD4^{+} T cells independent of CD8^{+} T cells (45). However, the evidence for a critical role of langerin^{+} DCs in CD8^{+} T cell activation do exist after gene gun DNA vaccination as well (46). LCs and cDC1s can mediate different humoral immune response through Langerin which may give us inspiration in development of vaccine effectiveness (47).

Langerin has been proposed as a frontline sentinel in the immunization process, e.g., HIV transmission (48) and Inflammatory Bowel Disease (49). As such, LC-DC clustering *via* langerin leads to DC maturation and facilitates antigen transfer of HIV-1 to DCs, which subsequently induces activation of CD8^{+} T cells (50). In contrast, it has been proposed that HIV-1 captured by langerin is internalized into BGs and then degraded. This would suggest that langerin does not enhance HIV-1 infection of T cells but rather prevents T-cell infection by viral clearance (51). Yet some research has conclusively shown that HIV was effectively transmitted to the primary target CD4^{+} T cells (52–54). The demonstration was confirmed in subsequent studies by Bertram groups (55, 56). Furthermore, langerin was revealed to induce HIV-1 specific humoral immunity in addition to cellular immunity (57). Further research is required in the area to define whether langerin promotes or inhibits immunity and under which specific conditions and if these specific conditions can be artificially controlled. This may open up new avenues for clinical prevention and treatment.

Langerin-expressing DCs in pulmonary immune-related diseases

Within the human lung, langerin is mainly expressed on the lung mucosa and the vascular wall (16). More specifically, staining is seen within the airway epithelium, lung parenchyma, visceral pleura (58), and lung draining LN (DLN) (6), and similar results are obtained in the mouse (33). Despite the link between skin and lung disease through the atopic march (59), research into the function of langerin in the lung and airway immune-related disease has not been studied in depth with much relating to the analysis of relative expression profiles in disease. Nevertheless, we can still speculate on the possible role of langerin based on the available evidence as shown in Table 1 to inspire more further research.

Lung carcinoma

Early studies examined langerin expression in bronchial biopsies of primary lung carcinomas from 12 patients and found infiltration of DCs within tumor tissues including LCs and CD1a^{+}/langerin^{+} cells interspersed among tumor cells (60). More recent research using high-throughput sequencing has provided a more complete picture of langerin expression in lung cancer. The depletion of langerin^{+} DCs before and after vaccination with VLP-gp33r (a lymphocytic choriomeningitis virus–derived peptide antigen) inhibits the growth of Lewis' lung carcinoma tumors expressing gp33 (LL-LCMV), leading to reduced cytotoxic CD8^{+} T cell activity. This highlights the importance of langerin in antigen cross-presentation of tumor peptides (61). In general, langerin plays a positive role

TABLE 1 Potential functions of langerin in pulmonary diseases.

Pulmonary diseases	Langerin potential functions	Immune trend
Lung carcinoma	Tumor peptides cross-presentation	$CD8^+$ T cell activation (61)
Asthma	Induce and maintain Th2 response	$CD4^+$ T cell activation (68)
Pulmonary fibrosis and PLCH	Pathogenic mutations	MAPK signaling alterations (86)
COPD	Induce Th1 response reacting to CS	$CD4^+$ T cell activation (89)
Microbial infection	Pathogen scouting	Neutrophil and macrophage recruitment (100)

CS, Cigarette smoking; MAPK, Mitogen-activated protein kinase.

in promoting the immune response during tumor immunity, which has been seen in other tumors such as oral cavity primary squamous cell carcinoma (62). In breast cancer tissues, CD1a and langerin staining was found in one-third of primary tumors but this did not correlate with clinicopathological data (63). This was divergent from previous findings from the same group that most LCs were resident within all tumor samples (64). However, with the update of cognition of immunological markers, CD1a and langerin expression may not discriminate LCs from $langerin^+$ cDC2 or $CD11c^+$ epidermal DCs (48, 55). It may lead to completely different conclusions in subsequent research.

In addition, tumor cells were found to promote langerin expression. Some, but not all, lung carcinomas produced GM-CSF and a good correlation exists between GM-CSF production and the number of $CD1a^+$ LCs infiltrating these tumors (65). Breast cancer cells can chemoattract $CD34^+$ progenitor cells through CCL20/MIP3α and promote the differentiation of progenitor cells into $langerin^+$ DCs depending upon the level of TGF-β present. These $langerin^+$ DCs differentiate into two types: $CD1a^+$ $langerin^+$ $CD86^+$ and $CD1a^{high}$ $langerin^-$ $CD86^-$ cells (66).

Using The Cancer Genome Atlas (TCGA) we analyzed the expression of langerin in Lung Squamous Cell Carcinoma (LUSC) (Figure 1A) and Lung Adenocarcinoma (LUAD) (Figure 1C) to identify any differential expression and the pathways associated with langerin up-regulation. Using this large database, we found significant up-regulation of langerin in both LUSC and LUAD which was associated with distinct gene ontology (GO) molecular pathways only some of which overlapped. The analysis showed that langerin in the two types of lung tumor was both positively correlated with immunity related signaling pathways, e.g., antigen processing and presentation, and endogenous lipid antigen *via* MHC class Ib (Figures 1B,D). These data provide a basis for further research on the role of langerin in tumor pathogenesis.

Asthma

In asthma, DCs are important not only for inducing T helper (Th) 2-cell sensitization but also for maintaining effector Th2-cell responses during ongoing allergic disease (67). In a mouse model of house dust mite-induced allergic asthma, subsequent LPS exposure resulted in enhanced migration of $langerin^+$ DCs from the lung to the draining lymph node and LPS-exposed $langerin^+$ DCs instructed $CD4^+$ T cells toward a Th2 response. Selective depletion of $langerin^+$ DCs prevented LPS-induced eosinophil recruitment and T-cell activation (68). In addition, langerin expression was up-regulated in induced sputum from asthmatic subjects and correlated with airway coagulation factor XIII (FXIII) and airflow limitation (69). Moreover, asthmatic human respiratory-tract DCs (hRTDC) expressed significantly higher levels of langerin than equivalent cells from control subjects. In addition, $langerin^+$ cells from sputum co-cultured with naive T cells increased T cell proliferation 2.5-fold (70). These results suggest potential langerin-specific novel therapeutic approaches for the treatment of severe asthma with irreversible airflow obstruction.

The largest lung DC population are the integrin αEβ7 positive and $I\text{-}A^{high}$ $CD11c^{high}$-DC population which express high levels of langerin and act to enable efficient antigen uptake and presentation (16). However, in an analysis of large airways and bronchopulmonary LNs in fatal asthma (FA), there were no statistical differences in the expression of $langerin^+$ DCs between the FA patients and control subjects (71). These differences in the expression of $langerin^+$ DCs in different studies may be due to analysis of different asthma immunophenotypes and/ or an effect of therapy. In addition, different sampling locations such as sputum, BALF, large airways, and bronchopulmonary LNs may contain different numbers of $langerin^+$ DCs. Therefore, further research is needed to elucidate the role of langerin in the pathogenesis and progression of asthma taking disease severity and subphenotypes into account.

Pulmonary fibrosis and pulmonary LCH

Pulmonary fibrosis is an umbrella term that covers idiopathic pulmonary fibrosis (IPF) and non-specific interstitial pneumonia, importantly the characteristics of the immature DCs that infiltrate during fibrosis and epithelial hyperplasia in these diseases are similar (72). Intraepithelial infiltrating $CD1a^+$/$langerin^+$ DCs committed to mucosal immunologic surveillance (73). High levels of langerin staining are also seen in sites of fibrosis in PLCH, which may indicate an important

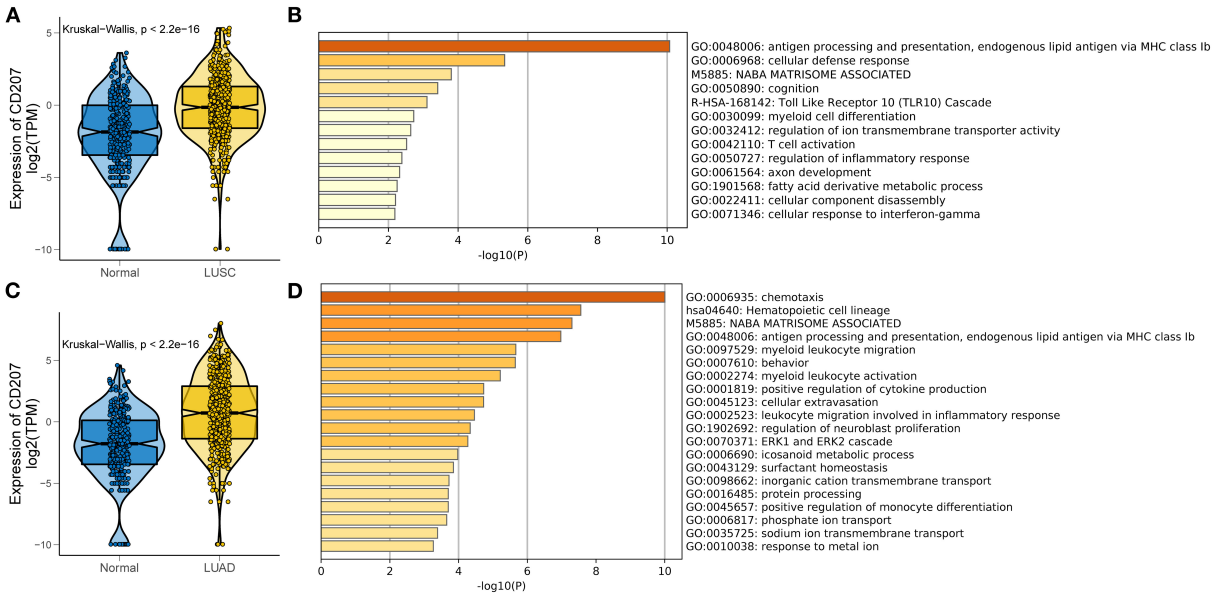

FIGURE 1
Expression and functional annotation of langerin in LUSC and LUAD in the TCGA RNA-seq datasets. **(A,C)** Boxplots visualizing significantly different expressions of langerin between normal and LUSC (and LUAD) tissues in TCGA database. **(B,D)** Bar plot showing the top 20 terms derived from the gene set enrichment of the differentially expressed genes in TCGA-LUSC (and LUAD) samples. The x-axis represents statistical significance.

connection between langerin expression and the pathological changes of fibrosis (74).

In adults, pulmonary LCH (PLCH) occurs predominantly in young smokers or ex-smokers (>90% of cases) with a peak incidence between the ages of 20 and 40 (75, 76). Patients with PLCH develop shortness of breath, pleuritic pain, or spontaneous pneumothoraces. There is evidence of obstruction, air trapping, and decreased carbon monoxide diffusing capacity (DLCO) which may help to identify patients with a poor prognosis (77). High-Resolution Computed Tomographic (HRCT) imaging of the chest is critical in the diagnosis of suspected PLCH and typically shows a combination of nodules, cavitated nodules, thick- and thin-walled cysts (78–80). Transbronchial lung biopsy is diagnostic in about 30% of cases and is valuable in excluding other diagnoses that mimic PLCH (81). PLCH presents as accumulation of LCs and other langerin-expressing DCs in the lungs (82). A comparison of BAL samples of patients with PLCH, sarcoidosis or IPF, found that patients suffering from PLCH had a significantly higher number of $CD1a^+$ and $langerin^+$ cells than the subjects with sarcoidosis and IPF (74).

A similar comparison was made between LCH and other interstitial, inflammatory, and infectious diseases as well. Counting the number of cells staining per high power field (400 x) in areas of highest density indicates that the number of $CD1a^+$ and $langerin^+$ cells in LCH lesions is more than two-fold that in interstitial pneumonia (83). Additional research has reported that Langerhans-like $CD1a^+$ cells are present with NRAS and BRAF mutations in patients (84), providing new insights into the pathogenesis of the disease. To date, langerin has been used as a diagnostic index of PLCH (85), but its true role in the pathophysiology or the intrapulmonary mechanism of the disease requires elucidation. A recently published report presents consensus recommendations that resulted from the discussions at the annual Histiocyte Society meeting in 2019 (5) which propose that the single-system PLCH may indeed be a clonal process for that recurrent Mitogen-activated protein kinase (MAPK) pathway alterations and BRAF-V600E mutations have been identified in lesions (86, 87). All questions are urgent for answers.

Chronic obstructive pulmonary disease

There is a significantly higher expression of langerin mRNA in human COPD lung tissue compared with those from healthy control subjects (88). The primary cause of COPD for most subjects is tobacco smoking, with other causes being air pollution and genetics. Interestingly, immunohistochemical staining of langerin expression in the small airways revealed more LC-type DCs (identified by langerin and the presence of BG) in current smokers without COPD and in COPD patients, vs. never smokers and ex-smokers without COPD (89). PLCH, which occurs predominantly in young smokers or ex-smokers, has high langerin positivity as a diagnostic indicator and shows the pathological manifestations in end-stage disease

(dense fibrosis, cystic changes, and honeycomb lungs) that are similar to that of emphysema. This suggests that langerin is involved in the pathophysiology of COPD particularly with lung destruction and airway remodeling. Taniguchi et al. firstly generate a glycosyltransferase, α1,6-fucosyltransferase (Fut8) knockout mice to discover COPD-like phenotypes in mouse model (90–93). To develop an effective clinical therapy application, candidate glycan keratan sulfate (KS) and the di-sulfated KS disaccharide L4, which were identified as specific glycan ligands to Langerin (94). It was supposed that KS-based glycomimetics may protect hijacking by viruses or bacteria in a langerin-dependent manner (95).

Microbial infection

Mediastinal lymph nodes contain increased numbers of cells co-expressing langerin and CD103 when the lung is infected with the virus, and depletion of lung langerin$^+$ DCs in langerin-DTR mice aggravates the severity of infection (96). Study of viral infection reveals that CD103$^+$ langerin$^+$ double-positive dermal DCs and langerin$^+$ epidermal LCs firstly upregulate innate immune response in the draining lymph node (97). CD103 binds integrin β7-ITGB7 to form the complete heterodimeric integrin molecule αEβ7 that the chief ligand is epithelial cellular adhesion molecule E-cadherin. Some CD103-expressing immune cells primarily reside on the epithelium in order to rapidly respond to both viral and bacterial infection (98). The considerable co-expression of langerin and CD103 inspire that whether there is related regulation of their, respectively, expression and whether αEβ7/E-cadherin-interaction enhance the receptor function of langerin.

As mentioned above, langerin is able to capture virus particles including HIV although the precise mechanism involved is unclear. Studies are underway in procaine models of infection to elucidate the key pathways by which langerin impacts lung viral infection (99). Furthermore, there is evidence that langerin plays a role in pathogen sensing, neutrophil and macrophage recruitment, and the downstream inflammatory processes. This is an exciting area for future research that may provide novel non-macrolide work therapeutic targets for acute exacerbations of lung diseases (100).

Conclusion

The current understanding of the role of langerin-expressing DCs in pulmonary diseases is lacking details although the evidence suggests that langerin plays a role in both the immuno-inflammatory aspects of the disease as well as on structural remodeling and exacerbations. DCs are key cells in initiating adaptive immunity and langerin acts as its surface receptor to sense external stimuli. However, it is clear that langerin possesses additional functions that make it an interesting target for future research. Considering the important role played by DCs in the pathogenesis of immune disorder of the lungs and airways, a deeper insight into langerin mechanisms may provide novel therapeutic modalities for immune and structural aspects of pulmonary immune-related diseases.

Author contributions

Conception and design: XY, SX, and YW. Manuscript writing: SX. Data analysis and interpretation: YL. Collection and assembly of literature: SX and YW. Language editing and proofreading: IA and XZ. Final approval of manuscript: all authors.

Funding

This research was supported by National Natural Science Foundation of China (No. 81870039).

Acknowledgments

The authors thank Liang Zhao for advice on bioinformatics analysis and thank Heng Fu for his support.

Conflict of interest

The authors declare that the research was conducted in the absence of any commercial or financial relationships that could be construed as a potential conflict of interest.

Publisher's note

References

1. Valladeau J, Ravel O, Dezutter-Dambuyant C, Moore K, Kleijmeer M, Liu Y, et al. Langerin, a novel C-type lectin specific to Langerhans cells, is an endocytic receptor that induces the formation of Birbeck granules. *Immunity.* (2000) 12:71–81. doi: 10.1016/S1074-7613(00)80160-0

2. Poulin LF, Henri S, de Bovis B, Devilard E, Kissenpfennig A, Malissen B. The dermis contains langerin+ dendritic cells that develop and function independently of epidermal Langerhans cells. *J Exp Med.* (2007) 204:3119–31. doi: 10.1084/jem.20071724

3. Bursch LS, Wang L, Igyarto B, Kissenpfennig A, Malissen B, Kaplan DH, et al. Identification of a novel population of Langerin+ dendritic cells. *J Exp Med.* (2007) 204:3147–56. doi: 10.1084/jem.20071966

4. Peters TL, McClain KL, Allen CE. Neither IL-17A mRNA nor IL-17A protein are detectable in Langerhans cell histiocytosis lesions. *Mol Ther.* (2011) 19:1433–9. doi: 10.1038/mt.2011.106

5. Goyal G, Tazi A, Go RS, Rech KL, Picarsic JL, Vassallo R, et al. International expert consensus recommendations for the diagnosis and treatment of Langerhans cell histiocytosis in adults. *Blood J Am Soc Hematol.* (2022) 139:2601–21. doi: 10.1182/blood.2021014343

6. Bigley V, McGovern N, Milne P, Dickinson R, Pagan S, Cookson S, et al. Langerin-expressing dendritic cells in human tissues are related to CD1c+ dendritic cells and distinct from Langerhans cells and CD141high XCR1+ dendritic cells. *J Leukoc Biol.* (2015) 97:627–34. doi: 10.1189/jlb.1HI0714-351R

7. Merad M, Ginhoux F, Collin M. Origin, homeostasis and function of Langerhans cells and other langerin-expressing dendritic cells. *Nat Rev Immunol.* (2008) 8:935–47. doi: 10.1038/nri2455

8. Nagao K, Ginhoux F, Leitner WW, Motegi S-I, Bennett CL, Clausen BE, et al. Murine epidermal Langerhans cells and langerin-expressing dermal dendritic cells are unrelated and exhibit distinct functions. *Proc Natl Acad Sci.* (2009) 106:3312–7. doi: 10.1073/pnas.0807126106

9. Valladeau J, Duvert-Frances V, Pin J-J, Dezutter-Dambuyant C, Vincent C, Massacrier C, et al. The monoclonal antibody DCGM4 recognizes Langerin, a protein specific of Langerhans cells, and is rapidly internalized from the cell surface. *Eur J Immunol.* (1999) 29:2695–704. doi: 10.1002/(SICI)1521-4141(199909)29:09<2695::AID-IMMU2695>3.0.CO;2-Q

10. Mohamadzadeh M, Berard F, Essert G, Chalouni C, Pulendran B, Davoust J, et al. Interleukin 15 skews monocyte differentiation into dendritic cells with features of Langerhans cells. *J Exp Med.* (2001) 194:1013–20. doi: 10.1084/jem.194.7.1013

11. Girolomoni G, Simon JC, Bergstresser PR, Cruz PD. Freshly isolated spleen dendritic cells and epidermal Langerhans cells undergo similar phenotypic and functional changes during short-term culture. *J Immunol.* (1990) 145:2820–6.

12. Vine EE, Rhodes JW, Warner van Dijk FA, Byrne SN, Bertram KM, Cunningham AL, Harman AN. HIV transmitting mononuclear phagocytes; integrating the old and new. *Mucosal Immunol.* (2022) 15:542–50. doi: 10.1038/s41385-022-00492-0

13. Harman AN, Bye CR, Nasr N, Sandgren KJ, Kim M, Mercier SK, et al. Identification of lineage relationships and novel markers of blood and skin human dendritic cells. *J Immunol.* (2013) 190:66–79. doi: 10.4049/jimmunol.1200779

14. Chun IY, Becker C, Wang Y, Marches F, Helft J, Leboeuf M, et al. Human CD1c+ dendritic cells drive the differentiation of CD103+ CD8+ mucosal effector T cells *via* the cytokine TGF-β. *Immunity.* (2013) 38:818–30. doi: 10.1016/j.immuni.2013.03.004

15. Cytlak U, Resteu A, Pagan S, Green K, Milne P, Maisuria S, et al. Differential IRF8 transcription factor requirement defines two pathways of dendritic cell development in humans. *Immunity.* (2020) 53:353–70. doi: 10.1016/j.immuni.2020.07.003

16. Sung S-SJ, Fu SM, Rose CE, Gaskin F, Ju S-T, Beaty SR, et al. major lung CD103 (αE)-β7 integrin-positive epithelial dendritic cell population expressing Langerin and tight junction proteins. *J Immunol.* (2006) 176:2161–72. doi: 10.4049/jimmunol.176.4.2161

17. Bedoui S, Whitney PG, Waithman J, Eidsmo L, Wakim L, Caminschi I, et al. Cross-presentation of viral and self antigens by skin-derived CD103+ dendritic cells. *Nat Immunol.* (2009) 10:488–95. doi: 10.1038/ni.1724

18. Vroman H, van Uden D, Bergen IM, van Hulst JA, Lukkes M, van Loo G, et al. Tnfaip3 expression in pulmonary conventional type 1 Langerin-expressing dendritic cells regulates T helper 2-mediated airway inflammation in mice. *Allergy.* (2020) 75:2587–98. doi: 10.1111/all.14334

19. Mollah ZU, Aiba S, Nakagawa S, Hara M, Manome H, Mizuashi M, et al. Macrophage colony-stimulating factor in cooperation with transforming growth factor-β1 induces the differentiation of CD34+ hematopoietic progenitor cells into Langerhans cells under serum-free conditions without granulocyte-macrophage colony-stimulating factor. *J Invest Dermatol.* (2003) 120:256–65. doi: 10.1046/j.1523-1747.2003.12036.x

20. Arrighi J-F, Soulas C, Hauser C, Saeland S, Chapuis B, Zubler RH, et al. TNF-α induces the generation of Langerin/(CD207)+ immature Langerhans-type dendritic cells from both CD14–CD1a–and CD14+ CD1a–precursors derived from CD34+ cord blood cells. *Eur J Immunol.* (2003) 33:2053–63. doi: 10.1002/eji.200323714

21. Kaplan DH, Li MO, Jenison MC, Shlomchik WD, Flavell RA, Shlomchik MJ. Autocrine/paracrine TGFβ1 is required for the development of epidermal Langerhans cells. *J Exp Med.* (2007) 204:2545–52. doi: 10.1084/jem.20071401

22. Mao A, Paharkova-Vatchkova V, Hardy J, Miller MM, Kovats S. Estrogen selectively promotes the differentiation of dendritic cells with characteristics of Langerhans cells. *J Immunol.* (2005) 175:5146–51. doi: 10.4049/jimmunol.175.8.5146

23. Hashimoto-Hill S, Friesen L, Park S, Im S, Kaplan MH, Kim CH. RARα supports the development of Langerhans cells and langerin-expressing conventional dendritic cells. *Nat Commun.* (2018) 9:1–13. doi: 10.1038/s41467-018-06341-8

24. Hoshino N, Katayama N, Shibasaki T, Ohishi K, Nishioka J, Masuya M, et al. A novel role for Notch ligand Delta-1 as a regulator of human Langerhans cell development from blood monocytes. *J Leukoc Biol.* (2005) 78:921–9. doi: 10.1189/jlb.1204746

25. Schwentner R, Jug G, Kauer MO, Schnöller T, Waidhofer-Söllner P, Holter W, et al. JAG2 signaling induces differentiation of CD14+ monocytes into Langerhans cell histiocytosis-like cells. *J Leukoc Biol.* (2019) 105:101–11. doi: 10.1002/JLB.1A0318-098R

26. Birbeck MS, Breathnach AS, Everall JD. An electron microscope study of basal melanocytes and high-level clear cells (langerhans cells) in vitiligo. *J Invest Dermatol.* (1961) 37:51–64. doi: 10.1038/jid.1961.80

27. Valladeau J, Dezutter-Dambuyant C, Saeland S. Langerin/CD207 sheds light on formation of birbeck granules and their possible function in Langerhans cells. *Immunol Res.* (2003) 28:93–107. doi: 10.1385/IR:28:2:93

28. Mc Dermott R, Ziylan U, Spehner D, Bausinger H, Lipsker D, Mommaas M, et al. Birbeck granules are subdomains of endosomal recycling compartment in human epidermal Langerhans cells, which form where Langerin accumulates. *Mol Biol Cell.* (2002) 13:317–35. doi: 10.1091/mbc.01-06-0300

29. Wolff K. The fine structure of the Langerhans cell granule. *J Cell Biol.* (1967) 35:468. doi: 10.1083/jcb.35.2.468

30. Oda T, Yanagisawa H, Shinmori H, Ogawa Y, Kawamura T. Cryo-electron tomography of Birbeck granules reveals the molecular mechanism of langerin lattice formation. *bioRxiv.* (2022) 11:e79990. doi: 10.1101/2022.02.24.481763

31. Ward EM, Stambach NS, Drickamer K, Taylor ME. Polymorphisms in human langerin affect stability and sugar binding activity. *J Biol Chem.* (2006) 281:15450–6. doi: 10.1074/jbc.M511502200

32. Chabrol E, Thépaut M, Dezutter-Dambuyant C, Vivès C, Marcoux J, Kahn R, et al. Alteration of the langerin oligomerization state affects Birbeck granule formation. *Biophys J.* (2015) 108:666–77. doi: 10.1016/j.bpj.2014.10.075

33. Takahara K, Omatsu Y, Yashima Y, Maeda Y, Tanaka S, Iyoda T, et al. Identification and expression of mouse Langerin (CD207) in dendritic cells. *Int Immunol.* (2002) 14:433–44. doi: 10.1093/intimm/14.5.433

34. Van Der Vlist M, Geijtenbeek TB. Langerin functions as an antiviral receptor on Langerhans cells. *Immunol Cell Biol.* (2010) 88:410–5. doi: 10.1038/icb.2010.32

35. Weis WI, Taylor ME, Drickamer K. The C-type lectin superfamily in the immune system. *Immunol Rev.* (1998) 163:19–34. doi: 10.1111/j.1600-065X.1998.tb01185.x

36. Stambach NS, Taylor ME. Characterization of carbohydrate recognition by langerin, a C-type lectin of Langerhans cells. *Glycobiology.* (2003) 13:401–10. doi: 10.1093/glycob/cwg045

37. Galustian C, Park CG, Chai W, Kiso M, Bruening SA, Kang Y-S, et al. High and low affinity carbohydrate ligands revealed for murine SIGN-R1 by carbohydrate array and cell binding approaches, and differing specificities for SIGN-R3 and langerin. *Int Immunol.* (2004) 16:853–66. doi: 10.1093/intimm/dxh089

38. de Jong MA, Vriend LE, Theelen B, Taylor ME, Fluitsma D, Boekhout T, et al. C-type lectin Langerin is a β-glucan receptor on human Langerhans cells that recognizes opportunistic and pathogenic fungi. *Mol Immunol.* (2010) 47:1216–25. doi: 10.1016/j.molimm.2009.12.016

39. Hunger RE, Sieling PA, Ochoa MT, Sugaya M, Burdick AE, Rea TH, et al. Langerhans cells utilize CD1a and langerin to efficiently present nonpeptide antigens to T cells. *J Clin Invest.* (2004) 113:701–8. doi: 10.1172/JCI200419655

40. Pena-Cruz V, Agosto LM, Akiyama H, Olson A, Moreau Y, Larrieux J-R, et al. HIV-1 replicates and persists in vaginal epithelial dendritic cells. *J Clin Invest.* (2018) 128:3439–44. doi: 10.1172/JCI98943

41. Valladeau J, Clair-Moninot V, Dezutter-Dambuyant C, Pin J-J, Kissenpfennig A, Mattéi M-G, et al. Identification of mouse langerin/CD207 in Langerhans cells and some dendritic cells of lymphoid tissues. *J Immunol.* (2002) 168:782–92. doi: 10.4049/jimmunol.168.2.782

42. Stoitzner P, Holzmann S, McLellan AD, Ivarsson L, Stössel H, Kapp M, et al. Visualization and characterization of migratory Langerhans cells in murine skin and lymph nodes by antibodies against Langerin/CD207. *J Invest Dermatol.* (2003) 120:266–74. doi: 10.1046/j.1523-1747.2003.12042.x

43. Hinata M, Kunita A, Abe H, Morishita Y, Sakuma K, Yamashita H, et al. Exosomes of Epstein-Barr virus-associated gastric carcinoma suppress dendritic cell maturation. *Microorganisms.* (2020) 8:1776. doi: 10.3390/microorganisms8111776

44. King IL, Kroenke MA, Segal BM. GM-CSF–dependent, CD103+ dermal dendritic cells play a critical role in Th effector cell differentiation after subcutaneous immunization. *J Exp Med.* (2010) 207:953–61. doi: 10.1084/jem.20091844

45. van der Vlist M, de Witte L, de Vries RD, Litjens M, de Jong MA, Fluitsma D, et al. Human Langerhans cells capture measles virus through Langerin and present viral antigens to CD4+ T cells but are incapable of cross-presentation. *Eur J Immunol.* (2011) 41:2619–31. doi: 10.1002/eji.201041305

46. Stoecklinger A, Eticha TD, Mesdaghi M, Kissenpfennig A, Malissen B, Thalhamer J, et al. Langerin+ dermal dendritic cells are critical for CD8+ T cell activation and IgH γ-1 class switching in response to gene gun vaccines. *J Immunol.* (2011) 186:1377–83. doi: 10.4049/jimmunol.1002557

47. Bouteau A, Kervevan J, Su Q, Zurawski SM, Contreras V, Dereuddre-Bosquet N, et al. subsets regulate humoral immune responses by supporting the differentiation of distinct Tfh cells. *Front Immunol.* (2019) 10:1134. doi: 10.3389/fimmu.2019.01134

48. Rhodes JW, Botting RA, Bertram KM, Vine EE, Rana H, Baharlou H, et al. Human anogenital monocyte-derived dendritic cells and langerin+ cDC2 are major HIV target cells. *Nat Commun.* (2021) 12:1–15. doi: 10.1038/s41467-021-22375-x

49. Fenton TM, Kelly A, Shuttleworth EE, Smedley C, Atakilit A, Powrie F, et al. Inflammatory cues enhance TGFβ activation by distinct subsets of human intestinal dendritic cells *via* integrin αvβ8. *Mucosal Immunol.* (2017) 10:624–34. doi: 10.1038/mi.2016.94

50. Ahmed Z, Kawamura T, Shimada S, Piguet V. The role of human dendritic cells in HIV-1 infection. *J Invest Dermatol.* (2015) 135:1225–33. doi: 10.1038/jid.2014.490

51. de Witte L, Nabatov A, Pion M, Fluitsma D, De Jong MA, de Gruijl T, et al. Langerin is a natural barrier to HIV-1 transmission by Langerhans cells. *Nat Med.* (2007) 13:367–71. doi: 10.1038/nm1541

52. Hladik F, Sakchalathorn P, Ballweber L, Lentz G, Fialkow M, Eschenbach D, et al. Initial events in establishing vaginal entry and infection by human immunodeficiency virus type-1. *Immunity.* (2007) 26:257–70. doi: 10.1016/j.immuni.2007.01.007

53. Ganor Y, Zhou Z, Tudor D, Schmitt A, Vacher-Lavenu MC, Gibault L, et al. Within 1 h, HIV-1 uses viral synapses to enter efficiently the inner, but not outer, foreskin mucosa and engages Langerhans–T cell conjugates. *Mucosal Immunol.* (2010) 3:506–22. doi: 10.1038/mi.2010.32

54. Patterson BK, Landay A, Siegel JN, Flener Z, Pessis D, Chaviano A, et al. Susceptibility to human immunodeficiency virus-1 infection of human foreskin and cervical tissue grown in explant culture. *Am J Pathol.* (2002) 161:867–73. doi: 10.1016/S0002-9440(10)64247-2

55. Bertram KM, Botting RA, Baharlou H, Rhodes JW, Rana H, Graham JD, et al. Identification of HIV transmitting CD11c+ human epidermal dendritic cells. *Nat Commun.* (2019) 10:1–15. doi: 10.1038/s41467-019-10697-w

56. Bertram KM, Truong NR, Smith JB, Kim M, Sandgren KJ, Feng KL, et al. Herpes Simplex Virus type 1 infects Langerhans cells and the novel epidermal dendritic cell, Epi-cDC2s, *via* different entry pathways. *PLoS Pathog.* (2021) 17:e1009536. doi: 10.1371/journal.ppat.1009536

57. Kervevan J, Bouteau A, Lanza JS, Hammoudi A, Zurawski S, Surenaud M, et al. Targeting human langerin promotes HIV-1 specific humoral immune responses. *PLoS Pathog.* (2021) 17:e1009749. doi: 10.1371/journal.ppat.1009749

58. Sertl K, Takemura T, Tschachler E, Ferrans VJ, Kaliner MA, Shevach EM. Dendritic cells with antigen-presenting capability reside in airway epithelium, lung parenchyma, and visceral pleura. *J Exp Med.* (1986) 163:436–51. doi: 10.1084/jem.163.2.436

59. Paller AS, Spergel JM, Mina-Osorio P, Irvine AD. The atopic march and atopic multimorbidity: many trajectories, many pathways. *J Allergy Clin Immunol.* (2019) 143:46–55. doi: 10.1016/j.jaci.2018.11.006

60. Bergeron A, El Hage F, Kambouchner M, Lecossier D, Tazi A. Characterisation of dendritic cell subsets in lung cancer micro-environments. *Eur Respir J.* (2006) 28:1170–7. doi: 10.1183/09031936.06.00114205

61. Li K, Peers-Adams A, Win SJ, Scullion S, Wilson M, Young VL, et al. Antigen incorporated in virus-like particles is delivered to specific dendritic cell subsets that induce an effective antitumor immune response *in vivo*. *J Immunother.* (2013) 36:11–9. doi: 10.1097/CJI.0b013e3182787f5e

62. O'Donnell RK, Mick R, Feldman M, Hino S, Wang Y, Brose MS, et al. Distribution of dendritic cell subtypes in primary oral squamous cell carcinoma is inconsistent with a functional response. *Cancer Lett.* (2007) 255:145–52. doi: 10.1016/j.canlet.2007.04.003

63. Treilleux I, Blay J-Y, Bendriss-Vermare N, Ray-Coquard I, Bachelot T, Guastalla J-P, et al. Dendritic cell infiltration and prognosis of early stage breast cancer. *Clin Cancer Res.* (2004) 10:7466–74. doi: 10.1158/1078-0432.CCR-04-0684

64. Bell D, Chomarat P, Broyles D, Netto G, Harb GM, Lebecque S, et al. In breast carcinoma tissue, immature dendritic cells reside within the tumor, whereas mature dendritic cells are located in peritumoral areas. *J Exp Med.* (1999) 190:1417–26. doi: 10.1084/jem.190.10.1417

65. Tazi A, Bouchonnet F, Grandsaigne M, Boumsell L, Hance AJ, Soler P. Evidence that granulocyte macrophage-colony-stimulating factor regulates the distribution and differentiated state of dendritic cells/Langerhans cells in human lung and lung cancers. *J Clin Invest.* (1993) 91:566–76. doi: 10.1172/JCI116236

66. Thomachot MC, Bendriss-Vermare N, Massacrier C, Biota C, Treilleux I, Goddard S, et al. Breast carcinoma cells promote the differentiation of CD34+ progenitors towards 2 different subpopulations of dendritic cells with CD1ahighCD86- Langerin-and CD1a+ CD86+ Langerin+ phenotypes. *Int J Cancer.* (2004) 110:710–20. doi: 10.1002/ijc.20146

67. Hammad H, Lambrecht BN. Dendritic cells and epithelial cells: linking innate and adaptive immunity in asthma. *Nat Rev Immunol.* (2008) 8:193–204. doi: 10.1038/nri2275

68. Ortiz-Stern A, Kanda A, Mionnet C, Cazareth J, Lazzari A, Fleury S, et al. Langerin+ dendritic cells are responsible for LPS-induced reactivation of allergen-specific Th2 responses in postasthmatic mice. *Mucosal Immunol.* (2011) 4:343–53. doi: 10.1038/mi.2010.73

69. Esnault S, Kelly EA, Sorkness RL, Evans MD, Busse WW, Jarjour NN. Airway factor XIII associates with type 2 inflammation and airway obstruction in asthmatic patients. *J Allergy Clin Immunol.* (2016) 137:767–73. doi: 10.1016/j.jaci.2015.05.053

70. McCarthy NE, Jones HA, Marks NA, Shiner RJ, Ind PW, Al-Hassi HO, et al. Inhaled allergen-driven CD1c up-regulation and enhanced antigen uptake by activated human respiratory-tract dendritic cells in atopic asthma. *Clin Exp Allergy.* (2007) 37:72–82. doi: 10.1111/j.1365-2222.2006.02631.x

71. Cagnoni EF, Ferreira DS, da Silva LFF, Petry ALNC, dos Santos ABG, Medeiros MCR, et al. Bronchopulmonary lymph nodes and large airway cell trafficking in patients with fatal asthma. *J Allergy Clin Immunol.* (2015) 135:1352–7. doi: 10.1016/j.jaci.2014.08.021

72. Marchal-Sommé J, Uzunhan Y, Marchand-Adam S, Kambouchner M, Valeyre D, Crestani B, et al. Dendritic cells accumulate in human fibrotic interstitial lung disease. *Am J Respir Crit Care Med.* (2007) 176:1007–14. doi: 10.1164/rccm.200609-1347OC

73. Vermaelen K, Pauwels R. Pulmonary dendritic cells. *Am J Respir Crit Care Med.* (2005) 172:530–51. doi: 10.1164/rccm.200410-1384SO

74. Smetana K, Měrička O, Saeland S, Homolka J, Brabec J, Gabius H-J. Diagnostic relevance of Langerin detection in cells from bronchoalveolar lavage of patients with pulmonary Langerhans cell histiocytosis, sarcoidosis and idiopathic pulmonary fibrosis. *Virchows Arch.* (2004) 444:171–4. doi: 10.1007/s00428-003-0952-6

75. Vassallo R, Harari S, Tazi A. Current understanding and management of pulmonary Langerhans cell histiocytosis. *Thorax.* (2017) 72:937–45. doi: 10.1136/thoraxjnl-2017-210125

76. Schönfeld N, Frank W, Wenig S, Uhrmeister P, Allica E, Preussler H, et al. Clinical and radiologic features, lung function and therapeutic results in pulmonary histiocytosis X. *Respiration.* (1993) 60:38–44. doi: 10.1159/000196171

77. Vassallo R, Ryu JH, Schroeder DR, Decker PA, Limper AH. Clinical outcomes of pulmonary Langerhans'-cell histiocytosis in adults. *N Engl J Med.* (2002) 346:484–90. doi: 10.1056/NEJMoa012087

78. Tazi A. Adult pulmonary Langerhans' cell histiocytosis. *Eur Respir J.* (2006) 27:1272–85. doi: 10.1183/09031936.06.00024004

79. Zinn DJ, Chakraborty R, Allen CE. Langerhans cell histiocytosis: emerging insights and clinical implications. *Oncol Williston Park NY.* (2016) 30:122–32.

80. Vassallo R, Ryu JH, Colby TV, Hartman T, Limper AH. Pulmonary Langerhans'-cell histiocytosis. *N Engl J Med.* (2000) 342:1969–78. doi: 10.1056/NEJM200006293422607

81. Harari S, Torre O, Cassandro R, Taveira-DaSilva AM, Moss J. Bronchoscopic diagnosis of Langerhans cell histiocytosis and lymphangioleiomyomatosis. *Respir Med.* (2012) 106:1286–92. doi: 10.1016/j.rmed.2012.06.012

82. Badalian-Very G, Vergilio J-A, Fleming M, Rollins BJ. Pathogenesis of Langerhans cell histiocytosis. *Annu Rev Pathol.* (2013) 8:1–20. doi: 10.1146/annurev-pathol-020712-163959

83. Sholl LM, Hornick JL, Pinkus JL, Pinkus GS, Padera RF. Immunohistochemical analysis of langerin in langerhans cell histiocytosis and pulmonary inflammatory and infectious diseases. *Am J Surg Pathol.* (2007) 31:947–52. doi: 10.1097/01.pas.0000249443.82971.bb

84. Zhang L, Pacheco-Rodriguez G, Steagall WK, Kato J, Colby TV, Haughey M, Moss J. BRAF and NRAS mutations in circulating Langerhans-like CD1a+ cells in a patient with pulmonary Langerhans' cell histiocytosis. *Eur Respir J.* (2017) 50:1700521. doi: 10.1183/13993003.00521-2017

85. Takizawa Y, Taniuchi N, Ghazizadeh M, Enomoto T, Sato M, Jin E, et al. Bronchoalveolar lavage fluid analysis provides diagnostic information on pulmonary Langerhans cell histiocytosis. *J Nippon Med Sch Nippon Ika Daigaku Zasshi.* (2009) 76:84–92. doi: 10.1272/jnms.76.84

86. Jouenne F, Chevret S, Bugnet E, Clappier E, Lorillon G, Meignin V, et al. Genetic landscape of adult Langerhans cell histiocytosis with lung involvement. *Eur Respir J.* (2020) 55:1901190. doi: 10.1183/13993003.01190-2019

87. Mourah S, How-Kit A, Meignin V, Gossot D, Lorillon G, Bugnet E, et al. Recurrent NRAS mutations in pulmonary Langerhans cell histiocytosis. *Eur Respir J.* (2016) 47:1785–96. doi: 10.1183/13993003.01677-2015

88. Vassallo R, Walters PR, Lamont J, Kottom TJ, Yi ES, Limper AH. Cigarette smoke promotes dendritic cell accumulation in COPD; a Lung Tissue Research Consortium study. *Respir Res.* (2010) 11:45. doi: 10.1186/1465-9921-11-45

89. Van Pottelberge GR, Bracke KR, Demedts IK, De Rijck K, Reinartz SM, van Drunen CM, et al. Selective accumulation of langerhans-type dendritic cells in small airways of patients with COPD. *Respir Res.* (2010) 11:35. doi: 10.1186/1465-9921-11-35

90. Wang X, Inoue S, Gu J, Miyoshi E, Noda K, Li W, et al. Dysregulation of TGF-beta1 receptor activation leads to abnormal lung development and emphysema-like phenotype in core fucose-deficient mice. *Proc Natl Acad Sci U S A.* (2005) 102:15791–6. doi: 10.1073/pnas.0507375102

91. Kobayashi S, Fujinawa R, Ota F, Kobayashi S, Angata T, Ueno M, et al. A single dose of lipopolysaccharide into mice with emphysema mimics human chronic obstructive pulmonary disease exacerbation as assessed by micro-computed tomography. *Am J Respir Cell Mol Biol.* (2013) 49:971–7. doi: 10.1165/rcmb.2013-0074OC

92. Kamio K, Yoshida T, Gao C, Ishii T, Ota F, Motegi T, et al. α1,6-Fucosyltransferase (Fut8) is implicated in vulnerability to elastase-induced emphysema in mice and a possible non-invasive predictive marker for disease progression and exacerbations in chronic obstructive pulmonary disease (COPD). *Biochem Biophys Res Commun.* (2012) 424:112–7. doi: 10.1016/j.bbrc.2012.06.081

93. Gao C, Maeno T, Ota F, Ueno M, Korekane H, Takamatsu S, et al. Sensitivity of heterozygous α1,6-fucosyltransferase knock-out mice to cigarette smoke-induced emphysema: implication of aberrant transforming growth factor-β signaling and matrix metalloproteinase gene expression. *J Biol Chem.* (2012) 287:16699–708. doi: 10.1074/jbc.M111.315333

94. Ota F, Hirayama T, Kizuka Y, Yamaguchi Y, Fujinawa R, Nagata M, et al. High affinity sugar ligands of C-type lectin receptor langerin. *Biochim Biophys Acta Gen Subj.* (2018) 1862:1592–601. doi: 10.1016/j.bbagen.2018.04.004

95. Ohkawa Y, Harada Y, Taniguchi N. Keratan sulfate-based glycomimetics using Langerin as a target for COPD: lessons from studies on Fut8 and core fucose. *Biochem Soc Trans.* (2021) 49:441–53. doi: 10.1042/BST20200780

96. GeurtsvanKessel CH, Willart MAM, van Rijt LS, Muskens F, Kool M, Baas C, et al. Clearance of influenza virus from the lung depends on migratory langerin+CD11b- but not plasmacytoid dendritic cells. *J Exp Med.* (2008) 205:1621–34. doi: 10.1084/jem.20071365

97. Wong E, Montoya B, Stotesbury C, Ferez M, Xu R-H, Sigal LJ. Langerhans cells orchestrate the protective antiviral innate immune response in the lymph node. *Cell Rep.* (2019) 29:3047–59.e3. doi: 10.1016/j.celrep.2019.10.118

98. Mei X, Li H, Zhou X, Cheng M, Cui K. The emerging role of tissue-resident memory CD8+ T lymphocytes in human digestive tract cancers. *Front Oncol.* (2021) 11:819505. doi: 10.3389/fonc.2021.819505

99. Maisonnasse P, Bouguyon E, Piton G, Ezquerra A, Urien C, Deloizy C, et al. The respiratory DC/macrophage network at steady-state and upon influenza infection in the swine biomedical model. *Mucosal Immunol.* (2016) 9:835–49. doi: 10.1038/mi.2015.105

100. De Simone M, Spagnuolo L, Lorè NI, Cigana C, De Fino I, Broman KW, et al. Mapping genetic determinants of host susceptibility to Pseudomonas aeruginosa lung infection in mice. *BMC Genomics.* (2016) 17:351. doi: 10.1186/s12864-016-2676-4

frontiers | Frontiers in Medicine

TYPE Original Research
PUBLISHED 20 September 2022
DOI 10.3389/fmed.2022.969487

OPEN ACCESS

EDITED BY
Yi Liu,
Shandong Provincial Hospital, China

REVIEWED BY
Rudolf Maria Huber,
Ludwig Maximilian University of Munich, Germany
Rafael A. Calderon-Candelario,
Miami VA Healthcare System, United States

*CORRESPONDENCE
Wei Li
weili126@126.com
Pingmin Wei
mpw1963@126.com

SPECIALTY SECTION
This article was submitted to Pulmonary Medicine, a section of the journal Frontiers in Medicine

RECEIVED 15 June 2022
ACCEPTED 01 September 2022
PUBLISHED 20 September 2022

CITATION
Li H, Zhao M, Fei G, Wang Z, Wang S, Wei P and Li W (2022) Epidemiological trends and incidence prediction of lung cancer in China based on the Global Burden of Disease study 2019. *Front. Med.* 9:969487. doi: 10.3389/fmed.2022.969487

Epidemiological trends and incidence prediction of lung cancer in China based on the Global Burden of Disease study 2019

Han Li[1], Meng Zhao[1], Gaoqiang Fei[1], Zemin Wang[1], Shuai Wang[1], Pingmin Wei[1]* and Wei Li[2]*

[1]Department of Epidemiology and Health Statistics, School of Public Health, Southeast University, Nanjing, China, [2]Department of Quality Management, Children's Hospital of Nanjing Medical University, Nanjing, China

Lung cancer remains the most common malignancy in China. This study aims to provide scientific support for the prevention and treatment of lung cancer by analyzing the epidemiological trends of lung cancer in China from 1990 to 2019. Based on the global health exchange database (GHDx), joinpoint and age-period-cohort analyses were performed to explore the trend of lung cancer incidence and mortality rates from 1990 to 2019. According to incidence rates from 1990 to 2019, a model was constructed to predict the incidence rates in the next 5 years. In addition, changes in risk factors associated with lung cancer deaths were compared between 1990 and 2019 and between males and females in 2019. The results are as follows. The age-standardized incidence rates (ASIRs), and age-standardized death rates (ASDRs) of lung cancer among Chinese had overall upward trends from 1990 to 2019. The ASDRs of females and males in China decreased since 2010. Interestingly, from 2016 to 2019, the ASIRs and ASDRs of females rose significantly. The age-period-cohort model showed that the incidence and mortality rates of lung cancer in China increased with age, and the growth rate accelerated after 45 years old. After 2004, the relative risks of lung cancer incidence increased with the passage of the period. Also, after the 1950–1954 birth cohort, the risks of lung cancer incidence and death began to decrease. The autoregressive integrated moving average (ARIMA) model predicted that the incidence rates of lung cancer in China would continue to rise in the next 5 years. The top five risk factors for lung cancer deaths of both genders in 2019 were smoking, ambient particulate matter pollution, secondhand smoke, high fasting plasma glucose, and household air pollution from solid fuels. The above results provided precise clues for the prevention and treatment of lung cancer in China.

KEYWORDS

lung cancer, China, epidemiological trends, prediction, Global Burden of Disease study

Introduction

According to the World Cancer Report 2020, there have been 2.2 million new cases of lung cancer worldwide, and deaths due to lung cancer will account for 18% of all deaths from cancer worldwide (1). Based on cancer statistics in China in 2016, lung cancer ranked first in terms of new cases (828,000) and deaths (657,000). Among males, lung cancer ranked first in the incidence and mortality rates of malignant tumors, while lung cancer ranked second in the incidence rate and first in the mortality rate among females from 2000 to 2016 (2). Previous study indicated that China serves one of the countries with the highest tracheal, bronchus, and lung cancer disease burden (3). There is no doubt that lung cancer has become a major public health problem and a huge social burden in China. It is of great significance to continue to carry out epidemiological research on lung cancer and strengthen the prevention and treatment of lung cancer to reduce the incidence and mortality of lung cancer in China. Lifestyle, environmental and occupational exposures are common risk factors for lung cancer (4), and understanding the deaths of lung cancer due to these risk factors is essential for disease management.

The Global Burden of Disease (GBD) project aggregated 354 diseases and injuries from 195 countries and territories worldwide, making it possible to analyze epidemiological trends of lung cancer in China (5). Therefore, based on the latest data published by the GBD project, the epidemiological trends from 1990 to 2019 in lung cancer in China were analyzed. Joinpoint and age-period-cohort models were developed based on incidence and death data to comprehensively analyze the epidemiological characteristics. Based on the incidence rates data, autoregressive integrated moving average (ARIMA) and support vector machine (SVM) models were used to construct models and finally the optimal model was selected to predict the incidence rates of lung cancer in the next 5 years. Additionally, the attributable risk factors for lung cancer deaths were also explored. The above analysis results might provide clues to the precise prevention and control of lung cancer.

Abbreviations: GHDx, Global health exchange database; DALY, Disability-Adjusted Life Year; ASIR, Age-standardized incidence rate; ASDR, Age-standardized death rate; GBD, Global Burden of Disease; SVM, Support vector machine; APC, Annual percentage change; AAPC, Average annual percentage change; RR, Rate ratio; NCI, National Cancer Institute; AR, Autoregressive Model; MA, Moving Average model; MSE, Mean square error; MAE, Mean absolute error; MAPE, Mean absolute percentage error; CI, confidence intervals; ARIMA, Autoregressive Integrated Moving Average model; LDCT, Low-dose computed tomography; CXR, chest X-ray.

Materials and methods

Data source

Incidence, deaths, and their age-standardized rates of lung cancer were downloaded from the GBD project (http://ghdx.healthdata.org/gbd-results-tool). In addition, 87 types of detailed risks were selected for identifying attributable risk factors for lung cancer deaths. By applying the comparative risk assessment (CRA) theory and counterfactual analysis, the proportions of lung cancer deaths caused by the above factors in the target population were calculated, that is, the population attributable score (PAF) of the risk factors (6).

Joinpoint regression analysis

Joinpoint regression is a widely used statistical method to analyze the long-term trends of incidence or mortality rates of tumors and chronic diseases. The core idea of the model is to build segmental regressions based on the temporal characteristics of the disease distribution, and then to evaluate the characteristics of disease variability specific to different intervals in more detail over the global time horizon (7). In this study, based on age-standardized incidence rates (ASIRs) and age-standardized death rates (ASDRs), joinpoint regression models were constructed by Joinpoint Regression Program (4.9.0.0) to analyze global and local change trends in incidence and mortality rates of lung cancer. The annual percentage change (APC) $[\left(e^{\beta}-1\right)\times 100\%]$ and average annual percentage change (AAPC) $[(e^{\sum \omega i\beta i/\sum \omega i}-1)\times 100\%]$ are used to describe the direction and magnitude of the changing trend, where β is the regression coefficient, and ωi is the number of years included in each segment. When APC or AAPC > 0, it means that the incidence or mortality rates of lung cancer show a rising trend. When APC or AAPC < 0, it means the incidence or mortality rates show a decreasing trend. $P < 0.05$ represents a statistically significant change.

Age-period-cohort analysis

The age-period-cohort model is based on Poisson distribution and uses three parameters: age, period, and birth cohort to reflect changes in the risks of disease incidence and death in the target population. And to quantify the effects of age, period, and cohort on incidence and death data based on controlling for interaction effects (8). In this study, an online tool provided by the National Cancer Institute (NCI) (http://analysistools.nci.nih.gov/apc/) was used to execute age-period-cohort analysis for the incidence and death of lung cancer (9). The tool performs the analysis using a built-in algorithm and the corresponding Wald test, with main parameters: net drift,

local drifts, longitudinal age curve, period rate ratio, and cohort rate ratio. 15 age groups (20–24, 25–29, ……, 85–89, 90–94), 6-period groups (1990–1994, 1995–1999, ……, 2015–2019), and 20 cohorts (1900–1904, 1905–1909, ……, 1995–1999) were included in age-period-cohort models.

Incidence prediction models

ARIMA time series model (p, d, q) which consists of an autoregressive model (AR) and a moving average model (MA) model have good accuracy and effectiveness in predicting the trend of future development of events, with p and q being the orders of AR and the order of MA, and d is the numbers of difference in stabilizing the term trend process (10). SPSS 25 was applied for ARIMA modeling in the study. SVM serves as a machine learning method that can be used for classification and regression prediction. A linear function was employed to predict the regression in a large space (11). In this study, the SVM model was developed through Python. ARIMA and SVM models were developed using the ASIRs of lung cancer in China from 1990 to 2014. Subsequently, the ASIRs of 2015–2019 were used to evaluate the predictive performance of the models. The evaluation indicators include mean square error (MSE) ($\frac{1}{n}\sum_{i=1}^{n}(yt-\hat{y}t)^2$), mean absolute error (MAE) ($\frac{1}{n}\sum \mid yt-\hat{y}t \mid$), and mean absolute percentage error (MAPE) ($\frac{1}{n}\sum(\frac{yt-\hat{y}t}{yt}) \times 100\%$), where yt is the actual value, $\hat{y}$t is the predicted value, and n is the number of predicted data.

Results

The general trends of incidence and mortality rates of lung cancer in China

From 1990 to 2019, the ASIRs of lung cancer in China showed an overall upward trend, with the highest in 2019 (Figure 1A). Figure 1B shows that the ASDRs of lung cancer in China increased overall from 1990 to 2010, with the highest in 2010. Since 2010, the ASDRs showed a slight downward trend. In general, the ASIRs and ASDRs of lung cancer in China were all higher than the global level.

Description of segmental trends in lung cancer incidence and mortality rates from 1990 to 2019

According to joinpoint analysis, ASIRs and ASDRs of lung cancer were on the rise for both males and females in China from 1990 to 2019 (All AAPC $>$ 0, $P < 0.001$) (Table 1). ASIRs and ASDRs for both sexes increased by an average of 1.1 and 0.8% per year, respectively. In addition, Figure 2 shows that the ASIRs and ASDRs of both sexes and females of lung cancer had upward trends during 1990–1997, 1997–2004 (All APC $>$ 0, $P < 0.05$), whereas it showed a downward trend during 2010–2016 (APC $<$ 0, $P < 0.05$). For males, ASIRs and ASDRs of lung cancer increased from 1994 to 1998, 1998 to 2004, and 2007 to 2010 (All APC $>$ 0, $P < 0.05$), while decreased from 2010 to 2019 (APC $<$ 0, $P < 0.05$). Interestingly, it can be observed that ASIRs and ASDRs of females showed a clear upward trend in 2016–2019, with APCs of 3.33 and 2.61, respectively.

The age, period, and cohort effects on lung cancer incidence and mortality rates

The wald test showed that the net drift, local drifts, period, and cohort effects of lung cancer incidence rates from 1990 to 2019 were all statistically significant ($P < 0.01$). However, for mortality rates of lung cancer, the local drifts and cohort effect were statistically significant ($P < 0.01$), while the net drift and period effect were not statistically significant (Table 2). For incidence rates, the net drift which represents the overall annual percentage change was 0.61% (95% confidence interval, CI: 0.38 to 0.84%), and the local drifts which represent additional age-specific variations were <0 before the 50–54 age group and >0 after that. Additionally, after the 60–64 age group, the local drifts of mortality rates started to be >0 (Figure 3A). This showed that the incidence rates of each age group were increasing over time, with an average increase of 0.61% per year. And the incidence rates after the 50–54 age group and mortality rates after the 60–64 age group showed an increasing trend with time, with the rest showing a decreasing trend.

As shown in Figure 3B, after correcting for period and cohort effects, the longitudinal age curves of lung cancer incidence and mortality rates in China were upward trends before the age group of 85–89. The incidence and mortality rates were at a low level in the 20–44 age group, and they increased rapidly after the 45–49 age group, reaching the peak in the 85–89 age group. As for the period effect (Figure 3C), the period-related RRs of incidence rates were on the rise from the 2000–2004 period group (RR = 1) to the 2015–2019 period group. Concerning cohort effects (Figure 3D), after adjusting the effects of period and age, the cohort risks of incidence and mortality rates were a single-peaked distribution, with the cohort risks of incidence and mortality reaching their highest in the 1950–1954 cohort (RR = 1.05, 95% CI: 1.00 to 1.10, RR = 1.02, 95% CI: 0.97 to 1.08).

Changes in attributed risk factors

As shown in Figure 4A, in 1990, smoking, household air pollution from solid fuels, and ambient particulate matter

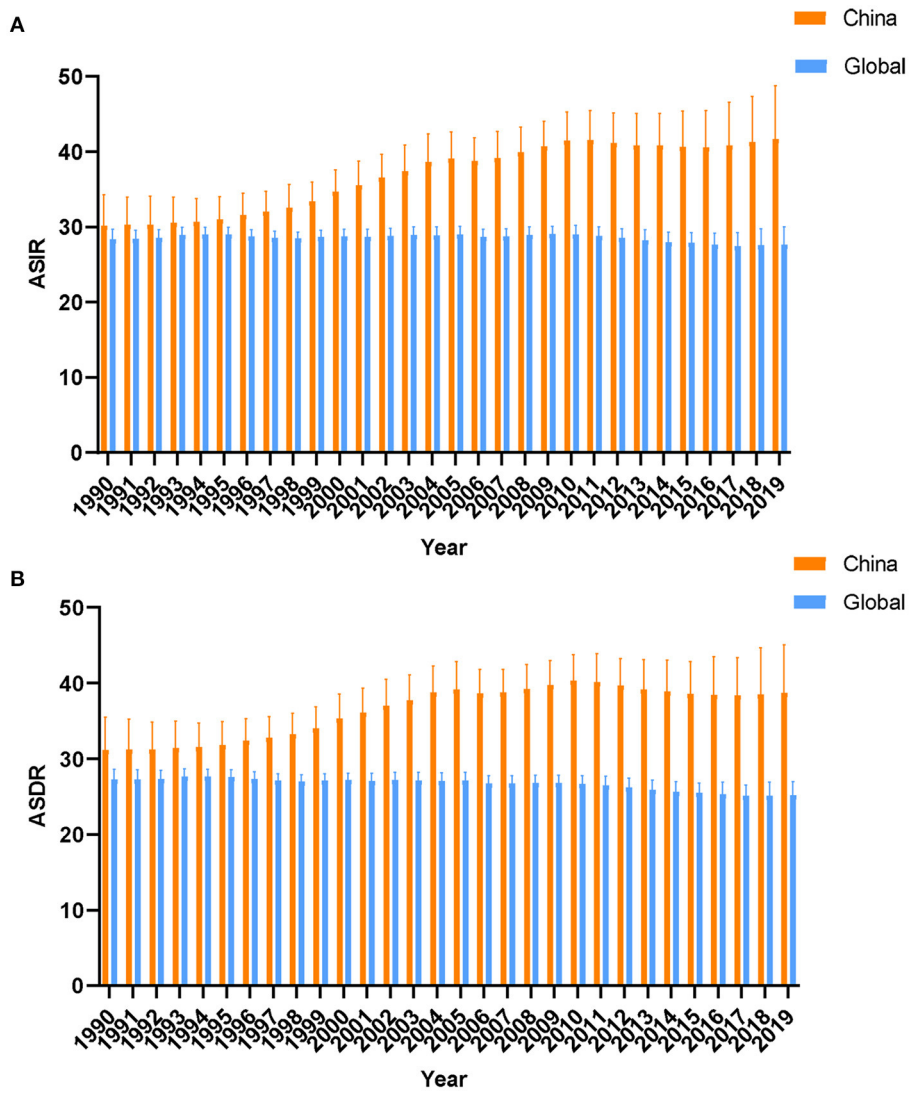

FIGURE 1
The trends of age-standard incidence rates **(A)** death rates **(B)** of lung cancer in global and China from 1990 to 2019.

pollution ranked the top three contributors to the deaths of lung cancer in China, causing 60.87%, 22.15%, and 10.83% of deaths, respectively. In 2019, the top three contributors to lung cancer deaths were smoking, ambient particulate matter pollution, and secondhand smoke, which contributed to 64.40%, 22.63%, and 7.83% of deaths, respectively. Among them, household air pollution from solid fuels dropped from the 2nd (22.15%) in 1990 to the 5th (4.91%) in 2019. And diet low in fruits and occupational exposure to silica dropped one place. However, the attribution ranking of ambient particulate matter pollution, secondhand smoke, high fasting plasma glucose, residential radon, and occupational exposure to asbestos was slightly up. As for changing trends of the risk factors subdivided by gender (Figures 4B,C), the attribution ranking of ambient particulate matter pollution and high fasting plasma glucose rose in males and females from 1990 to 2019. And the attribution ranking of household air pollution from solid fuels dropped from 1990 to 2019. Additionally, deaths of lung cancer in females for smoking increased from 19.56% to 26.58%. Furthermore, as shown in Figure 4D, the top three risk factors for lung cancer deaths in Chinese males in 2019 were smoking (82.03%), ambient particulate matter pollution (23.01%), and high fasting plasma glucose (7.28%). Nevertheless, smoking (26.58%), ambient particulate matter pollution (21.84%), and secondhand smoke (11.47%) ranked as the top three risk factors for the death of lung cancer in Chinese females in 2019. High fasting plasma glucose and occupational exposure to asbestos had a greater impact on lung cancer deaths in males than in females. In addition,

TABLE 1 Lung cancer incidence and mortality rates by sex in China, 1990–2019.

Year	ASIR			ASDR		
	Female	Male	Both	Female	Male	Both
1990	18.01	44.29	30.20	18.63	46.33	31.18
1991	18.23	44.21	30.30	18.83	46.18	31.24
1992	18.25	44.15	30.30	18.83	46.08	31.22
1993	18.56	44.38	30.58	19.12	46.26	31.47
1994	18.53	44.58	30.67	19.07	46.47	31.54
1995	18.51	45.28	31.01	19.02	47.14	31.85
1996	18.88	46.09	31.60	19.37	47.87	32.40
1997	19.18	46.78	32.08	19.63	48.51	32.83
1998	19.42	47.64	32.59	19.82	49.30	33.27
1999	19.89	48.81	33.38	20.26	50.44	34.03
2000	20.63	50.72	34.69	21.01	52.29	35.32
2001	21.10	52.02	35.55	21.46	53.54	36.13
2002	21.76	53.46	36.58	22.06	54.84	37.06
2003	22.27	54.71	37.44	22.49	55.87	37.78
2004	22.86	56.60	38.63	22.98	57.55	38.81
2005	23.04	57.47	39.10	23.06	58.26	39.15
2006	22.98	56.88	38.78	22.87	57.42	38.63
2007	23.13	57.65	39.19	22.84	57.84	38.78
2008	23.26	59.17	39.93	22.79	59.04	39.25
2009	23.45	60.73	40.70	22.82	60.27	39.77
2010	23.73	62.27	41.51	22.95	61.44	40.32
2011	23.61	62.57	41.53	22.75	61.51	40.18
2012	23.04	62.62	41.19	22.11	61.33	39.68
2013	22.76	62.36	40.86	21.75	60.82	39.19
2014	22.85	62.14	40.82	21.69	60.17	38.89
2015	22.67	62.06	40.68	21.43	59.84	38.60
2016	22.64	61.91	40.58	21.35	59.59	38.44
2017	23.31	61.69	40.88	21.80	58.84	38.40
2018	24.15	61.58	41.30	22.40	58.23	38.49
2019	24.76	61.74	41.71	22.86	58.10	38.70
AAPC(%)	1.1	1.2	1.1	0.7	0.8	0.8
95%CI	1	1	0.9	0.6	0.6	0.5
	1.3	1.3	1.4	0.9	1	1
P value	<0.001	<0.001	<0.001	<0.001	<0.001	<0.001

CI, confidence intervals.

secondhand smoke, household air pollution from solid fuels, residential radon, a diet low in fruits, and occupational exposure to silica had a slightly greater impact on lung cancer deaths in females than in males.

The prediction for lung cancer incidence in China in the future

Through the expert modeler of SPSS, the optimal model of ARIMA was determined to be (0, 2, 0). The Ljung-BOX test ($P = 0.99 > 0.05$) proved the constructed model was the white noise sequence. In addition, the SVM model was developed with kernel = "rbf", degree = 3, gamma = "auto", and C = 1. Table 3 shows the comparison of actual and predicted incidence rates in 2015–2019 of the two models. By comparing the goodness of fit of the two models (Table 4), the ARIMA (0, 2, 0) model with a better fitting effect was finally selected to predict the incidence rates of lung cancer in China in the next 5 years (2020–2024). The prediction results showed that the incidence rates of lung cancer in China will continue to rise in the next 5 years and might reach 44.10 /100,000 in 2024 (Table 5).

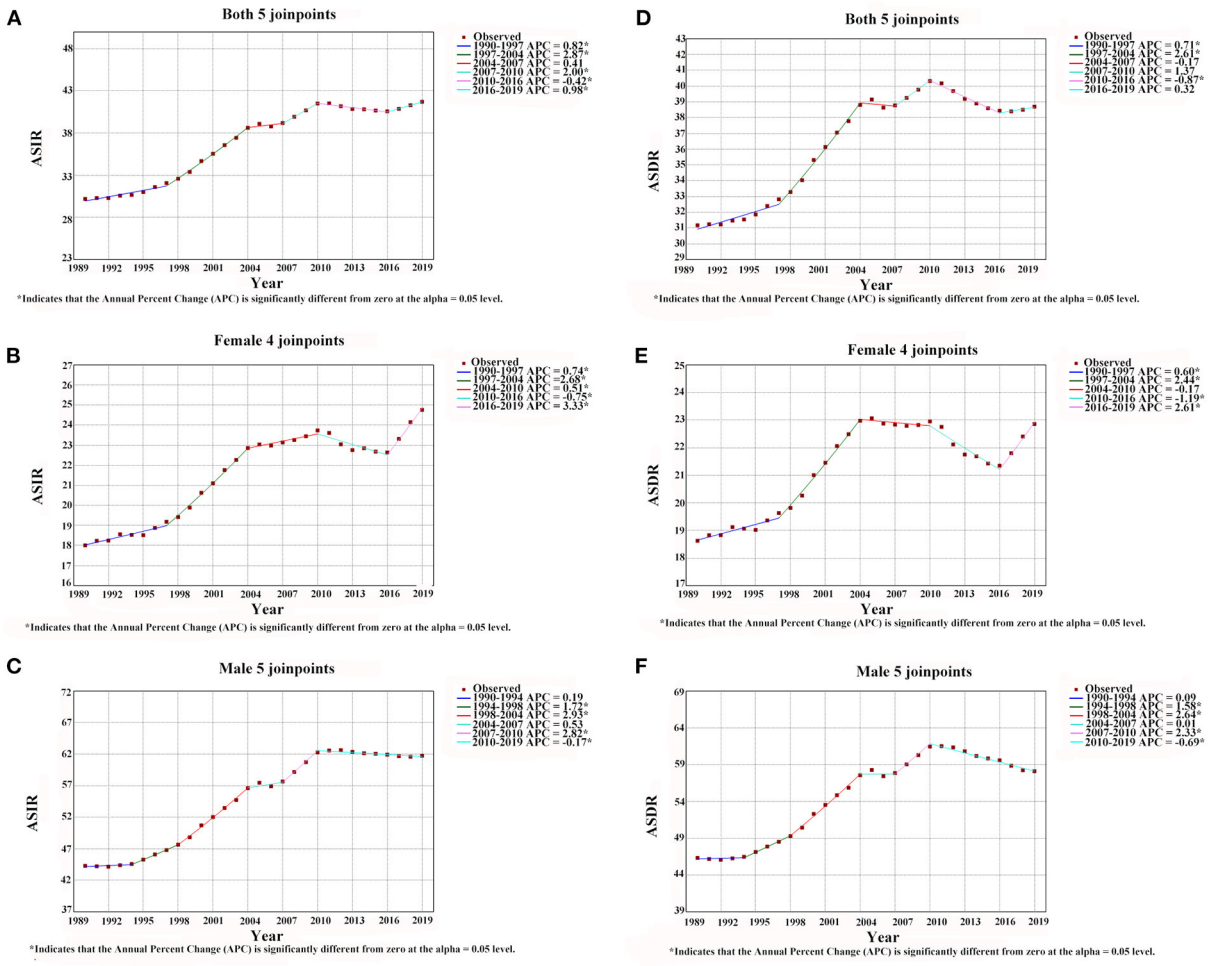

FIGURE 2
The results of joinpoint regression analysis for age-standard incidence rates and mortality rates of lung cancer in Chinese males [**(C)** incidence rate, **(F)** mortality rate], females [**(B)** incidence rate, **(E)** mortality rate] and both genders [**(A)** incidence rate, **(D)** mortality rate] from 1990 to 2019.

Discussion

With the rapid development of the economy, the lifestyle and disease spectrum of Chinese residents have changed dramatically. Among causes of death in China, lung cancer rose from the 8th in 1990 to the 4th in 2017. And as regards DALY (Disability-Adjusted Life Year) causes, lung cancer rose from 14th in 1990 to 4th in 2017 (12). Our study also indicated that lung cancer ASIRs and ASDRs increased overall in China from 1990 to 2019. Furthermore, joinpoint analysis indicated that ASDRs of females and males in China decreased since 2010. It is speculated that this might benefit from the initiation of low-dose computed tomography (LDCT) screening in 2010 in China (13). For the first time, the national lung screening trial research team demonstrated that LDCT screening reduced lung cancer mortality by 20% compared to chest X-ray (CXR) screening (14). The analysis results of this study also confirmed the necessity for early screening. Additionally, from 2016 to 2019, the ASIRs and ASDRs of females began to rise significantly again, with a rate of 3.33 and 2.61%, respectively. Cancer statistics in 2016 showed that for females, lung cancer was the second most common after breast cancer (2). Another epidemiological study in China showed that the average annual growth rate of lung cancer in women was greater than that in men from 2010 to 2015 (15, 16). In this study, it is found that the number of lung cancer deaths of females for smoking increased. This may be due to the rise in smoking rates in females in recent years. Moreover, lung cancer deaths from ambient particulate matter pollution increased as females work outside the home in recent years. Therefore, it is particularly significant to control these risk factors of lung cancer in females.

During the occurrence and development of diseases, individual characteristics such as age, birth cohort, and objective factors such as the social development period are all possible

TABLE 2 Wald Chi Square tests for estimable functions in the age-period-cohort model.

Null hypothesis	ASIR		ASDR	
	$\chi 2$	*P*	$\chi 2$	*P*
Net Drift = 0	26.63	<0.01	0.44	0.51
All age deviations = 0	1177.89	<0.01	722.44	<0.01
All period deviations = 0	8.67	0.07	7.71	0.10
All cohort deviations = 0	230.93	<0.01	197.77	<0.01
All period RR = 1	34.99	<0.01	7.89	0.16
All cohort RR = 1	439.96	<0.01	265.16	<0.01
All local drifts = Net Drift	225.55	<0.01	193.50	<0.01

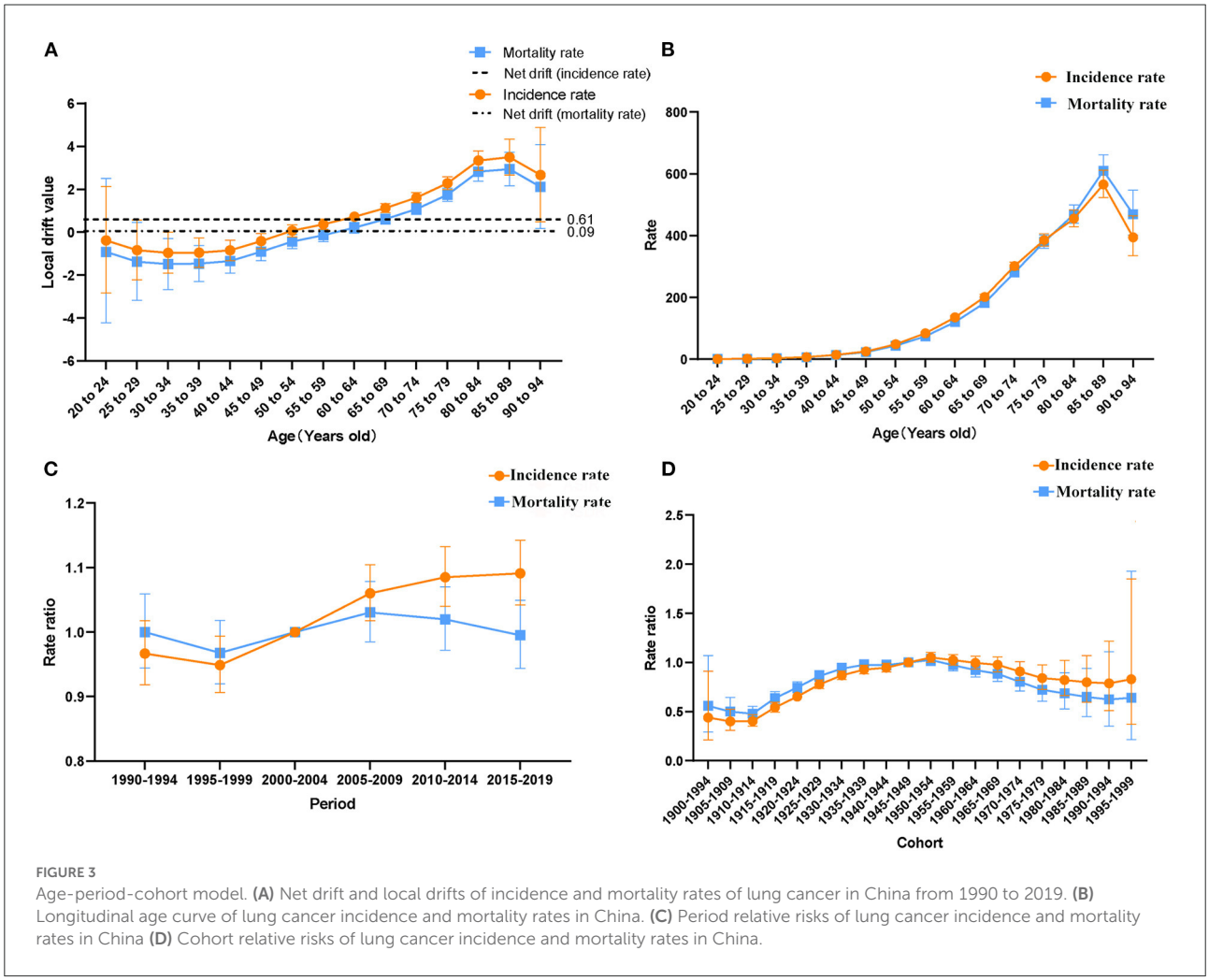

FIGURE 3
Age-period-cohort model. **(A)** Net drift and local drifts of incidence and mortality rates of lung cancer in China from 1990 to 2019. **(B)** Longitudinal age curve of lung cancer incidence and mortality rates in China. **(C)** Period relative risks of lung cancer incidence and mortality rates in China **(D)** Cohort relative risks of lung cancer incidence and mortality rates in China.

influencing factors. The age-period-cohort model has been widely used in lung cancer, colorectal cancer, cervical cancer, and other cancers, which is beneficial to reflect their changing trends more comprehensively, to seek the initiating factors and reasonable explanations for the occurrence and development of these cancers (17–19). In this study, the results of age effect analysis showed that the incidence and mortality rates of lung cancer in China increased with age, and the growth speed of the incidence and mortality rates accelerated after 45 years old. According to an analysis of China's 2016 cancer statistics, lung cancer is the most common cancer in males over 45 years old and females over 60 years old (2). On the one hand, the reason

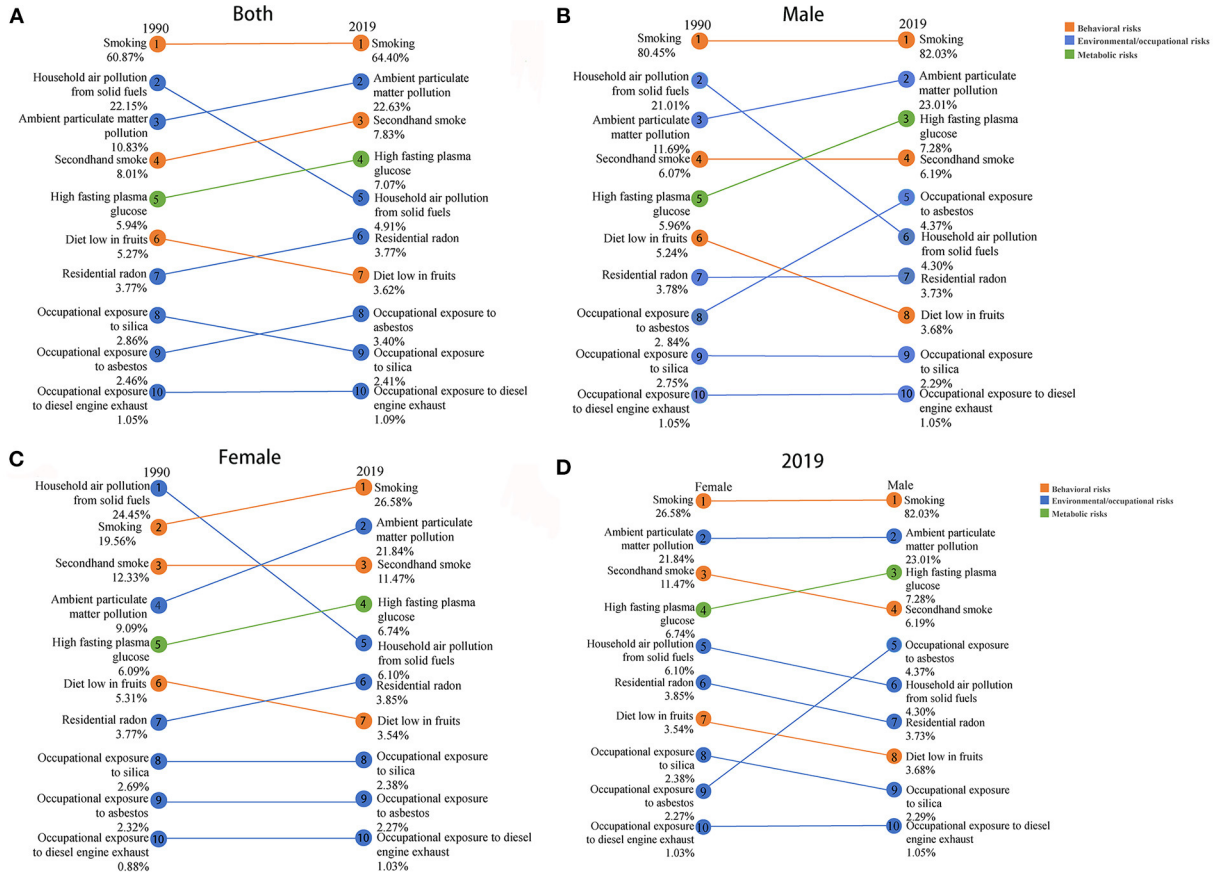

FIGURE 4
Comparisons of attributed risk factors of deaths between 1990 and 2019 in both genders **(A)** and males **(B)**, and females **(C)**, and between females and males in 2019 **(D)**.

might be that lung cancer is usually diagnosed at an advanced stage (20), resulting in a later age of diagnosis. On the other hand, the risk of incidence and death from lung cancer will increase due to the increase in underlying diseases and decline in physical fitness in the elderly (21), which is consistent with our findings. At present, China's aging situation is severe. In 2019, China's population over 65 years old accounted for about 11.5% of the total population (22). Thus, the incidence and death of lung cancer in the middle-aged and elderly population should be paid attention to. The period effect can be understood as the risks of incidence and mortality of diseases due to changes in natural conditions or social environment in a specific period. The period effect analysis in this paper pointed out that after 2004, the period effects of incidence rates increased over time. First of all, this might be related to the increased exposure of Chinese residents to risk factors caused by the rapid development of society and economy and the accelerated process of industrialization (23, 24). Then, with the living standards improvement of Chinese residents, the risk of lung cancer increased due to poor eating habits such as excessive intake of red meat (25), and low levels of vitamin D (26). What's more, it is speculated that this might be related to the increase in the number of patients diagnosed with lung cancer caused by the screening program for high-risk groups of lung cancer launched in 2010 (13). Furthermore, residents of different birth cohorts will experience different disease exposure risks due to the different social, economic, natural environments and other factors (27). In the present study, the cohort effects of incidence and mortality rates showed a unimodal distribution and peaked in the 1950–1954 birth cohort. From the birth cohort of 1914–1919 to the birth cohort of 1950–1954, the risks of incidence and mortality increased. The reason might be that the earlier generation is less educated and has poorer health literacy resulting in less awareness of risk factors and therefore increases risks of morbidity and mortality of lung cancer (28). However, after the 1950–1954 birth cohort, the risks of lung cancer morbidity and mortality began to decrease. For one thing, after the founding of new China, the health system has gradually improved, and more emphasis has been placed on the prevention and control of chronic diseases. For example,

TABLE 3 Comparison of actual and predicted incidence rates between ARIMA and SVM models.

Year	Actual value (1/100,000)	Predicted value (1/100,000)	
		ARIMA	SVM
2015	40.68	40.78	40.07
2016	40.58	40.73	39.60
2017	40.88	40.69	39.07
2018	41.30	40.66	38.52
2019	41.71	40.65	38.00

TABLE 4 Evaluation of the fitting effects of the two models.

Evaluation indicators	ARIMA	SVM
MAE	0.43	1.98
MSE	0.32	5.22
MAPE	0.0005	0.05

TABLE 5 The predicted values of ARIMA (0, 2, 0) model.

Year	Predicted value (1/10,0000)	95%CI
2020	42.14	41.29–43.00
2021	42.59	40.68–44.55
2022	43.06	39.88–46.43
2023	43.56	38.91–48.62
2024	44.10	37.83–51.14

the gradual improvement of China's medical insurance system reduces the medical burden on residents to a certain extent and enables timely treatment of lung cancer (29). For another thing, the younger generation is highly educated and has a strong sense of self-protection and high health literacy (30). Taken together, the younger generation has a lower risk of lung cancer morbidity and mortality.

The attributable risk factors for lung cancer deaths in China from 1990 to 2019 have changed. Lung cancer deaths due to household air pollution from solid fuels dropped from second to fifth. This is consistent with the results of another study in China (31). It could be seen that with the development of the times, household fuels in China were cleaner, and the indoor air has been purified. However, lung cancer deaths caused by ambient particulate matter pollution increased from the third to the second. It could be seen that with the process of industrialization, outdoor air pollution is still an important factor in the burden of lung cancer. And studies have shown that when smoking and air pollution affect men at the same time, the risk of developing lung cancer will be greatly increased (32). Our study found that deaths of lung cancer from smoking were the first in both 1900 and 2019. And the ranks of secondhand smoke rose from fourth to third. It means that the tobacco control policy in China has not worked well (14, 15). Also, deaths of lung cancer from high fasting plasma glucose increased. Hyperglycemia may accelerate cancer cell proliferation and is an independent predictor of survival in non-small cell lung cancer patients (33). Recently, eating habits have changed, which may explain this. In addition, the ranks of residential radon, and occupational exposure to asbestos all rose. Factors related to occupational exposure were also in the top ten. What's more, there were also differences in risk factors for lung cancer deaths in males and females in 2019. It's worth noting that occupational exposure to asbestos had a greater impact on lung cancer deaths in males than in females. The reason is that men have more exposure to asbestos in the workplace. Earlier research showed that men exposed to asbestos had a higher risk of developing lung cancer compared to men not exposed to asbestos (34). And females have longer exposure to household fuels and residential radon as they stay at home longer than males. Thus, household air pollution from solid fuels and residential radon had a greater impact on lung cancer deaths in females than in males. Based on the above understanding, the following suggestions are made: (1) Expanding the population of household clean fuel users, and encouraging the use of environmentally friendly decoration materials to purify indoor air. (2) Health education to improve public health literacy, combined with tobacco control policies, to reduce smoking rates. (3) Improving air quality while driving rapid economic growth. (4) Advancing diabetes screening and blood glucose monitoring. (5) Factors related to occupational exposure should also be paid attention to.

According to the forecast results of this study, the incidence rates of lung cancer in China might still increase in the next 5 years. Therefore, based on the analyses of epidemiological trends of lung cancer in China from 1990 to 2019 in the study, it can provide scientific reference for the prevention and control of lung cancer in the future. This study has the following limitations. Firstly, the incidence and death data from GBD are all estimates, and they are reconstructed from different sources. Secondly, this study only analyzes the epidemiological trends of lung cancer in the whole country, and cannot be specific to each province. Thirdly, in this study, the incidence rates of lung cancer were only predicted based on time series, but the occurrence of tumors is affected by many natural and social factors. In the future, more factors should be considered to optimize the model. Finally, the reported risk factors for GBD are limited, and more risk factors for lung cancer require further exploration.

Conclusion

In summary, the incidence, and mortality rates of lung cancer among Chinese residents increased from 1990 to 2019. The results of the joinpoint analysis showed that from 2016 to

2019, the incidence and mortality rates of female lung cancer increased significantly, while the incidence and mortality rates of male lung cancer decreased significantly. The age-period-cohort model showed that the incidence and mortality rates of lung cancer in China increase with age, and the growth speed of incidence and mortality rates accelerated after 45 years old. After 2004, the period effect of incidence rate increased over time, and the period risk of mortality rate continued to decline after 2009. Also, after the 1950–1954 birth cohort, the risks of lung cancer morbidity and mortality began to decrease. Smoking, ambient particulate matter pollution, household air pollution from solid fuels, secondhand smoke, and high fasting plasma glucose remain major risk factors for lung cancer deaths. And based on the prediction in this study, the incidence rate of lung cancer will increase in the next 5 years. Therefore, based on the above results, in the prevention and control of lung cancer, it is necessary to pay more attention to women and middle-aged and elderly people, carry out early diagnosis and early treatment and combine risk factors for comprehensive prevention and control.

Data availability statement

Publicly available datasets were analyzed in this study. This data can be found here: http://ghdx.healthdata.org/gbd-results-tool.

Author contributions

HL was responsible for the study conception and design. SW was responsible for manuscript preparation. ZW contributed to data acquisition, analysis, and interpretation. MZ and WL contributed to the review of the data. PW and GF contributed to the critical revision of the manuscript, obtained funding, and supervised the research. All authors have read and approved the final manuscript.

Funding

This work was supported by the Postgraduate Research & Practice Innovation Program of Jiangsu Province (KYCX22_0299).

Acknowledgments

We appreciate the works of the Global Burden of Disease study 2019 collaborators.

Conflict of interest

The authors declare that the research was conducted in the absence of any commercial or financial relationships that could be construed as a potential conflict of interest.

Publisher's note

References

1. Sung H, Ferlay J, Siegel RL, Laversanne M, Soerjomataram I, Jemal A, et al. Global cancer statistics 2020: GLOBOCAN estimates of incidence and mortality worldwide for 36 cancers in 185 countries. *CA Cancer J Clin.* (2021) 71:209–49. doi: 10.3322/caac.21660

2. Zheng R, Zhang S, Zeng H, Wang S, Sun K, Chen R, et al. Cancer incidence and mortality in China, 2016. *J Nat Cancer Center.* (2022). doi: 10.1016/j.jncc.2022.02.002

3. Deng Y, Zhao P, Zhou L, Xiang D, Hu J, Liu Y, et al. Epidemiological trends of tracheal, bronchus, and lung cancer at the global, regional, and national levels: a population-based study. *J Hematol Oncol.* (2020) 13:98. doi: 10.1186/s13045-020-00915-0

4. Barta JA, Powell CA, Wisnivesky JP. Global epidemiology of lung cancer. *Ann Glob Health.* (2019) 85:2419. doi: 10.5334/aogh.2419

5. Steel N, Ford JA, Newton JN, Davis ACJ, Vos T, Naghavi M, et al. Changes in health in the countries of the UK and 150 English local authority areas 1990–2016: a systematic analysis for the global burden of disease study 2016. *Lancet.* (2018) 392:1647–61. doi: 10.1016/S0140-6736(18)32207-4

6. GBD 2019 Risk Factors Collaborators. Global burden of 87 risk factors in 204 countries and territories, 1990–2019: a systematic analysis for the global burden of disease study 2019. *Lancet.* (2020) 396:1223–49. doi: 10.1016/S0140-6736(20)30752-2

7. Li HZ, Du LB. Application of Joinpoint regression model in cancer epidemiological time trend analysis. *Zhonghua Yu Fang Yi Xue Za Zhi.* (2020) 54:908–12. doi: 10.3760/cma.j.cn112150-20200616-00889

8. Scappini E. The estimable functions of age, period, and generation effects: a political application. *Qual Quant.* (2006) 40:759–81. doi: 10.1007/s11135-005-3267-7

9. Rosenberg PS, Check DP, Anderson WF, A. web tool for age-period-cohort analysis of cancer incidence and mortality rates. *Cancer Epidemiol Biomarkers Prev.* (2014) 23:2296–302. doi: 10.1158/1055-9965.EPI-14-0300

10. Singh S, Parmar KS, Makkhan SJS, Kaur J, Peshoria S, Kumar J. Study of ARIMA and least square support vector machine (LS-SVM) models for the prediction of SARS-CoV-2 confirmed cases in the most affected countries. *Chaos Solitons Fractals.* (2020) 139:110086. doi: 10.1016/j.chaos.2020.110086

11. Shirmohammadi-Khorram N, Tapak L, Hamidi O, Maryanaji Z. A comparison of three data mining time series models in prediction of monthly brucellosis surveillance data. *Zoonoses Public Health.* (2019) 66:759–72. doi: 10.1111/zph.12622

12. Zhou M, Wang H, Zeng X, Yin P, Zhu J, Chen W, et al. Mortality, morbidity, and risk factors in China and its provinces, 1990–2017: a systematic analysis for the global burden of disease study 2017. *Lancet.* (2019) 394:1145–58. doi: 10.1016/S0140-6736(19)30427-1

13. Zhou Q, Fan Y, Wu N, Huang Y, Wang Y, Li L, et al. Demonstration program of population-based lung cancer screening in China: rationale and study design. *Thorac Cancer*. (2014) 5:197–203. doi: 10.1111/1759-7714.12078

14. Aberle DR, Adams AM, Berg CD, Black WC, Clapp JD, Fagerstrom RM, et al. Reduced lung-cancer mortality with low-dose computed tomographic screening. *N Engl J Med*. (2011) 365:395–409. doi: 10.1056/NEJMoa1102873

15. Cao M, Chen W. Epidemiology of lung cancer in China. *Thorac Cancer*. (2019) 10:3–7. doi: 10.1111/1759-7714.12916

16. Wang N, Mengersen K, Tong S, Kimlin M, Zhou M, Wang L, et al. Lung cancer mortality in China: spatial and temporal trends among subpopulations. *Chest*. (2019) 156:972–83. doi: 10.1016/j.chest.2019.07.023

17. Stahlman S, Oetting A. Age-period-cohort analysis of colorectal cancer, service members aged 20–59 years, active component, U.S. Armed Forces, 1997–2016. *Msmr*. (2017) 24:12–9.

18. Deng Y, Peng L, Li N, Zhai Z, Xiang D, Ye X, et al. Tracheal, bronchus, and lung cancer burden and related risk factors in the United States and China. *Am J Transl Res*. (2021) 13:1928–51.

19. Guo M, Xu J, Du J. Trends in cervical cancer mortality in China from 1989 to 2018: an age-period-cohort study and Joinpoint analysis. *BMC Public Health*. (2021) 21:1329. doi: 10.1186/s12889-021-11401-8

20. Nooreldeen R, Bach H. Current and future development in lung cancer diagnosis. *Int J Mol Sci*. (2021) 22:8661. doi: 10.3390/ijms22168661

21. Gajra A, Akbar SA, Din NU. Management of Lung Cancer in the Elderly. *Clin Geriatr Med*. (2016) 32:81–95. doi: 10.1016/j.cger.2015.08.008

22. Man W, Wang S, Yang H. Exploring the spatial-temporal distribution and evolution of population aging and social-economic indicators in China. *BMC Public Health*. (2021) 21:966. doi: 10.1186/s12889-021-11032-z

23. Miao J, Wu X. Urbanization, socioeconomic status and health disparity in China. *Health Place*. (2016) 42:87–95. doi: 10.1016/j.healthplace.2016.09.008

24. Wang CY, Liu LF, Liu XL, Chen WJ, He GP. Mechanisms of lung cancer caused by cooking fumes exposure: a minor review (Δ). *Chin Med Sci J*. (2017) 32:193–7. doi: 10.24920/J1001-9294.2017.026

25. Xue XJ, Gao Q, Qiao JH, Zhang J, Xu CP, Liu J. Red and processed meat consumption and the risk of lung cancer: a dose-response meta-analysis of 33 published studies. *Int J Clin Exp Med*. (2014) 7:1542–53.

26. Malhotra J, Malvezzi M, Negri E, La Vecchia C, Boffetta P. Risk factors for lung cancer worldwide. *Eur Respir J*. (2016) 48:889–902. doi: 10.1183/13993003.00359-2016

27. Liu X, Yu C, Bi Y, Zhang ZJ. Trends and age-period-cohort effect on incidence and mortality of prostate cancer from 1990 to 2017 in China. *Public Health*. (2019) 172:70–80. doi: 10.1016/j.puhe.2019.04.016

28. Simmons RA, Cosgrove SC, Romney MC, Plumb JD, Brawer RO, Gonzalez ET, et al. Health literacy: cancer prevention strategies for early adults. *Am J Prev Med*. (2017) 53:S73–s7. doi: 10.1016/j.amepre.2017.03.016

29. Dou G, Wang Q, Ying X. Reducing the medical economic burden of health insurance in China: achievements and challenges. *Biosci Trends*. (2018) 12:215–9. doi: 10.5582/bst.2018.01054

30. Cohen AK, Syme SL. Education: a missed opportunity for public health intervention. *Am J Public Health*. (2013) 103:997–1001. doi: 10.2105/AJPH.2012.300993

31. Yin P, Brauer M, Cohen AJ, Wang H, Li J, Burnett RT, et al. The effect of air pollution on deaths, disease burden, and life expectancy across China and its provinces, 1990–2017: an analysis for the global burden of disease study 2017. *Lancet Planet Health*. (2020) 4:e386–e98. doi: 10.1016/S2542-5196(20)30161-3

32. Xing DF, Xu CD, Liao XY, Xing TY, Cheng SP, Hu MG, et al. Spatial association between outdoor air pollution and lung cancer incidence in China. *BMC Public Health*. (2019) 19:1377. doi: 10.1186/s12889-019-7740-y

33. Bergamino M, Rullan AJ, Saigí M, Peiró I, Montanya E, Palmero R, et al. Fasting plasma glucose is an independent predictor of survival in patients with locally advanced non-small cell lung cancer treated with concurrent chemoradiotherapy. *BMC Cancer*. (2019) 19:165. doi: 10.1186/s12885-019-5370-5

34. Lévêque E, Lacourt A, Philipps V, Luce D, Guénel P, Stücker I, et al. A new trajectory approach for investigating the association between an environmental or occupational exposure over lifetime and the risk of chronic disease: Application to smoking, asbestos, and lung cancer. *PLoS ONE*. (2020) 15:e0236736. doi: 10.1371/journal.pone.0236736

frontiers | Frontiers in Medicine

TYPE Original Research
PUBLISHED 05 October 2022
DOI 10.3389/fmed.2022.922239

OPEN ACCESS

EDITED BY
Yi Liu,
Shandong Provincial Hospital, China

REVIEWED BY
Mariaenrica Tinè,
University of Padua, Italy
Paul Zarogoulidis,
Euromedica General Clinic, Greece

*CORRESPONDENCE
Xuan Li
lixuan11299211@163.com
Changhui Wang
wang-chang-hui@hotmail.com
Shuanshuan Xie
xieshuanshuan@aliyun.com

SPECIALTY SECTION
This article was submitted to Pulmonary Medicine, a section of the journal Frontiers in Medicine

RECEIVED 17 April 2022
ACCEPTED 21 September 2022
PUBLISHED 05 October 2022

CITATION
Liang L, Duan H, Zhu H, Yang H, Li X, Wang C and Xie S (2022) Value of transbronchial needle aspiration combined with a rapid on-site evaluation of cytology in the diagnosis of pulmonary lesions.
Front. Med. 9:922239.
doi: 10.3389/fmed.2022.922239

Value of transbronchial needle aspiration combined with a rapid on-site evaluation of cytology in the diagnosis of pulmonary lesions

Long Liang[1], Hongxia Duan[2], Huiyuan Zhu[3], Huiqiong Yang[3], Xuan Li[1]*, Changhui Wang[1]* and Shuanshuan Xie[1]*

[1]Department of Respiratory Medicine, Shanghai Tenth People's Hospital, Tongji University School of Medicine, Shanghai, China, [2]Department of Oncology, Affiliated Hospital of Nantong University, Nantong, China, [3]Department of Pathology, Shanghai Tenth People's Hospital, Tongji University School of Medicine, Shanghai, China

Background: The diagnostic value of rapid on-site evaluation (ROSE) of cytology during endobronchial ultrasound-guided transbronchial needle aspiration (EBUS-TBNA) remains controversial. The purpose of this study was to validate the value of ROSE during the EUBS-TBNA procedure in the diagnosis of pulmonary lesions (PLs).

Methods: Enrolled in this study were 260 patients with nodules, masses, cavities, or inflammatory lesions on pulmonary CT images. They were assigned to undergo EBUS-TBNA with ROSE (n = 134) or without ROSE (n = 126). The diagnostic results of ROSE during EBUS-TBNA and the final pathologic reports were analyzed and compared by utilizing SPSS21.0 software to evaluate the sensitivity, specificity, positive predictive value (PPV), and negative predictive value (NPV). In addition, we further explored whether the ROSE method during EBUS-TBNA would improve the diagnostic yield and reduce the incidence of complications.

Results: The overall diagnostic yield of EBUS-TBNA for malignant diseases in the ROSE and the non-ROSE group were 29.9 and 11.1%, respectively. The sensitivity, specificity, PPV and NPV of the ROSE method during EBUS-TBNA were 97.4, 96.9, 92.5, and 98.90%, respectively. The result of the chi-square test effectively proved that ROSE operation during EBUS-TBNA contributes to the diagnosis of malignancy compared with the non-ROSE group (χ^2 = 13.858, $P < 0.001$). The number of punctures in the ROSE group was significantly lower than that in the non-ROSE group ($P < 0.001$).

Conclusion: ROSE examination during EBUS-TBNA could effectively improve the diagnostic yield of malignant diseases compared with the non-ROSE group and reduce the number of intraoperative punctures, which is a clinical application worth popularizing.

KEYWORDS

rapid on-site evaluation, endobronchial ultrasound-guided transbronchial needle aspiration, pulmonary lesions, diagnostic yield, complications

Introduction

Pulmonary nodules are one of the common radiological manifestations of pulmonary lesions (PLs). In recent years, the incidence of lung cancer has increased significantly worldwide ranking first among malignant diseases and has become a major disease endangering people's life and health (1). Interventional bronchoscopy is one of the most extensively used clinical approaches for the diagnosis of early lung cancer and other respiratory system-related diseases (2). Transbronchial needle aspiration (TBNA) has been widely used for the determination of focal properties adjacent to the trachea and bronchial walls, diagnosis of pulmonary hilar, and mediastinal lymph nodes, and staging of lung cancer (3). Unfortunately, tissue lesions could not be visualized in a real-time manner during the conventional TBNA procedure, thus increasing the possibility of causing accidental injury to the normal organs around the airway. With the advent of ultrasound probes mounted at the front end of the microscope, it has been made possible to enter the airway for ultrasound scanning, thus enabling the integration of the respective advantages of the above two techniques, known as endobronchial ultrasound-guided transbronchial needle aspiration (EBUS-TBNA) (4, 5).

Pathological examination remains the gold standard for the diagnosis of pulmonary malignant tumors. However, difficulty in sampling and time-consuming of the diagnostic procedure may delay the treatment, extend the length of hospitalization stay and increase the medical cost. In contrast, rapid on-site evaluation (ROSE) of cytology during EBUS-TBNA can realize the rapid diagnosis of lesions obtained and avoid the time-consuming defects in the pathological examination.

Several studies have reported the joint use of ROSE based on EBUS-TBNA (6), saying that the combined use of the above two technologies could provide the examiner with useful information on whether the puncture is successful, to enable him/her to evaluate the quality of specimens in a real-time manner, and to decide whether a repeated operation is necessary or not (7–9). However, there is still no agreement on whether ROSE technology could improve the diagnostic yield of lung malignancies. This retrospective study aimed to evaluate whether the ROSE method during EBUS-TBNA could effectively improve the diagnostic yield of lung malignancies and reduce surgery-related complications.

Abbreviations: ROSE, Rapid On-site Cytologic Evaluation; EBUS-TBNA, Endobronchial Ultrasound-guided Transbronchial Needle Aspiration; CT, Computerized Tomography; PPV, Positive Predictive Value; NPV, Negative Predictive Value.

Patients and methods

Screening of patients

This research was approved by the ethics committee of Shanghai Tenth People's Hospital affiliated with Tongji University (Shanghai, China; No. SHSY-IEC-4.1/20–21/01). All methods were carried out under the relevant guidelines and regulations. The study enrolled 260 patients who had undergone EBUS-TBNA with ROSE (n = 134) or without ROSE (n = 126) in the bronchoscopy room of the said hospital between 2018 and 2020. The clinical data of the patients in the two groups including sex, age, smoking history, accompanying symptoms, underlying diseases, and the length of hospitalization stay are presented in **Table 1**. Contraindications to bronchoscopy were examined before operation in all patients. In addition, routine examinations including electrocardiography, coagulation time, electrolytes, and infectious diseases were also performed before the operation. The inclusion criteria were patients older than 18 years whose chest CT scan showed ground glass or ordinary nodules, masses, and cavity or inflammatory manifestations. Not suitable for this procedure were patients with major diseases such as cachectic, a recent history of bronchial or lung trauma, bronchial asthma, myocardial infarction, and hematological diseases. Patients with incomplete information regarding discharge, transfer, or failure to follow up were also excluded (**Figure 1**).

Preoperative preparations and postoperative management

The patient was kept nil for at least 6 h before the procedure. Patients were placed in a supine position; intravenous access was

TABLE 1 Baseline characteristics of patients.

	ROSE (n = 134)	Non-ROSE (n = 126)	χ^2	P-value
Age (years, mean ± SD)	60.75 ± 12.75	60.56 12.75	/	0.904
Sex (n, %)			0.028	0.900
Male	79 (59.0%)	73 (57.9%)		
Female	55 (41.0%)	53 (42.1%)		
Smoking history (n, %)			0.334	0.575
No	101 (75.4%)	91 (72.2%)		
Yes	33 (24.6%)	35 (27.8%)		
Symptoms				
Dyspnea (n, %)			1.572	0.249
No	121 (90.3%)	119 (94.4%)		
Yes	13 (9.7%)	7 (5.6%)		
Cough (n, %)			0.800	0.442
No	80 (59.7%)	82 (65.1%)		
Yes	54 (40.3%)	44 (34.9%)		
Fever (n, %)			0.098	0.862
No	113 (84.3%)	108 (85.7%)		
Yes	21 (15.7%)	18 (14.3)		
Joint pain (n, %)			2.363	0.158
No	130 (97.0%)	117 (92.9%)		
Yes	4 (3.0%)	9 (7.1%)		
Basic diseases				
Hypertension (n, %)			1.335	0.303
No	107 (79.9%)	93 (73.8%)		
Yes	27 (20.1%)	33 (26.2)		
Diabetes (n, %)			1.096	0.327
No	114 (85.1%)	101 (80.2%)		
Yes	20 (14.9%)	25 (19.8%)		
Hypertension+ diabetes (n, %)			0.01	1.000
No	124 (92.5%)	117 (92.9%)		
Yes	10 (7.5%)	9 (7.1%)		
The length of hospitalization stay (mean ± SD)	9.03 ± 4.16	8.12 ± 3.55	/	0.059

ROSE, Rapid On-Site Evaluation.

established. Midazolam was administered by a pulmonologist for conscious sedation. Oxygen was given to the patient through the nasal catheter, and the basic life indicators including blood pressure, pulse, respiratory frequency, and oxygen saturation were monitored routinely during the whole operation process. A chest X-ray and routine blood examination were performed if uncomfortable symptoms or abnormal signs developed after this operation. For malignancies that failed to be detected by EBUS-TBNA, further CT-guided transthoracic puncture or open-chest surgery was required to obtain a reliable pathological tissue diagnosis.

A summary of the sample processing

The specimen absorbed into the needle cavity was gently pushed by the central tube core needle and spread over the slide as evenly as possible in a circle about 1 cm in diameter. A portion of the visible tissue fragment collected on the glass slide was transferred into a single container containing formalin for later histological examination, making sure that the tissue was immersed completely in formalin; the basic information of the specimen was marked on the surface of the bottle. The remaining specimen was divided into two sections and smeared onto two slides. The specimen remaining in the needle cavity and catheter cavity was washed down with normal saline and collected for microbiological analysis. The specimens in ROSE and non-ROSE groups were treated differently. One of the slides in the ROSE group was stained with Diff-quick cell staining solution AB (Zhuhai Beso Biotechnology Co., Ltd., Zhuhai, China) to observe the cell morphology and composition under the microscope by two experienced pathologists, who then decided whether sampling was completed successfully, or should be

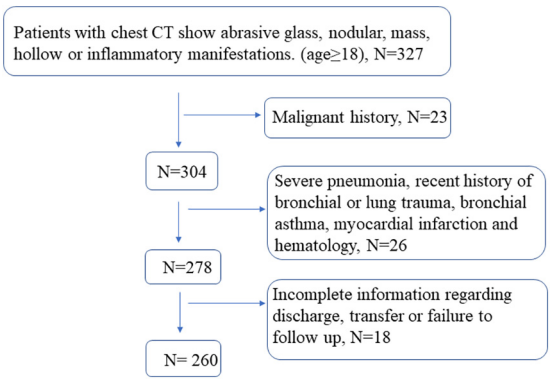

FIGURE 1
Standard flowchart for patient screening.

re-performed elsewhere. The other slide was placed in a bottle containing 95% alcohol for subsequent Papanicolaou staining and cytological examination. If abnormal cells were detected by ROSE, 2–3 more tissues needed to be taken at the same site. Otherwise, sampling would be continued in other sites to find whether there were diagnostic specimens that we needed. All non-ROSE specimens were fixed with 95% alcohol for cytological examination. The above processes are shown in Figure 2.

Diagnosis

The histological and cytological specimens were interpreted by two experienced pathologists. The final diagnostic results were determined by the pathological results of the histological biopsy. For suspicious cases or non-specific diagnostic results, thoracoscopic examination, mediastinal examination, or other surgical procedures were carried out according to the patient's wishes. For patients who were temporarily unwilling to undergo invasive examinations, preliminary conclusions could be obtained after considering the clinical symptoms, imaging findings, and laboratory examinations. A follow-up examination was performed once at least 6 months after EBUS-TBNA to further verify the original judgment according to the therapeutic effect. The diagnostic yield, sensitivity, specificity, positive predictive value (PPV), negative predictive value (NPV),

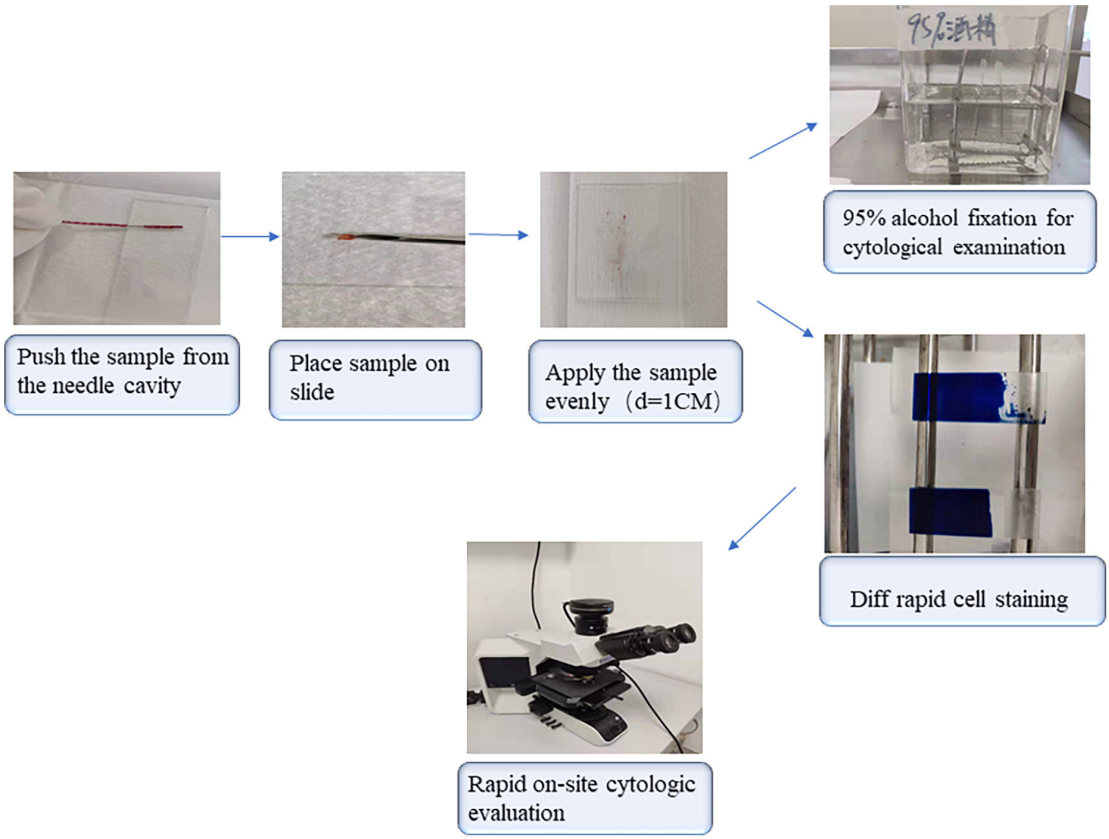

FIGURE 2
A flow diagram of procedure details.

and Youden index were calculated according to ROSE and pathological results.

Statistical analysis

The SPSS21.0 software was used for statistical analysis. Continuous variables were analyzed using a *t*-test, and dichotomous variables were analyzed using Pearson's χ^2-test or Fisher's exact test. Results were considered statistically significant only when the *P*-value was less than 0.05.

Results

Baseline characteristics of the patients

Our statistics showed no significant difference in sex ($P = 0.900$) and age ($P = 0.904$) between the two groups, and the number of smokers was approximately the same (33 vs. 35, $P = 0.575$). The main symptoms were cough (54 vs. 44), fever (21 vs. 18), dyspnea (13 vs. 7), and combined chest pain (4 vs. 9) in ROSE and non-ROSE groups. And there was no significant difference in these symptoms between the two groups ($\chi^2 = 0.800$, $P = 0.442$; $\chi^2 = 0.098$, $P = 0.862$; $\chi^2 = 1.572$, $P = 0.249$; $\chi^2 = 2.363$, $P = 0.158$, respectively). The most common underlying diseases in both groups were hypertension and diabetes. No significant statistical difference in terms of underlying diseases between the two groups ($\chi^2 = 1.335$, $P = 0.303$; $\chi^2 = 1.096$, $P = 0.327$; respectively). The average length of hospitalization stay was 9.03 days in the ROSE group and 8.12 days in the non-ROSE group, showing no significant difference between the two groups ($P = 0.059$) (as shown in **Table 1**). Data showed no significant statistical difference in the baseline characteristics including sex, age, smoking history, symptoms, associated underlying diseases, and hospitalization days between ROSE and non-ROSE groups.

Size, nature, and distribution characteristics of the lesions

We further analyzed the size, nature, and distribution location of lesions in the lung lobe between ROSE and non-ROSE groups. The specific distribution of lesions involved the right upper, right middle, right lower, left upper, left lingual, left lower, left pulmonary valve, lower or upper lobe of both lungs and all lungs. There were no significant differences in size ($P = 0.669$) and distribution ($P = 0.139$) of the lesions between the two groups. The lesions were divided into five categories according to their nature and characteristics: grinding nodules, common nodules, bumps, cavities and inflammatory exudations, which were significantly different between the two groups ($P = 0.008$) (**Table 2**).

Preliminary diagnosis and classification of benign and malignant diseases by using the method of rapid on-site evaluation during endobronchial ultrasound-guided transbronchial needle aspiration

Forty (29.9%) malignant nodules were detected in the ROSE group, including 26 cases of adenocarcinoma (AD), 12 cases of squamous cell carcinoma (SCC), and 2 cases of small cell lung cancer (SCLC). In addition, 2 cases of hamartoma, 1 case of synovial sarcoma, 1 case of tuberculosis, 3 cases of pulmonary abscesses, and 5 cases of fungal infections were detected as benign lesions. In the non-ROSE group, only 14 patients (11.1%) were diagnosed as malignant nodules by pathology, including 5 cases of AD, 4 cases of SCC, 4 cases of SCLC, and 1 case of cancer *in situ*. Furthermore, 1 case of dysplasia, 3 cases of lung abscess, and 3 cases of fungal infections were diagnosed as benign lesions in this group. Inflammatory nodules occupied a very large proportion in both the ROSE and non-ROSE groups (82 vs. 105) (as shown in **Supplementary Figure 1**). The statistical method of the chi-square test was adopted in our study, demonstrating that the application of ROSE technology during EBUS-TBNA contributes to the identification of benign and malignant tumors compared with the non-ROSE group as described in **Table 3** ($\chi^2 = 13.858$, $P < 0.001$).

Accuracy of diagnosis

The overall diagnostic yield of EBUS-TBNA for malignant diseases in the ROSE and non-ROSE groups were 29.9 and 11.1%, respectively (**Table 3**). It fully demonstrates that ROSE technology during EBUS-TBNA has an advantage in improving the diagnostic yield of malignant diseases compared to the non-ROSE group. The diagnostic accuracy of ROSE in PLs relative to the pathological results was calculated. The results showed that the sensitivity, specificity, PPV, and NPV of ROSE during EBUS-TBNA were 97.4, 96.9, 92.5, and 98.9%, respectively, and the Youden index was 94.3%, showing a good agreement with the pathological diagnosis (**Figure 3**).

Complications

The number of punctures for major target lesions in the ROSE group was significantly lower than that in the non-ROSE group ($P < 0.001$). No pneumothorax occurred in the ROSE group vs. 2 cases in the non-ROSE group. Hemoptysis occurred

in 86 cases in the ROSE group vs. 84 cases in the non-ROSE group, accounting for about 75% of the number of cases in each group and showing no statistically significant difference between the two groups (Table 4). None of the patients required further intensive care treatment.

Cytomorphological characteristics of the different lung cancer subtypes

Different lung cancers show their unique cytological features under the microscope. ROSE technique could achieve accurate subtyping of lung cancer based on the cytomorphologic features, especially in well-differentiated tumors. The general microscopic cytology morphology of SCC and AD are shown in Figure 4. The characteristics of the tumor cells are specifically depicted as follows: SCC cells adhered closely and showed clusters, with abnormal morphology of cancer cells and nuclei. AD cells gathered into closely distributed small cell clumps, with clear nucleoli and abundant cytoplasm. Figure 5 presents typical poorly differentiated morphological features of SCC by HE staining. The tumor cells were large and flat, with fusiform deeply stained nuclei and abundant cytoplasm. The diagnosis was confirmed by the immunoreactivity for P40

TABLE 2 Size, nature and distribution characteristics of the lesions.

	ROSE	Non-ROSE	χ^2	*P*-value
Lesion size (cm, mean ± SD)	1.51 ± 2.15	1.40 ± 1.82	/	0.669
Nature of lesion			13.650	0.008*
Grinding lesion	18	31		
Nodules	42	47		
Bump	20	19		
Cavity	5	0		
Inflammation	49	29		
Location of lesion			13.563	0.139
Right upper lobe	27	36		
Right middle lobe	12	12		
Right lower lobe	26	19		
Left upper division	20	27		
Left lingual lobe	7	4		
Left lower lobe	14	18		
Left pulmonary valve	1	1		
Lower lobe of both Lungs	4	1		
Upper lobe of both lungs	6	2		
Both lungs	17	6		

ROSE, Rapid On-Site Evaluation.
**P*-value less than 0.05 is statistically significant difference.

TABLE 3 Preliminary diagnosis and classification of benign and malignant diseases by using the method of ROSE during EBUS-TBNA.

Characteristics	ROSE (*n* = 134)	Non-ROSE (*n* = 126)	χ^2	*P*
Malignant(*n*, %)	40 (29.9%)	14 (11.1%)	13.858	<0.001***
Adenocarcinoma	26	5		
Squamous-cell carcinoma	12	4		
Small cell lung cancer	2	4		
Tis	0	1		
Benign (*n*,%)	94 (70.1%)	112 (88.9%)		
Hamartoma	2	0		
Dysplasia	0	1		
Synovial sarcoma	1	0		
Tuberculosis	1	0		
Abscess	3	3		
Mycotic infection	5	3		
Non-representative samples	82	105		

ROSE, Rapid On-Site Evaluation.
****P*-value less than 0.001 is statistically significant difference.

	Pathological Results	
ROSE	Cancer(n)	Normal(n)
POS	37	3
NEG	1	93

Sensitivity:	97.4%
Specificity:	96.9%
PPV :	92.5%
NPV :	98.9%
Youden index :	94.3%

FIGURE 3
Comparison of the ROSE diagnosis during EBUS-TBNA with the final pathological findings.

and P63 expression. Microscopically, HE staining under the microscope demonstrated that AD cells were mainly composed of cubic and columnar cells with large or irregular nuclear nuclei. Tumor tissues showed positive cytokeratin 7 and TTF-1 immunoreactivity (**Figure 6**). HE staining presented the following morphological features of SCLC tumor cells: small in size and round or oval in shape, mimicking lymphocytes, with rare cytoplasm and deeply stained nuclei. Abnormal cells were positive for TTF-1 immunoreactivity and negative for CD56 (**Figure 7**). Histological biopsy of pulmonary AD derived from metastatic gastrointestinal neoplasms is shown in **Figure 8**. Tumor cells were distributed in clusters and positive for Brg-1 and Claudin-4. The impossibility to afford rapid evaluation and analysis is the main disadvantage of using histological materials for pathological diagnosis. Conversely, the advantages are more attractive in that it can provide more tissue materials for immunohistochemical analysis, thus ensuring more convincing diagnostic results of certain tumor types.

Discussion

We collected multiple sample types in this study, including grinding glass lesions, nodules, masses, cavities, and inflammatory lesions. Our data suggest that there was a trend toward a higher diagnostic yield for malignant diseases in the ROSE group compared to the non-ROSE group. And we concluded that the diagnostic yield of the ROSE method during the EBUS-TBNA procedure for PLs was close to the result of pathological diagnosis. There is a good agreement between the above two methods. Another conclusion with clinical guidance that was also drawn from our study is that the number of punctures in the ROSE group was significantly lower than that in the non-ROSE group. There was no significant difference in hemoptysis between the two groups. The report of our study effectively demonstrated that the ROSE during EBUS-TBNA was a valuable diagnostic method to determine the nature of suspicious lesions.

Our findings have also been validated in several reports abroad. Some scholars have demonstrated a high rate of agreement between ROSE combined with EBUS-TBNA and the final pathological result and proved the effectiveness of ROSE in determining the quality and quantity of specimens (10, 11). Davenport (12) reported that ROSE could increase the detection rate of specimens containing malignant cells by comparing 73 aspirates using the technique with 134 routinely processed aspirates. Diette et al. (13) demonstrated that the ROSE technique could significantly improve the diagnostic yield in the evaluation of lung nodules or masses and/or hilar or mediastinal lymphadenopathies. The application value of ROSE in another interventional diagnosis for pulmonary malignant diseases should also be appreciated. A randomized trial performed by Mondoni et al. (14) showed that the ROSE method increased the cytological diagnostic sensitivity of TBLB from 76 to 97%. Lin et al. (15) collected information from 336 patients undergoing EBUS-TBB surgery, and the application of the ROSE method significantly improved diagnostic accuracy compared with EBUS-TBB without ROSE (88.4% vs. 68.0%, $P < 0.001$). Another study (16) showed a better diagnostic yield from 89.2% without ROSE to 92.1% with ROSE in sampling hilar–mediastinal lymphadenopathies in lung cancer. The utility of ROSE during EBUS-TBNA for lymph node staging and the mode of surgical resection in lung cancer has also been demonstrated in relevant studies (17, 18). This is mainly due to the stable and rapid diagnostic pattern of ROSE and the small demand for sample size. The occurrence of early cancer is often accompanied by the phenomenon of adjacent lymphadenopathy (19), and the clinical value of ROSE is to take full advantage of less sampling and fast diagnosis to achieve

TABLE 4 Comparison of complications between ROSE and non-ROSE groups.

Complications	ROSE (*n*)	Non-ROSE (*n*)	*P*-value
Pneumothorax	No	2	/
Hemoptysis	86	84	0.402
Number of punctures (mean ± SD)	2.07 ± 0.26	3.23 ± 0.42	<0.001***

ROSE, Rapid On-Site Evaluation.
***P-value less than 0.001 is statistically significant difference.

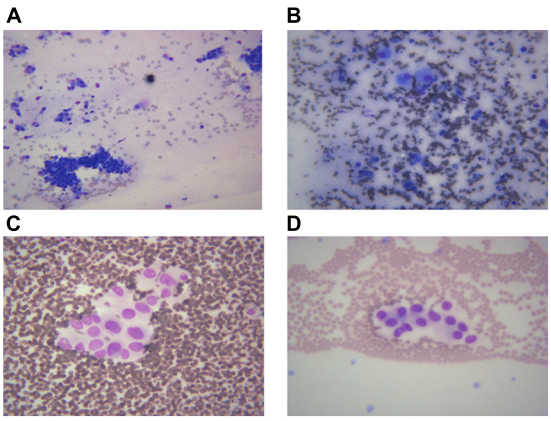

FIGURE 4
Images from different cancer types. According to the morphological characteristics of cells, ROSE can achieve accurate classification of lung cancer subtypes. **(A)** Squamous cell carcinoma, 400×; **(B)** adenocarcinoma derived from gastrointestinal cancer metastasis, 400×; **(C,D)** adenocarcinoma, 400×.

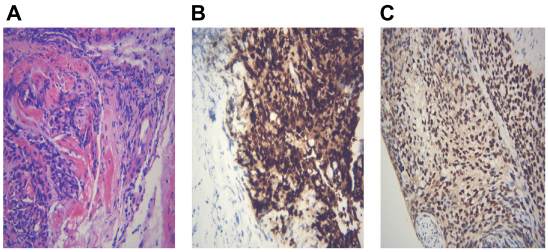

FIGURE 5
An example of histological biopsy from a poorly differentiated squamous cell carcinoma (SCC). **(A)** Shows typical poorly differentiated morphological features of SCC. The tumor cells are large and flat, with fusiform deeply stained nuclei and abundant cytoplasm (HE 400×). The diagnosis is confirmed by the immunoreactivity for P40 (**B**, IHC 400×) and P63 expression (**C**, IHC 400×). **(A)** Poorly differentiated SCC (HE 400×); **(B)** P40 400×; **(C)** P63 400×.

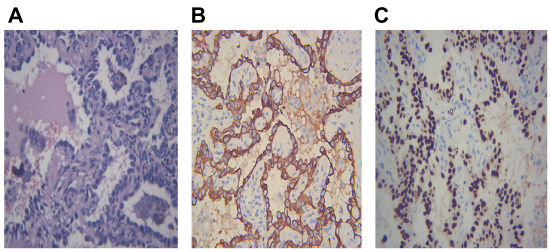

FIGURE 6
Demonstration of histological biopsy from adenocarcinoma. Under the microscope, adenocarcinoma consists of cubic and columnar cells with large or irregular nuclear nuclei and distinct nucleoli (**A**, HE 400×). Tumor cells show positive immunoreactivity for cytokeratin 7 and TTF-1 (**B,C** IHC 400×). **(A)** Adenocarcinoma HE 400×; **(B)** CK7 400×; **(C)** TTF-1 400×.

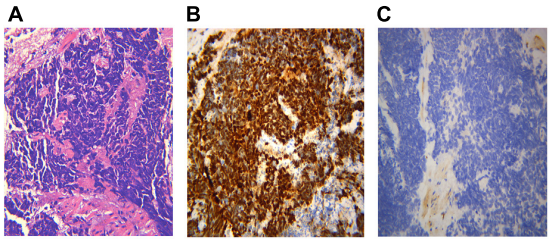

FIGURE 7
Histological biopsy of a case of small cell lung cancer (SCLC). HE staining presents the morphological features: tumor cells are small in size and round or oval in shape, mimicking lymphocytes, with rare cytoplasm, deeply stained nuclei and invisible nucleoli (**A**, HE 400×). Abnormal cells are positive for TTF-1 immunoreactivity (**B**, IHC 400×), and negative for CD56 (**C**, IHC 400×). **(A)** Small cell lung cancer HE 400×; **(B)** TTF-1 400×; **(C)** CD56(-) 400×.

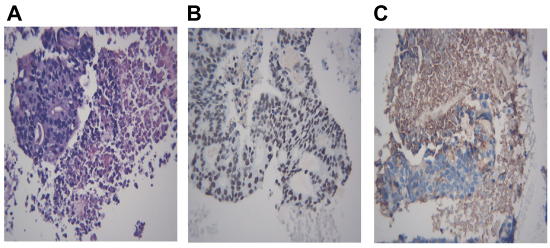

FIGURE 8
Histological biopsy of a pulmonary adenocarcinoma with metastasis from gastrointestinal neoplasm. Tumor cells are grouped in clusters (**A**, HE 400×) and positive for Brg-1 (**B**, IHC 400×) and Claudin-4 (**C**, IHC 400×). **(A)** Metastasis from gastrointestinal neoplasm, HE 400×; **(B)** Brg-1 400×; **(C)** Claudin-4 400×.

rapid identification of abnormal cells in lymph nodes (13, 20–24). ROSE enables rapid and accurate interpretation of cancerous tissues and surrounding cancerous tissues and then instructs clinicians to adjust the direction of puncture, which can reduce intraoperative traumas and facilitate the detection of diseased tissues (25–27), contributing to the choice of surgical modes (28–31). Although the clinical utility of ROSE has been reported in kinds of literature, it is still a controversial question on whether can be popularized in clinical practice. Some argue that ROSE does not benefit patients by improving the diagnostic yield for malignant diseases and is limited in clinical application due to the lack of professional pathologists (32, 33). However, our study strongly demonstrated that the ROSE method could improve the diagnostic yield of lung neoplastic diseases and not increase the risk of complications during the operation; instead, it significantly reduced the frequency of

punctures, eliminate unnecessary surgical traumas and bring more benefits to patients compared with the non-ROSE group. The good agreement between the ROSE diagnosis and the final pathological results is also well demonstrated, laying a solid theoretical foundation for the clinical application of ROSE. In the current era of precision medicine, ROSE services have become an important part of achieving rapid diagnosis and decision-making.

There are still some shortcomings in our study. First, the study was conducted in a single-center, which may affect the universality of the conclusion. In addition, this is a retrospective study, which may bring about bias in data collection and reliability of the results. Finally, the number of cases summarized in this study was relatively small.

Conclusion

In conclusion, the prevalence of the ROSE method during EBUS-TBNA is expected to upgrade the level of interventional bronchoscopy to a new profile, and to further meet the patients' needs for high-quality and accurately targeted medical services, and promote the development of medical undertakings around the world.

Data availability statement

The raw data supporting the conclusions of this article will be made available by the authors, without undue reservation.

Ethics statement

The studies involving human participants were reviewed and approved by the Ethics Committee of Shanghai Tenth People's Hospital affiliated with Tongji University. The patients/participants provided their written informed consent to participate in this study.

Author contributions

LL, HD, HZ, HY, XL, CW, and SX: conception and design and drafting of the manuscript. All authors: acquisition, statistical analysis, or interpretation of the data, review, and approved the final version of the manuscript.

Acknowledgments

We thank all the patients who donated their biological samples.

Conflict of interest

The authors declare that the research was conducted in the absence of any commercial or financial relationships that could be construed as a potential conflict of interest.

Publisher's note

All claims expressed in this article are solely those of the authors and do not necessarily represent those of their affiliated organizations, or those of the publisher, the editors and the reviewers. Any product that may be evaluated in this article, or claim that may be made by its manufacturer, is not guaranteed or endorsed by the publisher.

Supplementary material

The Supplementary Material for this article can be found online at: https://www.frontiersin.org/articles/10.3389/fmed.2022.922239/full#supplementary-material

SUPPLEMENTARY FIGURE 1
Preliminary diagnosis and classification of benign and malignant diseases by using the method of ROSE during EBUS-TBNA. Red, ROSE; Green, non-ROSE.

References

1. Bade BC, Dela Cruz CS. Lung cancer 2020: epidemiology, etiology, and prevention. *Clin Chest Med.* (2020) 41:1–24. doi: 10.1016/j.ccm.2019.10.001

2. Groitl H. The flexible bronchofiberscope in the intensive care unit (ICU)–the optimal postoperative care for the bronchial system. *Endoscopy.* (1981) 13:100–3. doi: 10.1055/s-2007-1021658

3. Mehta AC, Hood KL, Schwarz Y, Solomon SB. The evolutional history of electromagnetic navigation bronchoscopy: state of the art. *Chest.* (2018) 154:935–47. doi: 10.1016/j.chest.2018.04.029

4. Gupta D, Dadhwal DS, Agarwal R, Gupta N, Bal A, Aggarwal AN. Endobronchial ultrasound-guided transbronchial needle aspiration vs. conventional transbronchial needle aspiration in the diagnosis of sarcoidosis. *Chest.* (2014) 146:547–56. doi: 10.1378/chest.13-2339

5. Valentini I, Lazzari Agli L, Michieletto L, Innocenti M, Savoia F, Del Prato B, et al. Competence in flexible bronchoscopy and basic biopsy technique. *Panminerva Med.* (2019) 61:232–48. doi: 10.23736/S0031-0808.18.03563-2

6. Griffin AC, Schwartz LE, Baloch ZW. Utility of on-site evaluation of endobronchial ultrasound-guided transbronchial needle aspiration specimens. *Cytojournal.* (2011) 8:20. doi: 10.4103/1742-6413.90081

7. Oki M, Saka H, Kitagawa C, Kogure Y, Murata N, Adachi T, et al. Rapid on-site cytologic evaluation during endobronchial ultrasound-guided transbronchial needle aspiration for diagnosing lung cancer: a randomized study. *Respiration.* (2013) 85:486–92. doi: 10.1159/000346987

8. Pausawasdi N, Cheirsilpa K, Chalermwai W, Asokan I, Sriprayoon T, Charatcharoenwitthaya P. Endoscopic ultrasound-guided fine-needle biopsy using 22G franseen needles without rapid on-site evaluation for diagnosis of intraabdominal masses. *J Clin Med.* (2022) 11:1051. doi: 10.3390/jcm11041051

9. Sehgal IS, Dhooria S, Aggarwal AN, Agarwal R. Impact of Rapid On-Site Cytological Evaluation (ROSE) on the diagnostic yield of transbronchial needle aspiration during mediastinal lymph node sampling: systematic review and meta-analysis. *Chest.* (2018) 153:929–38. doi: 10.1016/j.chest.2017.11.004

10. Yuan M, Wang Y, Yin W, Xiao Y, Hu M, Hu Y. Efficacy of rapid on-site cytological evaluation (ROSE) by a pulmonologist in determining specimen adequacy and diagnostic accuracy in interventional diagnosis of lung lesions. *J Int Med Res.* (2021) 49:300060520982687. doi: 10.1177/0300060520982687

11. Nakajima T, Yasufuku K, Saegusa F, Fujiwara T, Sakairi Y, Hiroshima K, et al. Rapid on-site cytologic evaluation during endobronchial ultrasound-guided transbronchial needle aspiration for nodal staging in patients with lung cancer. *Ann Thorac Surg.* (2013) 95:1695–9. doi: 10.1016/j.athoracsur.2012.09.074

12. Davenport RD. Rapid on-site evaluation of transbronchial aspirates. *Chest.* (1990) 98:59–61. doi: 10.1378/chest.98.1.59

13. Diette GB, White P, Terry P, Jenckes M, Rosenthal D, Rubin HR. Utility of on-site cytopathology assessment for bronchoscopic evaluation of lung masses and adenopathy. *Chest.* (2000) 117:1186–90. doi: 10.1378/chest.117.4.1186

14. Mondoni M, Carlucci P, Di Marco F, Rossi S, Santus P, D'Adda A, et al. Rapid on-site evaluation improves needle aspiration sensitivity in the diagnosis of central lung cancers: a randomized trial. *Respiration.* (2013) 86:52–8. doi: 10.1159/000346998

15. Lin C-K, Jan IS, Yu K-L, Chang L-Y, Fan H-J, Wen Y-F, et al. Rapid on-site cytologic evaluation by pulmonologist improved diagnostic accuracy of endobronchial ultrasound-guided transbronchial biopsy. *J Formos Med Assoc.* (2020) 119:1684–92. doi: 10.1016/j.jfma.2020.01.001

16. Guo H, Liu S, Guo J, Li B, Li W, Lu Z, et al. Rapid on-site evaluation during endobronchial ultrasound-guided transbronchial needle aspiration for the diagnosis of hilar and mediastinal lymphadenopathy in patients with lung cancer. *Cancer Lett.* (2016) 371:182–6. doi: 10.1016/j.canlet.2015.11.038

17. Wada H, Nakajima T, Yasufuku K, Fujiwara T, Yoshida S, Suzuki M, et al. Lymph node staging by endobronchial ultrasound-guided transbronchial needle aspiration in patients with small cell lung cancer. *Ann Thorac Surg.* (2010) 90:229–34. doi: 10.1016/j.athoracsur.2010.03.106

18. Chen X, Wan B, Xu Y, Song Y, Zhan P, Huang L, et al. Efficacy of rapid on-site evaluation for diagnosing pulmonary lesions and mediastinal lymph nodes: a systematic review and meta-analysis. *Transl Lung Cancer Res.* (2019) 8:1029–44. doi: 10.21037/tlcr.2019.12.13

19. Kim ES, Bosquée L. The importance of accurate lymph node staging in early and locally advanced non-small cell lung cancer: an update on available techniques. *J Thorac Oncol.* (2007) 2(Suppl. 2):S59–67. doi: 10.1097/01.JTO.0000269738.13586.fd

20. Diacon AH, Schuurmans MM, Theron J, Louw M, Wright CA, Brundyn K, et al. Utility of rapid on-site evaluation of transbronchial needle aspirates. *Respiration.* (2005) 72:182–8. doi: 10.1159/000084050

21. Tournoy KG, Praet MM, Van Maele G, Van Meerbeeck JP. Esophageal endoscopic ultrasound with fine-needle aspiration with an on-site cytopathologist: high accuracy for the diagnosis of mediastinal lymphadenopathy. *Chest.* (2005) 128:3004–9. doi: 10.1378/chest.128.4.3004

22. Klapman JB, Logrono R, Dye CE, Waxman I. Clinical impact of on-site cytopathology interpretation on endoscopic ultrasound-guided fine needle aspiration. *Am J Gastroenterol.* (2003) 98:1289–94. doi: 10.1111/j.1572-0241.2003.07472.x

23. Jhala NC, Jhala DN, Chhieng DC, Eloubeidi MA, Eltoum IA. Endoscopic ultrasound-guided fine-needle aspiration. A cytopathologist's perspective. *Am J Clin Pathol.* (2003) 120:351–67. doi: 10.1309/MFRF-J0XY-JLN8-NVDP

24. Fassina A, Corradin M, Zardo D, Cappellesso R, Corbetti F, Fassan M. Role and accuracy of rapid on-site evaluation of CT-guided fine needle aspiration cytology of lung nodules. *Cytopathology.* (2011) 22:306–12. doi: 10.1111/j.1365-2303.2010.00802.x

25. Al-Abbadi MA, Bloom LI, Fatheree LA, Haack LA, Minkowitz G, Wilbur DC, et al. Adequate reimbursement is crucial to support cost-effective rapid on-site cytopathology evaluations. *Cytojournal.* (2010) 7:22. doi: 10.4103/1742-6413.71740

26. Dhillon I, Pitman MB, Demay RM, Archuletta P, Shidham VB. Compensation crisis related to the onsite adequacy evaluation during FNA procedures-Urgent proactive input from cytopathology community is critical to establish appropriate reimbursement for CPT code 88172 (or its new counterpart if introduced in the future). *Cytojournal.* (2010) 7:23. doi: 10.4103/1742-6413.71741

27. Gupta PK. Progression from on-site to point-of-care fine needle aspiration service: opportunities and challenges. *Cytojournal.* (2010) 7:6. doi: 10.4103/1742-6413.63195

28. Fang X, Cui T, Qiu J-Q, Zhang W-L, Duan H. Rapid on-site cytologic evaluation during endobronchial ultrasound-guided transbronchial biopsy. *J Formos Med Assoc.* (2021) 120:1412–3. doi: 10.1016/j.jfma.2020.12.006

29. Wang M, Levy G, Qin X, Adeniran AJ, Cai G. Fine-Needle Aspiration Biopsy of Intraocular Mass-Like Lesions. *Am J Clin Pathol.* (2021) 156:268–77. doi: 10.1093/ajcp/aqaa235

30. Lin C-K, Jan IS, Yu K-L, Chang L-Y, Fan H-J, Wen Y-F, et al. Rapid on-site cytologic evaluation by pulmonologist improved diagnostic accuracy of endobronchial ultrasound-guided transbronchial biopsy. *J Formos Med Assoc.* (2021) 120:1414–5. doi: 10.1016/j.jfma.2020.12.020

31. Torous VF, Lopez SH, Xu C, Sweeney BJ, Pitman MB. Performance of rapid on-site evaluation in breast fine-needle aspiration biopsies: identifying areas of diagnostic challenge. *Acta Cytol.* (2022) 66:1–13. doi: 10.1159/000518579

32. Yarmus L, Van der Kloot T, Lechtzin N, Napier M, Dressel D, Feller-Kopman D. A randomized prospective trial of the utility of rapid on-site evaluation of transbronchial needle aspirate specimens. *J Bronchology Interv Pulmonol.* (2011) 18:121–7. doi: 10.1097/LBR.0b013e31821707ee

33. Gu P, Zhao Y-Z, Jiang L-Y, Zhang W, Xin Y, Han B-H. Endobronchial ultrasound-guided transbronchial needle aspiration for staging of lung cancer: a systematic review and meta-analysis. *Eur J Cancer.* (2009) 45:1389–96. doi: 10.1016/j.ejca.2008.11.043

frontiers | Frontiers in Medicine

TYPE Original Research
PUBLISHED 05 October 2022
DOI 10.3389/fmed.2022.1007589

OPEN ACCESS

EDITED BY
Yi Liu,
Shandong Provincial Hospital, China

REVIEWED BY
Gunnar N. Hillerdal,
Karolinska University Hospital, Sweden
Mariaenrica Tinè,
University of Padua, Italy

*CORRESPONDENCE
Lihong Fan
fanlih@aliyun.com

†These authors share first authorship

SPECIALTY SECTION
This article was submitted to Pulmonary Medicine, a section of the journal Frontiers in Medicine

RECEIVED 01 August 2022
ACCEPTED 20 September 2022
PUBLISHED 05 October 2022

CITATION
Shen C, Wu Q, Xia Q, Cao C, Wang F, Li Z and Fan L (2022) Establishment of a malignancy and benignancy prediction model of sub-centimeter pulmonary ground-glass nodules based on the inflammation-cancer transformation theory. *Front. Med.* 9:1007589. doi: 10.3389/fmed.2022.1007589

Establishment of a malignancy and benignancy prediction model of sub-centimeter pulmonary ground-glass nodules based on the inflammation-cancer transformation theory

Changxing Shen[1†], Qiong Wu[2†], Qing Xia[1†], Chuanwu Cao[1], Fei Wang[1], Zhuang Li[1] and Lihong Fan[1*]

[1]Department of Integrated Traditional Chinese and Western Medicine, Shanghai Tenth People's Hospital, Tongji University School of Medicine, Shanghai, China, [2]Liangcheng Xincun Community Health Services Center, Shanghai University of Traditional Chinese Medicine, Shanghai, China

Background: In recent years, Chinese clinicians are frequently encountered by patients with multiple lung nodules and these intensity ground-glass nodules (GGNs) are usually small in size and some of them have no spicule sign. In addition, early lung cancer is diagnosed in large numbers of non-heavy smokers and individuals with no caner history. Obviously, the Mayo model is not applicable to these patients. The aim of the present study is to develop a new and more applicable model that can predict malignancy or benignancy of pulmonary GGNs based on the inflammation-cancer transformation theory.

Materials and methods: Included in this study were patients who underwent surgical resection or lung puncture biopsy of GGNs in Shanghai 10th People's Hospital between January 1, 2018 and May 31, 2021 with the inclusion criterion of the maximum diameter of GGN < 1.0 cm. All the included patients had their pulmonary GGNs diagnosed by postoperative pathology. The patient data were analyzed to establish a prediction model and the predictive value of the model was verified.

Results: Altogether 100 GGN patients who met the inclusion criteria were included for analysis. Based on the results of logistic stepwise regression analysis, a mathematical predication equation was established to calculate the malignancy probability as follows: Malignancy probability rate (p) = ex/(1 + ex); $p > 0.5$ was considered as malignant and $p \leq 0.5$ as benign, where $x = 0.9650 + [0.1791 \times$ T helper (Th) cell$] + [0.2921 \times$ mixed GGN (mGGN)$] + (0.4909 \times$ vascular convergence sign$) + (0.1058 \times$ chronic inflammation). According to this prediction model, the positive prediction rate was 73.3% and the negative prediction rate was 100% versus the positive prediction rate of 0% for the Mayo model.

Conclusion: By focusing on four major factors (chronic inflammation history, human Th cell, imaging vascular convergence sign and mGGNs), the present prediction model greatly improves the accuracy of malignancy or benignancy prediction of sub-centimeter pulmonary GGNs. This is a breakthrough innovation in this field.

KEYWORDS

prediction model, sub-centimeter, pulmonary GGNs, Mayo model, innovative

Background

Lung cancer is a malignant tumor ranking first in terms of both the incidence and mortality worldwide, primarily because of lacking early prediction and intervention. The Mayo model is a classic model for malignancy probability prediction of pulmonary nodules *via* synthetic analysis of age, smoking history, extra-thoracic tumor history, nodule diameter, the presence or absence of the spicule sign, and whether or not the nodule is located in the upper lung lobe. However, the pulmonary ground-glass nodules (GGNs) encountered in clinical practice are mostly multi-focal and small in size with no spicule sign. Furthermore, early lung cancer is diagnosed in large numbers of non-heavy smokers and individuals with no caner history (1, 2). In addition, more studies have reported chronic inflammation-cancer transformation in more sub-healthy individuals with pulmonary GGNs complicated with organ and tissue chronic inflammation due to the influence from the natural environment, food safety, and psychic pressure (3–5). For this reason, we need to ponder over the impact of these previously ignored factors on the pathogenesis of lung cancer and the predictive value, and establish a new and more applicable model for predicting malignancy or benignancy of pulmonary nodules for the sake of improving the diagnostic accuracy of early lung cancer, especially in China.

Patients and methods

Included in this study were patients who underwent surgical resection of GGNs in Shanghai 10th People's Hospital between January 1, 2018 and May 31, 2021 with the inclusion inclusion criterion of the maximum diameter of GGN < 1.0 cm.

The inclusion criteria were (1) patients who were found to have solitary nodules in the lung parenchyma on the CT image of our hospital; (2) the diameter of the nodule was 5 mm $<$ diameter $<$ 10 mm; (3) complete case information was available; (4) the diagnosis was confirmed by postoperative pathology; (5) tumor markers of CEA, SCC, NSE, and CYFRA21-1 were available; (6) all pulmonary nodules were followed up for more than 3 months; and (7) the patients had not received any preoperative treatment.

The exclusion criteria were (1) patients with diffuse pulmonary nodules; (2) solid pulmonary nodules; (3) calcified pulmonary nodules; (4) clinical data were incomplete; (5) patients who did not receive CT examination in our hospital; and (6) patients who had received chemotherapy, radiotherapy, or other treatments before operative.

Clinical data collection

Clinical data were collected from patients who had found pulmonary nodules in physical examinations but without receiving any treatment, including the sex, age, smoking history, personal tumor history, family tumor history, inflammation history of other tissue, and organs or chronic pulmonary inflammation history, and anxiety (international standard anxiety self rating scale, SAS) or depression (Self rating Depression Scale, SDS).

Histopathological criteria for judging pulmonary nodules

Malignancy of pulmonary nodules was confirmed by postoperative pathology of the surgical resected specimens. Benignancy of pulmonary nodules was confirmed by postoperative pathology of the surgical resected specimens. 100 patients underwent segmental pneumonectomy, and 100 nodule specimens were removed.

Laboratory evaluation

Blood inflammatory cytokines, T cell subsets and tumor biomarkers were detected within 1 month before surgery.

Imaging information collection

Imaging information included the pulmonary nodule type [mixed GGN (mGGN), pure GGN (pGGN)], whether the nodular lesion was accompanied with the vascular convergence sign, the spicule sign, a smooth or unsmooth boundary, the presence or absence of pleural indentation, the presence or absence of the vacuole sign, nodule diameter (mm), and whether or not the nodule was located in the upper lung lobe.

TABLE 1 Pathological results of pulmonary nodules in the model group.

Pathological type	Pathological result	$n = 100$
Malignant		**$n = 60$**
	In situ cancer	30
	Adenocarcinoma	24
	Squamous carcinoma	3
	Small-cell lung cancer	1
	Other malignant types	2
Benign		**$n = 40$**
	Inflammatory granuloma	18
	Tuberculoma	8
	Hamartoma	5
	Hemangioma	4
	Inflammatory pseudotumor	3
	Others	2

Statistical methods

The nodules were grouped according to the pathological results. Comparison between two groups was statistically analyzed by R language. The above 19 risk factors were analyzed by univariate analysis (whether the laboratory indexes were elevated or not, the baseline medical history, personal history and family history, and imaging signs were defined as binary variables: yes, 1, and no, 0; elevated, 1, and normal, 0). Significant differences in univariate analysis were subjected to multivariate logistic regression analysis. $p < 0.05$ was defined as statistically significant. Significant risk factors were used to establish a mathematical prediction equation as follows: Malignancy probability rate (p) = ex/(1 + ex); $p > 0.5$ was considered as malignant and $p \leq 0.5$ as benign.

Results

In the model group, 60 patients were diagnosed as having malignant pulmonary nodules by postoperative pathology of the surgically resected specimens, and 60 nodular lesions were treated; 40 patients were diagnosed as having benign pulmonary nodules by postoperative pathology of the surgically resected specimens, and 40 lesions were treated (Table 1). The results of univariate analysis of the 19 risk factors were shown in Table 2, compared with patients with benign pulmonary nodules, the results of

TABLE 2 Comparison of risk factors between malignant and benign groups in the model group.

Factors	Malignant group $n = 60$	Benign group $n = 40$	*P*
Sex (M/F)	27/33	20/20	0.09
Age (yr.)	51.82 ± 14.84	52.48 ± 10.40	0.12
Proinflammatory factor elevation (yes/no)	42/18	12/28	<0.05*
Th cell reduction (yes/no)	54/6	10/30	<0.05*
Tumor marker elevation (yes/no)	18/42	7/33	0.07
Mixed GGNs (yes/no)	56/4	5/35	<0.05*
Pure GGNs (yes/no)	2/58	10/30	<0.05*
Vascular convergence sign (yes/no)	60/0	6/34	<0.05*
Short spicule sign (yes/no)	4/56	0/40	0.56
Smooth boundary (yes/no)	0/60	10/30	<0.05*
Pleural indentation (yes/no)	8/52	0/40	0.19
Vacuole sign (yes/no)	6/54	2/38	0.21
Nodule diameter (mm)	9.43 ± 2.21	10.75 ± 2.42	0.18
Nodule in upper lobe (yes/no)	17/43	4/36	<0.05*
Smoking history (yes/no)	9/51	5/35	0.77
Personal tumor history (yes/no)	12/48	2/38	<0.05*
Family tumor history (yes/no)	4/56	1/39	<0.05*
Chronic inflammatory disease history (yes/no)	20/40	4/36	<0.05*
Anxiety/depression history (yes/no)	13/47	2/38	<0.05*

Th cell, T helper cell. *Statistically significant.

TABLE 3 Logistic regression analysis of risk factors for malignant nodules in the model group.

Factors	*B*	S.E.	*P*
Proinflammatory factor elevation (yes/no)	0.0047	0.0439	0.21
Th cell reduction (yeas/no)	0.1791	0.0524	0.01∗
mGGNs (yes/no)	0.2920	0.0664	0.001∗
pGGNs (yes/no)	−0.1061	0.0679	0.12
Vascular convergence sign (yes/no)	0.4908	0.0695	0.02∗
Smooth boundary (yes/no)	−0.1199	0.0725	0.22
Nodule in upper lobe (yes/no)	0.0677	0.0516	0.15
Personal tumor history (yes/no)	0.0024	0.0590	0.41
Family tumor history (yes/no)	0.1289	0.0825	0.32
Chronic inflammatory disease history (yes/no)	0.105845	0.046626	0.01∗
Anxiety/depression (yes/no)	0.0034	0.0027	0.09

*Statistically significant.

TABLE 4 Baseline data of patients in malignant and benign groups of the validation group.

Factors	Malignant group $n = 22$	Benign group $n = 18$	*p*
Sex (M/F)	12/10	9/9	0.86
Age (yr.)	54.55 ± 12.09	50.50 ± 8.43	0.09

differential analysis suggested that patients with malignant pulmonary nodules had significant differences in serum inflammatory factors, immune cells, imaging characteristics, history of chronic inflammation, history of tumor, and psychological factors (Table 2). Then Multivariate logistic stepwise regression analysis indicated that Th (helper T) cell reduction, mGGN, vascular convergence sign and chronic inflammatory disease history were significantly correlated with malignant nodules (Table 3). Based on the results of logistic stepwise regression analysis, a mathematical predication equation was established to calculate the malignancy probability as follows: Malignancy probability rate (p) = ex/(1 + ex); $p > 0.5$ was considered as malignant and $p \leq 0.5$ as benign. **X = 0.9650 + (0.1791 × Th cell) + (0.2921 × mGGN) + (0.4909 × vascular convergence sign) + (0.1058 × chronic inflammation)**

where e is a natural logarithm:

if the patient's Th cell was reduced before operation, Th cell = 1 (otherwise = 0);

if the patient's pulmonary nodule was mGGN before operation, mGGN = 1 (otherwise = 0);

if the patent's pulmonary nodule presented vascular convergent sign before operation, vascular convergent sign = 1 (otherwise = 0);

if the patient was complicated with a chronic inflammatory disease history, chronic inflammation = 1 (otherwise = 0).

In the validation group, 27 patients were diagnosed as having malignant pulmonary nodules by postoperative pathology of the surgically resected specimens or puncture biopsy, and 22 nodular lesions were treated; 18 patients were diagnosed as having benign pulmonary nodules by postoperative pathology of the surgically resected specimens, and 18 lesions were treated (Table 4). The predictive efficacy of the mathematical prediction model was judged by entering the data of the validation group into the model of the present study, using the pathological results as the gold standard, and drawing ROC curves by R language statistical software, AUC = 0.867. As shown in Figure 1, the positive prediction rate of our prediction model was 73.3%, and the negative prediction rate was 100% (Table 5). Compared with the new prediction model, Mayo model equation: $X = -6.8272 + (0.0391 \times \text{age}) + (0.7917 \times \text{smoking history}) + (1.3388 \times \text{malignant tumor history}) + (0.1274 \times \text{diameter}) + (1.0407 \times \text{spicule}) + (0.7838 \times \text{upper lobe})$. When the validation model data were entered into the Mayo model, the positive prediction value was 0 (Table 6).

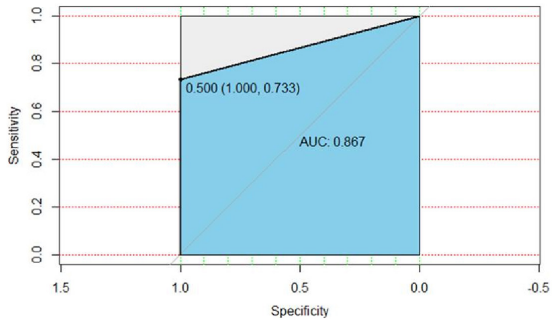

FIGURE 1
ROC curve of the validation group of the present model. AUC = 0.867, the specificity was 100%, the sensitivity was 73.3%, and the cut-off value of logistic regression was 0.5.

TABLE 5 Results of the present prediction model.

Pathological gold standard	Model prediction diagnosis		
	Malignant	Benign	Total
Malignant	22	8	30
Benign	0	10	10
Total	22	18	40

TABLE 6 The Mayo model prediction result.

Pathological gold standard	Model prediction diagnosis		
	Malignant	Benign	Total
Malignant	0	0	0
Benign	22	18	40
Total	22	18	40

Discussion

The incidence of sub-centimeter pulmonary nodules is high in China. As most of these nodules grow slowly and the volume doubling time varies from individual to individual, the diagnostic value of long-term follow-up observation of imaging changes of the nodules is often limited and may cause misdiagnosis of cancer (6). In the present study, we found that the positive prediction rate of the Mayo model on sub-centimeter pulmonary nodules was very low and not suitable for predicting the nature of sub-centimeter pulmonary nodules. In recent years, various models for predicting the nature of pulmonary nodules have been reported. Most of them are based on different pathophysiological characteristics of pulmonary nodules, including the prediction model by combining ctDNA with the imaging features, the prediction model based on pulmonary bloodstream transmission time, the prediction model using human plasma protein LG3BP and C163A, the prediction model using serum miRNA-21-5p, and imaging prediction model (7–15). Sub-centimeter GGNs are mostly *in situ* cancer with relatively low activity of cancer cell metabolism. For this reason, the diagnostic reliability of PETCT-based prediction model is questionable. In addition, most sub-centimeter pulmonary nodules have no short spicule sign, and the incidence of sub-centimeter pulmonary nodules does not increase with the increasing age of the patients (16, 17). As most of these prediction models only use a single aspect of risk factors to assess malignancy or benignancy of the nodules, their clinical prediction value is limited. To the best of our knowledge, there is no model that simultaneously uses a comprehensive spectrum of multiple factors to predict the nature of pulmonary GGNs with relatively small volumes.

Patients with pulmonary nodules are likely to have varying degrees of anxiety and depression, leading to immune dysfunction and low-grade inflammation (18). The inflammation-cancer transformation mechanism has been generally accepted, knowing that long-term chronic inflammation can lead to alterations of the human homeostasis, such as elevation of interleukin-6 (IL-6) as the representative of proinflammatory cytokines and decrease of Th cells in the body. In addition, tissue cell proliferation occurs upon inflammatory stimulation, which promotes new vessel formation to ensure nutrient supply (19). Chronic inflammation-mediated immune response change is an important regulatory factor for the development and evolution of human diseases (20). Studies have demonstrated that a high level of circulating IL-6 is correlated with adverse prognosis of various cancer types including non-small cell lung cancer (NSCLC). Inflammatory cytokines can stimulate the immune system and promote tumor growth, and change of T cell group and function is probably one of the mechanisms underlying the adverse prognosis of NSCLC patients with elevated level of IL-6 (21). The increase of neutrophil compartments in circulation is related to the generation of progranulocytes (IL-1β, IL-17A, TNFα, and IL-6) and elevation of Th2-related cytokines. In tumor patients with a relatively high level of neutrophils, T cell immune response is often reduced, as represented by the reduced expression of cytotoxic T cell genes including CD8A, CD8B, GZMA, and GZMB, the reduced number of CD3 + CD8 + cells, and the reduced expression of IFN-γ related genes (22). Studies have demonstrated the level of inflammatory cytokines is significantly higher and the level of CD4/CD8 is significantly lower in lung cancer and GGN patients as compared with that in patients with benign nodules. In addition, the anti-inflammatory and immune functions are reduced in lung cancer and pulmonary GGN patients, and therefore inflammatory cytokines and immune function can also be used as references for lung cancer prediction (23). Nowadays, natural environmental pollution, food safety, exposure to various irradiations in daily life, pressures from various social aspects, psychic factors, and chronic persistent infections are all factors that can cause the human sub-healthy status. These factors work together to cause chronic inflammation in different parts of the body. Most recent data have expanded the concept about the key role that inflammation plays in cancer development and progression. It has become clearer that the tumor microenvironment (TME) is mainly coordinated by inflammatory cells, and inflammation is an indispensable participant of tumorigenesis by promoting cancer cell proliferation, survival and migration (24, 25). The data obtained in our study also support the chronic inflammation history and Th cell as the lung cancer prediction indexes.

Mixed GGNs are a high-risk factor of primary lung cancer which has been recognized by most clinicians and researchers, and micro-infiltrating lung adenocarcinoma is often manifested by mGGNs (26–28). Vascular convergence is closely correlated with lung adenocarcinoma (29, 30). Vascular lung cancer tumors with vascular convergence sign are often nourished by multiple blood vessels which get assembled in the lung cancer. The clinical significance of this sign indicates the rich blood supply of the nodular lesion and a high probability of malignancy. Some studies reported that the sensitivity, specificity, and accuracy of using the vascular convergence sign as an indicator of lung cancer was 97.2, 68.8, and 93.7%, respectively, which is helpful for lung cancer prediction (21–35). Starting from the pathogenesis of human pulmonary nodules, the prediction model described in this study made a comprehensive analysis of multiple factors that may affect the development and progression of lung cancer, including the chronic inflammation history, family tumor hereditary history, GGN imaging characteristic, serum level of inflammatory cytokines, and T cell subset indexes. The results verified by the validation group show that this prediction model can minimize the misdiagnosis of malignant lung nodules with a high prediction rate and therefore is worthy of clinical promotion.

Conclusion

The prediction model described in this study is an innovative breakthrough in that it greatly improves the accuracy of predicting malignancy or benignancy of sub-centimeter pulmonary nodules by focusing on the four major factors (chronic inflammation history, human immune cell, imaging vascular convergence sign, and mGGNs), thus providing clinicians with an auxiliary tool for the diagnosis and interventional decision making of sub-centimeter pulmonary nodules.

Data availability statement

All datasets generated for this study are included in the article/**Supplementary material**.

Ethics statement

The studies involving human participants were reviewed and approved by the Ethics Committee of Shanghai Tenth People's Hospital, approval number: SHSY-IEC-5.0/22K122/P01. The patients/participants provided their written informed consent to participate in this study.

Author contributions

LF contributed substantially to the study design. QW and QX contributed substantially to the data providing. CS had full access to all data in the study, took responsibility for the integrity of the data, and the accuracy of the data analysis including and especially any adverse effects, and contributed substantially to the writing of the manuscript. CC and FW made contributions to the literature review, while ZL made contributions to the data processing. All authors contributed to the article and approved the submitted version.

Funding

The external funding approval had been obtained, the corresponding author LF had been awarded a grant for the study by the Shanghai Municipal Health Commission [grant number: ZY (2021–2023)-0205-05], which is a government agency in charge of the people's medical and health work.

Conflict of interest

The authors declare that the research was conducted in the absence of any commercial or financial relationships that could be construed as a potential conflict of interest.

Publisher's note

All claims expressed in this article are solely those of the authors and do not necessarily represent those of their affiliated organizations, or those of the publisher, the editors and the reviewers. Any product that may be evaluated in this article, or claim that may be made by its manufacturer, is not guaranteed or endorsed by the publisher.

Supplementary material

The Supplementary Material for this article can be found online at: https://www.frontiersin.org/articles/10.3389/fmed.2022.1007589/full#supplementary-material

References

1. Dubin S, Griffin D. Lung cancer in non-smokers. *Mo Med.* (2020) 117:375–9. doi: 10.1007/s10689-017-0044-4

2. Garrana SH, Dagogo-Jack I, Cobb R, Kuo AH, Mendoza DP, Zhang EW, et al. Clinical and imaging features of non-small-cell lung cancer in young patients. *Clin Lung Cancer.* (2021) 22:23–31.

3. Gomes M, Teixeira AL, Coelho A, Araújo A, Medeiros R. The role of inflammation in lung cancer. *Adv Exp Med Biol.* (2014) 816:1–23.

4. Tsay JJ, Tchou-Wong KM, Greenberg AK, Pass H, Rom WN. Aryl hydrocarbon receptor and lung cancer. *Anticancer Res.* (2013) 33:1247–56.

5. Wang YH, Li JQ, Shi JF, Que JY, Liu JJ, Lappin JM, et al. Depression and anxiety in relation to cancer incidence and mortality: A systematic review and meta-analysis of cohort studies. *Mol Psychiatry.* (2020) 25:1487–99. doi: 10.1038/s41380-019-0595-x

6. Borghesi A, Michelini S, Scrimieri A, Golemi S, Maroldi R. Solid Indeterminate pulmonary nodules of less than 300 mm3: Application of different volume doubling time cut-offs in clinical practice. *Diagnostics.* (2019) 9:62. doi: 10.3390/diagnostics9020062

7. Hu X, Ye W, Li Z, Chen C, Cheng S, Lv X, et al. Non-invasive evaluation for benign and malignant subcentimeter pulmonary ground-glass nodules (≤1 cm) based on CT texture analysis. *Br J Radiol.* (2020) 93:20190762. doi: 10.1259/bjr.20190762

8. Xing W, Sun H, Yan C, Zhao C, Wang D, Li M, et al. A prediction model based on DNA methylation biomarkers and radiological characteristics for identifying malignant from benign pulmonary nodules. *BMC Cancer.* (2021) 21:263. doi: 10.1186/s12885-021-08002-4

9. Zhang R, Tian P, Qiu Z, Liang Y, Li W. The growth feature and its diagnostic value for benign and malignant pulmonary nodules met in routine clinical practice. *J Thorac Dis.* (2020) 12:2019–30. doi: 10.21037/jtd-19-3591

10. Wang B, Sun F, Zheng XZ, Sun CY. A novel application of pulmonary transit time to differentiate between benign and malignant pulmonary nodules using myocardial contrast echocardiography. *Int J Cardiovasc Imaging.* (2021) 37:1215–23. doi: 10.1007/s10554-020-02104-z

11. Silvestri GA, Tanner NT, Kearney P, Vachani A, Massion PP, Porter A, et al. PANOPTIC trial team. Assessment of plasma proteomics biomarker's ability to distinguish benign from malignant lung nodules: Results of the PANOPTIC (pulmonary nodule plasma proteomic classifier) trial. *Chest.* (2018) 154:491–500. doi: 10.1016/j.chest.2018.02.012

12. Shen Y, Xu F, Zhu W, Hu H, Chen T, Li Q. Multiclassifier fusion based on radiomics features for the prediction of benign and malignant primary pulmonary solid nodules. *Ann Transl Med.* (2020) 8:171. doi: 10.21037/atm.2020.01.135

13. Palumbo B, Bianconi F, Palumbo I, Fravolini ML, Minestrini M, Nuvoli S, et al. Value of shape and texture features from 18F-FDG PET/CT to discriminate between benign and malignant solitary pulmonary nodules: An experimental evaluation. *Diagnostics.* (2020) 10:696. doi: 10.3390/diagnostics10090696

14. Chen W, Zhu D, Chen H, Luo J, Fu H. Predictive model for the diagnosis of benign/malignant small pulmonary nodules. *Medicine.* (2020) 99:e19452. doi: 10.1097/MD.0000000000019452

15. Li X, Zhang Q, Jin X, Cao L. Combining serum miRNAs, CEA, and CYFRA21-1 with imaging and clinical features to distinguish benign and malignant pulmonary nodules: A pilot study : Xianfeng Li et al.: Combining biomarker, imaging, and clinical features to distinguish pulmonary nodules. *World J Surg Oncol.* (2017) 15:107. doi: 10.1186/s12957-017-1171-y

16. Mi J, Wang S, Li X, Jiang G. [Clinical characteristics and prognosis of sub-centimeter lung adenocarcinoma]. *Zhongguo Fei Ai Za Zhi.* (2019) 22:500–6.

17. Truong MT, Ko JP, Rossi SE, Rossi I, Viswanathan C, Bruzzi JF, et al. Update in the evaluation of the solitary pulmonary nodule. *Radiographics.* (2014) 34:1658–79.

18. Wang L, Wei Y, Hu H, Zhang X, Zheng M, Fei G. [Correlation between anxiety, depression and changes in Th17/Treg and inflammatory levels in patients with pulmonary nodules]. *Zhongguo Fei Ai Za Zhi.* (2020) 23:554–60. doi: 10.3779/j.issn.1009-3419.2020.102.30

19. Ma SH, Le HB, Jia BH, Wang ZX, Xiao ZW, Cheng XL, et al. Peripheral pulmonary nodules: Relationship between multi-slice spiral CT perfusion imaging and tumor angiogenesis and VEGF expression. *BMC Cancer.* (2008) 8:186. doi: 10.1186/1471-2407-8-186

20. Larsen JM. The immune response to Prevotella bacteria in chronic inflammatory disease. *Immunology.* (2017) 151:363–74. doi: 10.1111/imm.12760

21. Rice SJ, Liu X, Zhang J, Jia B, Zheng H, Belani CP. Advanced NSCLC patients with high IL-6 levels have altered peripheral T cell population and signaling. *Lung Cancer.* (2019) 131:58–61. doi: 10.1016/j.lungcan.2019.03.014

22. Mitchell KG, Diao L, Karpinets T, Negrao MV, Tran HT, Parra ER, et al. Neutrophil expansion defines an immunoinhibitory peripheral and intratumoral inflammatory milieu in resected non-small cell lung cancer: A descriptive analysis of a prospectively immunoprofiled cohort. *J Immunother Cancer.* (2020) 8:e000405. doi: 10.1136/jitc-2019-000405

23. Liu CY, Xie WG, Wu S, Tian JW, Li J. A comparative study on inflammatory factors and immune functions of lung cancer and pulmonary ground-glass attenuation. *Eur Rev Med Pharmacol Sci.* (2017) 21:4098–103.

24. Coussens LM, Werb Z. Inflammation and cancer. *Nature.* (2002) 420:860–7.

25. Rani P, Pal D, Hegde RR, Hashim SR. Acetamides: Chemotherapeutic agents for inflammation-associated cancers. *J Chemother.* (2016) 28:255–65. doi: 10.1179/1973947815Y.0000000060

26. Zhou LN, Wu N, Zhao SJ, Yang L, Wang YL, Wang RB, et al. [HRCT features differentiate synchronous multiple primary lung adenocarcinomas from intrapulmonary metastases]. *Zhonghua Zhong Liu Za Zhi.* (2020) 42:449–55. doi: 10.3760/cma.j.cn112152-20200227-00126

27. Zhang Y, Qiang JW, Ye JD, Ye XD, Zhang J. High resolution CT in differentiating minimally invasive component in early lung adenocarcinoma. *Lung Cancer.* (2014) 84:236–41.

28. Ko JP, Naidich DP. Current readings: Radiologic interpretation of the part-solid nodule: Clinical relevance and novel technologies. *Semin Thorac Cardiovasc Surg.* (2014) 26:145–56. doi: 10.1053/j.semtcvs.2014.07.001

29. Yue JY, Chen J, Zhou FM, Hu Y, Li MX, Wu QW, et al. CT-pathologic correlation in lung adenocarcinoma and squamous cell carcinoma. *Medicine.* (2018) 97:e13362.

30. Aherne EA, Plodkowski AJ, Montecalvo J, Hayan S, Zheng J, Capanu M, et al. What CT characteristics of lepidic predominant pattern lung adenocarcinomas correlate with invasiveness on pathology? *Lung Cancer.* (2018) 118:83–9.

31. Xiong Z, Zhou H, Hu CP, Liu JK, Chen H, Chen W, et al. [Correlation between computed tomographic vascular convergence sign and enhancement value in patients with pulmonary nodules]. *Zhonghua Yi Xue Za Zhi.* (2013) 93:3015–8.

32. Snoeckx A, Reyntiens P, Desbuquoit D, Spinhoven MJ, Van Schil PE, van Meerbeeck JP, et al. Evaluation of the solitary pulmonary nodule: Size matters, but do not ignore the power of morphology. *Insights Imaging.* (2018) 9:73–86.

33. Xia T, Cai M, Zhuang Y, Ji X, Huang D, Lin L, et al. Risk factors for the growth of residual nodule in surgical patients with adenocarcinoma presenting as multifocal ground-glass nodules. *Eur J Radiol.* (2020) 133:109332.

34. Li Q, Li X, Li XY, He XQ, Chu ZG, Luo TY. Histological subtypes of solid-dominant invasive lung adenocarcinoma: Differentiation using dual-energy spectral CT. *Clin Radiol.* (2021) 76:.e1–77. doi: 10.1016/j.crad.2020.08.034

35. Chu ZG, Zhang Y, Li WJ, Li Q, Zheng YN, Lv FJ. Primary solid lung cancerous nodules with different sizes: Computed tomography features and their variations. *BMC Cancer.* (2019) 19:1060. doi: 10.1186/s12885-019-6274-0

frontiers | Frontiers in Medicine

TYPE Original Research
PUBLISHED 13 October 2022
DOI 10.3389/fmed.2022.946238

OPEN ACCESS

EDITED BY
Yi Liu,
Shandong Provincial Hospital, China

REVIEWED BY
Kai Zhang,
Ryerson University, Canada
Pin-Kuei Fu,
Taichung Veterans General Hospital, Taiwan
Vicente Benavides-Cordoba,
Pontificia Universidad Javeriana Cali, Colombia

*CORRESPONDENCE
Xiang-zhen Yuan
xzyuan1973@163.com
Shao-wei Li
li_shaowei81@hotmail.com

†These authors have contributed equally to this work

SPECIALTY SECTION
This article was submitted to Pulmonary Medicine, a section of the journal Frontiers in Medicine

RECEIVED 17 May 2022
ACCEPTED 20 September 2022
PUBLISHED 13 October 2022

CITATION
Zhu S-f, Wu X-x, Guo Y, Li P-f, Wang J-r, Liu M, Luo C-w, Yuan X-z and Li S-w (2022) A 16S rDNA sequencing-based analysis of airway microecology in patients with an acute exacerbation of chronic obstructive pulmonary disease: A cross-sectional study in Inner Mongolia, China. *Front. Med.* 9:946238. doi: 10.3389/fmed.2022.946238

A 16S rDNA sequencing-based analysis of airway microecology in patients with an acute exacerbation of chronic obstructive pulmonary disease: A cross-sectional study in Inner Mongolia, China

Shu-fen Zhu[1†], Xin-xin Wu[2†], Yan Guo[3], Peng-fei Li[4], Jing-ran Wang[2], Miao Liu[2], Cheng-wen Luo[5], Xiang-zhen Yuan[1*] and Shao-wei Li[6,7,8*]

[1]Physical Examination Center, The Affiliated Hospital of Inner Mongolia Medical University, Hohhot, China, [2]Inner Mongolia Medical University, Hohhot, China, [3]Department of Pathology, Inner Mongolia People's Hospital, Hohhot, China, [4]Department of Orthopaedics, Inner Mongolia People's Hospital, Hohhot, China, [5]Evidence-Based Medicine Center, Taizhou Hospital of Zhejiang Province, Wenzhou Medical University, Linhai, China, [6]Key Laboratory of Minimally Invasive Techniques & Rapid Rehabilitation of Digestive System Tumor of Zhejiang Province, Taizhou Hospital Affiliated to Wenzhou Medical University, Linhai, China, [7]Department of Gastroenterology, Taizhou Hospital of Zhejiang Province Affiliated to Wenzhou Medical University, Linhai, China, [8]Institute of Digestive Disease, Taizhou Hospital of Zhejiang Province Affiliated to Wenzhou Medical University, Linhai, China

Aim: To study the microecological characteristics of the airway and similarities and differences between healthy people and patients with the acute exacerbation of chronic obstructive pulmonary disease (AECOPD) in Inner Mongolia, and analyze the correlation between the characteristics of the airway microecological structure and clinical indicators of AECOPD patients.

Methods: Sputum samples from 36 healthy volunteers and 34 patients with AECOPD were detected by 16S rDNA high-throughput sequencing, and the airway microecological characteristics of healthy people and AECOPD patients were revealed by an alpha diversity analysis, beta diversity analysis, and LefSe difference analysis.

Results: There were differences in the airway microecological structure between healthy people and AECOPD patients in Inner Mongolia. The airway microbiota composition of AECOPD patients showed an increase in the abundance of common pathogens and a decrease in the abundance of commensal bacteria, and the airway microbial diversity in AECOPD patients was lower than that in healthy people. Long-term use of inhaled glucocorticoid + long-acting β2 agonist mixture (ICS + LABA), procalcitonin (PCT), blood monocyte count (MONO), hemoglobin (HGB), D-dimer (D-D),

and body temperature were negatively correlated with the alpha diversity of the airway micro-ecosystem.

Conclusion: The airway microecological composition of the AECOPD population in Inner Mongolia was different from that of the healthy population, and the airway microecological diversity was lower than that of the healthy population. The long-term use of ICS + LABA preparation by patients with AECOPD leads to lower alpha diversity. Alpha diversity was negatively correlated with inflammatory markers (PCT, MONO, D-dimer, body temperature) and HGB in AECOPD patients.

KEYWORDS

chronic obstructive pulmonary disease, acute exacerbation, airway microecology, 16s rDNA sequencing, sputum samples

Introduction

Chronic pulmonary disease obstructive (COPD) is a common chronic respiratory disease characterized by continuous airflow restriction (1). COPD patients suffer from the sudden exacerbation of symptoms and even respiratory failure, termed the acute exacerbation of chronic obstructive pulmonary disease (AECOPD). This is the main reason for increased mortality in patients with COPD. The pathogenesis of AECOPD is complex, involving infection, air pollution, high reactivity of the respiratory tract, and many other factors (2). In the past, because of the limitation of traditional sputum culture technology, the multiplication of one or several types of pathogenic bacteria was believed to be the main reason for AECOPD. However, with the emergence of a new generation of sequencing technology, the microecological structure of the airway was found to be closely associated with the onset of AECOPD and deterioration. After drug treatment, the microecology of the airway also changes in individual patients, which affects the course of the disease. In this background, we applied 16SrDNA high-throughput sequencing to analyze airway the microecology of healthy Han people and patients with AECOPD in Inner Mongolia in order to provide airway microecological data for these populations and to explore the correlation between the airway microecology and clinical indicators in AECOPD patients.

Materials and methods

Subjects and observations

The present study included individuals with AECOPD who were treated as inpatients in the Department of Respiratory and Critical Care Medicine, Affiliated Hospital of Inner Mongolia Medical University from January 2021 to December 2021. Healthy volunteers were recruited from individuals who underwent a physical examination at the same time. A total of 34 hospitalized AECOPD volunteers and 36 healthy volunteers were included in this study. The inclusion criteria for the AECOPD group were as follows: a diagnosis of AECOPD in line with the 2019 Global Initiative for Chronic Obstructive Pulmonary Disease (3), no history of antibiotic use in the 3 months before admission, and living in Inner Mongolia for a long time. Patients with bronchial asthma, pulmonary tuberculosis, interstitial lung disease, other chronic lung diseases, acute pulmonary edema, acute pulmonary embolism, acute heart failure, arrhythmia, other cardiopulmonary diseases, tumors, and autoimmune diseases were excluded from the study. The inclusion criteria for the healthy group were as follows: no chronic respiratory disease (e.g., COPD, pulmonary fibrosis, pulmonary tuberculosis, lung tumor, bronchial asthma, bronchiectasis, pulmonary sarcoidosis, etc.); no history of diseases affecting the immune system (e.g., blood system and autoimmune disease), age > 18 years; and living in Inner Mongolia for a long time. Patients who were unable to cooperate with sputum collection had a history of infection within the previous 3 months, or had a history of antibiotic use in the previous 3 months were excluded from the study. After obtaining their informed consent, sputum samples were collected from all volunteers and basic information, such as age, sex, and smoking status, was provided. Clinical case data were provided by volunteers in the AECOPD group. In addition, peripheral blood was extracted from all AECOPD patients before treatment on the day of admission and sent to the clinical laboratory of our hospital for a complete analysis of blood routine parameters, an evaluation of high-sensitivity C-reactive protein (hs-CRP), procalcitonin, a liver function test, sputum culture, and other analyses. All healthy volunteers came from the physical examination center of the same hospital. The physical examination items included lung function, chest CT, blood routine, liver function, kidney function, etc.

Methods

Collection of sputum samples

All subjects were repeatedly rinsed with normal saline to remove nasal and mouth secretions before sputum collection, and standards of operation were strictly observed during sputum collection in order to avoid contamination as far as possible. For objects with a large amount of sputum, the natural expectoration method was used to collect sputum samples, and the sputum from the deep part of the trachea was forcibly expectorated into sterile containers. For volunteers with no or low sputum volume, sputum samples were collected according to the improved Pin method (4): 3–5% gradient hypertonic saline air compression atomization was used for induction, the atomization time was 15 min, and the sputum was retained within 20 min. All sputum specimens were examined by sputum smear microscopy. Specimens with < 10 squamous cells/low magnification field and > 25 white blood cells/low magnification field were considered to be qualified sputum samples. Qualified sputum samples of at least 2 ml were collected in sterile cryopreservation tubes and frozen at -80°C within 2 h. Finally, the samples were uniformly sent to Hangzhou Lianchuan Biotechnology Co., Ltd., for a follow-up experimental analysis.

Bacterial deoxyribonucleic acid extraction, library construction, and a sequencing analysis

First, a Pathogenic Microbiome deoxyribonucleic acid (DNA) Kit (CWBIO) was used for the manual extraction of bacterial DNA from sputum samples. A PCR kit (New England Biolabs) was used with the341F (5'-CCTACGGGNGGCWGCAG-3'); 805R (5'-GACTACHVGGGTATCTAATCC-3') primer to amplify the V3-V4 specific fragment of the 16S rDNA gene. PCR products were purified by AMPure XT Beads (Beckman Coulter Genomics, USA), quantified by Qubit (Invitrogen, USA), and then were recovered by 2% agarose gel electrophoresis. The amplicon pools were prepared for sequencing and the size and quantity of the amplicon library were assessed on Agilent 2100 Bioanalyzer (Agilent, USA) and with the Library Quantification Kit for Illumina (Kapa Biosciences, Woburn, MA, USA), respectively. The libraries were sequenced on NovaSeq 6000 SP platform. Samples were sequenced on an Illumina NovaSeq platform paired-end reads were assigned to samples based on their unique barcode and truncated by cutting off the barcode and primer sequence. Paired-end reads were merged using FLASH (http://ccb.jhu.edu/software/FLASH/). Quality filtering on the raw reads was performed under specific filtering conditions to obtain high-quality clean tags according to the fqtrim (v0.94). Chimeric sequences were filtered using Vsearch software (v2.3.4). After dereplication using DADA2, we obtained the feature table and the feature sequence. According to the sequence of the ASV file using the SILVA (Release 138) database to NT-16s annotation database for species, the confidence threshold of the comments was determined to be 0.7.

Statistical analysis

The SPSS 22.0 software program was used for the basic statistical analysis of the data, and the T or T' test was used to measure data with normal distribution. Non-normal data were tested by a non-parametric Mann–Whitney U test. Qualitative data were compared using Pearson's chi-squared test. Spearman's rank correlation analysis was used to analyze the correlation between variables, and p-values of < 0.05 were considered to indicate statistical significance. A bioinformatics analysis was performed using the R software program (V2.5.4). An alpha diversity analysis and beta diversity analysis were performed based on the obtained ASV (feature) feature sequence and ASV (feature) abundance table. In the alpha diversity analysis, QIIME2 (2019.7) was used to calculate Observed-outs, Shannon, Chao1, and other indices, while the R software program was used to draw dilution curves and analyze differences between groups. Beta diversity was calculated by QIIME2 and plotted by the R software program. LEfSe was used to analyze the species differences between the groups. The threshold value of the linear discriminant analysis effect size (LEfSe) analysis in this project was set as LDA value > 4, $p < 0.05$.

We used the t-test to calculate the difference between two independent groups, assuming the effect size level of 0.8, the significance level of 0.05, and the power of 0.80. The target sample size was 54 participants. We allowed for a 20% participant dropout (reluctance to participate) and selected 68 participants as a conservative sample size. The sample size was calculated using the software G.Power 3.1.9.6.

Results

Basic information

A total of 36 healthy volunteers were included in this study (male, n = 17; female, n = 19; smokers, n = 15; non-smokers, n = 21; Smoking index, 425.21 ± 417.68; average age, 68.51 ± 11.28 years). The AECOPD group included 34 AECOPD patients (male, n = 20; female, n = 14; smokers, n = 18 smokers; non-smokers, n = 16; Smoking index, 447.83 ± 471.81; average age, 72.03 ± 7.72 years). There were no significant differences between the two groups in age, sex, or smoking habits ($p > 0.05$). The AECOPD included in this study were all severe patients who required hospitalization according to their comprehensive evaluation of clinical manifestations and laboratory tests.

The clinical data of the AECOPD patients included: disease course, test results on admission (hs-CRP, PCT, white blood cell count [WBC], neutrophil count [NEUT], neutrophil percentage [NEUT%], eosinophil count [EO], eosinophil ratio [EO%], lymphocyte count [LYM], lymphocyte ratio [LYM%], monocyte count [MONO], monocyte ratio [MONO%], basophil count [BASO%], basophil ratio [BASO%], hemoglobin [HGB], platelet count [PLT], prealbumin [PA], albumin [ALB], D-dimer [D-D]), body temperature, length of hospitalization, or long-term use of ICS + LABA mixed preparations (Table 1).

Airway microecological structure

In the healthy group, at the phylum level, Firmicutes, Proteobacteria, Bacteroidetes, Actinobacteria, and Fusobacteria constituted approximately 96.76% of the sequence in the community (Figure 1). At the genus level, the top 10 genera in the airway microecology of the healthy group were as follows Streptococcus, Neisseria, Prevotella-7, Porphyromonas, Haemophilus, Veillonella, Rothia, Alloprevotella, Actinomyces, and Fusobacterium, and these constituted approximately 73.63% of the sequences in the community (Figure 2).

In the AECOPD group at the phylum level, Firmicutes, Proteobacteria, Actinobacteria, Bacteroidetesa, and Fusobacteria constituted about 97.03% of the sequence in the community (Figure 3). The top 10 members of the genus were Streptococcus, Burkholderia, Veillonella, Actinomyces, Rothia, Neisseria, Prevotella-7, Klebsiella, Leptotrichia, and Pseudomonas; these constitute approximately 72.21% of the sequences in the community. Among the 34 AECOPD patients, most had a similar airway microecological composition, which maintained a dynamic balance among Pseudomonas, Burkholderia, and Veillonella. However, in some samples, Klebsiella and Pseudomonas were dominant (Figure 4).

TABLE 1 Clinical information of acute exacerbation of chronic obstructive pulmonary disease (AECOPD) volunteers.

Index	AECOPD patient ($n = 34$)
Course of disease (year, $x \pm s$)	11.79 ± 9.09
WBC ($\times 10^9$/L, $x \pm s$)	7.91 ± 2.91
NEUT ($\times 10^9$/L, $x \pm s$)	5.70 ± 2.64
NEUT% (%, $x \pm s$)	70.91 ± 11.43
LYM ($\times 10^9$/L, $x \pm s$)	1.39 ± 0.72
LYM% (%, $x \pm s$)	18.36 ± 8.34
MONO ($\times 10^9$/L, $x \pm s$)	0.53 ± 0.20
MONO% (%, $x \pm s$)	7.48 ± 4.48
EO ($\times 10^9$/L, $x \pm s$)	0.46 ± 0.99
EO% (%, $x \pm s$)	3.77 ± 5.48
BASO ($\times 10^9$/L, $x \pm s$)	0.04 ± 0.03
BASO% (%, $x \pm s$)	0.46 ± 0.35
HGB (g/L)	150.14 ± 26.10
PLT ($\times 10^9$/L, $x \pm s$)	197.15 ± 93.56
hs-CRP (mg/L)	14.79 ± 20.28
PCT (ng/mL)	0.54 ± 2.06
PA (mg/dL)	16.62 ± 7.00
ALB (g/L)	36.09 ± 7.73
D-D (μg/mL)	0.82 ± 0.84
Body temperature (°C)	36.6 ± 0.66
Length of stay (day)	8.88 ± 2.67
Use ICS + LABA (same)	17

LefSe difference analysis

LEfSe was used to further search for bacterial communities with significant differences between groups. There were 35 microorganisms with LDA values of > 4 at different classification levels (A: AECOPD group, B: healthy group). The relative abundance of Bacteroidetes in the healthy group increased at the phylum level. At the genus level, the relative abundance of Pseudomonas, Veillonella, and Burkholderia in the AECOPD group was increased in comparison to the healthy group. The relative abundance of Neisseria, Prevotella-7, Haemophilus, Alloprevotella, and Porphyromonas was decreased in comparison to the healthy group (Figure 5). Figure 6 shows an evolutionary clade demonstrating the difference in the abundance of biomarkers between the two groups using two different colors.

Alpha diversity

In this study, the complexity of the diversity of the microbial community was analyzed by the alpha diversity index (Observed-outs, Shannon, Simpson, Chao1). The dilution curve drawn by the Simpson index value as an ordinate tends to be flat, indicating that the current sequencing depth covers most microorganisms. The curve also indirectly reflected that the alpha diversity of airway bacteria in the healthy group was higher than that in the AECOPD group (Figure 7). Through the analysis of significant differences between groups, it was found that the alpha diversity of the airway bacteria in the healthy group was higher than that in the AECOPD group (Observed-outs, Shannon, Simpson, and Chao1 comparisons were all $p < 0.05$) (Figure 8).

Beta diversity analysis

In this study, a principal coordinate (PCoA) analysis based on the Weighted UniFrac distance was performed (ANOSIM, $p = 0.001$). The PC1 contribution rate was 50.31%, and the PC2 contribution rate was 14.91%, indicating differences in the

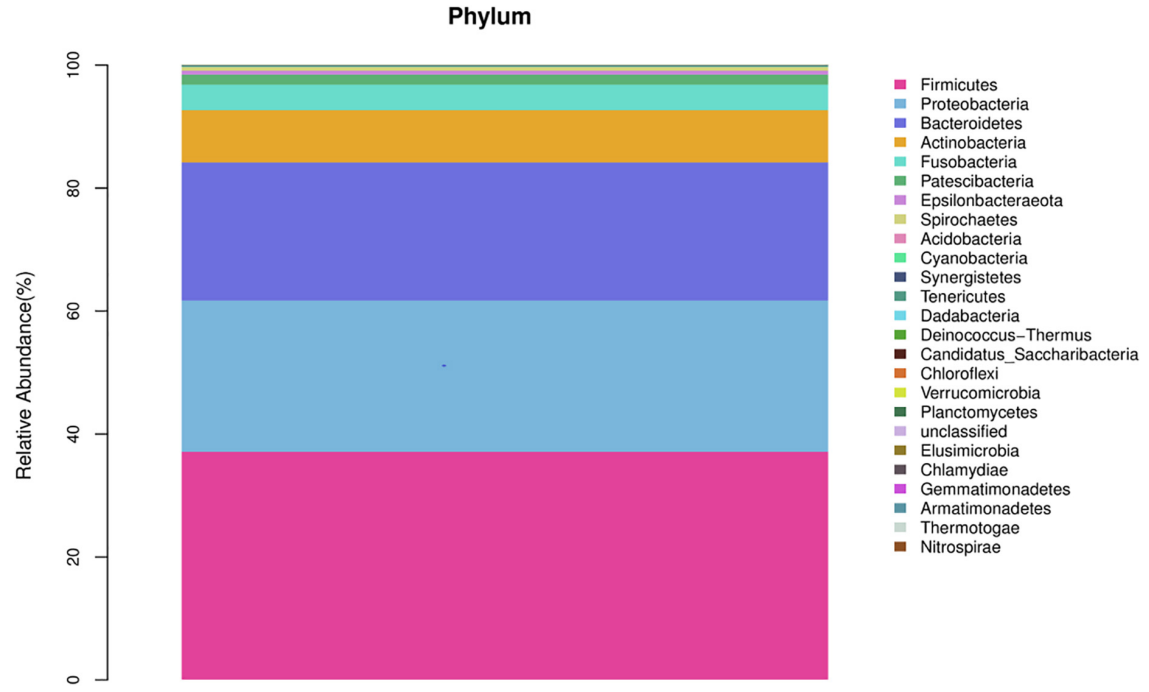

FIGURE 1
Histogram of microecological species distribution in healthy airways at the phylum level.

airway microecological structure between healthy individuals and patients with AECOPD (Figure 9).

Relationship between acute plus recombinant alpha diversity index and clinically relevant indicators in chronic obstructive pulmonary disease

We paid special attention to whether ICS + LABA affected the microecological structure of the airway, and the results showed that in the AECOPD group, ICS + LABA reduced alpha diversity (Observed-outs,*, Shannon*, Simpson*) (Table 2). LefSe was used to analyze the difference in flora between the two subgroups (Y: ICS + LABA, N: ICS + LABA), and it was found that the relative abundance of Actinomyces and Haemophilus was higher without ICS + LABA preparation (Figure 10).

In this paper, a Spearman rank correlation analysis was used to analyze the diversity index (Observed-outs, Shannon, Chao1) and blood routine parameters, and it was found that the MONO of AECOPD patients was negatively correlated with the alpha diversity of airway bacteria (Observed-outs, $r = 0.505$ **), PCT was negatively correlated with the alpha diversity of bacteria (Shannon, $r = -0.354$*), D-D was negatively correlated with the alpha diversity of the microflora (Observed-outs, $r = -0.372$*), body temperature was negatively correlated with the alpha diversity of the microflora (Observed-outs, $r = -0.540$**), and HGB was negatively correlated with the alpha diversity of the flora (Observed-outs, $r = -0.398$*) (Table 3).

Discussion

Although lung tissue is currently considered the preferred specimen for studying airway microecology, lung tissue specimens are difficult to obtain, and studies have found that upper airway and lower airway microflora are highly homologous, and there is no significant difference between the two species, except that the upper airway microflora is larger than the lower airway microflora (5). In addition, studies have shown that there is no significant difference in the composition of bacterial communities between spontaneous sputum samples and induced sputum samples (6). Thus, sputum was selected as the research sample in this study, and 16S rDNA high-throughput sequencing was performed to analyze and compare the airway microecology characteristics of AECOPD patients and healthy volunteers in Inner Mongolia. The correlation between the airway microecological diversity and clinical indicators, such as blood routine parameters, CRP, and PCT in patients with AECOPD was analyzed.

In our study, the airway flora structure of healthy volunteers in Inner Mongolia was mainly composed of Firmicutes, Proteobacteria, and Bacteroidetes, and the most common genera were Streptococcus, Neisseria, and Prevosia-7, which were

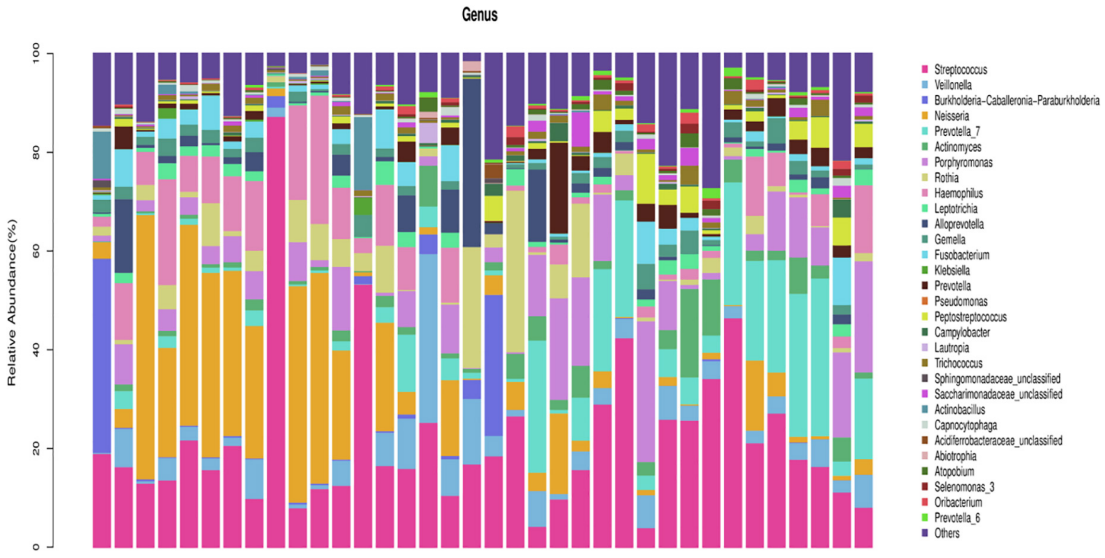

FIGURE 2
Histogram of microecological species distribution in healthy airways at the genus level.

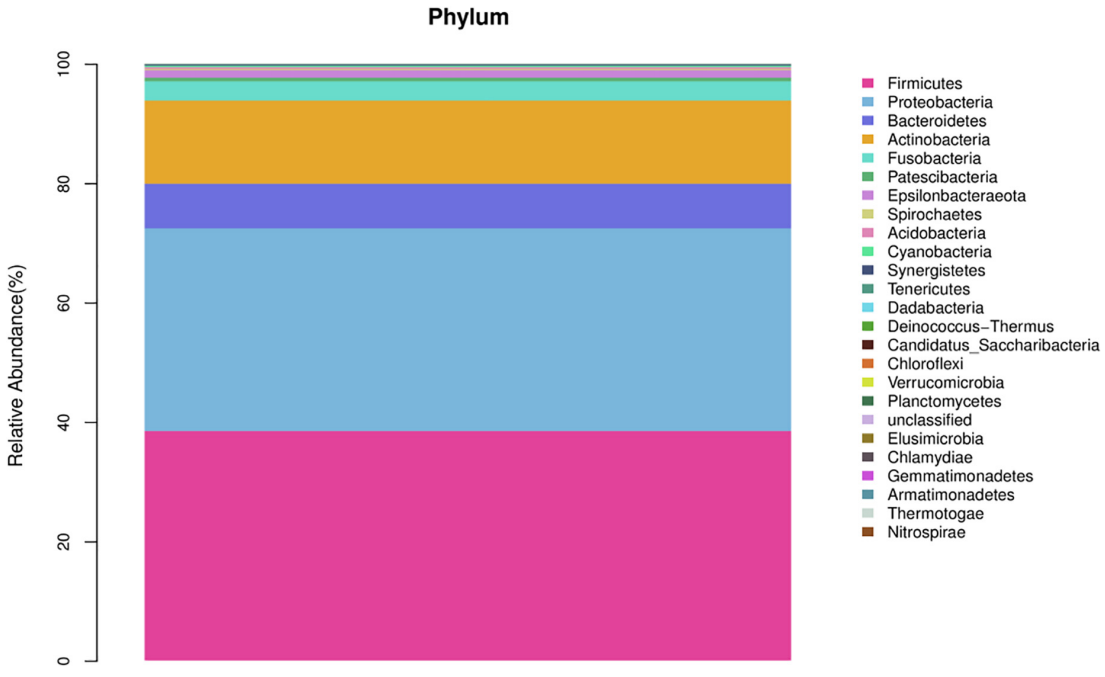

FIGURE 3
Composition of airway microbiota in the acute exacerbation of chronic obstructive pulmonary disease (AECOPD) group.

roughly in line with reports from Inner Mongolia and other countries (7–9); however, there were slight differences in each study. For example, Streptococcus, Prevotella, and Veillonella were the main factors in a multi-center study on the airway microecology of healthy people in the United States (8). In China, a study from Southern Medical University (9) showed that, at the genus level in the lower respiratory tract of healthy people, Streptococcus was the most numerous, followed by Prevotella and Neisseria. Considering the differences in the living environment, eating habits, genetics, and other aspects of the study subjects, these factors can be expected to have a certain impact on airway microecology (10), so

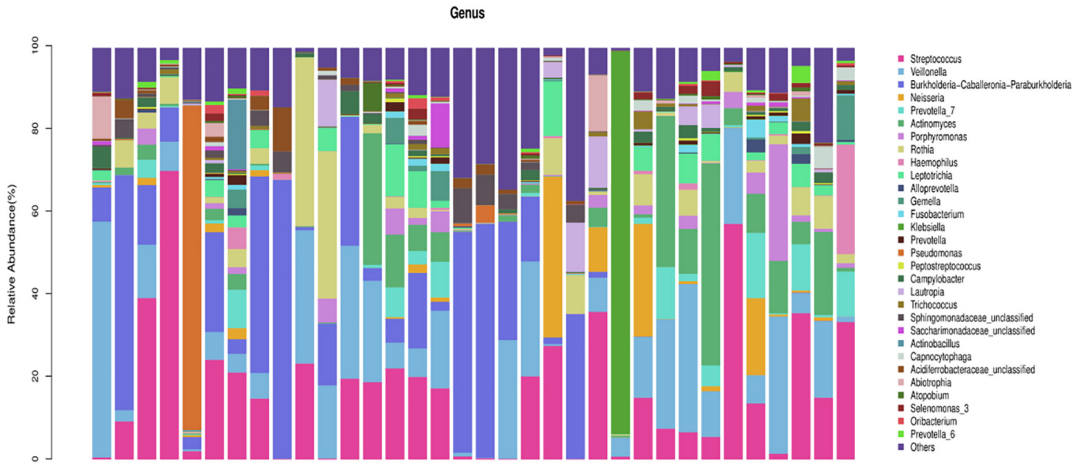

FIGURE 4
Composition of horizontal bacterial flora in the airway microecology of the acute exacerbation of chronic obstructive pulmonary disease (AECOPD) group.

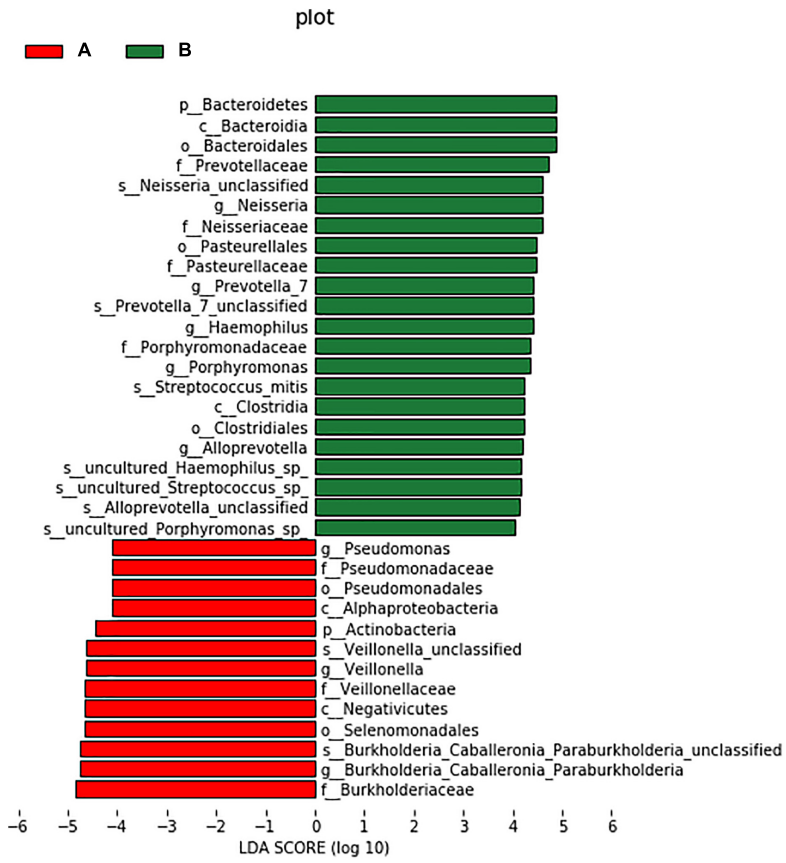

FIGURE 5
Histogram of the LDA value distribution of significantly different species.

the results may be different. For example, smoking will lead to a significant increase in the abundance of Streptococcus, and a decrease in common symbiotic bacteria (11). However, studies on the effects of race, climate, and diet on respiratory tract flora are still in the initial stage, and more in-depth studies are needed.

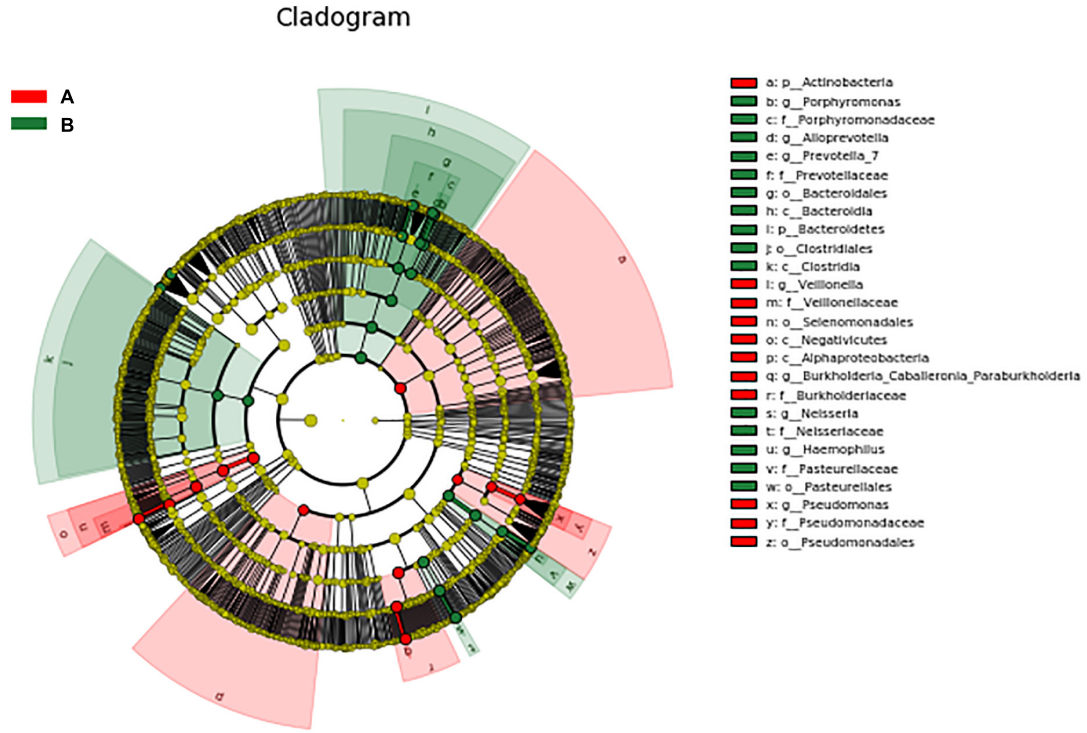

FIGURE 6
Evolutionary clade of significantly different species.

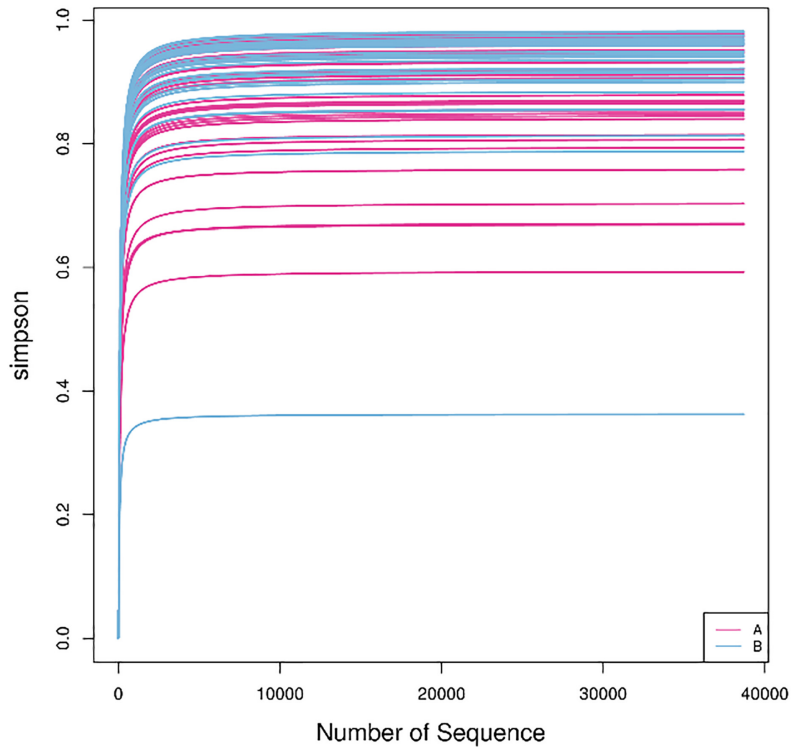

FIGURE 7
Dilution curve.

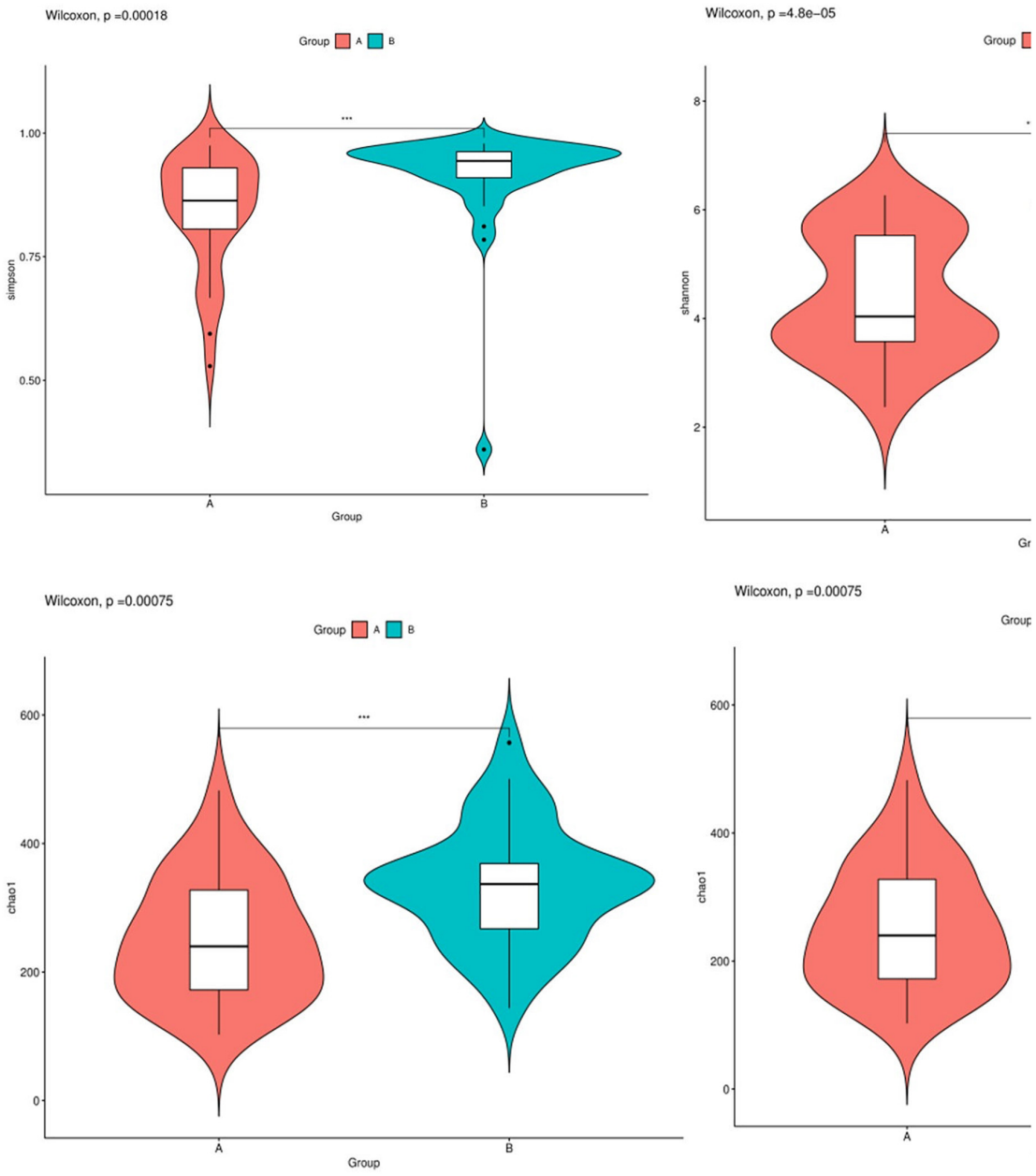

FIGURE 8
Difference analysis of alpha diversity index between groups.

In this experiment, Firmicutes and Proteobacteria were the main airway flora levels of AECOPD patients in Inner Mongolia. At the genus level, Streptococcus, Burkholderia, Veillonella, Actinobacteria, and Rothia are common, and LEfSe was used to analyze the difference in airway flora between healthy people and AECOPD patients. This analysis revealed that at the phylum level, the relative abundance of Bacteroidetes in the healthy group was higher; the relative abundance of pathogenic bacteria, such as Pseudomonas and Burkholderia, in the AECOPD group, was higher than that in the healthy group, and most of the genera that showed increased abundance in the AECOPD group belonged to Proteobacteria, which is in line with most previous reports (12, 13). However, there were differences. For example, in the study of Haldar et al. (13) the healthy population was dominated by Firmicutes and Bacteroidetes with relatively few Proteobacteria, while Proteobacteria were significantly increased in the COPD population and become the most important phylum. This may be due to factors such as age and smoking status among the COPD patients in each study. Studies have shown that the

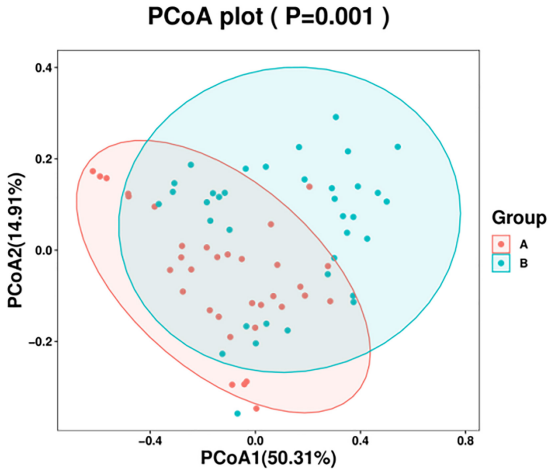

FIGURE 9
Principal coordinate (PcoA) analysis chart.

TABLE 2 Differences in alpha diversity of airway microflora and ICS + LABA in the acute exacerbation of chronic obstructive pulmonary disease (AECOPD) group [median (interquartile range)].

	ICS + LABA		*P*
	Exist	Inexistence	
Observed-OTUs	175.00 (139.00)	265.00 (148.50)	0.036*
Shannon	3.85 (1.00)	5.38 (2.09)	0.026*
Simpson	0.84 (0.11)	0.93 (0.11)	0.026*

*Expression $p < 0.05$.

TABLE 3 Correlation analysis of alpha diversity of the airway microflora and clinical indicators in acute exacerbation of chronic obstructive pulmonary disease (AECOPD) group (R correlation coefficient).

	Observed-OUTs	Shannon	Simpson
Age	−0.150	−0.181	−0.106
Disease course	−0.005	0.223	0.067
WBC	−0.320	0.115	0.069
NEUT	−0.186	0.063	0.071
NEUT%	−0.010	0.044	0.110
LYM	−0.044	0.013	−0.072
LYM%	0.157	−0.120	−0.189
MONO	−0.505**	0.075	0.094
MONO%	−0.150	0.091	0.075
EO	−0.036	−0.177	0.097
EO%	−0.093	−0.125	0.033
BASO	−0.125	0.125	0.150
BASO%	−0.150	−0.090	−0.097
HGB	−0.398*	0.205	0.145
PLT	0.021	−0.256	0.145
hs-CRP	−0.283	−0.079	−0.130
PCT	0.181	−0.354*	−0.292
PA	0.184	0.211	0.183
ALB	0.128	−0.099	0.055
D-D	−0.372*	0.116	0.108
Length of stay	−0.077	0.222	0.102
Body temperature	−0.540**	−0.038	0.018

**Expression $p < 0.01$, *expression $p < 0.05$.

airway microbiome of smokers has a higher load of pathogenic bacteria (e.g., Streptococcus pneumoniae, Haemophilus influenzae, and Pseudomonas aeruginosa) (14). However, no matter how these bacterial groups change, they generally change in the direction of increasing pathogenic bacteria and decreasing symbiotic bacteria. Commensal bacterial changes may be equally important in the development of COPD. Some people think that it may be because co-bacteria can—to a certain extent—inhibit the growth of potential pathogens belonging to the same genus or family (15). This may be with symbiotic bacteria and these potential pathogenic bacteria competing for colonization area and nutrients, and some studies have found that some bacteria can produce active substances, such as antimicrobial peptides to inhibit or kill other flora

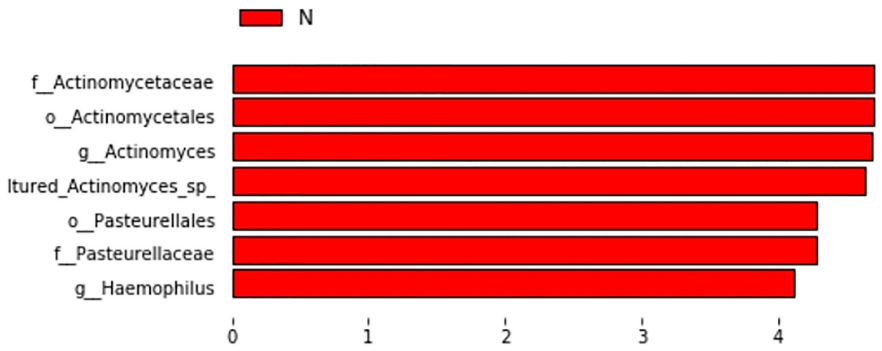

FIGURE 10
Histogram of LDA value distribution of significantly different species in subgroups.

(16). Similarly to our study, Wang et al. (17) also highlighted changes in non-pathogenic Proteobacteria in addition to the pathogenic microbiota during exacerbations, and it was found that Staphylococcus (potentially pathogenic bacteria) in the sputum of COPD patients and the absence of Veillonella, a potential commensal bacteria, were strongly associated with an increased risk of death after 1 year (18). This perspective highlights the importance of microbe-microbe interactions in maintaining homeostasis.

Our study showed that the alpha diversity of the airway microbiome in AECOPD patients was lower than that in healthy individuals, which is consistent with previous studies (6). This may be related to the proliferation of some pathogenic bacteria, which causes them to become dominant flora during acute exacerbations, inhibiting the growth of other flora, and resulting in a decline in flora diversity. Some studies have found that the decrease in diversity is related to the severity of the disease, and the microecology of patients with severe and advanced COPD was found to be lower than that of patients with moderate and severe disease (19). A study of the lung microbiome of COPD patients and a 1-year follow-up of the patients found that 1-year mortality increased significantly with a decrease in alpha diversity (18). These results suggest that airway microbial changes may be related to the exacerbation and prognosis of COPD.

A study showed that the airway microecology of patients with COPD could be significantly changed after 12 weeks of using ICS and or LABA preparations (20). Among the 34 patients with AECOPD included in this study, 17 of them used ICS + LABA on a regular basis. The medical history of preparations was more than half a year. To further study the effects of ICS and LABA on airway microecology, we analyzed the relationship between the diversity of airway flora in the AECOPD population and the use of ICS + LABA preparations. We found that the long-term inhalation of ICS + LABA preparations and alpha diversity was lower in AECOPD patients, and was associated with a relative reduction in Actinobacter and Haemophilus. Studies from Inner Mongolia and other countries have previously investigated the effects of hormones and long-acting β2 receptor agonists on the airway microecology, and also found that the treatment of COPD ICS can reduce the alpha diversity of the airway microecology (17, 21), but there is currently a lack of research on whether hormones can directly affect bacteria. However, studies have shown that, through indirect effects on the host, fluticasone, and budesonide inhibit the presence of *Haemophilus influenzae* in the airways (22), which is similar to our results. These data suggest that ICS may affect changes in the microbiome by promoting the growth of some bacteria and inhibiting others. However, there are few studies on the effect of β2 receptor agonists on airway microecology. At present, most clinical patients use a mixed preparation of ICS + LABA, which also makes it difficult to distinguish the specific effects of the two agents. Therefore, we need to better understand the effects of ICS, LABA, and other drugs on airway microecology, which may facilitate the more targeted use of these drugs.

This experiment found that PCT, MONO, D-dimer, body temperature, and airway microecological alpha diversity were negatively correlated. The elevation of these indicators all reflected the degree of inflammation in AECOPD, suggesting that the decrease in airway diversity may be associated with a more severe inflammatory response. This may be because the decline in the diversity of airway flora is due to the growth of pathogenic bacteria inhibiting the reproduction of other flora. Endotoxins and other metabolites produced by the mass reproduction of this pathogen can directly or indirectly affect the body's inflammatory response (23). Studies have shown that the flagellin of *Pseudomonas aeruginosa* can induce bronchial epithelial cells to produce interleukin-6 (IL-6) and interleukin-8 (IL-8) by affecting the signal transduction pathway, aggravating the inflammatory response. The underlying mechanism by which *Pseudomonas aeruginosa* causes acute exacerbations of COPD has also been explained (24). We also found that hemoglobin content in AECOPD patients was also negatively correlated with airway alpha diversity. Decreased airway diversity has been previously shown to be associated with more severe airflow obstruction (6, 25), and severe hypoxemia can lead to secondary polycythemia (26). These results suggest that the decrease in airway microbial diversity may be related to the level of inflammation and severity of the disease.

Conclusion

This study shows that the airway microecology of the AECOPD population in Inner Mongolia is different from that of the healthy population, and it is associated with drug use and some clinical indicators, which indicates that the airway microecological changes may be closely related to the acute attack of COPD. provides new ideas for diagnosis and treatment. There are many factors that affect airway microecology in the stable and acute stages of COPD. At present, this experiment has carried out part of the research on airway microecology in the acute exacerbation of COPD. In the next step, we need to use technologies such as metagenomics and metabolomics. The airway microecology (bacteria, fungi, viruses, etc.) of COPD patients with different stages and grades is analyzed by multi-factor, multi-center, and large samples to increase the influence of research results on the clinical diagnosis, treatment, and prognosis of COPD. Practical application.

Data availability statement

The datasets presented in this study can be found in online repositories. The name of the repository and accession number can be found below: China National

GeneBank (CNGB) Sequence Archive (CNSA), https://db.cngb.org/cnsa/, CNP0002927.

Ethics statement

The study was reviewed and approved by the Ethics Committee of Inner Mongolia Medical University Institutional Review Board (approval No. YKD2018170). The patients/participants provided their written informed consent to participate in this study.

Author contributions

S-FZ and X-XW designed and performed the experiments. YG, P-FL, J-RW, ML, and C-WL collected the data and performed the data analysis. X-ZY and S-WL designed the experiments and wrote the manuscript. All authors contributed to the article and approved the submitted version.

Funding

This work was supported in part by the Program of the National Natural Science Foundation of China (No. 61865014), the Medical Science and Technology Project of Zhejiang Province (No. 2021PY083), the Major Research Program of Taizhou Enze Medical Center (Grant No. 19EZZDA2), the Open Project Program of Key Laboratory of Minimally Invasive Techniques and Rapid Rehabilitation of Digestive System Tumor of Zhejiang Province (Nos. 21SZDSYS01 and 21SZDSYS09), and the Key Technology Research and Development Program of Zhejiang Province (No. 2019C03040).

Conflict of interest

The authors declare that the research was conducted in the absence of any commercial or financial relationships that could be construed as a potential conflict of interest.

Publisher's note

All claims expressed in this article are solely those of the authors and do not necessarily represent those of their affiliated organizations, or those of the publisher, the editors and the reviewers. Any product that may be evaluated in this article, or claim that may be made by its manufacturer, is not guaranteed or endorsed by the publisher.

References

1. Pauwels RA, Rabe KF. Burden and clinical features of Chronic Obstructive Pulmonary Disease (COPD). *Lancet.* (2004) 364:613–20. doi: 10.1016/S0140-6736(04)16855-4

2. Ritchie AI, Wedzicha JA. Definition, causes, pathogenesis, and consequences of chronic obstructive pulmonary disease exacerbations. *Clin Chest Med.* (2020) 41:421–38. doi: 10.1016/j.ccm.2020.06.007

3. Singh D, Agusti A, Anzueto A, Anzueto A, Barnes PJ, Bourbeau J, et al. Global strategy for the diagnosis, management, and prevention of chronic obstructive lung disease: the GOLD science committee report 2019. *Eur Respir J.* (2019) 53:1900164. doi: 10.1183/13993003.00164-2019

4. Pin I, Gibson PG, Kolendowicz R, Girgis-Gabardo A, Denburg JA, Hargreave FE, et al. Use of induced sputum cell counts to investigate airway inflammation in asthma. *Thorax.* (1992) 47:25–9. doi: 10.1136/thx.47.1.25

5. Guo MY, Chen HK, Ying HZ, Qiu FS, Wu JQ. The role of respiratory flora in the pathogenesis of chronic respiratory diseases. *BioMed Res Int.* (2021) 2021:6431862.

6. Mayhew D, Devos N, Lambert C, Brown JR, Clarke SC, Kim VL, et al. Longitudinal profiling of the lung microbiome in the AERIS study demonstrates repeatability of bacterial and eosinophilic COPD exacerbations. *Thorax.* (2018) 73:422–30. doi: 10.1136/thoraxjnl-2017-210408

7. Charlson ES, Bittinger K, Chen J, Diamond JM, Li H, Collman RG, et al. Assessing bacterial populations in the lung by replicate analysis of samples from the upper and lower respiratory tracts. *PLoS One.* (2012) 7:e42786. doi: 10.1371/journal.pone.0042786

8. Morris A, Beck JM, Schloss PD, Campbell TB, Crothers K, Curtis JL, et al. Comparison of the respiratory microbiome in healthy nonsmokers and smokers. *Am J Respir Crit Care Med.* (2013) 187:1067–75. doi: 10.1164/rccm.201210-1913OC

9. Liu HY, Li CX, Liang ZY, Zhang SY, Yang WY, Ye YM, et al. The interactions of airway bacterial and fungal communities in clinically stable asthma. *Front Microbiol.* (2020) 11:1647. doi: 10.3389/fmicb.2020.01647

10. Ploton MC, Abakka S, Amouyal E, Besnard C, Dufour L, El Harrif S, et al. [The lung microbiota. review]. *Arch Pediatr.* (2017) 24:667–74. doi: 10.1016/j.arcped.2017.04.007

11. Turek EM, Cox MJ, Hunter M, Hui J, James P, Willis-Owen SAG, et al. Airway microbial communities, smoking and asthma in a general population sample. *EBioMed.* (2021) 71:103538. doi: 10.1016/j.ebiom.2021.103538

12. Pragman AA, Lyu T, Baller JA, Hui J, James P, Willis-Owen SAG, et al. The lung tissue microbiota of mild and moderate chronic obstructive pulmonary disease. *Microbiome.* (2018) 6:7. doi: 10.1186/s40168-017-0381-4

13. Haldar K, George L, Wang Z, Mistry V, Ramsheh MY, Free RC, et al. The sputum microbiome is distinct between COPD and health, independent of smoking history. *Respir Res.* (2020) 21:183. doi: 10.1186/s12931-020-01448-3

14. Ghosh B, Gaike AH, Pyasi K, Brashier B, Das VV, Londhe JD, et al. Bacterial load and defective monocyte-derived macrophage bacterial phagocytosis in biomass smoke-related COPD. *Eur Respir J.* (2019) 53:1702273. doi: 10.1183/13993003.02273-2017

15. Iwase T, Uehara Y, Shinji H, Tajima A, Seo H, Takada K, et al. *Staphylococcus epidermidis* Esp inhibits *Staphylococcus aureus* biofilm formation and nasal colonization. *Nature.* (2010) 465:346–9. doi: 10.1038/nature09074

16. Boparai JK, Sharma PK. Mini review on antimicrobial peptides, sources, mechanism and recent applications. *Protein Pept Lett.* (2020) 27:4–16. doi: 10.2174/18755305MTAwENDE80

17. Wang Z, Bafadhel M, Haldar K, Spivak A, Mayhew D, Miller BE, et al. Lung microbiome dynamics in COPD exacerbations. *Eur Respir J.* (2016) 47:1082–92.

18. Leitao Filho FS, Alotaibi NM, Ngan D, Tam S, Yang J, Hollander Z, et al. Sputum microbiome is associated with 1-year mortality after chronic obstructive pulmonary disease hospitalizations. *Am J Respir Crit Care Med.* (2019) 199:1205–13. doi: 10.1164/rccm.201806-1135OC

19. Garcia-Nuñez M, Millares L, Pomares X, Ferrari R, Pérez-Brocal V, Gallego M, et al. Severity-related changes of bronchial microbiome in chronic obstructive pulmonary disease. *J Clin Microbiol.* (2014) 52:4217–23. doi: 10.1128/JCM.01967-14

20. Leitao Filho FS, Takiguchi H, Akata K, Ra SW, Moon JY, Kim HK, et al. Effects of inhaled corticosteroid/long-acting β(2)-agonist combination on the airway microbiome of patients with chronic obstructive pulmonary disease: a randomized controlled clinical trial (DISARM). *Am J Respir Crit Care Med.* (2021) 204:1143–52. doi: 10.1164/rccm.202102-0289OC

21. Qi YJ, Sun XJ, Wang Z, Bin YF, Li YH, Zhong XN, et al. Richness of sputum microbiome in acute exacerbations of eosinophilic chronic obstructive pulmonary disease. *Chin Med J.* (2020) 133:542–51. doi: 10.1097/CM9.0000000000000677

22. Wagner C, Goldmann T, Rohmann K, Rupp J, Marwitz S, Rotta Detto Loria J. Budesonide inhibits intracellular infection with non-typeable *Haemophilus influenzae* despite its anti-inflammatory effects in respiratory cells and human lung tissue: a role for p38 MAP kinase. *Respiration.* (2015) 90:416–25. doi: 10.1159/000439226

23. Sommariva M, Le Noci V, Bianchi F, Camelliti S, Balsari A, Tagliabue E, et al. The lung microbiota: role in maintaining pulmonary immune homeostasis and its implications in cancer development and therapy. *Cell Mol Life Sci.* (2020) 77:2739–49. doi: 10.1007/s00018-020-03452-8

24. Nakamoto K, Watanabe M, Sada M, Inui T, Nakamura M, Honda K, et al. *Pseudomonas aeruginosa*-derived flagellin stimulates IL-6 and IL-8 production in human bronchial epithelial cells: a potential mechanism for progression and exacerbation of COPD. *Exp Lung Res.* (2019) 45:255–66. doi: 10.1080/01902148.2019.1665147

25. Galiana A, Aguirre E, Rodriguez JC, Mira A, Santibañez M, Candela I, et al. Sputum microbiota in moderate versus severe patients with COPD. *Eur Respir J.* (2014) 43:1787–90. doi: 10.1183/09031936.00191513

26. Zhang J, DeMeo DL, Silverman EK, Make BJ, Wade RC, Wells JM, et al. Secondary polycythemia in chronic obstructive pulmonary disease: prevalence and risk factors. *BMC Pulmon Med.* (2021) 21:235. doi: 10.1186/s12890-021-01585-5

frontiers | Frontiers in Medicine

TYPE Systematic Review
PUBLISHED 07 November 2022
DOI 10.3389/fmed.2022.941944

OPEN ACCESS

EDITED BY
Yi Liu,
Shandong Provincial Hospital, China

REVIEWED BY
Jia Mi,
Binzhou Medical University, China
Tadesse Bekele Tafesse,
Haramaya University, Ethiopia

*CORRESPONDENCE
Wenquan Niu
niuwenquan@zryhyy.com.cn
Qi Zhang
zhangqikeyan@163.com

SPECIALTY SECTION
This article was submitted to Pulmonary Medicine, a section of the journal Frontiers in Medicine

RECEIVED 12 May 2022
ACCEPTED 15 September 2022
PUBLISHED 07 November 2022

CITATION
Hui Q, Hao Y, Ye F, Pang B, Niu W and Zhang Q (2022) Genetically high angiotensin-converting enzyme concentrations causally increase asthma risk: A meta-analysis using Mendelian randomization. *Front. Med.* 9:941944. doi: 10.3389/fmed.2022.941944

Genetically high angiotensin-converting enzyme concentrations causally increase asthma risk: A meta-analysis using Mendelian randomization

Qin Hui[1], Ying Hao[2], Fang Ye[1], Bo Pang[1], Wenquan Niu[2]* and Qi Zhang[1]*

[1]Department of Pediatrics, China-Japan Friendship Hospital, Beijing, China, [2]Institute of Clinical Medical Sciences, China-Japan Friendship Hospital, Beijing, China

Objectives: This meta-analysis aimed to test the association of angiotensin-converting enzyme (*ACE*) gene I/D polymorphism with asthma risk and circulating ACE changes.

Methods: Public literature retrieval, publication selection, and information extraction were completed independently by two investigators. Effect-size values are expressed as odds ratios (ORs) or standardized mean differences (SMDs) with a 95% confidence interval (95% CI).

Results: Nineteen studies (2,888 patients and 9,549 controls) fulfilled the eligibility criteria. Overall investigations demonstrated that *ACE* gene I/D polymorphism was significantly associated with asthma risk under allelic (OR, 95% CI: 1.26, 1.08 to 1.48), homozygous genotypic (1.50, 1.09 to 2.06), and recessive (1.53, 1.24 to 1.89) models with moderate heterogeneity (I^2 statistic: 64% to 79%). Subsidiary investigations recorded that race, matched status, asthma diagnosis, sample size, and age possibly accounted for the existence of significant heterogeneity. Relative to carriers with the II genotype, those with the DD genotype, ID genotype, and the combination of DD and ID genotypes had significantly higher concentrations of circulating ACE (WMD: 3.13, 2.07, and 2.83 U/L, respectively, $p < 0.05$). Adoption of Mendelian randomization analyses revealed that one unit increment in circulating ACE concentrations was found to be significantly associated with a 1.14-fold increased risk of asthma (95% CI: 1.02 to 4.24).

Conclusion: We provided strong meta-analytical evidence supporting the causal implication of high circulating ACE concentrations in the development of asthma.

KEYWORDS

angiotensin-converting enzyme, asthma, meta-analysis, polymorphism, Mendelian randomization

Introduction

Asthma is a highly heritable disease. The heritability of childhood asthma reached as high as 82% (1). A long list of asthma-susceptibility genes has been identified (2, 3). However, no consensus exists on which gene actually involves the pathogenesis of asthma, even with genome-wide association studies (4–6). In this regard, the candidate gene approach still represents an alternative strategy (7). Based on a known biological function, a gene can be a candidate to precipitate asthma. Importantly, the gene can be screened to see which mutation actually embodies its function. One such case is the insertion/deletion (I/D) polymorphism in the gene coding angiotensin-converting enzyme (ACE).

The association of *ACE* gene I/D polymorphism with asthma has been widely studied. For example, the DD genotype of the *ACE* gene was overrepresented in patients with asthma relative to healthy controls (8). In an early meta-analysis, the DD homozygote carriers had an overall about 60% increased risk of asthma compared with the II + ID carriers, and this risk was more evident in Asians (9). A recent meta-analysis in children indicated that *ACE* gene I/D polymorphism was associated with a significant risk of asthma (10). Other studies, however, did not reveal any significance between this polymorphism and asthma risk (11–13). The reasons behind this inconsistency are multiple, likely because of differences in origins, baseline characteristics of study participants, diagnosis criteria of asthma, and statistical power to derive significance. To this point, the synthesis of individually underpowered studies with the same research goals can help shed some light on these reasons.

To yield robust evidence, we aimed to perform an updated meta-analysis and test the association of *ACE* gene I/D polymorphism with asthma risk and changes in circulating ACE concentrations. Meanwhile, heterogeneity sources attributable to inconsistent observations were explored.

Methods

Performance guidelines

This meta-analysis was performed according to the guidelines in the preferred reporting items for systematic reviews and meta-analyses (PRISMA) statement. The PRISMA checklist is shown in Supplementary Table 1, and the PRISMA flow diagram is shown in Figure 1.

Search strategies

Using predefined key terms, four electronic databases—PubMed, HuGE Navigator, EMBASE (Excerpt Medica Database), and Web of Science—were searched from literature inception through March 2022. Key terms used for searching possibly eligible publications were formulated using the MeSH (Medical Subject Headings) database and are expressed in the Boolean format, that is ("asthma" or "atopic") and ("polymorphism" or "SNP" or "variant" or "mutation" or "variation" or "genetic" or "genotype" or "allele") and ("ACE" or "angiotensin-converting enzyme" or "angiotensin I converting enzyme" or "ACE1" or "DCP" or "DCP1" or "CD143").

Initial screening of searched publications was restricted to the English language and human beings. The search was also extended to the reference lists of major publications (reviews and meta-analyses) retrieved. The search was independently performed by two investigators (Q. H. and F. Y.), and any difference in numbers was resolved *via* discussion and a consensus was attained.

Inclusion criteria

Included publications must concurrently meet the following four criteria: (i) class of evidence: case-control design; (ii) outcome: asthma with clear definition; (iii) necessary data: genotype counts (or allele counts in the absence of genotype counts) of *ACE* gene I/D polymorphism between patients with asthma and controls, or circulating ACE concentrations across I/D genotypes in either patients or controls or both; and (iv) genotype determination: valid methodology.

Exclusion criteria

Publications were excluded if one or more of the following criteria were met: (i) type of publication: review, letter to editor or correspondence, editorial, comment, conference abstract, and case report or series; (ii) publication with duplicate participant samples; (iii) involvement of only cases; (iv) endpoint other than asthma; and (v) unpublished data.

Publication selection

The selection of eligible publications was handled in two steps. First, the title and abstract (if available) were reviewed and removal was applied based on exclusion criteria. After the first round of publication removal, the full text was read and eligibility was checked based on inclusion criteria.

The selection process of eligible publications was completed independently by two investigators (Q. H. and F. Y.), and any divergence was solved by discussion and if necessary by a third investigator (W. N.).

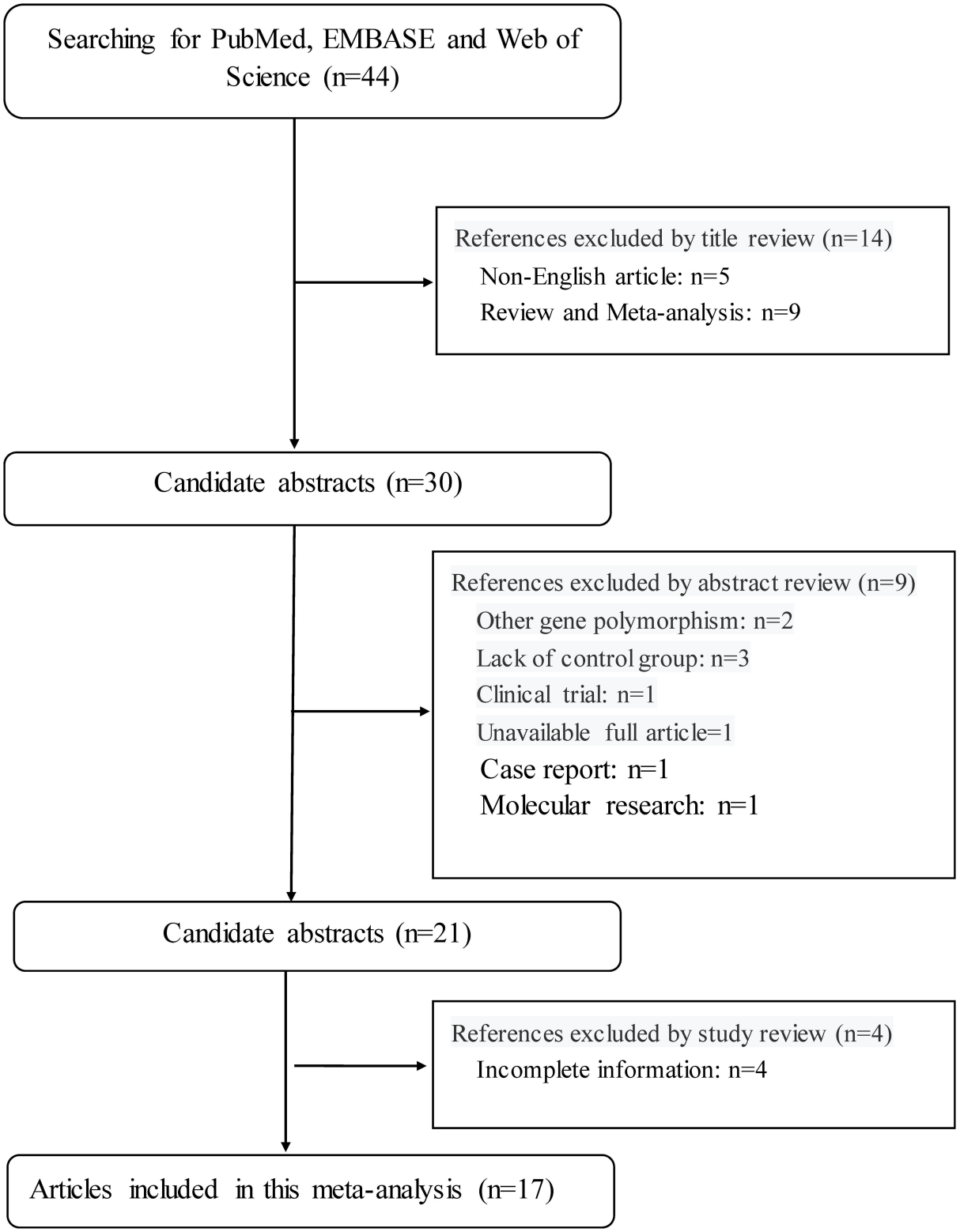

FIGURE 1
The PRISMA flowchart illustrates the selection process of qualified articles in this meta-analysis.

Information extraction

By the use of a uniform data extraction Excel sheet, information from each qualified publication was independently extracted by two investigators (Q. H. and F. Y.), and two Excel sheets were compared by kappa statistics. Any disagreement was solved by rechecking the full text until a consensus was attained.

The first author's name, year of publication, country where participants were enrolled, race, sample size, design, source of controls, matched condition, diagnosis of asthma, genotype counts of *ACE* gene I/D polymorphism, and baseline characteristics of study participants, including age, gender, and ACE concentrations in circulation, were all extracted.

Statistical analyses

STATA software version 14.1 for Windows (Stata Corp, College Station, Texas) was utilized for this meta-analysis. The association of *ACE* gene I/D polymorphism with the risk of asthma was measured by odds ratio (OR) with a 95% confidence interval (95% CI). Changes in circulating ACE concentrations between genotypes of this polymorphism were denoted by standardized mean difference (SMD) with a 95% CI. Both OR and SMD were derived under the random-effects model, because in the absence of heterogeneity, fixed-effects and random-effects models yield very similar estimates, whereas, in the presence of heterogeneity, the random-effects model is preferred (14). In the case of the significant association of *ACE* gene I/D polymorphism with asthma risk and ACE changes in circulation, the Mendelian randomization technique was employed to infer the possible causality between circulating ACE and asthma.

Between-study heterogeneity was measured by the inconsistency index (I^2) statistic. I^2 denotes the percent of variability observed between studies that are the result of heterogeneity but not a chance observation. Higher I^2 indicates a higher likelihood of heterogeneity. An I^2 statistic of over 50% is indicative of significant heterogeneity. The sources of heterogeneity were statistical, clinical, and methodological aspects. To track these sources, subsidiary analyses according to pre-specified factors (including sample size, race, matched condition, source of controls, and diagnosis of asthma) and meta-regression analyses of both continuous and categorical factors were carried out. Subgroups involving two or more studies are displayed.

In addition, cumulative analyses were conducted to see the impact of the first publication on subsequent publications and evolution of accumulated estimates over time. Sensitivity analyses were conducted to see the impact of any single study on the overall effect-size estimate by removing an individual study each time to check whether any of these estimates can bias the overall estimates.

Publication bias was assessed by Begg's funnel plot. If the funnel shape is asymmetrically inverted, it suggests a correlation between pooled estimate and study size (publication bias or small study bias). From a statistical aspect, publication bias was measured by Egger's test, which appraises funnel asymmetry with a significance level set at 10%.

Results

Qualified publications

By the use of key terms, searching four public databases yielded 44 publications in the English language. Application of inclusion criteria and exclusion criteria, 17 of 44 publications were qualified for synthesis in this meta-analysis (8, 12, 13, 15–28).

In total, 19 independent studies were isolated from 17 qualified publications, including 2,888 patients with asthma and 9,549 controls, among who the genotypes of *ACE* gene I/D polymorphism were assayed with validated typing methods. Out of 19 independent studies, 3 (including 431 subjects) provided data on the changes in circulating ACE concentrations across the genotypes of this polymorphism.

Baseline characteristics

The baseline characteristics of qualified studies are shown in Table 1. Thirteen studies were performed among adults, three among children, and one among both.

Overall analyses

The association between *ACE* gene I/D polymorphism and asthma risk was separately evaluated under allelic, homozygous genotypic, dominant, and recessive models of inheritance. Figure 2 shows the overall forest plots of the four models. This polymorphism was significantly associated with asthma risk in the allelic model, with the D allele corresponding to 1.26 times more likely to have asthma than the I allele (95% CI: 1.08 to 1.48). Significance was also noticed under homozygous genotypic (DD vs. II: OR = 1.50, 95% CI: 1.09 to 2.06) and recessive (DD vs. ID plus II: OR = 1.53, 95% CI: 1.24 to 1.89) models. However, there was no observable association under the dominant model (DD plus DI vs. II: OR = 1.14, 95% CI: 0.87 to 1.48). As of between-study heterogeneity, the I^2 statistic ranged from 64 to 79% across the four models of inheritance, suggesting that diversity in effect-size estimates was not due to chance.

In addition, this association was also evaluated under the heterozygous model of inheritance (Supplementary Figure 1),

TABLE 1 Study characteristics from all qualified publications in this meta-analysis.

Author	Year	Object	Country	Race	Design	Diagnosis	Source	Control feature	Sample size		Allele in cases		Allele in controls		Genotypes in cases			Genotypes in controls		
									Case	Control	D	I	D	I	DD	ID	II	DD	ID	II
Benessiano	1997	Adults	France	Caucasians	Cross-sectional	ATS	Hospital	Healthy	79	54	104	54	61	47	37	30	12	15	31	8
Tomita	1998	Adults	Japan	East Asians	Cross-sectional	ATS	Population	Healthy	71	142	55	87	101	183	9	37	25	16	69	57
Holla	1998	Adults	Czech	Caucasians	Cross-sectional	ATS	Hospital	Healthy	161	141	169	111	133	149	52	65	23	29	75	37
Gao	1998	Adults	UK	Caucasians	Cross-sectional	Doctor	Hospital	Healthy	150	150	174	126	167	133	55	64	31	48	71	31
Gao	1998	Adults	Japan	East Asians	Cross-sectional	Doctor	Hospital	Healthy	200	100	171	229	98	102	42	87	71	25	48	27
Gao	1998	Children	Japan	East Asians	Cross-sectional	Doctor	Hospital	Healthy	100	100	95	105	98	102	27	41	32	25	48	27
Chagani	1999	Adults	Canada	Caucasians	Cross-sectional	Doctor	Hospital	Healthy	224	252	258	204	274	224	79	100	52	72	130	47
Nakahama	1999	Adults	Japan	East Asians	Cross-sectional	ATS	Hospital	Non-asthma	119	208	94	144	152	264	22	50	47	28	96	84
Gao	2000	Adults	China	East Asians	Cross-sectional	ATS	Hospital	Healthy	50	50	61	39	42	58	23	15	12	8	26	16
Lee	2000	Adults	Korea	East Asians	Cross-sectional	ATS	Hospital	Healthy	167	121	244	376	96	146	43	158	109	23	50	48
Yildiz	2004	Adults	Turkey	Middle Eastern	Cross-sectional	ATS	Hospital	Healthy	49	49	47	37	46	46	15	17	10	13	20	13
Urhan	2004	Adults	Turkey	Middle Eastern	Cross-sectional	ATS	Hospital	Healthy	100	88	108	92	84	92	30	48	22	14	56	18
Lue	2006	Children	Taiwan	East Asians	Cross-sectional	ATS	Hospital	Non-asthma	105	102	74	136	50	154	17	40	48	4	42	56
Eryuksel	2009	Adults	Turkey	Middle Eastern	Cross-sectional	ATS	Hospital	Healthy	97	96	122	72	84	108	39	44	14	18	48	30
Lee	2009	Adults	Denmark	Caucasians	Cross-sectional	Self-report	Hospital	Non-asthma	602	7,079	646	574	8,587	8,261	166	314	130	2,208	4,171	2,045
Guo	2009	Children	China	East Asians	Prospective	GINA	Hospital	Non-asthma	149	165	178	120	122	208	71	36	42	41	40	84
Shafei	2011	Adults	Egypt	Middle Eastern	Cross-sectional	GINA	Hospital	Healthy	30	30	40	20	32	28	14	12	4	10	12	8
Bora	2013	Children	Turkey	Middle Eastern	Cross-sectional	Doctor	Hospital	Non-asthma	102	101	120	84	104	98	32	56	14	22	60	19
Saba	2016	Adults	Pakistan	Middle Eastern	Cross-sectional	Doctor	Hospital	Healthy	333	521	328	338	600	442	94	140	99	137	326	58

and there was no hint of statistical significance (D/I vs. II: OR = 0.96, 95% CI: 0.74 to 1.25). Considering the opposite effects of allele D and allele I on asthma risk, the heterozygous model is only interrogated in overall analyses.

Cumulative and influential analyses

Supplementary Figures 2, 3 exhibit the cumulative and influential analyses on the association between *ACE* gene I/D

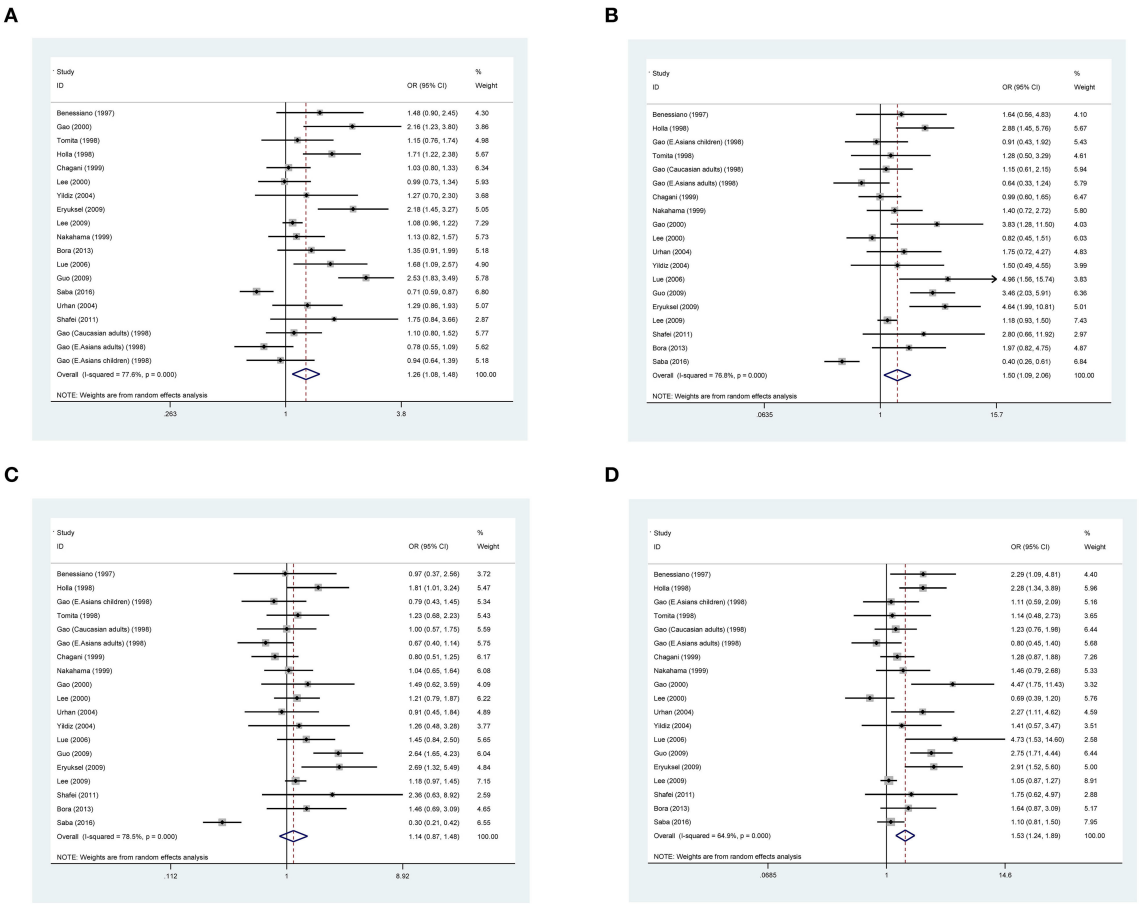

FIGURE 2
Forest plots of the angiotensin-converting enzyme (ACE) gene insertion/deletion (I/D) polymorphism in association with asthma under allelic **(A)**, homozygous genotypic **(B)**, dominant models **(C)**, and recessive model **(D)**.

polymorphism and asthma risk, respectively. The cumulative impact over time was stabilized since the year 2000. Influential analyses were conducted by evaluating the impact of each study on the pooled OR *via* the deletion of one study each time, which revealed no single study impacted the pooled ORs significantly.

Publication bias

Figure 3 shows Begg's funnel plot inspecting the potential satisfaction of publication bias under the allelic model. The Begg's funnel plot seemed asymmetrical by inspection, which was confirmed by Egger's test, with the probability being 0.052.

Subgroup analyses

As summarized in Table 2, the association between *ACE* gene I/D polymorphism and asthma risk was examined upon stratification by several potential factors on a categorical scale under the four models of inheritance.

It is worth noticing that race, matched status, asthma diagnosis, sample size, and age were possible sources of between-study heterogeneity, particularly under the recessive model. For example, the mutation of *ACE* gene I/D polymorphism was associated with the significant risk of asthma in Caucasians under allelic and recessive models, with the odds reaching 1.19 (95% CI: 1.00 to 1.41) and 1.41 (95% CI: 1.04 to 1.90), respectively, and no significance was observed in East Asians, irrespective of the models of inheritance.

The majority of subgroups showed improved between-study heterogeneity by pooling studies with homogeneous characteristics of interest.

Meta-regression analyses

An alternative way to explore sources of between-study heterogeneity is to perform meta-regression analyses. By

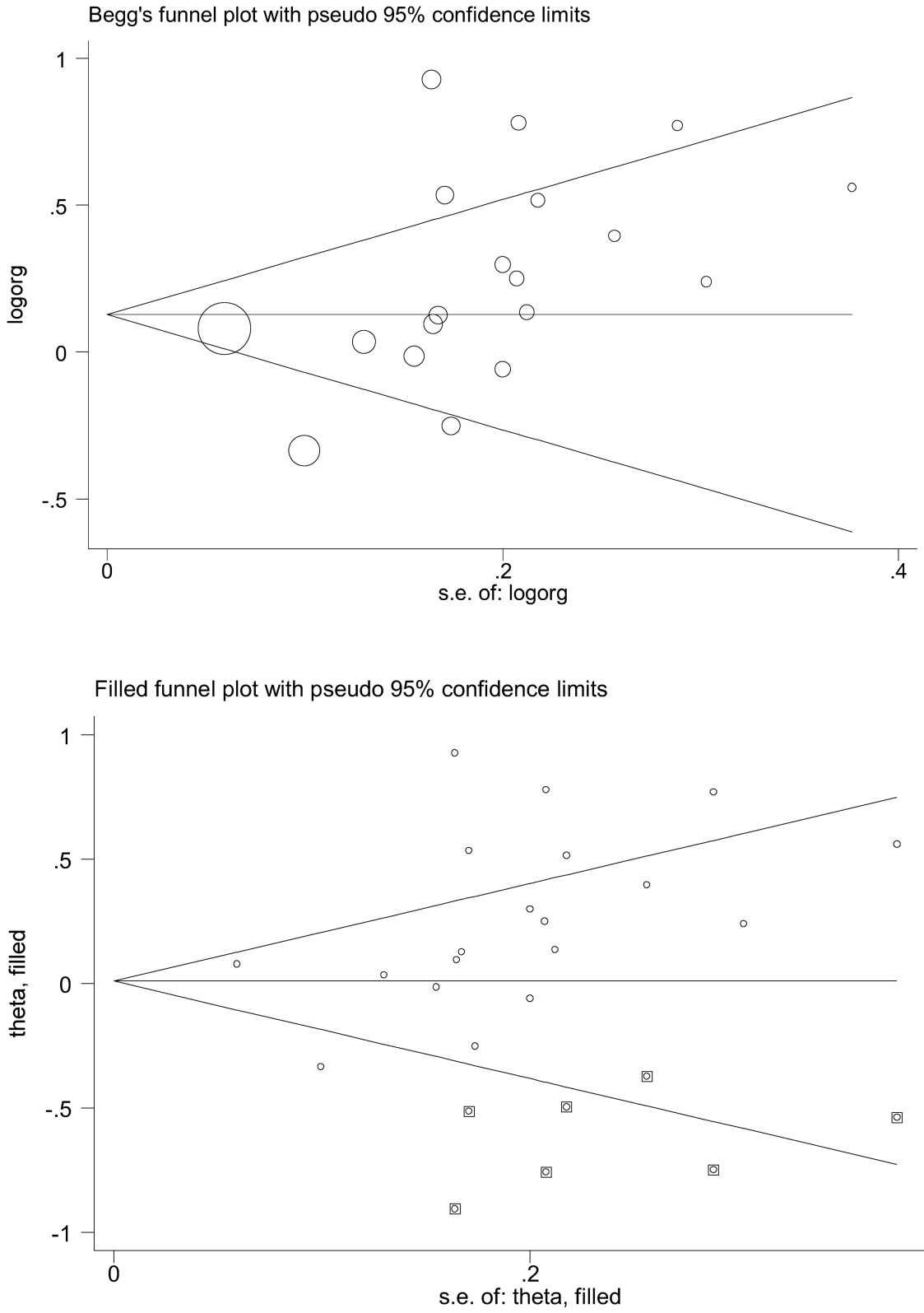

FIGURE 3
Begg's and filled funnel plots of the angiotensin-converting enzyme (ACE) gene insertion/deletion (I/D) polymorphism in association with asthma under the allelic model.

TABLE 2 Subgroup analyses of *ACE* gene I/D polymorphisms in association with asthma.

Subgroups	Studies	Allele model (D vs. I)					Homozygous genotype model (DD vs. II)					Dominant model (DD+DI vs. II)					Recessive model (DD vs. DI+II)				
	(cases/controls)	OR	LCI	UCI	*p*	I^2 (%)	OR	LCI	UCI	*p*	I^2 (%)	OR	LCI	UCI	*p*	I^2 (%)	OR	LCI	UCI	*p*	I^2 (%)
By race																					
Caucasians	1,216/7,676	1.19	1.00	1.41	0.05	49.7	1.32	0.96	1.82	0.08	42.5	1.12	0.89	1.41	0.34	24.6	1.41	1.04	1.90	0.03	62.1
East Asians	961/988	1.29	0.96	1.74	0.10	80.6	1.56	0.91	2.66	0.10	75.2	1.21	0.89	1.66	0.22	61.8	1.55	0.96	2.52	0.08	75.8
Middle Eastern	711/885	1.31	0.87	1.98	0.20	84.3	1.66	0.65	4.21	0.29	86.5	1.15	0.49	2.73	0.75	88.7	1.67	1.17	2.38	0.01	45.6
By design																					
Cross-sectional	2,739/9,384	1.19	1.04	1.38	0.01	69.3	1.4	1.03	1.91	0.03	72.70	1.07	0.83	1.38	0.60	75.20	1.45	1.18	1.78	0.00	59.00
Prospective	149/165	2.53	1.83	3.49	0.00	NA	3.46	2.03	5.91	0.00	NA	2.64	1.65	4.23	0.00	NA	2.75	1.71	4.44	0.00	NA
By matched status																					
Yes	707/979	1.34	0.77	2.32	0.30	91.7	1.62	0.53	4.93	0.39	91.50	1.11	0.44	2.81	0.83	93.50	1.76	1.02	3.03	0.04	72.30
No	2,181/8,570	1.22	1.06	1.41	0.01	58.8	1.43	1.09	1.88	0.01	55.80	1.12	0.94	1.34	0.19	30.50	1.47	1.16	1.87	0.00	63.20
By diagnosis																					
ATS	998/1,051	1.42	1.12	1.69	0.00	46.0	1.99	1.34	2.96	0.00	52.30	1.31	1.08	1.60	0.01	0.00	1.92	1.33	2.79	0.00	61.60
GINA	179/195	2.39	1.76	3.2	0.00	0.0	3.38	2.05	5.57	0.00	0.00	2.61	1.68	4.06	0.00	0.00	2.55	1.65	3.93	0.00	0.00
Doctor	1,109/1,224	0.94	0.77	1.15	0.55	60.8	0.85	0.54	1.34	0.48	69.90	0.72	0.45	1.17	0.19	80.70	1.16	0.97	1.39	0.12	0.00
Self-report	602/7,079	1.08	0.964	1.22	0.18	NA	1.18	0.93	1.5	0.17	NA	1.18	0.97	1.45	0.10	NA	1.05	0.88	1.27	0.59	NA
By sample size																					
>250	2,105/8,737	1.13	0.91	1.41	0.28	85.5	1.39	0.99	1.99	0.06	80.40	1.10	0.82	1.48	0.52	82.90	1.43	1.15	1.79	0.00	66.60
<250	783/812	1.44	1.21	1.71	0.00	30.4	2.21	1.24	3.94	0.01	0.00	1.38	0.82	2.24	0.23	0.00	2.25	1.41	3.59	0.00	9.60
By age																					
Children	456/468	1.54	0.99	2.37	0.05	80.7	2.28	1.11	4.69	0.03	69.90	1.48	0.87	2.51	0.15	69.40	2.04	1.19	3.48	0.01	60.90
Adults	2,432/9,081	1.19	1.01	1.39	0.03	71.9	1.33	0.95	1.86	0.09	74.10	1.06	0.79	1.42	0.72	78.50	1.41	1.14	1.76	0.00	60.30

ACE, angiotensin-converting enzyme; OR, odds ratio; LCI, 95% lower confidence interval; UCI, 95% upper confidence interval; I^2, inconsistency index; NA, not available.

10.3389/fmed.2022.941944

TABLE 3 Mean changes in circulating ACE concentrations between carriers of different genotypes of *ACE* gene I/D polymorphism.

Models	Studies	WMD	95% LCI	95% UCI	*p*	I^2 (%)	Egger's *P*-value
DD vs. II	3	3.13	0.50	5.77	0.02	96	0.59
ID vs. II	3	2.07	0.33	3.81	0.02	96	0.42
DD+ID vs. II	3	2.83	0.38	5.28	0.02	97.9	0.63

ACE, angiotensin-converting enzyme; WMD, weighted mean difference; 95% LCI, 95% lower confidence interval; 95% UCI, 95% upper confidence interval; I^2, inconsistency index.

regressing age, gender, asthma severity, race, matched status, asthma diagnosis, sample size, and study design (Supplementary Table 2), no hints of significance were seen at a significance level of 5%.

Genotype–phenotype analyses

The relationship between *ACE* gene I/D polymorphism and circulating ACE concentrations is shown in Table 3. Relative to carriers with the II genotype, those with the DD genotype, ID genotype, and the combined DD and ID genotypes showed significantly higher concentrations of circulating ACE (WMD: 3.13, 2.07, and 2.83 U/L, respectively, $p < 0.05$ for all).

Mendelian randomization analyses

Given the significance observed in both genotype-disease and genotype–phenotype analyses, the Mendelian randomization technique was utilized to infer the possible causal association between circulating ACE and asthma risk. Under the assumptions of the Mendelian randomization technique and by use of *ACE* gene I/D polymorphism as an instrumental variable, one unit increment in circulating ACE concentrations was found to be significantly associated with a 1.14-fold increased risk of asthma (95% CI: 1.02 to 4.24) under the homozygous genotypic model.

Discussion

The aim of this meta-analysis was to test the association of *ACE* gene I/D polymorphism with asthma risk and circulating ACE changes as well as explore sources for heterogeneity in the English literature. Through a comprehensive pooling of 19 independent studies involving 2,888 cases and 9,549 controls, this polymorphism was associated with a significant risk of asthma and changes in circulating ACE concentrations. Importantly, further adoption of the Mendelian randomization technique revealed that genetically increased ACE concentrations were causally associated with an increased risk of asthma. To the best of our knowledge, this is thus far the first meta-analytical evidence concerning the causal relation between circulating ACE and asthma risk in the literature.

It is well-known that asthma is a chronic pulmonary disease characterized by intermittent and reversible airflow obstruction (29). The exact etiology of asthma currently remains elusive; however, there is convincing evidence that asthma is a highly inheritable disease (1, 30). To shed light on the genetic profiles of asthma and seek reasons attributable to the inconsistency of previous individual studies, we, in this meta-analysis, aimed to test the association of *ACE* gene I/D polymorphism with asthma risk, as well as with circulating ACE concentrations. Our genotype-disease and genotype–phenotype analyses showed that carriers of the mutant DD homozygote had a 50% increased risk of asthma and 3.13 U/L increased concentrations of circulating ACE relative to the wild II homozygote. Under the assumptions of the Mendelian randomization technique, it is expected that circulating ACE may be a causal risk factor for the development of asthma. The implication of circulating ACE in asthma is biologically plausible. There is evidence that ACE expressed in the lungs plays a key role in the pathogenesis of bronchial asthma. It is because ACE can mediate the proliferation of smooth vascular muscle cells (31), which affects aggregation and adhesion of platelets and monocytes and consequently leads to excessive bronchiectasis (32). The biological mechanism behind the causal implication of circulating ACE in asthma is not clear at present (33). It is reasonable to speculate that if involved, the mutation of I/D polymorphism can alter the expression of ACE in circulation or tissues, which triggers the development of asthma.

It is also worth noticing that according to our subsidiary analyses, differences in race, matched status, asthma diagnosis, sample size, and age might account for previously diverging findings of individual studies. Taking race as an example, we found that the susceptibility of *ACE* gene I/D polymorphism to asthma was race-dependent, with significance observed in Caucasians but not in East Asians, in agreement with the findings of previous studies (16, 18, 19, 21, 34). Indeed, asthma is a multifactorial disease to which genetic, environmental, and lifestyle-related factors contribute jointly (35). For feasibility reasons, it is recommended to construct a list of candidate genetic determinants for asthma in each racial group. Moreover, diagnostic criteria for asthma can also confound the association between *ACE* gene I/D polymorphism and asthma risk. In

this meta-analysis, significance was observed in studies based on ATS and GINA criteria, whereas there was no observable significance in studies with self-reported asthma. To derive a reliable estimate, it is important to diagnose asthma formally. Differing from the observations of subsidiary analyses, we failed to reveal any statistical significance in meta-regression analyses, an alternative method to explore sources of between-study heterogeneity. It is of practical importance to bear in mind that meta-regression analyses, albeit enabling covariates in either continuous or categorical format to be regressed, do not have the methodological rigor of a properly designed study that is intended to test the effect of these covariates formally (36).

Another important finding is the obvious changes in circulating ACE between genotypes of *ACE* gene I/D polymorphism. Considering the fact that the I/D polymorphism is located in the 16th intron, it is unlikely to be functional at the transcription level. There is a possibility that this polymorphism is strongly linked to another functional locus in either the promoter or exon or 3′-untranslated region of the *ACE* gene that is responsible for the regulation of circulating ACE concentrations. Further genomic and functional explorations of the *ACE* gene are encouraged.

Limitations

Several limitations should be acknowledged in this meta-analysis. First, this meta-analysis synthesized evidence from publications written in the English language, and selection bias cannot be excluded. Second, all included studies are cross-sectionally designed; however, causality was inferred by means of the Mendelian randomization technique. Third, only a few features were commonly provided by the majority of included studies, and it is expected that more features are needed to examine their potential confounding impact on between-study heterogeneity. Fourth, there was moderate evidence of publication bias, which might limit the generalizability of our findings.

Conclusion

Taken together, we, for the first time, provided systematic evidence supporting the causal implication of high circulating ACE in the development of asthma by means of the Mendelian randomization technique. Further experimental studies are needed to determine the culprit genetic loci in the *ACE* gene that can simultaneously regulate circulating ACE concentrations and precipitate the onset and progression of asthma.

Data availability statement

The original contributions presented in the study are included in the article/Supplementary material, further inquiries can be directed to the corresponding authors.

Author contributions

QZ and WN planned and designed the study, and directed its implementation. QH and FY contributed to data acquisition. QH, YH, and BP conducted statistical analyses. QH and WN wrote and revised the manuscript. All authors read and approved the final manuscript prior to submission.

Funding

This work was financially supported by the CAMS Innovation Fund for Medical Sciences (2021-12M-C&T-B-089) and the National Natural Science Foundation of China (Grant number: 81970042).

Conflict of interest

The authors declare that the research was conducted in the absence of any commercial or financial relationships that could be construed as a potential conflict of interest.

Publisher's note

Supplementary material

The Supplementary Material for this article can be found online at: https://www.frontiersin.org/articles/10.3389/fmed.2022.941944/full#supplementary-material

References

1. Ullemar V, Magnusson PKE, Lundholm C, Zettergren A, Melen E, Lichtenstein P, et al. Heritability and confirmation of genetic association studies for childhood asthma in twins. *Allergy*. (2016) 71:230–8. doi: 10.1111/all.12783

2. Bansal M, Garg M, Agrawal A. Advances in asthma genetics. *Adv Genet*. (2021) 107:1–32. doi: 10.1016/bs.adgen.2020.11.001

3. Ober C. Asthma genetics in the post-GWAS era. *Ann Am Thorac Soc*. (2016) 13(Suppl. 1):S85–90. doi: 10.1513/AnnalsATS.201507-459MG

4. Hirota T, Takahashi A, Kubo M, Tatsuhiko T, Tomita K, Doi D, et al. Genome-wide association study identifies three new susceptibility loci for adult asthma in the Japanese population. *Nat Genet*. (2011) 43:893–6. doi: 10.1038/ng.887

5. Bonnelykke K, Sleiman P, Nielsen K, Kreiner-Moller E, Mercader JM, Belgrave D, et al. A genome-wide association study identifies CDHR3 as a susceptibility locus for early childhood asthma with severe exacerbations. *Nat Genet*. (2014) 46:51–5. doi: 10.1038/ng.2830

6. Anantharaman R, Andiappan AK, Nikanth PP, Suri BK, Wang DY, Chew FT. Genome-wide association study identifies PERLD1 as asthma candidate gene. *BMC Med Genet*. (2011) 12:170. doi: 10.1186/1471-2350-12-170

7. Raita Y, Zhu Z, Camargo CA, Freishtat RJ, Ngo D, Liang L, et al. Relationship of soluble interleukin-6 receptors with asthma: a mendelian randomization study. *Front Med*. (2021) 8:665057. doi: 10.3389/fmed.2021.665057

8. Benessiano J, Crestani B, Mestari F, Klouche W, Neukirch F, Hacein-Bey S, et al. High frequency of a deletion polymorphism of the angiotensin-converting enzyme gene in asthma. *J Allergy Clin Immunol*. (1997) 99:53–7. doi: 10.1016/S0091-6749(97)70300-2

9. Zhang YG, Li XB, Zhang J, Huang J, He C, Deng Y, et al. The I/D polymorphism of angiotensin-converting enzyme gene and asthma risk: a meta-analysis. *Allergy*. (2011) 66:197–205. doi: 10.1111/j.1398-9995.2010.02438.x

10. Shao Z, Jin H, Sun H, Dong C, Xu B, Zha L. Angiotensin-converting enzyme insertion/deletion polymorphism and susceptibility to pediatric asthma: a meta-analysis. *J Renin Angiotensin Aldosterone Syst*. (2020) 21:1470320320923475. doi: 10.1177/1470320320923475

11. Rad IA, Bagheri M, Rahimi-Rad MH. Deletion allele of the ACE gene is not a risk factor for asthma predisposition. *Pneumologia*. (2011) 60:208–12. doi: 10.1081/jas-120026073

12. Yildiz P, Oflaz H, Cine N, Genchallac H, Erginel-Unaltuna N, Yildiz A, et al. Endothelial dysfunction in patients with asthma: the role of polymorphisms of ACE and endothelial NOS genes. *J Asthma*. (2004) 41:159–66. doi: 10.1081/JAS-120026073

13. Gao PS, Mao XQ, Kawai M, Enomoto T, Sasaki S, Shaldon SR, et al. Lack of association between ACE gene polymorphisms and atopy and asthma in British and Japanese populations. *Clin Genet*. (1998) 54:245–7. doi: 10.1111/j.1399-0004.1998.tb04294.x

14. Cohn LD, Becker BJ. How meta-analysis increases statistical power. *Psychol Methods*.(2003) 8:243–53. doi: 10.1037/1082-989X.8.3.243

15. Urhan M, Degirmenci I, Harmanci E, Gunes HV, Metintas M, Basaran A. High frequency of DD polymorphism of the angiotensin-converting enzyme gene in Turkish asthmatic patients. *Allergy Asthma Proc*. (2004) 25:243–7.

16. Tomita H, Sato S, Matsuda R, Ogisu N, Mori T, Niimi T, et al. Genetic polymorphism of the angiotensin-converting enzyme (ACE) in asthmatic patients. *Respir Med*. (1998) 92:1305–10. doi: 10.1016/S0954-6111(98)90134-2

17. Saba N, Yusuf O, Rehman S, Munir S, Ahmad leS, Mansoor A, et al. An angiotensin I-converting enzyme insertion/detion polymorphism is associated with Pakistani asthmatic cases and controls. *J Biosci*. (2016) 41:439–44. doi: 10.1007/s12038-016-9617-x

18. Nakahama H, Obata K, Nakajima T, Nakamura H, Kitada O, Sugita M, et al. Renin-angiotensin system component gene polymorphism in Japanese bronchial asthma patients. *J Asthma*. (1999) 36:187–93. doi: 10.3109/02770909909056316

19. Lee YC, Cheon KT, Lee HB, Kim W, Rhee YK, Kim DS. Gene polymorphisms of endothelial nitric oxide synthase and angiotensin-converting enzyme in patients with asthma. *Allergy*. (2000) 55:959–63. doi: 10.1034/j.1398-9995.2000.00724.x

20. Lee J, Nordestgaard BG, Dahl M. Elevated ACE activity is not associated with asthma, COPD, and COPD co-morbidity. *Respir Med*. (2009) 103:1286–92. doi: 10.1016/j.rmed.2009.04.003

21. Hollá L, Văsku A, Znojil V, Sisková L, Vácha J. Association of 3 gene polymorphisms with atopic diseases. *J Allergy Clin Immunol*. (1999) 103:702–8. doi: 10.1016/S0091-6749(99)70246-0

22. Gao J, Lin Y, Xiao Y, Xu K, Xu W, Zhu Y, et al. Polymorphism of angiotensin-converting enzyme gene and genetic susceptibility to asthma with familial aggregation. *Chin Med Sci J*. (2000) 15:24–8.

23. Eryüksel E, Ceyhan BB, Bircan R, Avşar M, Cirakoglu B. Angiotensin converting enzyme gene polymorphism in Turkish asthmatic patients. *J Asthma*. (2009) 46:335–8. doi: 10.1080/02770900802660972

24. El-Shafei MS, Farres MN, Shahin RY. Evaluation of angiotensin converting enzyme gene polymorphism and susceptibility to bronchial asthma among Egyptians. *Allergol Immunopathol*. (2012) 40:275–80. doi: 10.1016/j.aller.2011.05.010

25. Chagani T, Pare PD, Zhu S, Weir TD, Bai TR, Behbehani NA, et al. Prevalence of tumor necrosis factor-alpha and angiotensin converting enzyme polymorphisms in mild/moderate and fatal/near-fatal asthma. *Am J Respir Crit Care Med*. (1999) 160:278–82. doi: 10.1164/ajrccm.160.1.9808032

26. Lue KH, Ku MS, Li C, Sun HL, Lee HS, Chou MC. ACE gene polymorphism might disclose why some Taiwanese children with allergic rhinitis develop asthma symptoms but others do not. *Pediatr Allergy Immunol*. (2006) 17:508–13. doi: 10.1111/j.1399-3038.2006.00452.x

27. Guo S, Zhang JH, Yan YD, Ding YF, Sheng JY. Association between renin-angiotensin system gene polymorphism and recurrent wheezing in Chinese children: a 4-year follow-up study. *J Int Med Res*. (2009) 37:351–8. doi: 10.1177/147323000903700209

28. Bora E, Soylar R, Ayyildiz ZA, Uzuner N, Bozkaya OG, Ercal D, et al. Plasminogen activator inhibitor-1 and angiotensin converting enzyme gene polymorphisms in Turkish asthmatic children. *Allergol Immunopathol*. (2013) 41:11–6. doi: 10.1016/j.aller.2011.12.003

29. Bush A. Pathophysiological mechanisms of asthma. *Front Pediatr*. (2019) 7:68. doi: 10.3389/fped.2019.00068

30. Wang TN, Chao YY, Wang TH, ChenCJ, Ko YC. Familial risk of asthma among adolescents and their relatives in Taiwan. *J Asthma*. (2001) 38:485–94. doi: 10.1081/JAS-100105869

31. Tong Y, Ye C, Ren XS, Qiu Y, Zang YH, Xiong XQ, et al. Exosome-mediated transfer of ACE (angiotensin-converting enzyme) from adventitial fibroblasts of spontaneously hypertensive rats promotes vascular smooth muscle cell migration. *Hypertension*. (2018) 72:881–8. doi: 10.1161/HYPERTENSIONAHA.118.11375

32. Rechkina. Models of gen-gene interaction in determining the severity of bronchial asthma in children. *Am J Intern Med*. (2020) 8:182–91. doi: 10.11648/j.ajim.20200804.17

33. Krynytska I. The association of angiotensin-converting enzyme gene insertion/deletion polymorphism with bronchial asthma. *Pol Merkur Lekarski*. (2021) XLIX:442–4.

34. Ding QL, Sun SF, Cao C, Deng ZC. Association between angiotensin-converting enzyme I/D polymorphism and asthma risk: a meta-analysis involving 11,897 subjects. *J Asthma*. (2012) 49:557–62. doi: 10.3109/02770903.2012.685540

35. Tan LD, Alismail A, Ariue B. Asthma guidelines: comparison of the National Heart, Lung, and Blood Institute Expert Panel Report 4 with Global Initiative for Asthma 2021. *Curr Opin Pulm Med*. (2022) 28:234–44. doi: 10.1097/MCP.0000000000000867

36. Munafo MR, Flint J. Meta-analysis of genetic association studies. *Trends Genet*. (2004) 20:439–44. doi: 10.1016/j.tig.2004.06.014

Frontiers in Medicine

Translating medical research and innovation into improved patient care

A multidisciplinary journal which advances our medical knowledge. It supports the translation of scientific advances into new therapies and diagnostic tools that will improve patient care.

Discover the latest Research Topics

See more →

Frontiers

Avenue du Tribunal-Fédéral 34
1005 Lausanne, Switzerland
frontiersin.org

Contact us

+41 (0)21 510 17 00
frontiersin.org/about/contact